Sensing and Retrograde Signalling of Mitochondrial Metabolic States in Plants

Dissertation der Fakultät für Biologie der Ludwig-Maximilians-Universität München

Vorgelegt von
Ann-Christine König

München, Juni 2014

Gutachter:

Dr. Iris Finkemeier (Erstgutachter)

Prof. Dr. Jörg Nickelsen (Zweitgutachter)

Prof. Dr. Wolfgang Enard

Prof. Dr. Thorsten Mascher

PD. Dr. Bolle

Prof. Dr. Günther Heubl

Tag der Dissertations Abgabe: 18.06.2014

Tag der mündlichen Prüfung: 26.09.2014

Table of contents

I. Summary

Plants are exposed to always changing environmental conditions because of their sessile nature. For an optimal development and growth, plants have to be able to adapt to these changing conditions such as alterations in light intensities, temperature differences, salt stress as well as pathogen attacks. The acclimation of the plant metabolism can occur by the synthesis of new proteins which are directly or indirectly capable to protect cellular components from damage due to oxidative stress for example. Most sensitive to oxidative inhibition are metabolic pathways connected to electron transport chains which are housed in the plant organelles, mitochondria and chloroplasts, and which are the major energy sources for plant cells. Because both organelles lost most of their genomes during evolution, the majority of their required proteins are expressed in the nucleus, translated in the cytosol and posttranslationally imported into the target organelle. This requires a fine-tuned and constant communication between the nucleus and the organelles as well as interplay between chloroplasts and mitochondria themselves. Mitochondria indirectly provide reducing equivalents for the chloroplast and supply the cells with ATP in the dark and when ATP supply from chloroplasts is not sufficient. In this thesis, the communication of mitochondria with the nucleus and the posttranslational regulation of mitochondrial metabolic enzymes have been investigated. Mitochondria house the tricarboxylic acid (TCA) cycle in which acetyl-CoA and carboxylic acids are used in a series of decarboxylation reactions to produce reducing equivalents used during oxidative phosphorylation for ATP synthesis. As organic acids are the major players in the TCA cycle and they reflect both the redox and the metabolic state of the cell, they represent putative candidates to act as regulators of gene expression. We propose citrate as a possible signalling molecule to report on the metabolic state of mitochondria as it can be transported between organelles and we were able to demonstrate that perturbation in cellular citrate concentrations strongly correlate with changes in transcript abundances. After citrate treatment, the main functional affected gene targets were photosynthesis, cell wall, biotic stress, and protein synthesis. Similar categories were observed to be changed after mitochondrial impairment and therefore they were concluded as main targets of mitochondrial retrograde signalling. Additionally we showed that the transcript response to citrate is distinct from other organic acids and that induction of genes occurs in a time and concentration dependent manner.

Intracellular mitochondrial citrate levels depend on the action of citrate synthase which we found to be redox-regulated. Citrate synthase is catalyzing the first committed step of the TCA cycle in which oxaloacetate and acetyl-CoA are converted to citrate. Our results indicate

that citrate synthase can be deactivated by oxidation and reactivated by thioredoxin which probably enables the proper folding of citrate synthase. Further high molecular weight complexes of citrate synthase were observed either because of multimeric aggregates or association with high molecular weight complexes with proteins from oxidative phosphorylation (OXPHOS). By site-directed mutagenesis the cysteine residues important for activity and redox regulation of citrate synthase were discovered. Until now almost nothing was known about the posttranslational regulation of TCA cycle enzymes and here we provide first insight into the redox regulation of citrate synthase.

Posttranslational modifications, like redox regulation, are in general efficient molecular mechanisms to modify the activity of important metabolic enzymes. A further yet largely unexplored posttranslational modification is the acetylation of the ε-amino group of lysine residues on proteins investigated in the third part of this thesis. Lysine acetylation is dependent on the acetyl-CoA pools and can be reverted by the action of lysine deacetylases. We explored the extent of lysine acetylation in plant mitochondria. By liquid chromatography–mass spectrometry (LC-MS/MS) analysis the acetylome of Arabidopsis mitochondria was revealed, including 120 proteins and 243 acetylated sites. All TCA cycle enzymes carry at least one acetylation site and several enzymes of OXPHOS were identified as lysine-acetylated. The high number of lysine-acetylated proteins suggests that this modification has a regulatory role in mitochondrial metabolism maybe under adverse environmental conditions. In *in vitro* analysis, the abundance of non-enzymatic lysine acetylation depending on elevated pH and acetyl-CoA concentrations has been investigated. Furthermore, we characterized a novel sirtuin-type lysine deacetylase, Silent Information Regulator2 homolog (SRT2) in Arabidopsis mitochondria. We were able to demonstrate that SRT2 is mainly localized at the inner mitochondrial membrane and is interacting with several protein complexes in energy metabolism such as complex I, the ATP/ADP carries, and a subunit of the ATP-synthase. An increased ADP uptake was discovered for the knockout mutant as well as changes in sugars and amino acid contents compared to wild type plants. In conclusion, this work provides a first insight into the fine-tuning of mitochondrial metabolism which is achieved by retrograde regulation and possibly mediated by citrate as signalling molecule. Furthermore, novel post-translational regulatory processes in *Arabidopsis* mitochondria were uncovered, such as the redox regulation of citrate synthase and the regulation of mitochondrial metabolism by lysine acetylation with SRT2 as active mitochondrial deacetylase.

II. Zusammenfassung

Pflanzen sind durch ihre sessile Lebensweise ständig wechselnden Umweltbedingungen ausgesetzt. Für eine optimale Entwicklung und optimales Wachstum müssen Pflanzen dazu in der Lage sein, sich wechselnden Bedingungen wie Lichtintensität, Temperaturunterschiede, Salzstress und Pathogenbefall anzupassen. Die Adaption des Pflanzenmetabolismus kann zum Beispiel durch die Synthese oder Regulation von Proteinen erfolgen, die direkt oder indirekt dazu fähig sind zelluläre Bestandteile vor Schäden wie z.B. Oxidation zu bewahren. Besonders metabolische Vorgänge in den pflanzlichen Organellen, welche mit dem Transport von Elektronen verbunden sind, erweisen sich als sehr empfindlich gegenüber Oxidation. Da Mitochondrien und Chloroplasten im Laufe der Evolution den größten Teil ihres Genoms verloren haben, müssen benötigte Proteine im Zellkern exprimiert, im Zytosol translatiert und anschließend posttranslational in das Zielorganell importiert werden. Dies setzt eine Feinregulation und ständige Kommunikation zwischen dem Zellkern und den Organellen voraus. Im Zuge dieser Arbeit wurde sowohl die Kommunikation zwischen Mitochondrien und dem Zellkern, als auch die posttranslationale Regulation mitochondrialer metabolischer Enzyme untersucht. In Mitochondrien findet der Citratzyklus statt, in welchem Reduktionsäquivalente aus Acetyl-CoA und Carbonsäuren in einer Reihe von Decarboxylierungsreaktionen gewonnen werden. Diese werden in der Oxidativen Phosphorylierung (OXPHOS) zur ATP-Produktion verwendet. Die Konzentrationen der Carbonsäuren des Citratzyklus spiegeln den Redoxstatus und den metabolischen Zustand der Mitochondrien wieder. Aus diesem Grund sind Carbonsäuren mögliche Kandidaten, welche an der Regulation der Genexpression beteiligt sein könnten. Citrat besitzt die Grundvoraussetzungen um als Signalmolekül mitochondrialer metabolischer Zustände zu dienen, da es zwischen den Organellen transportiert werden kann. In dieser Arbeit konnte gezeigt werden, dass die zelluläre Citratkonzentration einen starken Einfluss auf den Transkriptionsspiegel hat. Nach der Behandlung von *Arabidopsis*-Blättern mit Citrat, zeigten sich vor allem Änderungen in der Transkriptmenge folgender Gen-Gruppen: Photosynthese, Zellwandaufbau, biotischen Stress und Proteinbiosynthese. Zusätzlich konnte gezeigt werden, dass die Antwort auf Citrat sich von anderen Carbonsäuren und Zuckern unterscheidet und die Transkriptregulation sowohl Zeit- als auch konzentrationsabhängig erfolgt.

Intrazelluläre Citratspiegel sind mitunter abhängig von der Aktivität der Citrat-Synthase, für welche in dieser Studie bewiesen werden konnte, dass sie über die Redox-Regulation von Disulfidbrücken kontrolliert wird. Die Redox-Regulation der Citrat Synthase beruht auf einer Deaktivierung durch Oxidation und Reaktivierung durch Thioredoxine, welche

wahrscheinlich eine funktionelle Faltung der Citrat-Synthase begünstigen. Zusätzlich wurden hoch molekulare Komplexe der Citrat-Synthase entdeckt, welche entweder durch multimere Aggregationen oder durch transiente Interaktionen mit den hochmolekularen Komplexen der OXPHOS-Proteine zustande kommen. Durch die Mutation der sechs Cysteinreste in der Citrat-Synthase wurden jene Cysteine aufgedeckt, welche für die Aktivität und die Redox-Regulation verantwortlich sind. Bisher war nur wenig über die posttranslationale Regulation der Citratzyklus Enzyme bekannt. Diese Arbeit kann nun erstmalig eine Redox-Abhängigkeit der Citrat-Synthase darlegen.

Generell sind posttranslationale Modifikationen wie die Redox-Regulation von Proteinen effiziente molekulare Mechanismen, um die Aktivität von wichtigen Enzymen zu steuern. Im dritten Teil dieser Arbeit wurde die bis jetzt zum größten Teil unerforschte posttranslationale Modifikation der Lysin-Acetylierung behandelt, die eng an die mitochondriale Acetyl-CoA Konzentration gekoppelt ist. Die Lysin-Acetylierung von Proteinen erfolgt an der ε-Aminogruppe eines Lysins und wird reversibel durch Lysin-Deacetylasen reguliert. In dieser Arbeit wurde das Ausmaß der Lysin-Acetylierung von mitochondrialen Proteinen in Arabidopsis mit Hilfe von LC-MS/MS Analysen untersucht und es wurden 120 Lysin-acetylierte Proteine und 243 acetylierte Lysin-Seitenketten identifiziert. Diese große Anzahl an Lysin-acetylierten Proteinen lässt eine regulatorische Funktion im mitochondrialen Metabolismus vermuten. In *in vitro* Experimenten wurde die enzymatisch unabhängige Acetylierung gezeigt, welche von einem erhöhten pH-Wert und der Acetyl-CoA-Konzentration abhängig ist. Ebenfalls wurde eine mitochondriale Sirtuin-Typ Lysin-Deacetylase, Silent Information Regulator2 homolog (SRT2), charakterisiert. Es konnte gezeigt werden, dass SRT2 hauptsächlich an der inneren mitochondrialen Membran lokalisiert ist und mit mehreren Proteinkomplexen, welche am Energie-Metabolismus beteiligt sind, interagiert. Unter den Interaktionspartnern befinden sich sowohl Komplex I, die ATP/ADP-Carrier-Proteine und eine Untereinheit der ATP-Synthase. An isolierten Mitochondrien der Knockout-Mutante konnte ein erhöhter ADP Import festgestellt werden, was auf eine Regulation des ATP/ADP-Carries durch Lysin-Acetylierung schließen lässt. Die vorliegende kumulative Arbeit hat somit in ihren drei Haupteilen zu unserem Verständnis der Fein-Regulation des mitochondrialen Metabolismus durch retrograde Regulation und posttranslationaler Mechanismen, wie der Redox-Regulierung der Citrat-Synthase und der Regulation von mitochondrialen Proteinen durch die Lysine-Acetylierung, beigetragen.

III. Aim of the Thesis

In this work, putative signalling molecules as well as fine-tuning mechanisms of mitochondrial metabolism by posttranslational modifications were investigated. Mitochondria are key players in the plant energy metabolism producing ATP and providing reducing equivalents to the cell. Adjustment of metabolic function is regulated by the mitochondrial proteome. Acclimatization of mitochondria can either occur by the synthesis of new proteins or by activity manipulation of already available enzymes. The synthesis of new proteins is almost exclusively controlled by the nucleus except for some mitochondrial-encoded respiratory subunits. In order to supply mitochondria with new proteins, signals that sense the status of the organelle and communicate it back to the nucleus, are required. Nearly nothing is known about mitochondrial retrograde signalling in plants. Therefore the aim of this work was the investigations of the underlying regulatory mechanisms and identification of putative signalling molecules. As second part the adjustment of mitochondrial metabolic enzymes by posttranslational modifications as well as the first plant mitochondrial deacetylase were explored.

IV. List of Publications

[1] Schwarzländer M, **König AC**, Sweetlove LJ, Finkemeier I. The impact of impaired mitochondrial function on retrograde signalling: a meta-analysis of transcriptomic responses. J Exp Bot. 2012; 63(4):1735-50

[2] Finkemeier I, **König AC**, Heard W, Nunes-Nesi A, Pham PA, Leister D, Fernie AR, Sweetlove LJ. Transcriptomic analysis of the role of carboxylic acids in metabolite signaling in Arabidopsis leaves. Plant Physiol. 2013; 162(1):239-53

[3] Schmidtmann E, **König AC**, Orwat A, Leister D, Hartl M, Finkemeier I. Redox regulation of Arabidopsis mitochondrial citrate synthase. Mol Plant. 2014; 7(1):156-69

[4] Braun HP, Binder S, Brennicke A, Eubel H, Fernie AR, Finkemeier I, Klodmann J, **König AC**, Kühn K, Meyer E, Obata T, Schwarzländer M, Takenaka M, Zehrmann A. The life of plant mitochondrial complex I. Mitochondrion. 2014 pii: S1567-7249(14)00020-8

[5] **König AC** *, Hartl M*, Pham PA, Laxa M, Boersema PJ, Orwat A, Kalitventseva I, Plöchinger M, Braun HP, Leister D, Mann M, Wachter A, Fernie AR, Finkemeier I. The Arabidopsis class II sirtuin is a lysine deacetylase and interacts with mitochondrial energy metabolism. Plant Physiol. 2014; 164(3):1401-14. (*both authors contributed equally to the work)

[6] **König AC**, Hartl M, Boersema PJ, Mann M, Finkemeier I. The mitochondrial lysine acetylome of Arabidopsis. Mitochondrion. 2014 pii: S1567-7249

[7] Hartl M *, **König AC** *, Finkemeier I. Identification of lysine-acetylated mitochondrial proteins and their acetylation sites. Submitted to Spinger, Methods in Molecular Biology on Plant Mitochondria. (*both authors contributed equally to the work)

V. Abbreviations

2D-BN-PAGE	Two-dimensional blue native polyacrylamide gelelectrophoresis
2-OG	Oxoglutarate
AA	Antimycin A
AAC1-3	ATP/ADP carriers 1-3
ABA	Abscisic acid
AOX1	Alternative oxidase 1
A. thaliana	*Arabidopsis thaliana*
ANAC13	NAC domain protein 13
BR	Brassinosteroid
CI1	Citrate-induced 1
CI	Complex I; NADH dehydrogenase complex
CII	Complex II; Succinate dehydrogenase
CII	Complex III; Cytochrome bc_1 complex
CIV	Complex IV; Cytochrome c oxidase
CV	Complex V; ATP-synthase
CA2	Gamma carbonic anhydrase 2
COX	Cytochrome-c oxidase
CS	Citrate synthase
CS4	Recombinant Arabidopsis CS 4 protein
Cyt c	Cytochrome c
DIC	Di-and tricarboxylate transporter
E. coli	*Escherichia coli*
ETC	Electron transport chain
FER1	Ferritin1
GA	Gibberellic acid
GC-MS	Gas chromatography-mass spectrometry
GCN5L1	GCN5 (general control of amino acid synthesis 5)-like 1
GDH	Glutamate dehydrogenase
H_2O_2	Hydrogen peroxide
HAT	Histone acetyltransferase
HDAC	Histone deacetylase
IMS	Intermembrane space
JA	Jasmonic acid

KAT	Lysine Acetyltransferase
KDAC	Lysine deacetylase
LC-MS/MS	Liquid chromatography–mass spectrometry
McpS	Methyl-accepting chemotaxis receptor protein
MRR	Mitochondrial retrograde regulation
MRS	Mitochondrial retrograde signaling
MS	Mass spectrometry
noxy	Nonresponding to oxylipins
NTR	Thioredoxin reductase
OAA	Oxaloacetate
OSCP	Oligomycin sensitivity conferral protein
OXPHOS	Oxidative phosphorylation
PDC	Pyruvate dehydrogenase complex
PORA	Protochlorophyllide oxidoreductase A
PTM	Posttranslational modification
qDELLA	*quadruple DELLA* mutant
QRT-PCR	Quantitative real-time PCR
ROS	Reactive oxygen species
RuBisCo	Ribulose-1,5-bisphosphate carboxylase/oxygenase
SA	Salicylic acid
SAM-MT	SAM-dependent methyltransferase
SC	Supercomplex
Sir2	Silent information regulator 2
SIRT	Sirtuin
SRT2	Silent Information Regulator 1 homolog from class II
TCA	Tricarboxylic acid cycle
TF	Transcription factor
TRX	Thioredoxins
TRXi	Inactive mutant form of *E.coli* TRX
UQ	Ubiquinone
UQH	Ubiquinol
VDAC1-3	Voltage dependent anion channels 1-3

1. General Introduction

Communication between organelles – an overview

Mitochondria and chloroplasts are semi-autonomous organelles of higher plant cells. They are of endosymbiontic origin, with the assumption that mitochondria derive from proteobacteria and chloroplasts from cyanobacteria (Arnold, 1982; Deusch et al., 2008; Esser et al., 2004; Mirabdullaev, 1985; Martin et al., 2002). During the development of higher land plants genetic information was distributed between the organelles which requires the formation of compartments. As a consequence, mitochondria and chloroplasts lost their independence during evolution and work in a complex network together with the nucleus and the rest of the cell. Although the organelles still host their own genomes, most of their original genetic material was transferred to the nucleus. For this reason, proteins required in the organelles have to be transcribed in the nucleus, synthesized in the cytosol and imported into the target organelle (Woodson and Chory, 2008). Not only does the expression of genes in the nucleus need to be adjusted to constantly changing environmental conditions, but there is also a continuous need for particular proteins in the organelles, which allow them to acclimate to these environmental alterations.

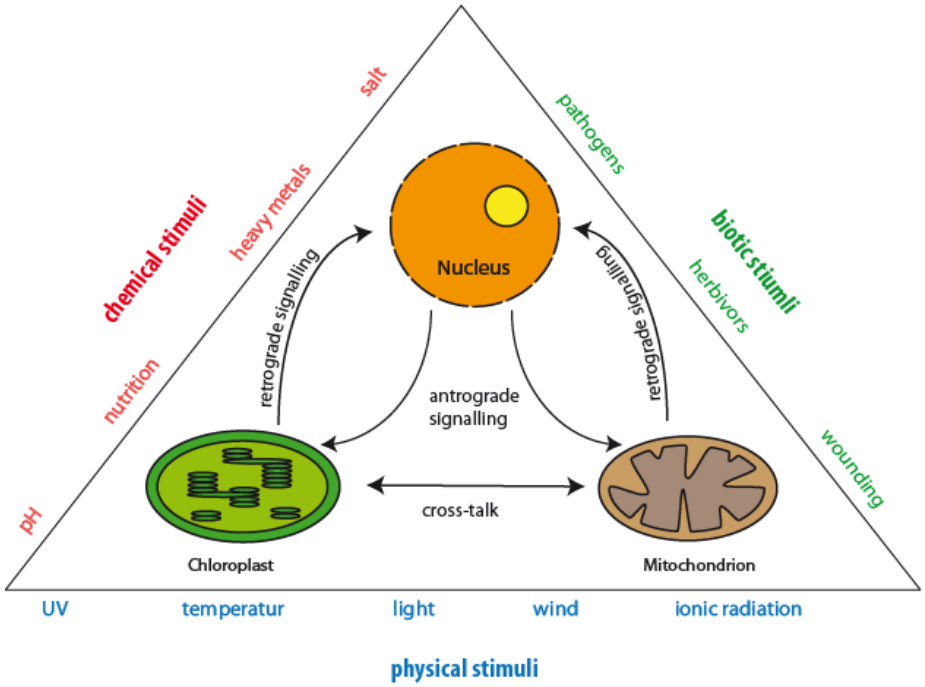

Fig. 1. Overview of signalling pathways between nucleus, mitochondria, and chloroplasts. Nucleus to organelle: anterograde signalling; organelle to nucleus: retrograde signalling; organelle to organelle signalling: cross-talk. Factors triggering signalling pathways can be chemical, biotic or physical stimuli.

In this study, two strategies of mitochondrial metabolic fine-tuning in *Arabidopsis thaliana* were investigated and are discussed in the following: (1) Retrograde regulation of gene expression and signalling molecules possibly involved, and (2) lysine acetylation on mitochondrial proteins as a posttranslational modification with putative regulatory functions.
Thus, three ways of signalling have been described: (I) anterograde control (nucleus to organelle) for signals sensed by the nucleus which allow the organelles to acclimate to environmental changes, (II) retrograde control (organelle to nucleus), which is needed to control the nuclear gene expression in concert with the metabolic and developmental state of the organelle, and (III) mitochondria to chloroplast cross-talk to coordinate metabolic pathways and requirements between the two endosymbiotic organelles (Fig. 1).

1.1. Main functions of mitochondria in plant cells

Besides chloroplasts, mitochondria are responsible for supplying energy in the form of ATP to the plant cell. In addition, an extensive range of other metabolic processes take place in mitochondria including amino acid synthesis, fatty acid metabolism as well as photorespiration (Fernie et al., 2004). As their mammalian counterparts, plant mitochondria host the tricarboxylic acid cycle (TCA), which reduces NAD and FAD to NAD(P)H and FADH, respectively, during the decarboxylation of carboxylic acids and provides energy for the oxidative phosphorylation of ATP (Fig. 2). Besides the TCA cycle, plant mitochondria also contain an electron transport chain that consists of four large protein complexes (CI, CII, CIII, CIV). Together with complex V (CV), these complexes build the classical oxidative phosphorylation pathway for ATP synthesis (Fig. 2). Starting with CI also called NADH dehydrogenase complex, electrons are shuttled through the complex by iron-sulfur clusters followed by the reduction of ubiquinone (UQ), while protons are pumped across the inner mitochondrial membrane from the matrix to the intermembrane space (Baradaran et al., 2013). Additionally, CI has several plant-specific subunits such as the carbonic anhydrases (Perales et al., 2005; Sunderhaus et al., 2006) which are unique to the plant kingdom. CII, or succinate dehydrogenase, is a component of both, the TCA cyle as well as of the electron transport chain. CII does not translocate protons, but rather by the conversion of succinate to fumarate, electrons are shuttled through CII and transferred to UQ. Ubiquinol (UQH), the reduced form of UQ, releases its electron at CIII (the cytochrome bc_1 complex) which transfers them in the Q-cycle onto cytochrome c (cyt c). CIII protons are shuttled again into the intermembrane space. At CIV, the cytochrome c oxidase, electrons are transferred from cyt c to oxygen, which is reduced to water in a four electron transfer step. This represents the

final step of the classical electron transport chain found in animals and plants (reviewed in Millar et a., 2011). At CIV protons are again pumped into the intermembrane space. This proton gradient between matrix and intermembrane space is finally used at CV, also called ATP synthase, in order to produce ATP from ADP and P_i.

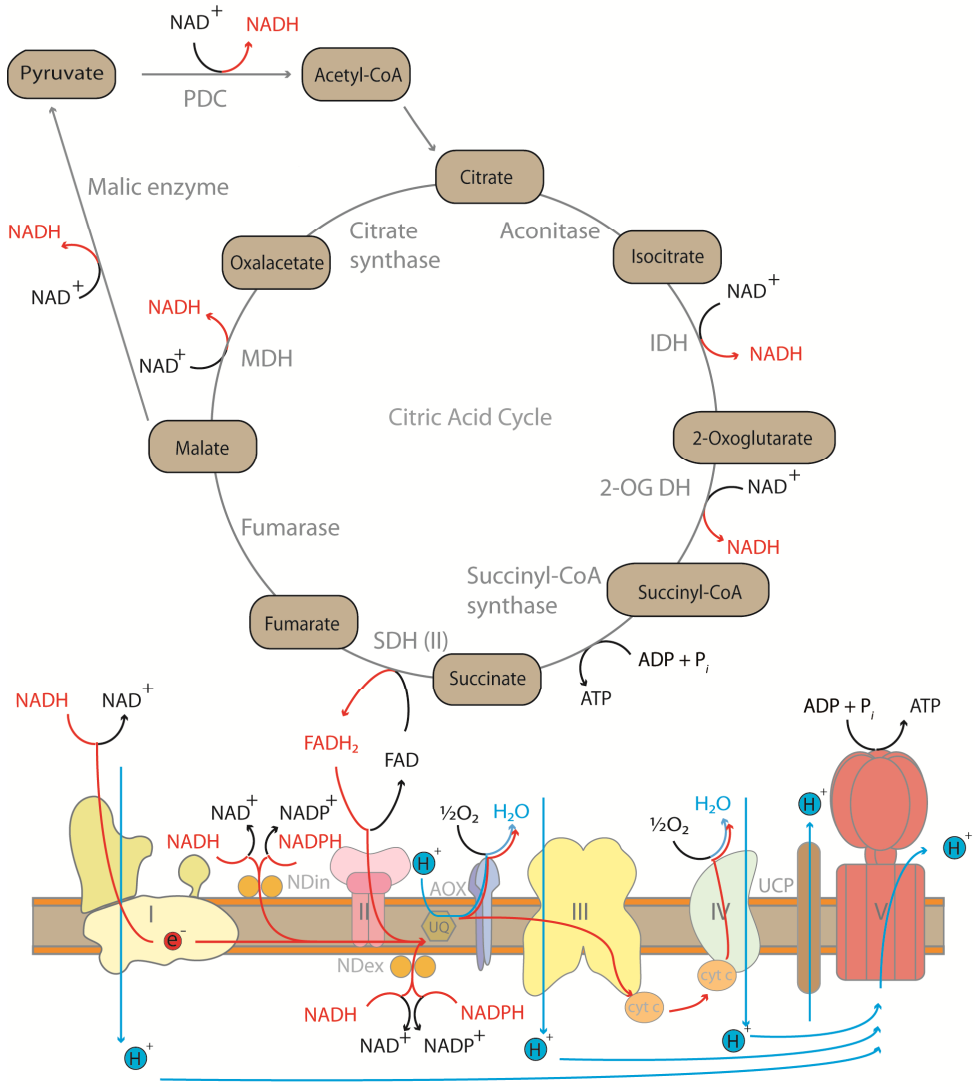

Fig. 2. Simplified scheme of the plant mitochondrial TCA cycle and respiratory chain. PDC, pyruvate dehydrogenase complex; IDH, isocitrate dehydrogenase; 2-OG DH, α-ketoglurate dehydrogenase; SDH, succinyl Co-A synthase; MDH, malate dehydrogenase; I, complex I; II, complex II; III, complex III; IV, complex IV; AOX, alternative oxidase; UCP, uncoupling protein; NDin, internal dehydrogenase; DDex, external dehydrogenase. Reducing equivalents are either depicted in red for the reduced form or in black for the oxidized form. Arrows in blue symbolize the flow of the protons and arrows in red of the electrons.

Besides the classical oxidative phosphorylation pathway, plant mitochondria contain alternative respiratory proteins such as the alternative oxidase (AOX), which participates in the electron transport chain (Moore and Siedow, 1991). The AOX exists in plants, some fungi as well as in unicellular organisms and uses electrons directly from the UQH pool to reduce

oxygen to water in order to bypass CIII without the generation of a proton gradient (Vanlerberghe and McIntosh, 1997). It is well established that AOX, with AOX1 as the most stress-induced isoform, prevents the over-reduction of the UQH pool and thereby decreases reactive oxygen species (ROS) production, especially when the plant experiences stress (Maxwell et al., 1999). Aside from AOX, plant mitochondria host additional $NAD(P)^+$ dehydrogenases along with CI, of which two are facing towards the intermembrane space and another two towards the mitochondrial matrix (Moller and Rasmusson, 1998). Compared to CI, these NAD(P)H dehydrogenases are rotenone-insensitive and they do not participate in the generation of a proton gradient. By reducing NAD(P)H and transferring electrons directly to AOX via the UQH pool, they help to avoid over-reduction of the cyt c-dependent respiratory pathway (Moller, 2001).

1.2. Mitochondrial retrograde signalling in plants

Impact of impaired mitochondria

In the case of impaired metabolic functions due to environmental stress, the communication between chloroplast, mitochondria, and the nucleus must operate in an efficient way in order to adapt to new conditions. This is important because mitochondria and chloroplasts are metabolically interdependent (Gardestrom, 1996; Hoefnagel et al., 1998; Kromer, 1995). Substrates produced by photosynthesis are necessary for mitochondrial respiration and mitochondria supply the chloroplast with carboxylic acids and other metabolites during photosynthesis. Besides the exchange of substrates, chloroplasts also depend on mitochondria in order to prevent photoinhibition by utilizing the redox equivalents arriving from the chloroplast during the day. This is mainly reported to happen with the assistance of AOX1, which exists next to the conventional cytochrome-c oxidase (COX)-dependent oxidative phosphorylation pathway (McDonald et al., 2002). It is estimated that around 60% of the mitochondrial electrons run through the AOX pathway during light, while during night the electron flux decreases (Atkin et al., 1993). It is well established that AOX1 (transcript and protein) is regulated in a retrograde dependent manner, mainly under stress conditions (Djajanegara et al., 2002; Vanlerberghe and McIntosh, 1994, 1996). Especially in terms of high light conditions AOX1 transcript levels are increased, suggesting that photoreceptors mediate light-induced AOX1 expression (Xu et al., 2011). Interestingly, the transcription factor (TF) ABI4 was identified as a repressor of AOX1 (Giraud et al., 2009). ABI4 itself was already described as a nuclear component mediating chloroplast retrograde signalling by

inhibiting light-induced expression of nuclear photosynthetic genes (Koussevitzky et al., 2007). This interplay reflects the importance of maintaining mitochondrial functions, and their impairment would have drastic effects on photosynthesis (Carrari et al., 2003; Dutilleul et al., 2003; Nunes-Nesi et al., 2005). ABI4 was the first identified downstream component of mitochondrial retrograde regulation (MRR) and until now nothing is known about the identity of mitochondrial retrograde signals (MRSs) that are directly transmitted from the mitochondria. One approach to study the mitochondrial retrograde regulation to the nucleus and crosstalk between the organelles is the comparison of transcription levels. The availability of public microarray data under various stress conditions as well as the study of mutants with mitochondrial dysfunctions offers a good tool as a research source (Leister et al., 2011; Van Aken et al., 2009). Until now, a widespread genomic analysis concerning the influence of impaired mitochondria on gene transcription was missing and was subject of publication [1].

Metabolites in mitochondrial retrograde signalling

In the last two decades deep insights into retrograde control were achieved, but mainly in regards to the plastid-to-nucleus signalling (Kleine et al., 2009; Pesaresi et al., 2007; Woodson and Chory, 2008). Several factors are believed to be involved in retrograde control, such as redox signalling, tetrapyrrole signalling, sugar signalling as well as signalling based on ROS (reviewed in Leister, 2005). ROS, which are produced during inhibited oxidative phosphorylation, are well-known stress factors in plants. As a consequence of stress-induced ROS production, the retrograde regulated AOX1 transcript is up-regulated (Maxwell et al., 2002; Millar et al., 2001; Norman et al., 2004; Vanlerberghe and McIntosh, 1994). However, the role of ROS as signalling molecules is under debate as they are either too short-lived to reach the nucleus (as it is the case of singlet oxygen), or, like hydrogen peroxide (H_2O_2) which is permeable but not confined to a particular compartment, too unspecific (Moller and Sweetlove, 2010). Interestingly, gene expression studies using the TCA cycle inhibitor monofluoroacetate as an effector molecule show the induction of AOX transcript level without increasing ROS (Umbach et al., 2012). Increased mitochondrial ROS levels can lead to the inhibition of several TCA cycle enzymes, especially by damaging proteins including aconitase (Morgan et al., 2008). A decrease in aconitase activity can then cause a reduction in the conversion of citrate to isocitrate, resulting in the accumulation of citrate, which leads to the induction of mitochondrial AOX1 transcript levels (Gray et al., 2004). For this reason, the question is posed as to whether or not ROS themselves may trigger MRR, or if it might be the increase in levels of mitochondrial organic acids such as citrate. For example, it has been

already demonstrated that metabolites are involved in gene expression changes of prokaryotes as well as eukaryotes (Sellick and Reece, 2005). Especially sugars and nitrate, which represent relevant metabolites in the plant cell, are known to regulate the expression of metabolic genes (Coruzzi and Zhou, 2001; Price et al., 2004; Stitt, 1999; Usadel et al., 2008). Several sugar-sensing pathways are reported to exist in plants, but little insight into these signalling pathways has been achieved so far (Rolland et al., 2006). One enzyme involved in sugar sensing is the hexokinase 1, which was found by characterizing mutants with altered sugar sensitivity, grown on high sugar media (Cho et al., 2006; Moore et al., 2003). Another energy-sensing kinase is the sucrose nonfermenting1-realted kinase (SNRK1) which plays a role in signalling energy and nutrient deficiency in order to sustain metabolic homeostasis (Baena-Gonzalez and Sheen, 2008). Although sugars as signalling molecules have been well demonstrated in plants, the question of whether or not other metabolites may participate in signalling pathways has become more prominent (Lancien and Roberts, 2006; Templeton and Moorhead, 2004; van Schooten et al., 2006). As previously described, intermediates of the TCA cycle represent promising candidate molecules for mediating MRR, as they reflect both the metabolic and redox status of the organelle and are known to be transported between compartments. The first investigations of retrograde signalling were performed in yeast mitochondria (Liao and Butow, 1993) in which initial evidence for TCA cycle metabolites having a role in nuclear gene expression changes was reported (McCammon et al., 2003). In the study of McCammon at al. (2003) eight different TCA cycle mutants exhibited changes in nuclear gene expression which were correlated with altered levels of citrate, oxaloacetate (OAA), succinate, and malate. In addition, it was demonstrated that in human cells citrate, succinate, fumarate, 2-oxoglutarate and the closely related metabolite 2-hydroxyglutarate (in its reduced form) all have signalling functions (Gomez et al., 2010; Hewitson et al., 2007; Wellen et al., 2009; Yang et al., 2012). Therefore, carboxylic acids and particularly citrate appear to play an interesting role in MRR, which was the objective of publication [2].

1.3. Protein posttranslational modifications connected to mitochondrial metabolism

Organellar retrograde signalling implies that a signal is released, recognized and transduced to the nucleus. As a consequence, transcriptome changes followed by proteome changes can be observed. A different mechanism to alter orgarnellar protein function depending on environmental conditions is to modify the properties of proteins which are already present via posttranslational modifications (PTMs). PTMs alter protein function and turnover by adding a chemical group to one or more amino acid residues of the protein. This process can be highly

flexible, meaning that the modification can be reversed to the initial unmodified state. Therefore, PTMs offer regulatory networks which can be a continuously fine-tuned. Several hundred different types of PTMs such as phosphorylation, ubiquitination, adenylation, ribosylation, redox modification, and acetylation have already been described to date (Deribe et al., 2010; Wold, 1981).

Redox regulation

In plants, the redox milieu is well known to alter important metabolic processes such as the Calvin cycle and starch synthesis (Buchanan, 1991). Therefore, redox regulation is a mechanism that offers the possibility for the cell to regulate the catalytic activity of many metabolic enzymes by altering the redox state of cysteine residues (Scheibe and Dietz, 2012). Inter- or intramolecular disulfide bridges in enzymes can be formed by the activity of thioredoxin (TRX) (Buchanan, 1984; Schurmann and Buchanan, 2008). TRXs themselves must be activated by reduction, which is achieved by the action of NADPH-dependent thioredoxin reductases (NTR). The interplay of these two enzymes is described as the TRX/NTR-system. Very little is known about the posttranslational regulation of TCA cycle enzymes, however in an *in vitro* analysis several enzymes including citrate synthase were identified as TRX targets (Yoshida et al., 2013). The regulation of citrate synthase depending on the mitochondrial TRX/NTR-system will be further discussed in publication [3], which also has implications for citrate as a signalling molecule.

Lysine acetylation

Besides redox regulation, another recent upcoming mitochondrial PTM is the acetylation of the ε-amino group of lysine residues on proteins (Fig. 3). Lysine acetylation can also be coupled to the activity of citrate synthase as it uses acetyl-CoA as a substrate. Lysine acetylation was discovered in the 1960s as a PTM of histone proteins regulating DNA-histone interaction as well as the interaction with several other proteins (Allfrey and Mirsky, 1964; Phillips, 1963). Histone acetylation takes place at the ε-amino-group of specific lysine residues and is of major regulatory significance. It influences transcriptional regulation by changing the interaction of transcription factors with chromatin. Lysine residues of histone tails are exposed from the core of the nucleosome and are the target of lysine acetylation and other PTMs, methylation in particular. The transfer of the acetyl group is mediated by histone acetyltransferases (HATs) and reversed by histone deacetylases (HDACs). The first protein discovered to be lysine-acetylated but not nuclear localized was alpha-tubulin of

Chlamydomonas axonemal microtubules more than 20 years ago (Lhernault and Rosenbaum, 1983, 1985a, b). From then on, the discovery of lysine acetylation on non-histone proteins increased and is now known to occur in various organisms as well as subcellular localisations in bacteria, yeast, plant, and animal cells (Choudhary et al., 2009; Finkemeier et al., 2011; Henriksen et al., 2012; Lundby et al., 2012; Melo-Braga et al., 2012; Smith-Hammond et al., 2014; Weinert et al., 2013; Weinert et al., 2011; Wu et al., 2013). Following of the discovery of the non-nuclear acetylated proteins, the names of the responsible enzymes have been changed to lysine acetyltransferases (KATs) and lysine deacetylases (KDACs) (Allis et al., 2007) (Fig. 3). Acetylation can also change the protein properties of non-histone proteins by masking the positive charge of the lysine residue. This can impact on the biochemical functions as well as the catalytic activity, protein-protein and protein-DNA interactions of the traget protein. In higher plants, lysine acetylation has only recently been discovered also to occur on non-histone proteins (Finkemeier et al., 2011; Wu et al., 2011). For example, subunits of the plastid encoded ATP synthase and the large subunit of ribulose 1, 5-bisphosphate carboxylase/oxygenase (RuBisCO) in chloroplasts were shown to carry lysine acetylated sites, demonstrating that acetylation occurs in the organelle and not before protein import. The acetylation of RuBisCO was shown to decrease its activity in *in vitro* experiments (Finkemeier et al., 2011). Apart from this, the relevance of lysine acetylation as well as its regulatory functions is almost completely unknown, although its potential regulatory role is of great interest for future investigations. Compared to other organisms little is known about lysine acetylation in plants, especially in respect to mitochondria. Finkemeier et al. (2011) discovered only seven mitochondrial proteins to be lysine-acetylated. This number is suprisingly low considering all TCA cycle enzymes that were found to be lysine-acetylated in organisms such as bacteria and human (Rardin et al., 2013; Wang et al., 2010). The identification of lysine-acetylated proteins in plant mitochondria was investigated in publications [5] and [6].

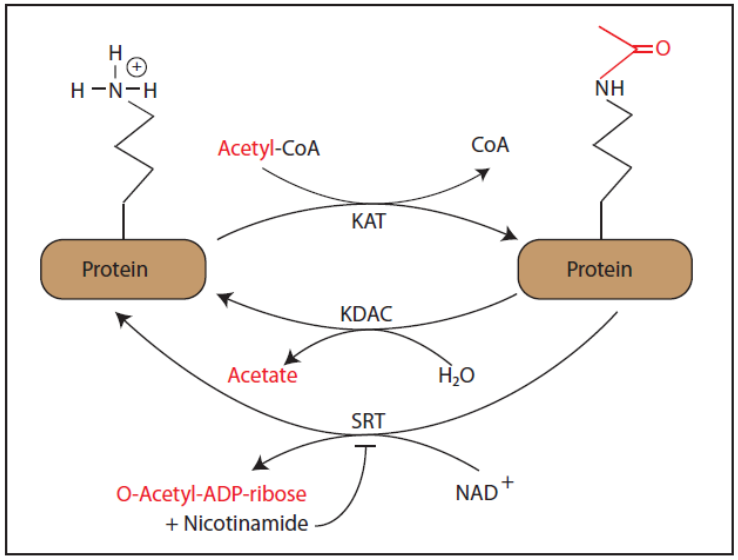

Fig. 3. Scheme of enzyme-dependent lysine acetylation and deacetylation. KAT, lysine acetyltransferases; KDAC, lysine deacetylase; SRT, Silent Information Regulator1 homolog. KATs transfer an acetyl group from acetyl-CoA onto a lysine residue by releasing CoA. KDACs remove the acetyl group by producing acetate. SRTs belong to different class of lysine deacetylases which use NAD^+ as a co-factor to remove the acetyl group from the lysine residue by producing O-acetyl-ADP ribose and nicotinamide. Nicotinamide inhibits SRT activity.

Regulators of lysine acetylation

As mentioned before, lysine acetylation of proteins is regulated by KATs and KDACs which catalyse the reversible reaction of lysine acetylation. This occurs by transferring an acetyl moiety from acetyl-CoA onto a ε-amino-group of a lysine side chain and by releasing CoA-SH. The reverse reaction is catalyzed by KDACs, which remove the acetyl group by the production of acetate (Fig. 3). In *Arabidopsis*, little is known about the action of KATs and most of what is known is related to histone acetylation. KATs are categorized into A and B type of enzymes depending on their nuclear or cytosolic localization (Chen and Tian, 2007). By sequence homology at least 12 KATs were identified in *Arabidopsis* to date (Earley et al., 2007; Pandey et al., 2002; Servet et al., 2010). Concerning KDACs, 18 members of putative histone deacetylases have been described in *Arabidopsis* (Pandey et al., 2002). Non-nuclear localized deacetylases are mainly described for the group of sirtuin (SIRT) family of NAD^+-dependent deacetylases (Blander and Guarente, 2004). The SIRT family in humans includes nuclear-, cytosol-, and mitochondria-localized members (North et al., 2003; Schwer et al., 2002). Besides the sirtuins, other KDACs are suspected to be non-nuclear proteins such as HDAC5, HDAC8 and HDAC14, which are believed to be expressed in the cytosol, chloroplasts or mitochondria. Sirtuins are named after the silent information regulator 2 (Sir2) in yeast and are highly conserved across species from bacteria to humans (Frye, 2000). They

play an essential role in regulating lysine deacetylation in several different compartments and are associated with lifespan extension in yeast, nematodes, and flies (Rogina and Helfand, 2004; Sinclair and Guarente, 1997; Tissenbaum and Guarente, 2001). As sirtuin activity depends on the presence of NAD^+ as a co-factor, they are discussed as likely candidates in regulating metabolic states of the cell. Together with NADH as a counterpart, NAD^+ is responsible for maintaining the redox balance in the cell. During the deacetylation reaction of sirtuins NAD^+ and the acetyl moiety are converted into nicotinamide and 2′-*O*-acetyl-ADP-ribose (Fig. 3). Based on phylogenetic analysis, sirtuins can be divided into five groups, I-IV and U, whereas group U is just appearing in Gram-positive bacteria (Frye, 2000). Mammals express seven sirtuin proteins (SIRT1-7) which display diverse functions and cellular localizations. While SIRT1, SIRT6 and SIRT7 are mainly localized in the nucleus, SIRT2 is of cytoplasmatic localization. Interestingly, SIRT3, SIRT4 and SIRT5 are targeted to the mitochondria, executing different catalytic reactions, with SIRT3 as the main mitochondrial deacetylase. The Arabidopsis genome encodes just two sirtuin-type genes belonging to two different classes: silent Information Regulator1 homolog (SRT1; At5g55760) from class IV, and SRT2 (At5g09230) from class II (Pandey et al., 2002). While SRT1 is believed to be localized in the nucleus, SRT2 has a predicted mitochondrial localization. Until now, nothing was known about the activity or any function of plant sirtuins. Therefore, it was our goal to investigate the function of the predicted mitochondrial class II sirtuin SRT2 of Arabidopsis which was addressed in publication [5].

2. Summarizing Discussion

2.1. Dysfunctions in mitochondria result in transcriptional changes of distinct metabolic and regulatory pathways

Mitochondria play a central role in the energy metabolism in animals as well as in plants. Therefore the organelle has to be highly flexible in order to adapt to the changing environmental conditions. Upon environmental stress conditions, plant mitochondrial function can be disturbed and the interplay between metabolic pathways, different organelles, as well as signalling networks will be affected. To restore metabolic functions, a MRS has to be sent to the nucleus to regulate gene transcription to control the levels of required proteins. The AOX1 protein is a well-known read out marker for MRR and is induced in the case of mitochondrial dysfunction, for example after antimycin A (AA) as well as rotenone treatment (Clifton et al., 2005; Vanlerberghe and McIntosh, 1997). However, the overall effect on gene transcription concerning mitochondrial impairment has been largely unknown until now. Therefore, in publication [1], transcriptomic analyses after several impairments of mitochondrial proteins were performed. Eight different published transcriptomic datasets and three unpublished datasets of our own were compared and analyzed. In our study, transcriptional consequences of the following impairments within the mitochondria were examined: (I) CI mutants (*ndufa1*, *ndufs4*) which were affected in CI protein abundance and the inhibition of CI by rotenone (Clifton et al., 2005; Meyer et al., 2009). (II) AOX mutant (*aox1a*) which had no immunodetectable AOX protein (Giraud et al., 2009). (III) CIII was inhibited by AA. (IV) CV mutants which express the unedited form of the CV subunit 9 in *Arabidopsis* flowers under the control of APETAL 3 and A9 promoter (*AP3-uATP9*, *AP9-uATP9*) and oligomycin treatment which inhibits CV (Busi et al., 2011) (V) mitochondrial DNA mutants (*msh1×recA*) which exhibit compromised recombination surveillance of the mitochondrial genome (Shedge et al., 2010). (VI) Loss of mitochondrial superoxide dismutase by inducible RNA (*msd1*). (VII) Peroxiredoxin-II F knockout mutant (*prxII F*) (Fig. 4).

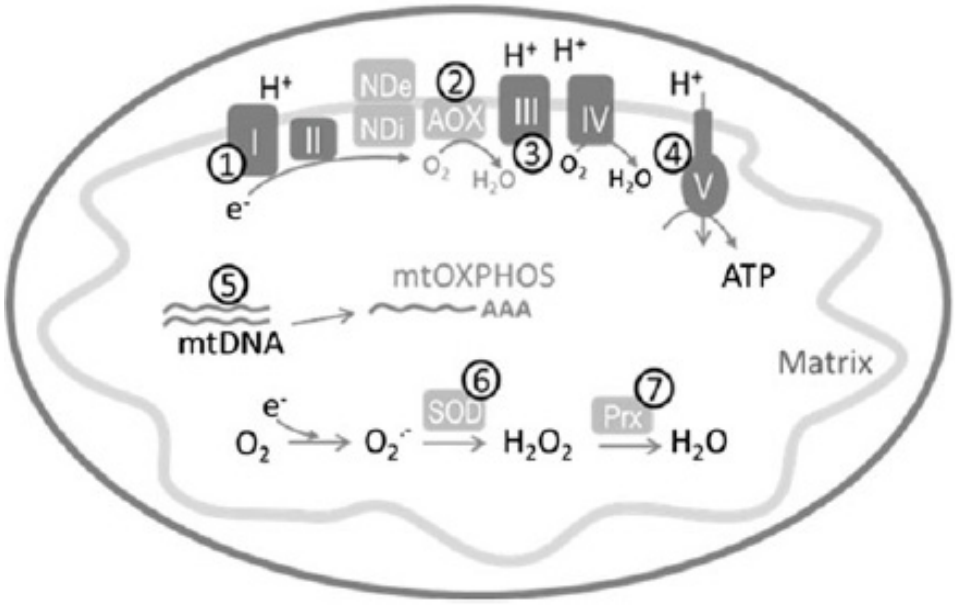

Fig. 4: Overview of microarray experiments dealing with mitochondrial impairments. Numbers depict treatments or mutations affecting mitochondrial targets. (1) Complex I: *ndufa1*, *ndufs4*, and rotenone. (2) AOX: *aox1a*. (3) Complex III: antimycin A. (4) Complex V: *AP3-uATP9*, *AP9-uATP9*, and oligomycin, (5) mtDNA: *msh1×recA*. (6) MnSOD: *msd1*. (7) PeroxiredoxinII F: *prxII F*. (publication [1], Fig. 1).

On the one hand, the transcriptomic datasets included stable mutants which can most likely display pleiotropic or acclimation responses, and on the other hand transient inhibitor treatments of mitochondrial complexes. The overlap of regulated genes between all treatments and mutants is intended to reflect the actual changes in transcript levels caused by mitochondrial impairment. Details of transcriptional changes concerning CI, CII, AOX, CIII, CV, mtDNA, and ROS are discussed in publication [1]. In conclusion, this study points out that MRR triggered by impairment of mitochondria mainly affects three categories of genes coding for proteins with the following functions: protein synthesis, photosynthetic light reactions, and plant pathogen defense (Fig. 5).

With respect to protein synthesis, two different effects have been discovered between chemical treatment and stable mutants. Whereas treatment with AA, rotenone, and oligomycin induced a down-regulation of transcripts involved in protein synthesis, the stable mutants like *ndufa1*, *ndufs4, msh1×recA, msd1,* and *aox1a* caused an up-regulation ([1] Fig. 2). This suggests that acute mitochondrial impairment by chemical treatments lead to signalling events which cause down-regulation of protein synthesis, whereas acclimated stable mutants show compensation reactions and an accumulation of protein synthesis transcripts.

In seven data sets, genes of the photosynthetic light reactions showed a significant down-regulation of transcripts, but an opposite trend in the *aox1a* mutant ([1] Fig. 3). This is

remarkable as AOX1 is known to be retrograde-regulated, especially under stress conditions (Djajanegara et al., 2002; Vanlerberghe and McIntosh, 1994, 1996). The opposite effect on photosynthetic gene-transcription supports the hypothesis that AOX itself is not only a marker transcript for MRR, but is also involved in MRR itself. It seems that signals which are usually transmitted due to the presence of AOX cause a down-regulation of photosynthetic genes, and in the *aox1a* mutant these signals are absent leading to an up-regulation of photosynthetic transcripts. In *Chlamydomonas reinhardtii* for example, the inhibition of the mitochondrial electron transport chain by AA showed an inhibition of psaE mRNA, and the AOX inhibitor SHAM resulted in an up-regulation of psaE transcription (Matsuo and Obokata, 2006). This indicates that the flux through the conventional COX-dependent oxidative phosphorylation pathway and the AOX-dependent alternative pathway might transmit different MRS.

As a third functional category, we discovered gene expression changes related to pathogen defense. Recently, a link between mitochondrial function and pathogen defense was demonstrated in the non-responding to oxylipins (*noxy*) mutants. The *noxy* mutants were found as unknown mitochondrial proteins with increased AOX1a expression, and which formed mitochondrial aggregates. Due to the fact that MRR is impaired, they show increased sensitivity to *Pseudomonas syringae* infection which is reflected by a decreased activation of salicylic acid-responding genes (Vellosillo et al., 2013).

In this study, we defined ten transcripts showing orchestrated regulation in terms of stress conditions which can be considered as general mitochondrial stress marker genes ([1] Tab.3). Strikingly, one of the ten marker genes, NAC domain protein 13 (*ANAC13*, At1g32870) has recently been identified together with ANAC016, ANAC017, ANAC053, and ANAC078 to bind a specific cis-element found in MRR-regulated genes (De Clercq et al., 2013). ANAC13 triggers increased oxidative stress tolerance by binding to a mitochondria dysfunction related cis-element, thereby inducing MRR genes. Hence, ANAC13 was identified as a TF mediating MRR. The fact that ANAC13 was found in our transcript analysis before the function was investigated proves the scientific relevance provided by the meta-analysis. Another interesting marker gene is At2g41380, which codes for an embryo-abundant protein-related protein which has predicted SAM-dependent methyltransferase activity (SAM-MT). SAM-MT was already identified as a mitochondrial stress defense marker gene in earlier studies (Van Aken et al., 2009). Interestingly, we also discovered that SAM-MT transcript levels are increased after citrate treatment, a phenomenon which was investigated in more detail in publication [2]. The function of the other marker transcripts in MRR is unclear so far, but candidates such as the protein phosphates 2C will be interesting for future investigations.

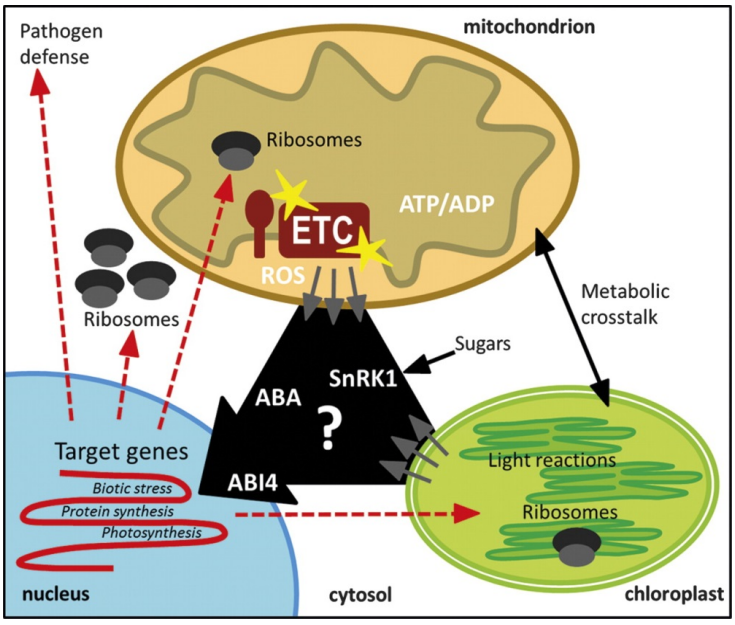

Fig. 5: Schematic representation of the working model for mitochondrial retrograde signalling triggered by various respiratory impairments. An orchestrated regulation of transcriptional read-out markers was found for the functional categories 'light reactions', 'protein synthesis', and 'plant–pathogen interactions' (depicted in red). The actual key players and components in the mitochondrial retrograde signalling pathway are still unknown and might involve known ABA, ROS, and energy signalling pathways (depicted in white). The transcription factor ABI4 is a known target of retrograde signalling from mitochondria and plastids (Giraud et al., 2009) (publication [1], Fig. 4).

2.2. Carboxylic acid treatment results in distinct changes of nuclear transcripts

As previously described, mitochondrial dysfunction leads to overall changes in the transcriptome. These changes are believed to be derived from MRS which carry information about the mitochondrial metabolic status and cause transcriptional changes within the nucleus. Nothing is known about the type of information transduced between mitochondria and nucleus. Some known key players in retrograde control are abscisic acid (ABA) and ROS, as well as energy signalling pathways mediated by sugars (reviewed in Leister et al., 2005). Carboxylic acids represent good candidates to mediate MRR as they originate from mitochondria and can easily be transported between compartments, but they also reflect the metabolic state of mitochondria. In publication [2], carboxylic acids were investigated as putative MRS in a transcriptome analysis with the main focus on citrate. Until now, no comparative analysis was performed in plants, therefore we investigated the effect of citrate and other organic acids on transcriptional regulation in *Arabidopsis* leaves.

For a more comprehensive view as to what extent transcript levels are changed after carboxylic acid treatment, we selected citrate and malate to perform whole transcriptome microarray analysis. In general, a wide range of transcriptional changes were observed with

very little overlap between the two carboxylic acids ([2] Fig. 1). Hence, we concluded that malate and citrate might convey different information within the cell. One possible explanation is that citrate and malate have different chemical properties as well as cellular functions. Citrate, for example, is of great importance for chelating iron molecules which in their free form are highly toxic for the cell (Haydon and Cobbett, 2007). Likewise, in human cells it was reported that citrate is also involved in the regulation of gene expression because cytosolic citrate can be converted into acetyl-CoA, which is important for histone acetylation and thus transcriptional regulation (Wellen et al., 2009). Malate, on the other hand, is involved in stomata closure and indirectly transfers reducing equivalents from chloroplast to mitochondria under high plastidic NADPH/$NADP^+$ levels (Heineke et al., 1992; Scheibe, 2004). Considering these facts, it is of great interest that malate showed a slight but significant up-regulation of photosynthetic transcripts in general, whereas citrate treatment caused the opposite effect. This could be due to different signalling functions concerning their specific role in the plant cell. The fact that many genes encoding metabolic proteins were affected indicates that citrate abundance is involved in feedback control. Our data suggest that the cell uses different organic acids depending on the energy and nutrient status to communicate different metabolic signals to the nucleus, which then result in distinct alterations of transcript levels. Because of the striking expressional changes after citrate treatment we performed the following experiments mainly based on citrate as an effector molecule.

As citrate showed the strongest influence on transcript levels, we selected 18 marker transcripts and validated the citrate effect by quantitative real-time (QRT)-PCR. The inductive or repressive response of citrate on the marker genes could be confirmed and further time- and concentration-dependent effects on gene expression were revealed ([2] Fig. 2). By gas chromatography-mass spectrometry (GC-MS)-based metabolite profiling we confirmed that down-stream metabolites of citrate were not affected, however increased sugar levels were detected upon citrate treatment ([2] Fig. 3). In general, it is difficult to demonstrate that a particular metabolite is the actual signalling molecule because of the downstream metabolites that also affect signalling. For example, one method which was used to prove that sugars act as signalling metabolites was to use non-metabolisable sugar analogues (Jang and Sheen, 1994). Also in *Anabaena* it was demonstrated for example that 2-oxogluteric acid (2-OG) is not just a key player in the TCA cycle but is as well involved in sensing nitrogen starvation (Bastet et al., 2010; Chen et al., 2006). To demonstrate that 2-OG itself acts as signalling molecule and not further downstream metabolites, a non-metabolisable 2-OG was used. Additionally it was shown that the two carboxylic acid terminals and the 5 carbon atom of the

synthesized non-metabolisable 2-OG were both essential for signalling function (Wang et al., 2014). To prove the specific effect of citrate, we selected tricarballylate as an analogue (Fig. 6).

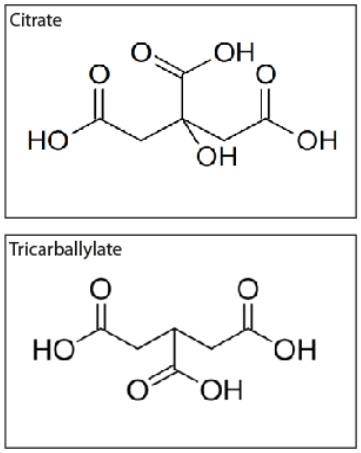

Fig. 6: Chemical structure of citrate (2-hydroxypropane-1,2,3-tricarboxylic acid) and tricarballylate (propane-1,2,3-tricarboxylic acid). Citrate has an additional hydroxyl group which might a pivotal role in citrate signalling.

Tricarballylate has similar properties as citrate and can be transported between cells, but it cannot be metabolized (Wolffram et al., 1993). Therefore, we treated WT leaf slices with either 10 mM citrate or tricarballylate for 4 h and analyzed some of the marker genes by QRT-PCR ([2] Fig. 5). Citrate and tricarballylate treatments resulted in similar transcriptional response, although tricarballylate was slightly less efficient in the extent of the transcript change. The stronger effects in transcript abundance after citrate treatment could either derive from downstream metabolites or it is also possible that tricarballylate is not that well-perceived by a putative citrate-sensor due to its slightly different structure. The second hypothesis is more likely as no changes in metabolite contents were observed after tricarballylate treatment which indicates that the properties of the molecule itself are enough to induce transcriptional changes and it can be assumed that a specific citrate-binding protein might exist. In agreement with this, a tricarboxylate chemoreceptor McpS (for methyl-accepting chemotaxis receptor protein) in bacteria was found to be activated by citrate. However, neither isocitrate nor tricarballylate were able to activate the receptor indicating that the hydroxy group is involved in protein binding and recognition of McpS (Lacal et al., 2010). To gain further insight into citrate signalling and the effects on transcription we compared our microarray data with publicly available microarray data sets by using genevestigator ([2] Fig. 6). A high degree of similarity in transcript levels was detected for biotic stress responses, especially after *Pseudomonas syringae* infection or flagellin 22 treatment. This is of great interest because citrate has an inhibitory effect on gram-negative bacteria by destabilizing their plasma membrane (Boziaris and Adams, 1999; Vaara, 1992). Thus, citrate

could feed into the signalling response regarding pathogen defense. Besides the influence on pathogen-related transcripts, the cluster analyses also revealed an impact on gibberellin (GA) regulated genes. To further investigate the role of citrate within plant hormone signalling, several mutants with defects in hormone signalling pathways that convey signals derived from GA, jasmonic acid (JA), salicylic acid (SA), and brassinosteroid (BR) were analyzed ([2] Fig. 7). Most significant changes in transcript abundance of our marker genes after citrate treatment were observed in the *bak1* (*elg*; brassinosteroid hypersensitive; (Whippo and Hangarter, 2005) mutant background and in the *quadruple DELLA* (*qDELLA*; relief of growth repression, methyl jasmonate, and GA insensitive; (Cheng et al., 2004; Navarro et al., 2008) mutant. In future studies it has to be investigated if citrate acts as a signalling molecule that interferes with signalling pathways of BR and GA.

Marker transcripts and their response to carboxylic acids

As explained above we selected 18 marker transcripts that responded to altered citrate levels ([2] Table 1.) to test their response to carboxylic acids and in different mutant backgrounds. In the following section the four most important marker transcripts *CI1, FER1, SAM-MT* and *OEP16-1* (Table 1) will be discussed in more detail with respect to their function.

Table1. List of marker transcripts responding to citrate. Arrows indicate the up or down-regulation of transcripts levels after 10 mM of citrate treatment for 4 h analysed by QRT-PCR ([2] Fig. 2).

Identifier	Short description	Description	Function	Citrate 10 mM 4h
At1g73120	CI1	*CITRATE-INDUCED1*	Unknown function	↑
At5g01600	FER1	*FERRITIN1*	iron homeostasis	↑
At2g41380	SAM-MT	*SAM-DEPENDENT METHYLTRANSFERASE*	Unknown function	↑
At2g28900	OEP16-1	*OUTER-ENVELOPE PROTEIN16-1*	Shuttling of amino acids across the outer envelope of the plastid and pre-protein transport of the PORA	↓

The marker genes were chosen from the regulated transcripts which showed a more than 2-fold change after citrate treatment.

CI1 showed the highest up-regulation after citrate treatment and was induced in a time- and concentration-dependent manner reaching the highest transcript levels with a treatment of

10 mM citrate and 8 h incubation (about 15-fold; $\log_2 = 3.89$) ([2] Fig. 2). Additionally, CI1 transcript levels were analyzed after treatment with different carboxylic acids and sugars ([2] Fig. 4) to investigate the specificity of citrate. Especially CI1 showed a highly selective induction of transcript levels after citrate treatment and a down-regulation for all other organic acids tested, even for isocitrate, which is very similar to citrate. These findings demonstrated that citrate signalling is unique compared to other organic acids. The non-fermentable citrate analogue tricarballylate induced transcript levels of CI1 as well, although to a lesser extent ([2] Fig. 5). Because of the strong inductive effect of citrate on CI1 transcript level it would be of great interest to learn more about this unknown protein in the future and whether it has a function in citrate signalling.

Besides CI1, FER1 was also increased more than 2-fold after citrate treatment. Ferritins are key players in complexing free iron and their transcript levels increase in conditions of high iron concentration. (Briat and Lebrun, 1999; Briat and Lobreaux, 1998; Lobreaux et al., 1992). The transcript levels of FER1 showed similar patterns in comparison to CI1. FER1 induction after citrate treatment is of great interest because ferritins play an essential role in cellular iron homeostasis. Recently, it was demonstrated that ferritins are involved in protecting cells from ROS production (Ravet et al., 2009). This finding is also interesting in respect to the fact that oxidative stress also leads to a rise in citrate levels (Gupta et al., 2012; Lehmann et al., 2009; Morgan et al., 2008; Vanlerberghe and McIntosh, 1994). Ferritins and citrate have a remarkable overlap in function as they are both capable of chelating iron. It can therefore be speculated whether citrate not only plays a role in regulating iron homeostasis by acting as a chelator, but also as a MRS which activates iron responsive genes.

While FER1 represents an iron stress-related gene we also discovered another stress responsive gene, SAM-MT, as a general marker gene of mitochondrial stress which was already described in publication [1] as well as in Van Aken et al., 2009. SAM-MT is up-regulated after citrate treatment in a time- and concentration-dependent manner. Unlike CI1, whose transcript levels are specifically altered only after citrate treatment, isocitrate and sugars can also induce the transcript accumulation of SAM-MT ([2] Fig.4). However, SAM-MT transcript levels were elevated in the same amount after tricarballylate as after citrate treatment ([2] Fig. 5). The mechanism behind SAM-MT transcriptional induction and what role this protein plays in MRR will be of great interest for our understanding of the regulatory mechanisms of MRR.

Citrate treatment did not only cause an up-regulation of transcripts. We also chose the marker transcript OEP16-1, which showed a significant down-regulation of transcript levels. The

regulation of OEP16-1 transcription following treatment with other organic acids was more variable, showing an up-regulation after sugar treatment and a down-regulation after citrate, acetate, and OAA treatment. OEP16-1 is located in the plastid envelope membrane and two putative functions were reported for it: shuttling of amino acids across the outer envelope of the plastid and involvement of pre-protein transport of the protochlorophyllide oxidoreductase A (PORA) which is under debate (Philippar et al., 2007; Pohlmeyer et al., 1997; Pollmann et al., 2007; Pudelski et al., 2012). OEP16-1 is the major isoform in *Arabidopsis* leaves and early embryo development, whereas the second isoform OEP16-2 is mainly expressed in late seed development and is highly responsive to ABA. In contrast, ABA treatment in embryos exhibited a 2-fold down regulation of OEP16-1 transcription (Pudelski et al., 2012). Strikingly, citrate treatment in the ABI4 mutant still causes a decrease in OEP16-1 transcription. Therefore, citrate and ABA seem to operate in two different signalling pathways which reduce OEP16-1 transcription.

2.3. Correlation between MRR and citrate-dependent transcriptional changes

In publication [1] the general transcriptional response after mitochondrial impairment was investigated and three main pathways were found to be affected: protein synthesis, pathogen defense, and photosynthetic light reactions (Fig. 5). By comparing these results with the insights we achieved in publication [2], it becomes clear that the transcriptional response after mitochondrial impairment and citrate treatment do overlap in several categories. The MapMan analysis of citrate treatments also revealed significant regulation of the functional categories: protein synthesis, biotic stress, synthesis, and cell wall synthesis ([2] Supplemental Table S2).

Nuclear-encoded transcripts of protein synthesis represent one category that was discovered to be regulated after mitochondrial impairment and also after citrate treatment. As previously explained in terms of mitochondrial dysfunction, a general orchestrated down-regulation of transcripts involved in protein biosynthesis was observed for the short-term inhibition experiments (AA, rotenone, and oligomycin), whereas the stable mutants showed a general up-regulation, which could be part of the acclimation response ([1] Fig. 2). The expressional pattern for the *ndufa1* mutant was slightly different compared to the other stable mutants showing an up-regulation in mitochondrial ribosomal transcripts and a down-regulation in plastidic ribosomal transcripts (Fig. 7 A). Transcriptional changes after citrate treatment are similar to those observed in the *ndufa1* mutant (Fig. 7 A). By comparing general changes in gene expression an overlap of 392 transcripts can also be discovered, which represents more

than 50% of all regulated transcripts observed after citrate treatment (Fig. 7 B). Meyer et al. (2009) already reported on induced organic acids contents in the *ndufa1* mutant. This may derive from the higher flux through glycolysis and the TCA cycle to compensate lowered ATP production from the OXPHOS. Also, the formation and dissociation of supercomplexes (SC) has recently been discussed to have effects on metabolic switches to either favour biosynthetic pathways or energy producing pathways (Genova and Lenaz, 2014; Lapuente-Brun et al., 2013). Thus, an orchestrated transcriptional regulation after citrate treatment and in the *ndufa1* mutant can be explained by the induction of organic acids due to the loss of CI which feeds into MRS. It will be interesting to learn more about the interplay between the loss of CI and citrate signalling in the future.

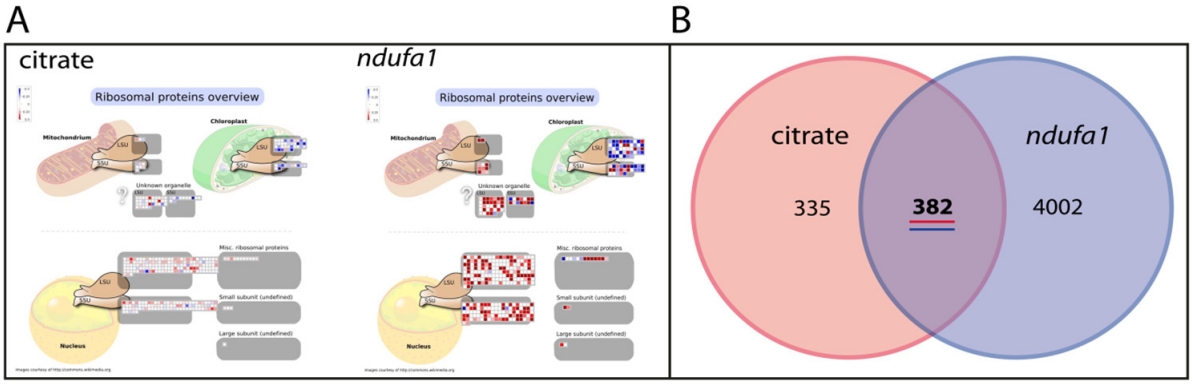

Fig. 7: Comparison of gene expression response after citrate treatment and in the *ndufa1* mutant. (A) Regulated transcripts of the functional group 'ribosomal proteins' in response to citrate treatment and mitochondrial impairment. The display has been adopted from the MapMan software. Boxes represent individual transcripts, and blue and red indicate up- and down-regulation, respectively (log2 ratios). (B) Venn diagram of significantly regulated transcripts detected in citrate and *ndufa1* microarrays. A total of 717 and 4384 transcripts were significantly regulated by a threshold of 0.3 according to MapMan analysis. A significant overlap of 382 transcripts was detected under both conditions.

Transcripts encoding for photosynthetic light reactions were as well not only regulated after mitochondrial impairment, but also after citrate treatment causing a general down-regulation of transcripts (Fig. 8). In a further step it would be important to reveal if the different mutants and chemically treated plants used in publication [1] also show differences in organic acid levels, especially citrate. As discussed before, the only mutant that showed an up-regulation in photosynthetic transcription was *aox1a*. The AOX transcript and protein was previously shown to be up-regulated after citrate treatment in tobacco (Gray et al., 2004). It would be interesting to reveal if the *aox1a* mutant still shows the same changes in transcript levels after citrate treatment or if citrate signalling is impaired in the mutant. As described earlier, the

AOX1 promoter was used as a read-out marker for MRR in a forward genetic screen to identify mutants with impaired AOX transcript induction. These mutants were named *regulators of alternative oxidase1a (rao)*. A membrane bound NAC TF (ANAC017) was found to be a regulator for MRR. ANAC017 is localized in the endoplasmatic reticulum and after inhibition of CIII by AA treatment, a rhomboid protease is activated and cleaves ANAC017, which can then migrate to the nucleus and activate *AOX1* expression (Ng et al., 2013). In future experiments the *roa* mutants could be used to see if the AOX promoter is still induced after citrate treatment, and if not, it is very likely that citrate has similar effects on signalling as AA or maybe even leads to the same signalling pathway activating the rhomboid protease.

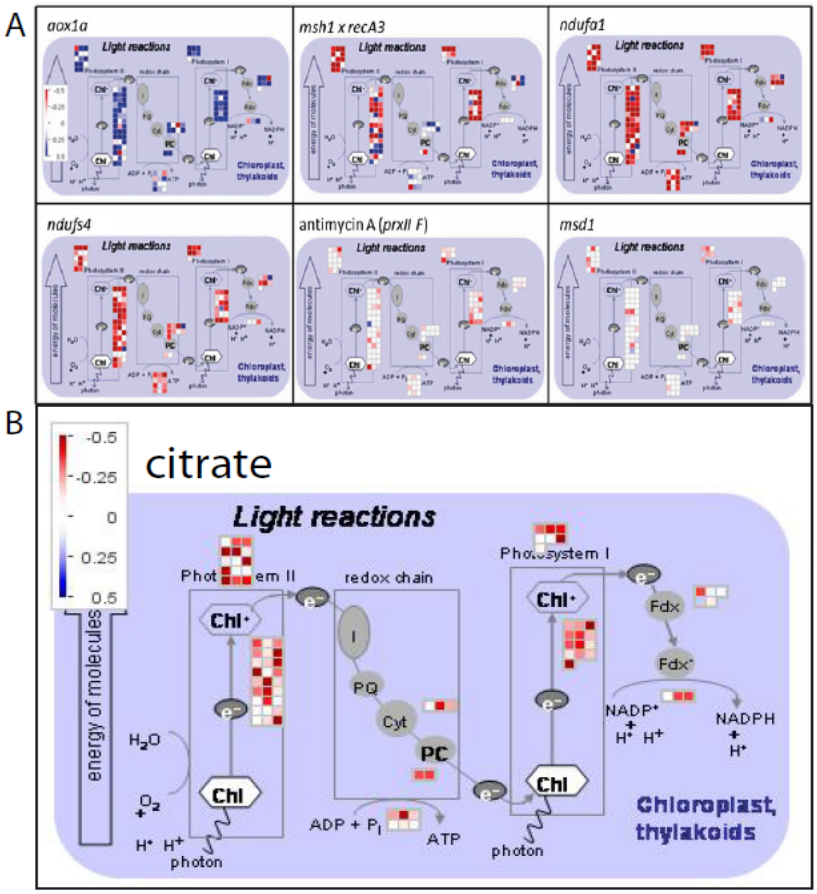

Fig. 8: Regulated transcripts of the functional group 'photosynthetic light reactions' in response to (A) mitochondrial impairments ([1] Fig. 3) and (B) after citrate treatment. The display has been adopted from the MapMan software. Boxes represent individual transcripts, and blue and red indicate up- and down-regulation, respectively (log2 ratios).

2.4. Redox regulation of mitochondrial citrate synthase

Our previous results indicate that the regulation of intracellular mitochondrial citrate levels might be important in the activation of MRR. Therefore, we were interested to understand how citrate synthase (CS) activity is regulated. CS catalyzes the first committed step in the TCA cycle to form citrate using acetyl-CoA and OAA. Not much is known about how CS

activity is regulated in mitochondria. One hypothesis is that activity of CS depends on the nutrient status which is reflected by the redox milieu of the cell. In mitochondria the redox state is determined by the ratio of $NAD(P)^+$ to NADPH. The AOX is one good example for being regulated in a redox-dependent manner. The TRX/NTR-system is able to reduce a disulfide bridge in the AOX dimer, activating the enzyme (Gelhaye et al., 2004). Likewise, the CS was discovered as an *in vitro* TRX-target (Yoshida et al., 2013) which therefore offered a great starting point to investigate the redox regulation of CS. The *Arabidopsis* CS (CS4) contains six cysteine residues in total and we were interested in their possible role in redox-regulation. As CS4 was just characterized by sequence homology until now, we first confirmed the enzymatic activity of CS4 ([3] Fig. 2). Like the pig heart CS, CS4 forms also dimers around 100 kDa but as well higher molecular weight complexes of up to 1000 kDa ([3] Fig. 3). This could be either due to CS4 multimers or a transient interaction with high molecular weight complexes from the respiratory chain. An interaction between CS and electron transport chain (ETC) complexes has not been verified in plants yet, but by 2D-BN-PAGE we demonstrated that CS4 was also detected around 1000 kDa which co-migrates with the molecular weight of free CI ([3] Fig. 3 A). Interestingly, CI is also supposed to be redox regulated and contains targets of glutaredoxins and TRXs further discussed in publication [4] (Balmer et al., 2004; Rouhier et al., 2005; Yoshida et al., 2013).

To investigate the redox regulation of CS4, we mutated all present cysteine residues by site-directed mutagenesis into serine. The six different CS4 variants are referred to as Cys108, Cys209, Cys325, Cys365, Cys439, and Cys467 ([3] Fig. 1). Activity measurements were performed to investigate the importance of each cysteine for the enzyme activity. Strikingly, Cys108 and Cys325 had a very low activity compared to CS4, and Cys365 which is the most conserved cysteine, showed an activity reduction of 60%-80% ([3] Fig. 4). By addition of H_2O_2 to oxidize the protein, CS4 activity could be reduced by half. Interestingly, no further inhibition was observed for Cys108 and Cys325. In contrast, Cys365 showed a fourth less activity after H_2O_2 treatment. As TRX was identified as an *in vitro* interaction partner (Yoshida et al., 2013), we investigated TRX-dependent activation of the different CS4 variations. CS4 itself showed an activity increase of eight times in the presence of TRX and also Cys108 and Cys325 exhibited activation. Only Cys365 showed very little induction of activity ([3] Fig. 4). To further confirm the TRX interaction, we used a mutated *E.coli* TRX (TRXi) (further explanation see publication [3]) which forms stable interactions with the target protein. CS4, Cys108 and Cys325 variably bind TRXi while Cys365 does not show any

interaction ([3] Fig. 5). By summing up all these results we propose the following model (Fig. 9):

Cys325 forms an intermolecular disulfide bridge leading to dimer formation whereas Cys108 and Cys365 form an intramolecular disulfide bridge under non-reducing conditions. The disulfide-dependent dimer represents the inactive state of CS. Activation is followed by TRX, which releases the dimer formation and offers the enzyme to re-fold. Compared to the inactive state, the active enzyme of CS4 is also a dimer but it is not disulfide-dependent. Thus, in the future it would be interesting to investigate if the different redox states occur *in vivo* and regulate citrate levels in the cell. Redox signalling is already known to be involved in chloroplast retrograde signalling (Leister, 2005; Pfannschmidt et al., 2001) and for future experiments it would be interesting to find out if citrate signalling is downstream and dependent on redox signalling in the first place.

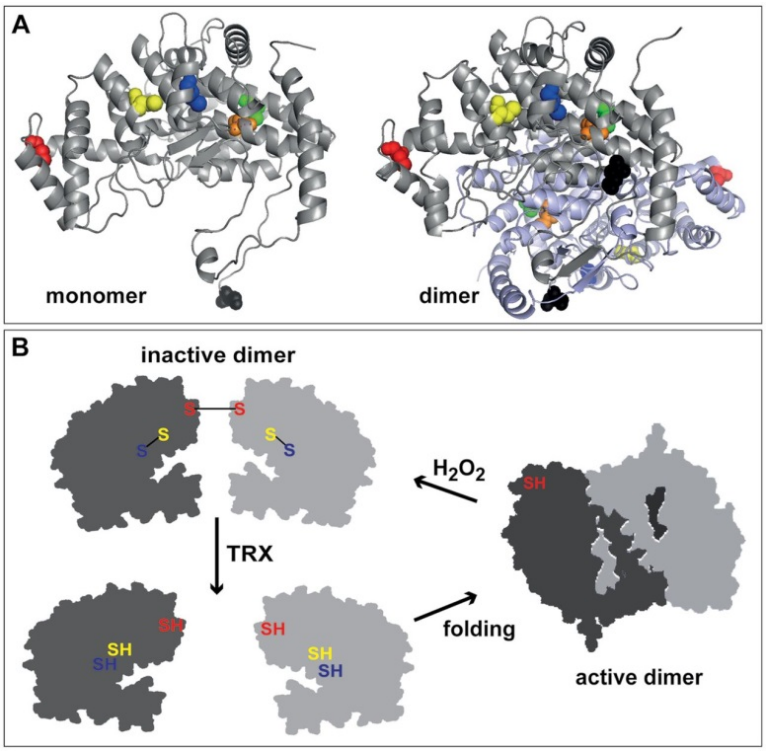

Fig. 9: Scheme of redox regulation of *Arabidopsis* citrate synthase. The oxidized form of citrate synthase forms mixed disulfides. An intermolecular disulfide bridge between Cys325 (red) is formed. Additionally, Cys108 (blue) and Cys365 (yellow) can form an intramolecular disulfide bridge next to others. In the presence of TRX, the disulfide bonds are reduced and the active dimer which is independent on disulfides can be formed. Oxidants like hydrogen peroxide can again lead to an inactivation of citrate synthase enzyme (publication [3], Fig. 7).

2.5. Acetyl-CoA dependent lysine acetylation of mitochondrial proteins

Acetyl-CoA is another metabolite in mitochondria which can impact mitochondrial functions due to lysine acetylation of proteins. This might occur under oxidizing conditions when CS activity is impaired and acetyl-CoA levels might rise and would be available for lysine

acetylation. In the previous chapter MRR was discussed in the context of mitochondrial impairment and the influence of increased citrate levels on MRR. In the following section the impact of lysine acetylation on plant mitochondrial function will be presented.

Since a lack of knowledge on the extent of lysine acetylated proteins in plant mitochondria existed, it was our goal to shed light on the existing plant mitochondrial acetylome and to reveal putative regulatory functions.

By mass spectrometry (MS) analysis, 120 lysine-acetylated mitochondria proteins of *Arabidopsis* including 243 lysine-acetylated sites were discovered ([6] Tab.1, method see publication [7]). We categorized the identified lysine-acetylated proteins into functional groups and discovered that 17% of the identified proteins belong to the TCA cycle and 13% to the respiratory chain ([6] Fig. 1). Relative to the total amount of proteins participating in the TCA cycle on the basis of MapMan bin annotations, 38% of them are lysine-acetylated. Our results are consistent with other studies in bacteria and animals showing that actually all TCA cycle enzymes were identified as lysine-acetylated (Wang et al., 2010; Zhao et al., 2010). Compared to the total number of proteins identified from the TCA-cycle, only 12% of the proteins participating in the ETC were identified although the ETC consists of many more proteins than the TCA cycle. The most likely explanation for this is that the TCA cycle enzymes are situated in the matrix of mitochondria and usually do not appear in SC, thus they are probably more accessible for lysine acetylation. Proteins of the ETC are partially hidden in the inner mitochondrial membrane and they likely form SC which would prevent the acetylation of lysine residues. To verify the MS analysis we performed two dimensional blue native (2D-BN-PAGE) as second approach to detect mitochondrial lysine acetylated proteins followed by Western blot analysis using the anti-acetyllysine antibody ([6] Fig. 4, method see publication [7]). We confirmed the very low abundance of lysine-acetylated proteins in SC I/III_2. In line with the MS analysis, CV exhibited the highest number of lysine acetylation sites within the ETC, and CIII carried no obvious lysine acetylated proteins. In Fig. 10, lysine-acetylated proteins are depicted within the TCA cycle and the ETC. The following chapter provides some more insights into the possible regulatory functions of lysine acetylation on important enzymes.

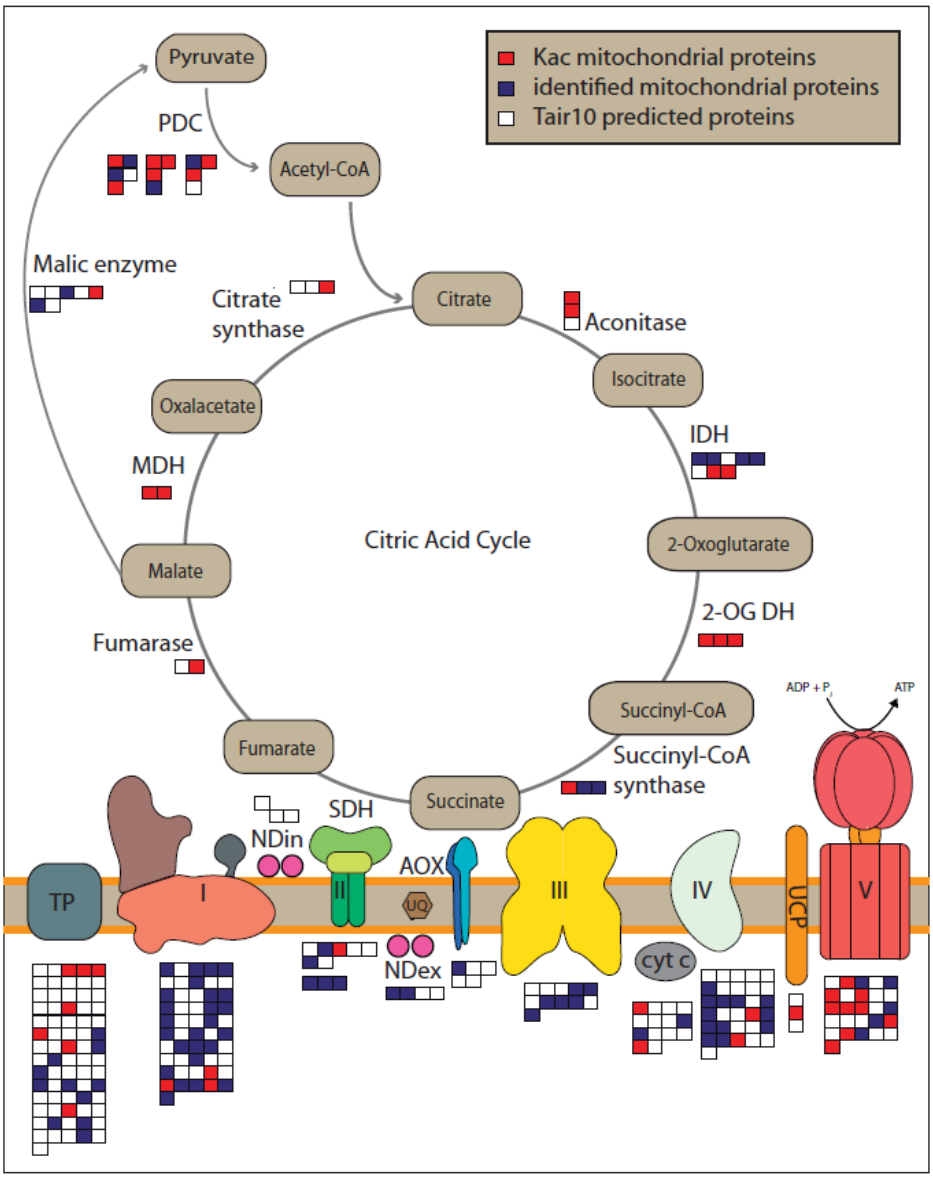

Fig. 10: Overview of identified Arabidopsis lysine-acetylated proteins from mitochondrial energy metabolism. Proteins functional categories were annotated using MapMan (Thimm et al., 2003). Boxes in blue indicate identified non-acetylated proteins before enrichment, red boxes show identified lysine-acetylated proteins and white boxes indicate TAIR10 proteins not identified in the LC-MS/MS analysis. AOX, alternative oxidase; TCA, tricarboxylic acid; TP, transporter; I, complex I; II, complex II; III, complex III; IV, complex IV (publication [6]).

Comparison of lysine acetylation of mitochondrial proteins in different species

The mitochondrial pyruvate dehydrogenase complex (PDC) acts as a link between glycolysis and the TCA cycle. It catalyzes the rate limiting step of the TCA cycle which is the oxidative decarboxylation of pyruvate by the release of acetyl-CoA and the reduction of NAD^+ to NADH. Acetyl-coA is the substrate of protein acetylation, and it is the first substrate of the TCA cycle and plays an important role for fatty acid synthesis, isoprenoids and a number of secondary metabolites. Hence, regulation of the PDC activity serves as an important switch

for many metabolic pathways. Feedback activity regulation of the PDC by lysine acetylation seems likely since we have shown in publication [6] that acetylation is dependent on the amount of acetyl-CoA. However, such a mechanism for PDC is not proven yet, whereas in yeast it was demonstrated that the deletion of PDC results in a general decrease in lysine acetylation, the study also indicating that there is a direct link between intracellular acetyl-CoA concentrations and the acetylation state of proteins (Weinert et al., 2014). Recently, it has been discovered in mammalian cells that lysine acetylation and phosphorylation act hierarchically in concert to control molecular composition as well as activity of PDC (Fan et al., 2014). In future research the overlap in regulatory pathways concerning lysine acetylation and phosphorylation is a promising path for research in plants.

For CS we were able to demonstrate that the activity was regulated in a redox dependent manner by the action of TRX (publication [3]). Nothing is known so far as to how lysine acetylation affects CS activity. As an acetyl-CoA consuming enzyme, CS also controls mitochondrial acetyl-CoA levels. Weinert et al., 2014 demonstrated that the lack of CS in yeast leads to increased acetyl-CoA levels in the mitochondria which correlate with an increase in lysine acetylation. Additionally, CS indirectly affects acetyl-CoA levels in the cytosol because citrate can be exported from mitochondria and converted by ATP-dependent citrate-lyase into acetyl-CoA (Fatland et al., 2002; Fatland et al., 2005). It would be interesting to investigate the effect of lysine acetylation on CS also in correlation with the knowledge that citrate possibly leads to MRS [2].

Concerning the remaining enzymes in the TCA cycle, it is known for mammalian cells that the activity of malate dehydrogenase is stimulated by lysine acetylation while isocitrate dehydrogenase as well as succinate dehydrogenase activities are repressed (Guan and Xiong, 2011). Similar observations were made for the cytosolic NAD^+-dependent malate dehydrogenase from *Arabidopsis* (Finkemeier et al., 2011). These opposing effects are not yet understood in detail and might reflect the complex network of specific KATs and KDACs as regulators of these enzymes.

Taking a closer look at the ETC, the only subunit of CI that was identified by MS analysis as lysine-acetylated in *Arabidopsis* was the gamma carbonic anhydrase 2 (CA2) which is involved in the assembly of CI as well as in SC formation (Perales et al., 2005). It will be of great relevance to find out if acetylation of CA2 is involved in CI stabilization. As previously, explained the loss of CI in the *ndufa1* mutant has an impact on transcription levels and therefore it would be interesting to investigate if acetylation of CA2 contributes into MRR by stabilizing or destabilizing CI.

The OXPHOS protein complex with the highest number of lysine-acetylated proteins is CV. Also in other species, CV has an outstanding number of lysine acetylation sites but actually very little is known about their function. In mice, it was already demonstrated that the number of acetylation sites on CV varies during fasting or feeding, suggesting that lysine acetylation is a dynamic PTM which depends on cellular energy status (Kane and Van Eyk, 2009). Only for the oligomycin sensitivity conferral protein (OSCP) subunit in mammalian cells it has been reported that an increase in lysine acetylation leads to decreased ATP levels. The regulation of the OSCP acetylation status is dependent on the action of Sirt3 (Wu et al., 2013). In our studies the OSCP subunit was not identified as a lysine-acetylated protein. This might suggest that the OSCP subunit of *Arabidopsis* might not be regulated by lysine acetylation or that an unknown KDAC regulates the deacetylation of OSCP in *Arabidopsis.*

Beside proteins of the TCA cycle and the ETC, mitochondrial transporter proteins were also discovered as lysine-acetylated. Strikingly, all mitochondrial voltage dependent anion channels 1-3 (VDAC1-3) were found to be acetylated which was also observed in other species. VDACs play an essential role in regulating metabolite transport between mitochondria and the cytoplasm (Colombini, 2004; Homble et al., 2012). In mouse and human liver mitochondria for example, VDACs contain several lysine acetylated sites (Kerner et al., 2012; Kim et al., 2006; Schwer et al., 2009; Yang et al., 2011; Zhao et al., 2010). Because VDACs are the most abundant mitochondrial outer membrane proteins it is of high interest to better understand their regulation and the involvement of lysine acetylation. Besides VDACs, we also identified a dicarboxylate/tricarboxylate carrier as lysine-acetylated which possibly transports citrate. As described earlier citrate plays a pivotal role in MRR as well as in the control of acetyl-CoA levels in the cytosol. By controlling the transport of citrate into the cytosol an additional layer of regulating acetyl-CoA levels would be provided. The ATP/ADP carriers 1-3 (AAC1-3) were also found to be acetylated which was investigated in more detail in publication [5] and will be discussed below (subchapter 2.7).

Mechanisms that regulate lysine acetylation levels

As mitochondria show a high number of lysine-acetylated proteins the question arose how this PTM is transferred onto the protein. In the nucleus the acetylation of histone proteins is catalyzed by HATs. Interestingly, no HAT/KAT has been found in plant organelles until now and also for other species just one single KAT, the GCN5-related KAT, GCNAL1 was found to be localized in human mitochondria (Scott et al., 2012). However, lysine acetylation was also found on mitochondrial encoded proteins which implies that the acetylation reaction can

occur within the organelle (Hirschey et al., 2011). In contrast, the knowledge about orgarnellar KDACS is increasing rapidly with sirtuins as predominant non-nuclear localized deacetylases. The action of sirtuin homologues in *Arabidopsis* will be discussed in the next chapter and publication [5]. In plants, no mitochondrial KAT has been identified so far but we were able to demonstrate that lysine acetylation can also occur non-enzymatically similar to what was observed for mice mitochondria. Wagner and Payne, 2013 demonstrated that lysine acetylation can occur non-enzymatically on isolated mice mitochondria in *in vitro* experiments. Non-enzymatic lysine acetylation requires a high pH which is part of the physiology of mitochondria. In contrast to cytosolic pH of 7, the mitochondrial matrix has a pH of 7.9-8.0. Additionally, acetyl-CoA levels can reach concentrations of around 1.5 mM. To mimic these conditions we isolated plant mitochondria and treated them with different pH and with or without addition of acetyl-CoA ([6] Fig. 5). At pH 8 and an acetyl-CoA concentration of 5 mM a maximum level of acetylation was reached, which could be even increased by denaturing mitochondria before treatment. The presence of non-enzymatic acetylation may explain the absence of KATs in organelles. However, it does not rule out the presence of KATs, also because the pH in the intermembrane space (IMS) is even lower than in the cytosol (Porcelli et al., 2005) and acetylated lysines were identified on IMS proteins. Therefore, it would be interesting to discover which of the acetylated proteins we found in our study are localized to the IMS. But if the control is not on the level of KATs, it is likely that acetylation control is based on KDACs which is already proposed for SIRT3 in mice mitochondria. It protects mitochondrial enzymes and proteins from chemical acetylation-induced impairment (Hirschey et al., 2011). In *Arabidopsis,* two sirtuin-type like KDACs exist, whereas one of the two is localized in mitochondria [5] and which will be discussed in the next section.

2.6. The Arabidopsis sirtuin SRT2 fine tunes mitochondrial metabolism

Sirtuins have essential roles in mammalian metabolism and several deacetylases have been discovered to be localized in mitochondria. The mitochondrial sirtuins are of innovative clinical relevance, because they are supposed to be important factor regulating longevity (Satoh et al., 2011). Almost nothing was known about deacetylases in plant mitochondria when we started our research. Mammalian cells possess three sirtuins localized in mitochondria (SIRT3-5) which have diverse functions. SIRT3 is the master deacetylase regulating overall protein acetylation levels within mammalian mitochondria. In publication [5], we investigated SRT2, which was the only sirtuin in *Arabidopsis* predicted to be localized

in mitochondria. Basic characterizations of the SRT2 protein confirmed the localization at the inner mitochondrial membrane and that SRT2 possess deacetylases activity. Knockout plants of SRT2, *srt2-1*, did not possess any obvious growth phenotype different from WT. However, by comparing *srt2-1* to the WT, increased lysine acetylation levels in several CV subunits, the ATP/ADP carrier proteins AAC1 to AAC3 and VDAC1 to VDAC4, A BOUT DE SOUFFLE, and di- and tricarboxylate transporter protein were observed ([5] Fig. 4). The interaction of SRT2 with AAC1 to AAC3 as well as the ATPase F1 complex alpha subunit was confirmed by two independent pull-down approaches ([5] Fig. 5). AAC carrier proteins are important in energy metabolism in eukaryotic cells, as they supply the cytosol with ATP (Haferkamp et al., 2002). In intact mitochondria, matrix ATP is usually transported against cytosolic ADP in a 1:1 exchange ratio via the AAC carriers, while they are unable to transport AMP (Klingenberg, 2008). Strikingly, we could demonstrate that the ADP uptake rate in *srt2-1* mitochondria was enhanced compared to WT ([5] Fig. 6). Therefore, we hypothesized that increased acetylation levels stimulate ADP import into mitochondria. Interestingly, mice which lack SIRT3 exhibit increased acetylation levels of the AAC proteins (Rardin et al., 2013). Hence, the acetylation level of the AACs seems to be regulated by sirtuins also in other species. We concluded that SRT2 contributes to the regulation of the ATP/ADP carrier by regulation of the transport rate via deacetylation. No changes in the total ATP amount were discovered between *srt2-1* and WT whereas the ADP amount was increased. Additionally, the ATP/ADP ratio was elevated in the *srt2-1* as well as some changes in other metabolite levels were observed such as increased glycine and serine levels but decreased contents in sugars, amino acids and some organic acids. Due to the changes in total ATP/ADP ratio in *srt2-1* compared WT, oxygen measurements were performed to analyze respiratory activities. No significant changes in respiration rates of the OXPHOS complexes were observed, however the respiratory control ratio, which indicates the coupling of respiration to ATP synthesis, was significantly decreased in *srt2-1* mitochondria compared to the wild type ([5] Fig. 6). Hence, we concluded that SRT2 appears to be responsible for the fine tuning of energy metabolism in mitochondria.

Similar to our results, it was found out recently that the mammalian SIRT4 which shares 42% protein sequence homology with SRT2 is also involved in energy mitochondrial ATP homeostasis (Ho et al., 2013). Hence, it would be interesting to find out if the redox state of NAD^+/NADH might affect ADP import via SRT2 activation. High NAD^+ levels should increase the activity of SRT2 because it is used as a substrate. In plants, nothing is known so far as to whether lysine acetylation is redox dependent and so it offers a challenging research

field in the future. Interestingly, we discovered CI only with the pull-down experiment as a putative interaction partner. In mitochondria, CI consumes most of the NADH for oxidation to NAD^+ and therefore it provides the substrate for SRT2. In general, CI together with the alternative NAD(P)H dehydrogenases is supposed to control redox homeostasis by regulating cellular NADH concentration [4]. One could speculate if SRT2 would have more interaction partners under conditions where increased protein acetylation can be observed. All our experiments were performed under standard growth conditions, but it would be interesting to find out if extreme conditions like oxidative stress, starvation, drought etc. would change the level of lysine acetylation and therefore offer more targets for SRT2 in plant mitochondria. In conclusion, we discovered SRT2 as an active mitochondrial lysine deacetylase which interacts with the ATP/ADP carries in order to regulate the transport of ADP into mitochondria (Fig. 11).

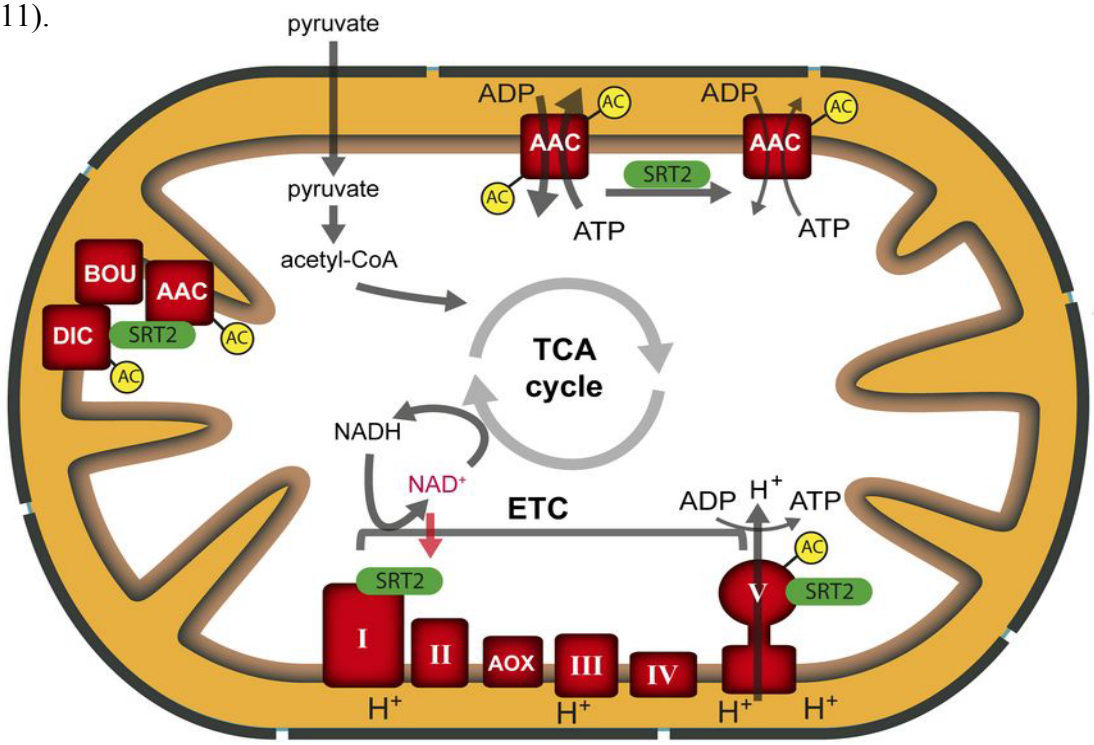

Fig. 11: Working hypothesis of SRT2 in plant mitochondria. SRT2 is dependent on NAD^+ as substrate and interacts with the 76 kDa subunit of complex I. SRT2 interacts and most likely deacetylates the ATP synthase (complex V) as well as a complex containing the AAC proteins AAC1 to AAC3, the putative di-and tricarboxylate transporter (DIC), and the metabolite transporter BOU. Lys acetylation sites of SRT2 interaction partners are indicated (AC). (publication [5]).

3. Conclusion and Outlook

In conclusion, this work shows that citrate-triggered retrograde signalling and lysine acetylation of proteins are important contributors in fine-tuning mitochondrial metabolism. Fig. 12 shows a summary of results achieved in this work. It reflects the connections and the interplay of mitochondrial metabolic fine-tuning regulated by MRS and lysine acetylation.

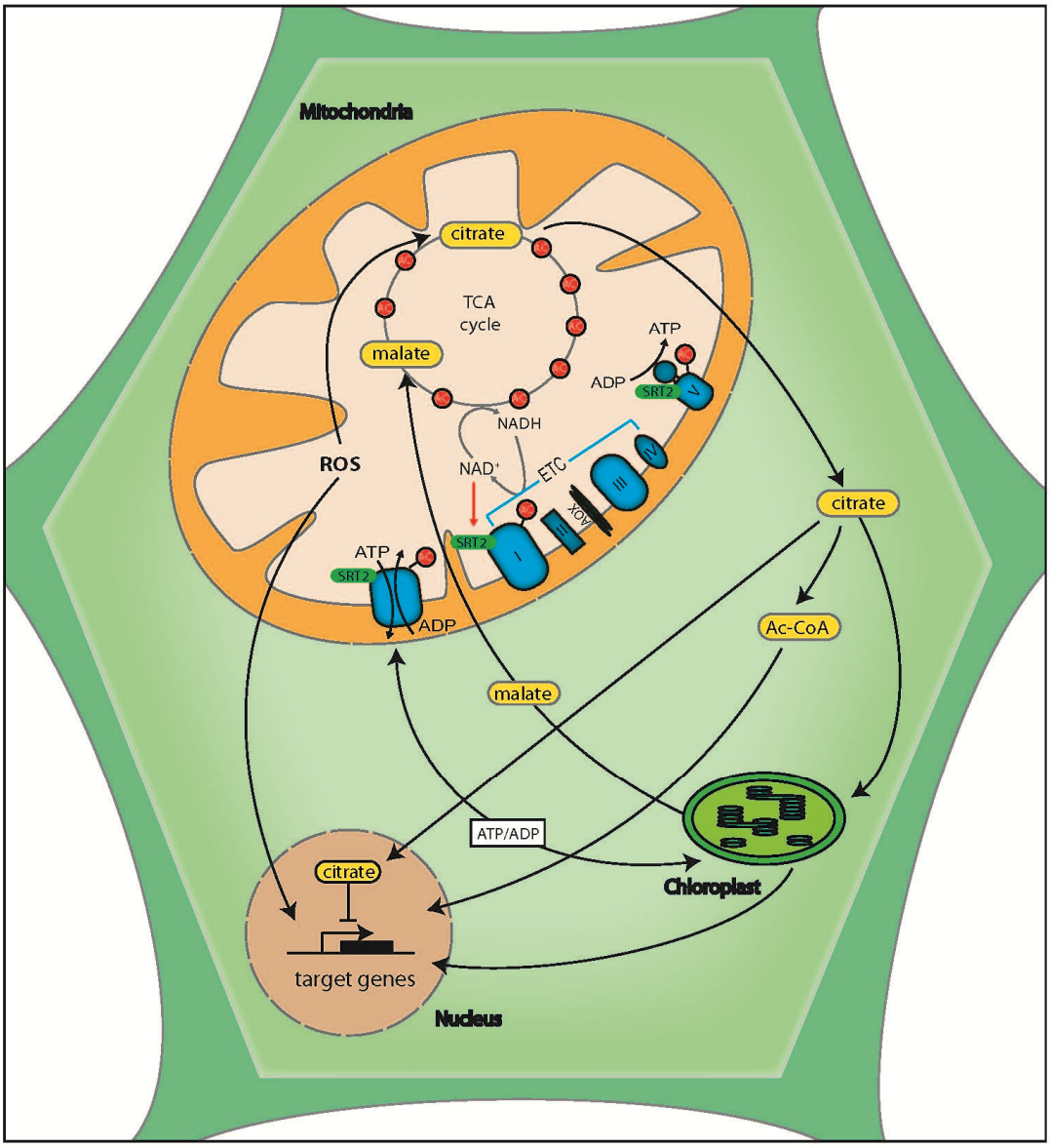

Fig. 12: Summarizing working model of mitochondrial metabolic fine-tuning by retrograde signalling and lysine acetylation. SRT2 was discovered as a lysine deacetylase which is dependent on NAD^+ as substrate (red arrow). It interacts with the 76-kD subunit of complex I and most likely deacetylates the ATP synthase (complex V) as well as a complex containing the AAC proteins AAC1 to AAC3. Additionally, all proteins from the TCA cycle were found to be lysine acetylated. Substrates of the tricarboxylic acid (TCA) cycle, such as malate and citrate can shuttle between mitochondria and the cytosol as well as ATP and ADP (ATP/ADP). Citrate was identified as possible retrograde signalling molecule inducing or inhibiting target gene transcription. ROS is indicated as known retrograde signal.

3.1. Future perspectives of transcriptional regulation triggered by citrate

We found good evidence that citrate can act as a signalling molecule. Specific changes in gene expression were observed upon citrate feeding that did not occur with other organic acids and feeding of external citrate showed a reprogramming of transcripts which was very similar to the response in gene expression that occurred after mitochondrial perturbation. Especially three different groups of target genes were affected including photosynthetic light reactions, protein synthesis, and pathogen defense. It is not clear yet if citrate directly binds to TF regulating gene expression or if altered citrate concentrations are perceived by a receptor which triggers a signalling cascade. Recently, a signalling cascade for AA perception was discovered which includes activation of a rhomboid protease cleaving ANAC017 which then shuttles to the nucleus and activates *AOX1* expression (Ng et al., 2013). Because citrate can also increase AOX1 transcript levels, it would be interesting to investigate if citrate also leads into the ANAC17 mediated MRR pathway. Many open questions remain to be answered in the future, e.g. how is citrate signalling transduced in the cell and what mechanisms control the transcriptional changes. As we only analyzed the change in transcript levels after external addition of citrate it would be interesting to see the effect of locally induced citrate concentration on a sub-cellular level. This could be achieved by over-expressing CS in mitochondria. Furthermore, mutants impaired in citrate transport could give deeper insights into citrate-mediated MRR. To identify novel cis-elements which are responsible for the transcriptional activation after citrate treatment promoter-luciferase constructs of citrate-inducible genes have been designed. 2000 bp of the promoter region were fused to a luciferase gene and stably transformed into *Arabidopsis*. To elucidate the region responsible for the citrate-dependent promoter activation, deletion constructs of the promoter region will be constructed. After narrowing down the promoter, yeast one hybrid screens and EMSA assays can be performed to identify citrate-dependent promoter motifs and their DNA-binding proteins. To identify proteins which are involved in citrate signalling, an affinity chromatography could be carried out. A citrate mimic can be coupled to an agarose column and incubated with total plant extract as well as organellar fractions to pull down citrate-binding proteins which can then be detected via MS. To uncover how changes in the appearance of key metabolites such as citrate and other carboxylic acids influence signalling within the plant cell and how they are perceived will be challenging for the future.

3.2. Research outlook for lysine acetylation on metabolic enzymes

In the second part of my work, the abundance of lysine acetylation in plant mitochondria was investigated. In total 120 proteins of several functional groups including TCA cycle enzymes as well as proteins from the OXPHOS were discovered. Until now, regulation of lysine acetylation is thought to be controlled by KATs and KDACs. While no orgarnellar KAT has been discovered in plants, here we demonstrated that lysine acetylation can occur non-enzymatically because of the basic pH in the mitochondrial matrix. Hence, it seems more likely that acetylation levels are mainly controlled by KDACs. We characterized a sirtuin-type like KDAC, SRT2, which was supposed to be the only mitochondrial sirtuin in *Arabidopsis*. We could confirm the mitochondrial localization as well as the deacetylase activity of SRT2. No obvious phenotype was visible in the knockout plants but changed lysine acetylation levels for proteins of CV as well as for the ATP/ADP carriers were observed. Strikingly, an enhanced ADP uptake in the *srt2-1* knockout mutant was detected as well as changed ATP/ADP ratios. Additionally, we observed changes in metabolic levels with increased glycine and serine levels, while sugars, some amino acids and organic acids were significantly decreased in abundance. We hypothesized that SRT2 is involved in fine-tuning mitochondrial metabolism by interacting with the ATP/ADP carries. Many interesting research questions concerning mitochondrial lysine emanate from our recent findings. After the discovery of the lysine acetylome in mitochondria, the functional relevance now has to be investigated. Does lysine acetylation change activity of metabolic enzymes in plant mitochondria? In other species several mitochondrial enzymes regulated by lysine acetylation were uncovered in the last years, for example the malate dehydrogenase and the superoxide dismutase 2 in human cells (Qiu et al., 2010; Tao et al., 2010; Zhao et al., 2010); the succinate dehydrogenase complex, subunit A as well as the aldehyde dehydrogenase 2 in mouse (Cimen et al., 2010; Lu et al., 2011). One possible approach to investigate the relevance of specific lysine residues is to perform site-directed mutagenesis. The exchange of lysine to arginine is supposed to mimic the non-acetylated state and the exchange to glutamine the acetylated state. An interesting candidate for using site-directed mutagenesis is the PDC complex as it is of great importance for the TCA cycle and it controls acetyl-CoA levels in mitochondria. The next question which should be answered is, when and how does lysine acetylation vary in mitochondria. Does lysine acetylation depend on the redox state of the organelle and does it reflect the metabolic state? How does lysine acetylation change in terms of abiotic and biotic stress conditions and what is the impact on enzyme activity? To answer these questions, we have to learn more about the lysine acetylation regulating enzymes. As no orgarnellar KAT has been discovered

so far the question arises if they exist in organelles at all or if lysine acetylation only occurs non-enzymatically. We found SRT2 as the only sirtuin type KDACs in mitochondria but other KDACs might exist as well. To answer these questions it will be critical to dissect these regulatory enzymes in more detail.

4. References

Allfrey, V.G., and Mirsky, A.E. (1964). Structural modifications of histones and their possible role in regulation of RNA synthesis. Science *144*, 559.
Allis, C.D., Berger, S.L., Cote, J., Dent, S., Jenuwien, T., Kouzarides, T., Pillus, L., Reinberg, D., Shi, Y., Shiekhattar, R., *et al.* (2007). New nomenclature for chromatin-modifying enzymes. Cell *131*, 633-636.
Arnold, C.G. (1982). The phylogenetic origin of mitochondria and plastids. Biol Zbl *101*, 365-374.
Atkin, O.K., Cummins, W.R., and Collier, D.E. (1993). Light induction of alternative pathway capacity in leaf slices of belgium endive. Plant Cell Environ *16*, 231-235.
Baena-Gonzalez, E., and Sheen, J. (2008). Convergent energy and stress signaling. Trends Plant Sci *13*, 474-482.
Balmer, Y., Vensel, W.H., Tanaka, C.K., Hurkman, W.J., Gelhaye, E., Rouhier, N., Jacquot, J.P., Manieri, W., Schurmann, P., Droux, M., *et al.* (2004). Thioredoxin links redox to the regulation of fundamental processes of plant mitochondria. Proceedings of the National Academy of Sciences of the United States of America *101*, 2642-2647.
Baradaran, R., Berrisford, J.M., Minhas, G.S., and Sazanov, L.A. (2013). Crystal structure of the entire respiratory complex I. Nature *494*, 443-448.
Bastet, L., Boileau, C., Bedu, S., Janicki, A., Latifi, A., and Zhang, C.C. (2010). NtcA regulates patA expression in Anabaena sp. strain PCC 7120. Journal of Bacteriology *192*, 5257-5259.
Blander, G., and Guarente, L. (2004). The Sir2 family of protein deacetylases. Annual Review of Biochemistry *73*, 417-435.
Boziaris, I.S., and Adams, M.R. (1999). Effect of chelators and nisin produced in situ on inhibition and inactivation of Gram negatives. International Journal of Food Microbiology *53*, 105-113.
Briat, J.F., and Lebrun, M. (1999). Plant responses to metal toxicity. Cr Acad Sci *322*, 43-54.
Briat, J.F., and Lobreaux, S. (1998). Iron storage and ferritin in plants. Met Ions Biol Syst *35*, 563-584.
Buchanan, B.B. (1984). The ferredoxin/thioredoxin system: a key element in the regulatory function of light in photosynthesis. Bioscience *34*, 378-383.
Buchanan, B.B. (1991). Regulation of Co2 assimilation in oxygenic photosynthesis - the ferredoxin thioredoxin system - perspective on its discovery, present status, and future-development. Arch Biochem Biophys *288*, 1-9.
Busi, M.V., Gomez-Lobato, M.E., Rius, S.P., Turowski, V.R., Casati, P., Zabaleta, E.J., Gomez-Casati, D.F., and Araya, A. (2011). Effect of mitochondrial dysfunction on carbon metabolism and gene expression in flower tissues of Arabidopsis thaliana. Molecular Plant *4*, 127-143.
Carrari, F., Nunes-Nesi, A., Gibon, Y., Lytovchenko, A., Loureiro, M.E., and Fernie, A.R. (2003). Reduced expression of aconitase results in an enhanced rate of photosynthesis and marked shifts in carbon partitioning in illuminated leaves of wild species tomato. Plant Physiology *133*, 1322-1335.
Chen, H., Laurent, S., Bedu, S., Ziarelli, F., Chen, H.L., Cheng, Y., Zhang, C.C., and Peng, L. (2006). Studying the signaling role of 2-oxoglutaric acid using analogs that mimic the ketone and ketal forms of 2-oxoglutaric acid. Chemistry and Biology *13*, 849-856.
Chen, Z.J., and Tian, L. (2007). Roles of dynamic and reversible histone acetylation in plant development and polyploidy. BBA-Gene Struct Expr *1769*, 295-307.
Cheng, H., Qin, L., Lee, S., Fu, X., Richards, D.E., Cao, D., Luo, D., Harberd, N.P., and Peng, J. (2004). Gibberellin regulates Arabidopsis floral development via suppression of DELLA protein function. Development *131*, 1055-1064.

Cho, Y.H., Yoo, S.D., and Sheen, J. (2006). Regulatory functions of nuclear hexokinase1 complex in glucose signaling. Cell *127*, 579-589.
Choudhary, C., Kumar, C., Gnad, F., Nielsen, M.L., Rehman, M., Walther, T.C., Olsen, J.V., and Mann, M. (2009). Lysine acetylation targets protein complexes and co-regulates major cellular functions. Science *325*, 834-840.
Cimen, H., Han, M.J., Yang, Y.J., Tong, Q., Koc, H., and Koc, E.C. (2010). Regulation of succinate dehydrogenase activity by SIRT3 in mammalian mitochondria. Biochemistry *49*, 304-311.
Clifton, R., Lister, R., Parker, K.L., Sappl, P.G., Elhafez, D., Millar, A.H., Day, D.A., and Whelan, J. (2005). Stress-induced co-expression of alternative respiratory chain components in Arabidopsis thaliana. Plant Molecular Biology *58*, 193-212.
Colombini, M. (2004). VDAC: The channel at the interface between mitochondria and the cytosol. Molecular and Cellular Biochemistry *256*, 107-115.
Coruzzi, G.M., and Zhou, L. (2001). Carbon and nitrogen sensing and signaling in plants: emerging 'matrix effects'. Current Opinion in Plant Biology *4*, 247-253.
De Clercq, I., Vermeirssen, V., Van Aken, O., Vandepoele, K., Murcha, M.W., Law, S.R., Inze, A., Ng, S., Ivanova, A., Rombaut, D., *et al.* (2013). The membrane-bound NAC transcription factor ANAC013 functions in mitochondrial retrograde regulation of the oxidative stress response in Arabidopsis. The Plant Cell *25*, 3472-3490.
Deribe, Y.L., Pawson, T., and Dikic, I. (2010). Post-translational modifications in signal integration. Nature Structural and Molecular Biology *17*, 666-672.
Deusch, O., Landan, G., Roettger, M., Gruenheit, N., Kowallik, K.V., Allen, J.F., Martin, W., and Dagan, T. (2008). Genes of cyanobacterial origin in plant nuclear genomes point to a heterocyst-forming plastid ancestor. Mol Biol Evol *25*, 748-761.
Djajanegara, I., Finnegan, P.M., Mathieu, C., McCabe, T., Whelan, J., and Day, D.A. (2002). Regulation of alternative oxidase gene expression in soybean. Plant Mol Biol *50*, 735-742.
Dutilleul, C., Driscoll, S., Cornic, G., De Paepe, R., Foyer, C.H., and Noctor, G. (2003). Functional mitochondrial complex I is required by tobacco leaves for optimal photosynthetic performance in photorespiratory conditions and during transients. Plant Physiology *131*, 264-275.
Earley, K.W., Shook, M.S., Brower-Toland, B., Hicks, L., and Pikaard, C.S. (2007). In vitro specificities of Arabidopsis co-activator histone acetyltransferases: implications for histone hyperacetylation in gene activation. The Plant Journal : for Cell and Molecular Biology *52*, 615-626.
Esser, C., Ahmadinejad, N., Wiegand, C., Rotte, C., Sebastiani, F., Gelius-Dietrich, G., Henze, K., Kretschmann, E., Richly, E., Leister, D., *et al.* (2004). A genome phylogeny for mitochondria among alpha-proteobacteria and a predominantly eubacterial ancestry of yeast nuclear genes. Mol Biol Evol *21*, 1643-1660.
Fan, J., Shan, C.L., Kang, H.B., Elf, S., Xie, J.X., Tucker, M., Gu, T.L., Aguiar, M., Lonning, S., Chen, H.B., *et al.* (2014). Tyr phosphorylation of PDP1 toggles recruitment between ACAT1 and SIRT3 to regulate the pyruvate dehydrogenase complex. Molecular Cell *53*, 534-548.
Fatland, B.L., Ke, J., Anderson, M.D., Mentzen, W.I., Cui, L.W., Allred, C.C., Johnston, J.L., Nikolau, B.J., and Wurtele, E.S. (2002). Molecular characterization of a heteromeric ATP-citrate lyase that generates cytosolic acetyl-coenzyme A in Arabidopsis. Plant Physiology *130*, 740-756.
Fatland, B.L., Nikolau, B.J., and Wurtele, E.S. (2005). Reverse genetic characterization of cytosolic acetyl-CoA generation by ATP-citrate lyase in Arabidopsis. The Plant Cell *17*, 182-203.

Fernie, A.R., Carrari, F., and Sweetlove, L.J. (2004). Respiratory metabolism: glycolysis, the TCA cycle and mitochondrial electron transport. Current Opinion in Plant Biology *7*, 254-261.
Finkemeier, I., Laxa, M., Miguet, L., Howden, A.J., and Sweetlove, L.J. (2011). Proteins of diverse function and subcellular location are lysine acetylated in Arabidopsis. Plant Physiology *155*, 1779-1790.
Frye, R.A. (2000). Phylogenetic classification of prokaryotic and eukaryotic Sir2-like proteins. Biochemical and Biophysical Research Communications *273*, 793-798.
Gardestrom, P. (1996). Interactions between mitochondria and chloroplasts. Bba-Bioenergetics *1275*, 38-40.
Gelhaye, E., Rouhier, N., Gerard, J., Jolivet, Y., Gualberto, J., Navrot, N., Ohlsson, P.I., Wingsle, G., Hirasawa, M., Knaff, D.B., *et al.* (2004). A specific form of thioredoxin h occurs in plant mitochondria and regulates the alternative oxidase. Proceedings of the National Academy of Sciences of the United States of America *101*, 14545-14550.
Genova, M.L., and Lenaz, G. (2014). Functional role of mitochondrial respiratory supercomplexes. Bba *1837*, 427-443.
Giraud, E., Van Aken, O., Ho, L.H.M., and Whelan, J. (2009). The transcription factor ABI4 is a regulator of mitochondrial retrograde expression of ALTERNATIVE OXIDASE1a. Plant Physiology *150*, 1286-1296.
Gomez, M.A., Alisaraie, L., Shio, M.T., Berghuis, A.M., Lebrun, C., Gautier-Luneau, I., and Olivier, M. (2010). Protein tyrosine phosphatases are regulated by mononuclear iron dicitrate. Journal of Biological Chemistry *285*, 24620-24628.
Gray, G.R., Maxwell, D.P., Villarimo, A.R., and McIntosh, L. (2004). Mitochondria/nuclear signaling of alternative oxidase gene expression occurs through distinct pathways involving organic acids and reactive oxygen species. Plant Cell Reports *23*, 497-503.
Guan, K.L., and Xiong, Y. (2011). Regulation of intermediary metabolism by protein acetylation. Trends in Biochemical Sciences *36*, 108-116.
Gupta, K.J., Shah, J.K., Brotman, Y., Jahnke, K., Willmitzer, L., Kaiser, W.M., Bauwe, H., and Igamberdiev, A.U. (2012). Inhibition of aconitase by nitric oxide leads to induction of the alternative oxidase and to a shift of metabolism towards biosynthesis of amino acids. J Exp Bot. *63*, 1773-1784.
Haferkamp, I., Hackstein, J.H.P., Voncken, F.G.J., Schmit, G., and Tjaden, J. (2002). Functional integration of mitochondrial and hydrogenosomal ADP/ATP carriers in the Escherichia coli membrane reveals different biochemical characteristics for plants, mammals and anaerobic chytrids. European Journal of Biochemistry *269*, 3172-3181.
Haydon, M.J., and Cobbett, C.S. (2007). Transporters of ligands for essential metal ions in plants. New Phytologist *174*, 499-506.
Heineke, D., Sonnewald, U., Bussis, D., Gunter, G., Leidreiter, K., Wilke, I., Raschke, K., Willmitzer, L., and Heldt, H.W. (1992). Apoplastic Expression of yeast-derived invertase in potato - effects on photosynthesis, leaf solute composition, water relations, and tuber composition. Plant Physiology *100*, 301-308.
Henriksen, P., Wagner, S.A., Weinert, B.T., Sharma, S., Bacinskaja, G., Rehman, M., Juffer, A.H., Walther, T.C., Lisby, M., and Choudhary, C. (2012). Proteome-wide analysis of lysine acetylation suggests its broad regulatory scope in Saccharomyces cerevisiae. Molecular and Cellular Proteomics : MCP *11*, 1510-1522.
Hewitson, K.S., Lienard, B.M., McDonough, M.A., Clifton, I.J., Butler, D., Soares, A.S., Oldham, N.J., McNeill, L.A., and Schofield, C.J. (2007). Structural and mechanistic studies on the inhibition of the hypoxia-inducible transcription factor hydroxylases by tricarboxylic acid cycle intermediates. The Journal of Biological Chemistry *282*, 3293-3301.

Hirschey, M.D., Shimazu, T., Jing, E., Grueter, C.A., Collins, A.M., Aouizerat, B., Stancakova, A., Goetzman, E., Lam, M.M., Schwer, B.*, et al.* (2011). SIRT3 Deficiency and mitochondrial protein hyperacetylation accelerate the development of the metabolic syndrome. Molecular Cell *44*, 177-190.
Ho, L., Titus, A.S., Banerjee, K.K., George, S., Lin, W., Deota, S., Saha, A.K., Nakamura, K., Gut, P., Verdin, E.*, et al.* (2013). SIRT4 regulates ATP homeostasis and mediates a retrograde signaling via AMPK. Aging *5*, 835-849.
Hoefnagel, M.H.N., Atkin, O.K., and Wiskich, J.T. (1998). Interdependence between chloroplasts and mitochondria in the light and the dark. Bba-Bioenergetics *1366*, 235-255.
Homble, F., Krammer, E.M., and Prevost, M. (2012). Plant VDAC: Facts and speculations. Bba-Biomembranes *1818*, 1486-1501.
Jang, J.C., and Sheen, J. (1994). Sugar sensing in higher plants. The Plant Cell *6*, 1665-1679.
Kane, L.A., and Van Eyk, J.E. (2009). Post-translational modifications of ATP synthase in the heart: biology and function. Journal of Bioenergetics and Biomembranes *41*, 145-150.
Kerner, J., Lee, K., Tandler, B., and Hoppel, C.L. (2012). VDAC proteomics: Post-translation modifications. Bba-Biomembranes *1818*, 1520-1525.
Kim, S.C., Sprung, R., Chen, Y., Xu, Y.D., Ball, H., Pei, J.M., Cheng, T.L., Kho, Y., Xiao, H., Xiao, L.*, et al.* (2006). Substrate and functional diversity of lysine acetylation revealed by a proteomics survey. Molecular Cell *23*, 607-618.
Kleine, T., Voigt, C., and Leister, D. (2009). Plastid signalling to the nucleus: messengers still lost in the mists? Trends in Genetics : TIG *25*, 185-192.
Klingenberg, M. (2008). The ADP and ATP transport in mitochondria and its carrier. Bba-Biomembranes *1778*, 1978-2021.
Koussevitzky, S., Nott, A., Mockler, T.C., Hong, F., Sachetto-Martins, G., Surpin, M., Lim, J., Mittler, R., and Chory, J. (2007). Signals from chloroplasts converge to regulate nuclear gene expression. Science *316*, 715-719.
Kromer, S. (1995). Respiration during Photosynthesis. Annual Review of Plant Physiology and Plant Molecular Biology *46*, 45-70.
Lacal, J., Alfonso, C., Liu, X., Parales, R.E., Morel, B., Conejero-Lara, F., Rivas, G., Duque, E., Ramos, J.L., and Krell, T. (2010). Identification of a chemoreceptor for tricarboxylic acid cycle intermediates: differential chemotactic response towards receptor ligands. The Journal of Biological Chemistry *285*, 23126-23136.
Lancien, M., and Roberts, M.R. (2006). Regulation of Arabidopsis thaliana 14-3-3 gene expression by gamma-aminobutyric acid. Plant Cell Environ *29*, 1430-1436.
Lapuente-Brun, E., Moreno-Loshuertos, R., Acin-Perez, R., Latorre-Pellicer, A., Colas, C., **Balsa, E., Perales-Clemente, E., Quiros, P.M., Calvo, E., Rodriguez-Hernandez, M.A.*, et al.*** (2013). Supercomplex assembly determines electron flux in the mitochondrial electron transport chain. Science *340*, 1567-1570.
Lehmann, M., Schwarzlander, M., Obata, T., Sirikantaramas, S., Burow, M., Olsen, C.E., Tohge, T., Fricker, M.D., Moller, B.L., Fernie, A.R.*, et al.* (2009). The metabolic response of Arabidopsis roots to oxidative stress is distinct from that of heterotrophic cells in culture and highlights a complex relationship between the levels of transcripts, metabolites, and flux. Molecular Plant *2*, 390-406.
Leister, D. (2005). Genomics-based dissection of the cross-talk of chloroplasts with the nucleus and mitochondria in Arabidopsis. Gene *354*, 110-116.
Leister, D., Wang, X., Haberer, G., Mayer, K.F., and Kleine, T. (2011). Intracompartmental and intercompartmental transcriptional networks coordinate the expression of genes for organellar functions. Plant Physiology *157*, 386-404.
Lhernault, S.W., and Rosenbaum, J.L. (1983). Chlamydomonas alpha-tubulin is posttranslationally modified in the flagella during flagellar assembly. J Cell Biol *97*, 258-263.

Lhernault, S.W., and Rosenbaum, J.L. (1985a). Chlamydomonas alpha-tubulin is posttranslationally modified by acetylation on the epsilon-amino group of a lysine. Biochemistry-Us *24*, 473-478.
Lhernault, S.W., and Rosenbaum, J.L. (1985b). Reversal of the posttranslational modification on chlamydomonas flagellar alpha-tubulin occurs during flagellar resorption. J Cell Biol *100*, 457-462.
Liao, X., and Butow, R.A. (1993). RTG1 and RTG2: two yeast genes required for a novel path of communication from mitochondria to the nucleus. Cell *72*, 61-71.
Lobreaux, S., Yewdall, S.J., Briat, J.F., and Harrison, P.M. (1992). Amino-acid sequence and predicted three-dimensional structure of pea seed (Pisum sativum) ferritin. The Biochemical Journal *288 (Pt 3)*, 931-939.
Lu, Z.P., Bourdi, M., Li, J.H., Aponte, A.M., Chen, Y., Lombard, D.B., Gucek, M., Pohl, L.R., and Sack, M.N. (2011). SIRT3-dependent deacetylation exacerbates acetaminophen hepatotoxicity. EMBO reports *12*, 840-846.
Lundby, A., Lage, K., Weinert, B.T., Bekker-Jensen, D.B., Secher, A., Skovgaard, T., Kelstrup, C.D., Dmytriyev, A., Choudhary, C., Lundby, C.*, et al.* (2012). Proteomic analysis of lysine acetylation sites in rat tissues reveals organ specificity and subcellular patterns. Cell Reports *2*, 419-431.
Martin, W., Rujan, T., Richly, E., Hansen, A., Cornelsen, S., Lins, T., Leister, D., Stoebe, B., Hasegawa, M., and Penny, D. (2002). Evolutionary analysis of Arabidopsis, cyanobacterial, and chloroplast genomes reveals plastid phylogeny and thousands of cyanobacterial genes in the nucleus. Proceedings of the National Academy of Sciences of the United States of America *99*, 12246-12251.
Matsuo, M., and Obokata, J. (2006). Remote control of photosynthetic genes by the mitochondrial respiratory chain. The Plant journal : for Cell and Molecular Biology *47*, 873-882.
Maxwell, D.P., Nickels, R., and McIntosh, L. (2002). Evidence of mitochondrial involvement in the transduction of signals required for the induction of genes associated with pathogen attack and senescence. The Plant journal : for Cell and Molecular Biology *29*, 269-279.
Maxwell, D.P., Wang, Y., and McIntosh, L. (1999). The alternative oxidase lowers mitochondrial reactive oxygen production in plant cells. Proceedings of the National Academy of Sciences of the United States of America *96*, 8271-8276.
McCammon, M.T., Epstein, C.B., Przybyla-Zawislak, B., McAlister-Henn, L., and Butow, R.A. (2003). Global transcription analysis of Krebs tricarboxylic acid cycle mutants reveals an alternating pattern of gene expression and effects on hypoxic and oxidative genes. Molecular Biology of the Cell *14*, 958-972.
McDonald, A.E., Sieger, S.M., and Vanlerberghe, G.C. (2002). Methods and approaches to study plant mitochondrial alternative oxidase. Physiologia Plantarum *116*, 135-143.
Melo-Braga, M.N., Verano-Braga, T., Leon, I.R., Antonacci, D., Nogueira, F.C., Thelen, J.J., Larsen, M.R., and Palmisano, G. (2012). Modulation of protein phosphorylation, N-glycosylation and Lys-acetylation in grape (Vitis vinifera) mesocarp and exocarp owing to Lobesia botrana infection. Molecular and Cellular Proteomics *11*, 945-956.
Meyer, E.H., Tomaz, T., Carroll, A.J., Estavillo, G., Delannoy, E., Tanz, S.K., Small, I.D., Pogson, B.J., and Millar, A.H. (2009). Remodeled respiration in ndufs4 with low phosphorylation efficiency suppresses Arabidopsis germination and growth and alters control of metabolism at night. Plant Physiology *151*, 603-619.
Millar A. H., Whelan J., Soole K. L., Day D. A. (2011). Organization and regulation of mitochondrial respiration in plants. Annual Review of Plant Physiology and Plant Molecular Biology. 62, 79–104

Millar, A.H., Sweetlove, L.J., Giege, P., and Leaver, C.J. (2001). Analysis of the Arabidopsis mitochondrial proteome. Plant Physiology *127*, 1711-1727.
Mirabdullaev, I.M. (1985). The Evolution of plastids and origin of cyanobacteria. Zh Obshch Biol *46*, 483-490.
Moller, I.M. (2001). Plant mitochondria and oxidative stress: electron transport, NADPH turnover, and metabolism of reactive oxygen species. Annual Review of Plant Physiology and Plant Molecular Biology *52*, 561-591.
Moller, I.M., and Rasmusson, A.G. (1998). The role of NADP in the mitochondrial matrix. Trends Plant Sci *3*, 21-27.
Moller, I.M., and Sweetlove, L.J. (2010). ROS signalling-specificity is required. Trends Plant Sci *15*, 370-374.
Moore, A.L., and Siedow, J.N. (1991). The regulation and nature of the cyanide-resistant alternative oxidase of plant mitochondria. Bba. *1059*, 121-140.
Moore, B., Zhou, L., Rolland, F., Hall, Q., Cheng, W.H., Liu, Y.X., Hwang, I., Jones, T., and Sheen, J. (2003). Role of the Arabidopsis glucose sensor HXK1 in nutrient, light, and hormonal signaling. Science *300*, 332-336.
Morgan, M.J., Lehmann, M., Schwarzlander, M., Baxter, C.J., Sienkiewicz-Porzucek, A., Williams, T.C., Schauer, N., Fernie, A.R., Fricker, M.D., Ratcliffe, R.G.*, et al.* (2008). Decrease in manganese superoxide dismutase leads to reduced root growth and affects tricarboxylic acid cycle flux and mitochondrial redox homeostasis. Plant Physiology *147*, 101-114.
Navarro, L., Bari, R., Achard, P., Lison, P., Nemri, A., Harberd, N.P., and Jones, J.D. (2008). DELLAs control plant immune responses by modulating the balance of jasmonic acid and salicylic acid signaling. Current Biology. *18*, 650-655.
Ng, S., Ivanova, A., Duncan, O., Law, S.R., Van Aken, O., De Clercq, I., Wang, Y., Carrie, C., Xu, L., Kmiec, B.*, et al.* (2013). A membrane-bound NAC transcription factor, ANAC017, mediates mitochondrial retrograde signaling in Arabidopsis. The Plant Cell *25*, 3450-3471.
Norman, C., Howell, K.A., Millar, A.H., Whelan, J.M., and Day, D.A. (2004). Salicylic acid is an uncoupler and inhibitor of mitochondrial electron transport. Plant Physiology *134*, 492-501.
North, B.J., Marshall, B.L., Borra, M.T., Denu, J.M., and Verdin, E. (2003). The human Sir2 ortholog, SIRT2, is an NAD(+)-dependent tubulin deacetylase. Molecular Cell *11*, 437-444.
Nunes-Nesi, A., Carrari, F., Lytovchenko, A., Smith, A.M.O., Loureiro, M.E., Ratcliffe, R.G., Sweetlove, L.J., and Fernie, A.R. (2005). Enhanced photosynthetic performance and growth as a consequence of decreasing mitochondrial malate dehydrogenase activity in transgenic tomato plants. Plant Physiology *137*, 611-622.
Pandey, R., Muller, A., Napoli, C.A., Selinger, D.A., Pikaard, C.S., Richards, E.J., Bender, J., Mount, D.W., and Jorgensen, R.A. (2002). Analysis of histone acetyltransferase and histone deacetylase families of Arabidopsis thaliana suggests functional diversification of chromatin modification among multicellular eukaryotes. Nucleic Acids Res *30*, 5036-5055.
Perales, M., Eubel, H., Heinemeyer, J., Colaneri, A., Zabaleta, E., and Braun, H.P. (2005). Disruption of a nuclear gene encoding a mitochondrial gamma carbonic anhydrase reduces complex I and supercomplex I + III2 levels and alters mitochondrial physiology in Arabidopsis. Journal of Molecular Biology *350*, 263-277.
Pesaresi, P., Schneider, A., Kleine, T., and Leister, D. (2007). Interorganellar communication. Current Opinion in Plant Biology *10*, 600-606.
Pfannschmidt, T., Schutze, K., Brost, M., and Oelmuller, R. (2001). A novel mechanism of nuclear photosynthesis gene regulation by redox signals from the chloroplast during photosystem stoichiometry adjustment. Journal of Biological Chemistry *276*, 36125-36130.

Philippar, K., Geis, T., Ilkavets, I., Oster, U., Schwenkert, S., Meurer, J., and Soll, J. (2007). Chloroplast biogenesis: the use of mutants to study the etioplast-chloroplast transition. Proceedings of the National Academy of Sciences of the United States of America *104*, 678-683.
Phillips, D.M. (1963). The presence of acetyl groups of histones. The Biochemical Journal *87*, 258-263.
Pohlmeyer, K., Soll, J., Steinkamp, T., Hinnah, S., and Wagner, R. (1997). Isolation and characterization of an amino acid-selective channel protein present in the chloroplastic outer envelope membrane. Proceedings of the National Academy of Sciences of the United States of America *94*, 9504-9509.
Pollmann, S., Springer, A., Buhr, F., Lahroussi, A., Samol, I., Bonneville, J.M., Tichtinsky, G., von Wettstein, D., Reinbothe, C., and Reinbothe, S. (2007). A plant porphyria related to defects in plastid import of protochlorophyllide oxidoreductase A. Proceedings of the National Academy of Sciences of the United States of America *104*, 2019-2023.
Porcelli, A.M., Ghelli, A., Zanna, C., Pinton, P., Rizzuto, R., and Rugolo, M. (2005). pH difference across the outer mitochondrial membrane measured with a green fluorescent protein mutant. Biochemical and Biophysical Research Communications *326*, 799-804.
Price, J., Laxmi, A., St Martin, S.K., and Jang, J.C. (2004). Global transcription profiling reveals multiple sugar signal transduction mechanisms in Arabidopsis. Plant Cell *16*, 2128-2150.
Pudelski, B., Schock, A., Hoth, S., Radchuk, R., Weber, H., Hofmann, J., Sonnewald, U., Soll, J., and Philippar, K. (2012). The plastid outer envelope protein OEP16 affects metabolic fluxes during ABA-controlled seed development and germination. J Exp Bot. *63*, 1919-1936.
Qiu, X., Brown, K., Hirschey, M.D., Verdin, E., and Chen, D. (2010). Calorie restriction reduces oxidative stress by SIRT3-mediated SOD2 activation. Cell Metabolism *12*, 662-667.
Rardin, M.J., Newman, J.C., Held, J.M., Cusack, M.P., Sorensen, D.J., Li, B.A., Schilling, B., Mooney, S.D., Kahn, C.R., Verdin, E.*, et al.* (2013). Label-free quantitative proteomics of the lysine acetylome in mitochondria identifies substrates of SIRT3 in metabolic pathways. Proceedings of the National Academy of Sciences of the United States of America *110*, 6601-6606.
Ravet, K., Touraine, B., Boucherez, J., Briat, J.F., Gaymard, F., and Cellier, F. (2009). Ferritins control interaction between iron homeostasis and oxidative stress in Arabidopsis. Plant Journal *57*, 400-412.
Rogina, B., and Helfand, S.L. (2004). Sir2 mediates longevity in the fly through a pathway related to calorie restriction. Proceedings of the National Academy of Sciences of the United States of America *101*, 15998-16003.
Rolland, F., Baena-Gonzalez, E., and Sheen, J. (2006). Sugar sensing and signaling in plants: Conserved and novel mechanisms. Annu Rev Plant Biol *57*, 675-709.
Rouhier, N., Villarejo, A., Srivastava, M., Gelhaye, E., Keech, O., Droux, M., Finkemeier, I., Samuelsson, G., Dietz, K.J., Jacquot, J.P.*, et al.* (2005). Identification of plant glutaredoxin targets. Antioxidants and Redox Signaling *7*, 919-929.
Satoh, A., Stein, L., and Imai, S. (2011). The role of mammalian sirtuins in the regulation of metabolism, aging, and longevity. Handbook of Experimental Pharmacology *206*, 125-162.
Scheibe, R. (2004). Malate valves to balance cellular energy supply. Physiologia Plantarum *120*, 21-26.
Scheibe, R., and Dietz, K.J. (2012). Reduction-oxidation network for flexible adjustment of cellular metabolism in photoautotrophic cells. Plant Cell Environ *35*, 202-216.
Schurmann, P., and Buchanan, B.B. (2008). The ferredoxin/thioredoxin system of oxygenic photosynthesis. Antioxidants and Redox Signaling *10*, 1235-1274.

Schwer, B., Eckersdorff, M., Li, Y., Silva, J.C., Fermin, D., Kurtev, M.V., Giallourakis, C., Comb, M.J., Alt, F.W., and Lombard, D.B. (2009). Calorie restriction alters mitochondrial protein acetylation. Aging Cell *8*, 604-606.
Schwer, B., North, B.J., Frye, R.A., Ott, M., and Verdin, E. (2002). The human silent information regulator NO homologue hSIRT3 is a mitochondrial nicotinamide adenine dinucleotide-dependent deacetylase. J Cell Biol *158*, 647-657.
Scott, I., Webster, B.R., Li, J.H., and Sack, M.N. (2012). Identification of a molecular component of the mitochondrial acetyltransferase programme: a novel role for GCN5L1. Biochemical Journal *443*, 655-661.
Sellick, C.A., and Reece, R.J. (2005). Eukaryotic transcription factors as direct nutrient sensors. Trends Biochem Sci *30*, 405-412.
Servet, C., Silva, N.C.E., and Zhou, D.X. (2010). Histone acetyltransferase AtGCN5/HAG1 is a versatile regulator of developmental and inducible gene expression in Arabidopsis. Molecular Plant *3*, 670-677.
Shedge, V., Davila, J., Arrieta-Montiel, M.P., Mohammed, S., and Mackenzie, S.A. (2010). Extensive rearrangement of the Arabidopsis mitochondrial genome elicits cellular conditions for thermotolerance. Plant Physiology *152*, 1960-1970.
Sinclair, D.A., and Guarente, L. (1997). Extrachromosomal rDNA circles - A cause of aging in yeast. Cell *91*, 1033-1042.
Smith-Hammond, C.L., Swatek, K.N., Johnston, M.L., Thelen, J.J., and Miernyk, J.A. (2014). Initial description of the developing soybean seed protein Lys-N(epsilon)-acetylome. Journal of Proteomics *96*, 56-66.
Stitt, M. (1999). Nitrate regulation of metabolism and growth. Current Opinion in Plant Biology *2*, 178-186.
Sunderhaus, S., Dudkina, N.V., Jansch, L., Klodmann, J., Heinemeyer, J., Perales, M., Zabaleta, E., Boekema, E.J., and Braun, H.P. (2006). Carbonic anhydrase subunits form a matrix-exposed domain attached to the membrane arm of mitochondrial complex I in plants. The Journal of Biological Chemistry *281*, 6482-6488.
Tao, R.D., Coleman, M.C., Pennington, J.D., Ozden, O., Park, S.H., Jiang, H.Y., Kim, H.S., Flynn, C.R., Hill, S., McDonald, W.H., *et al.* (2010). Sirt3-mediated deacetylation of evolutionarily conserved lysine 122 regulates MnSOD activity in response to stress. Molecular Cell *40*, 893-904.
Templeton, G.W., and Moorhead, G.B. (2004). A renaissance of metabolite sensing and signaling: from modular domains to riboswitches. Plant Cell *16*, 2252-2257.
Tissenbaum, H.A., and Guarente, L. (2001). Increased dosage of a sir-2 gene extends lifespan in Caenorhabditis elegans. Nature *410*, 227-230.
Umbach, A.L., Zarkovic, J., Yu, J.P., Ruckle, M.E., McIntosh, L., Hock, J.J., Bingham, S., White, S.J., George, R.M., Subbaiah, C.C., *et al.* (2012). Comparison of Intact Arabidopsis thaliana leaf transcript profiles during treatment with inhibitors of mitochondrial electron transport and TCA Cycle. Plos One *7*.
Usadel, B., Blasing, O.E., Gibon, Y., Retzlaff, K., Hohne, M., Gunther, M., and Stitt, M. (2008). Global transcript levels respond to small changes of the carbon status during progressive exhaustion of carbohydrates in Arabidopsis rosettes. Plant Physiology *146*, 1834-1861.
Vaara, M. (1992). Agents That Increase the Permeability of the Outer-Membrane. Microbiol Rev *56*, 395-411.
Van Aken, O., Zhang, B., Carrie, C., Uggalla, V., Paynter, E., Giraud, E., and Whelan, J. (2009). Defining the mitochondrial stress response in Arabidopsis thaliana. Molecular Plant *2*, 1310-1324.
van Schooten, B., Testerink, C., and Munnik, T. (2006). Signalling diacylglycerol pyrophosphate, a new phosphatidic acid metabolite. Bba-Mol Cell Biol L *1761*, 151-159.

Vanlerberghe, G.C., and McIntosh, L. (1994). Mitochondrial electron transport regulation of nuclear gene expression. Studies with the alternative oxidase gene of tobacco. Plant Physiology *105*, 867-874.
Vanlerberghe, G.C., and McIntosh, L. (1996). Signals regulating the expression of the nuclear gene encoding alternative oxidase of plant mitochondria. Plant Physiology *111*, 589-595.
Vanlerberghe, G.C., and McIntosh, L. (1997). ALTERNATIVE OXIDASE: From gene to function. Annual Review of Plant Physiology and Plant Molecular Biology *48*, 703-734.
Vellosillo, T., Aguilera, V., Marcos, R., Bartsch, M., Vicente, J., Cascon, T., Hamberg, M., and Castresana, C. (2013). Defense activated by 9-lipoxygenase-derived oxylipins requires specific mitochondrial proteins. Plant Physiology *161*, 617-627.
Wagner, G.R., and Payne, R.M. (2013). Widespread and enzyme-independent N-is an element of-acetylation and N-is an element of-succinylation of proteins in the chemical conditions of the mitochondrial matrix. Journal of Biological Chemistry *288*, 29036-29045.
Wang, Y., Liu, X., Laurini, E., Posocco, P., Ziarelli, F., Fermeglia, M., Qu, F., Pricl, S., Zhang, C.C., and Peng, L. (2014). Mimicking the 2-oxoglutaric acid signalling function using molecular probes: insights from structural and functional investigations. Organic and Biomolecular Chemistry.
Wang, Q., Zhang, Y., Yang, C., Xiong, H., Lin, Y., Yao, J., Li, H., Xie, L., Zhao, W., Yao, Y.*, et al.* (2010). Acetylation of metabolic enzymes coordinates carbon source utilization and metabolic flux. Science *327*, 1004-1007.
Weinert, B.T., Iesmantavicius, V., Moustafa, T., Scholz, C., Wagner, S.A., Magnes, C., Zechner, R., and Choudhary, C. (2014). Acetylation dynamics and stoichiometry in Saccharomyces cerevisiae. Molecular Systems Biology *10*, 716.
Weinert, B.T., Iesmantavicius, V., Wagner, S.A., Scholz, C., Gummesson, B., Beli, P., Nystrom, T., and Choudhary, C. (2013). Acetyl-phosphate is a critical determinant of lysine acetylation in E. coli. Mol Cell *51*, 265-272.
Weinert, B.T., Wagner, S.A., Horn, H., Henriksen, P., Liu, W.R., Olsen, J.V., Jensen, L.J., and Choudhary, C. (2011). Proteome-wide mapping of the Drosophila acetylome demonstrates a high degree of conservation of lysine acetylation. Science Signaling *4*, ra48.
Wellen, K.E., Hatzivassiliou, G., Sachdeva, U.M., Bui, T.V., Cross, J.R., and Thompson, C.B. (2009). ATP-Citrate lyase links cellular metabolism to histone acetylation. Science *324*, 1076-1080.
Whippo, C.W., and Hangarter, R.P. (2005). A brassinosteroid-hypersensitive mutant of BAK1 indicates that a convergence of photomorphogenic and hormonal signaling modulates phototropism. Plant Physiology *139*, 448-457.
Wold, F. (1981). In vivo chemical modification of proteins (post-translational modification). Annual Review of Biochemistry *50*, 783-814.
Wolffram, S., Zimmermann, W., and Scharrer, E. (1993). Transport of tricarballylate by intestinal brush-border membrane vesicles from steers. Experimental Physiology *78*, 473-484.
Woodson, J.D., and Chory, J. (2008). Coordination of gene expression between organellar and nuclear genomes. Nat Rev Genet *9*, 383-395.
Wu, X., Oh, M.H., Schwarz, E.M., Larue, C.T., Sivaguru, M., Imai, B.S., Yau, P.M., Ort, D.R., and Huber, S.C. (2011). Lysine acetylation is a widespread protein modification for diverse proteins in Arabidopsis. Plant Physiology *155*, 1769-1778.
Wu, Y.T., Lee, H.C., Liao, C.C., and Wei, Y.H. (2013). Regulation of mitochondrial F(o)F(1)ATPase activity by Sirt3-catalyzed deacetylation and its deficiency in human cells harboring 4977bp deletion of mitochondrial DNA. Bba *1832*, 216-227.
Xu, F., Yuan, S., and Lin, H.H. (2011). Response of mitochondrial alternative oxidase (AOX) to light signals. Plant Signaling and Behavior *6*, 55-58.

Yang, L., Vaitheesvaran, B., Hartil, K., Robinson, A.J., Hoopmann, M.R., Eng, J.K., Kurland, I.J., and Bruce, J.E. (2011). The fasted/fed mouse metabolic acetylome: N6-acetylation differences suggest acetylation coordinates organ-specific fuel switching. Journal of Proteome Research *10*, 4134-4149.
Yang, M., Soga, T., Pollard, P.J., and Adam, J. (2012). The emerging role of fumarate as an oncometabolite. Frontiers in Oncology *2*, 85.
Yoshida, K., Noguchi, K., Motohashi, K., and Hisabori, T. (2013). Systematic exploration of thioredoxin target proteins in plant mitochondria. Plant and Cell Physiology *54*, 875-892.
Zhao, S.M., Xu, W., Jiang, W.Q., Yu, W., Lin, Y., Zhang, T.F., Yao, J., Zhou, L., Zeng, Y.X., **Li, H.,** ***et al***. (2010). Regulation of Cellular Metabolism by Protein Lysine Acetylation. Science *327*, 1000-1004.

VI. Declaration of Own contributions

[1] Schwarzländer M, **König AC**, Sweetlove LJ, Finkemeier I. The impact of impaired mitochondrial function on retrograde signalling: a meta-analysis of transcriptomic responses. J Exp Bot. 2012; 63(4):1735-50

König AC contributed with a literature research and helped with writing of the manuscript.

[2] Finkemeier I, **König AC**, Heard W, Nunes-Nesi A, Pham PA, Leister D, Fernie AR, Sweetlove LJ. Transcriptomic analysis of the role of carboxylic acids in metabolite signaling in Arabidopsis leaves. Plant Physiol. 2013; 162(1):239-53

König AC conducted the effector treatment experiments, RNA isolation, cDNA synthesis, and QRT-PCR together with Finkemeier I (Fig.2, 4). König AC conducted the effector treatment with the citrate analog tricarballylate, RNA isolation, cDNA synthesis, QRT-PCR and data analysis (Fig. 5). König AC contributed to writing of the manuscript.

[3] Schmidtmann E, **König AC**, Orwat A, Leister D, Hartl M, Finkemeier I. Redox regulation of Arabidopsis mitochondrial citrate synthase. Mol Plant. 2014; 7(1):156-69

2D-BN-PAGE was performed by König AC (Fig. 3 A) as well as Western blots of diagonal 2D-SDS-PAGE of citrate synthase from Arabidopsis mitochondria (Fig. 6 A). Working theory and model was created by König AC (Fig. 7). König AC contributed to writing of the manuscript and composed all figures in this publication.

[4] Braun HP, Binder S, Brennicke A, Eubel H, Fernie AR, Finkemeier I, Klodmann J, **König AC**, Kühn K, Meyer E, Obata T, Schwarzländer M, Takenaka M, Zehrmann A. The life of plant mitochondrial complex I. Mitochondrion. 2014 pii: S1567-7249(14)00020-8

König AC performed in silico data analysis on complex I posttranslational modifications as well as presequences analysis of complex I subunits in Arabidopsis and rice (Supp. table 4).

[5] **König AC** *, Hartl M*, Pham PA, Laxa M, Boersema PJ, Orwat A, Kalitventseva I, Plöchinger M, Braun HP, Leister D, Mann M, Wachter A, Fernie AR, Finkemeier I. The Arabidopsis class II sirtuin is a lysine deacetylase and interacts with mitochondrial energy metabolism. Plant Physiol. 2014; 164(3):1401-14. (*both authors contributed equally to the work)

Protoplast isolation and fluorescent microscopy analysis were performed by König AC as well as Western blot analysis of SRT2 abundance (Fig. 2 A, B). Mitochondria isolation, 2D-BN-PAGE, and Western blot analysis were done by König AC as well as graphic design (Fig. 4). Mitochondria isolation, pull-down experiment with antibody specific for Arabidopsis SRT2 and antibody specific for GFP were done by König AC (Fig. 5 A, B). Scheme of the AAC carrier protein was modeled and graphically designed by König AC (Fig.5 D). ATP, ADP measurements and 14C-ADP uptake into isolated mitochondria were performed by König AC as well as statistical analysis and graphic design (Fig. 6 D, E, F, G). Theory and working model

was created by König AC (Fig. 7). König AC wrote materials and methods for own experiments. König AC contributed overall with writing of the manuscript and experimental design.

[6] **König AC**, Hartl M, Boersema PJ, Mann M, Finkemeier I. The mitochondrial lysine acetylome of Arabidopsis. Mitochondrion. 2014 pii: S1567-7249

All experiments were performed by König AC apart from LC-MS/MS analysis itself and generation of the sequence logo (Fig. 3). The publication was written by König AC with the help of Hartl M and Finkemeier I. The figures were graphically designed by König AC. Experiments were designed by König AC under the guidance of Finkemeier I.

[7] Hartl M *, **König AC** *, Finkemeier I. Identification of lysine-acetylated mitochondrial proteins and their acetylation sites. Submitted to Spinger, Methods in Molecular Biology on Plant Mitochondria. (*both authors contributed equally to the work)

Summary and introduction was written by König AC with the help of Hartl M and Finkemeier I. The method for detecting lysine acetylation in mitochondrial protein complexes of Arabidopsis by 2D BN/SDS-PAGE and Western blot analysis was established and written by König AC.

VII. Curriculum Vitae

Name: Ann-Christine König
Date of Birth: 11th July 1984, Dieburg
Nationality: German

EDUCATION

Since 01/2014 **Ph.D. study in Plant Physiology, Max Planck Institute for plant breeding in Cologne (AG Finkemeier)**

12/2010 -12/2013 **Ph.D. study in Plant Physiology, Ludwig-Maximilians University Munich (AG Leister, AK Finkemeier)**

- Research project: "Metabolite sensing and signalling in plant mitochondria."

09/2009 - 06/2010 **Diploma thesis in Plant Physiology, Ludwig-Maximilians University Munich (AG Leister, AK Bolle)**

- Research project: "The Role of Phosphatases in the Phytochrome-A-Signal Transduction". (final mark: 1.3)

09/2007 - 06/2008 **ERASMUS scholarship, University of Aberdeen, Scotland**

- Courses in: Genetics, the molecular control of cell function, basic molecular technologies for biologists, the molecular biology of the cell.

10/2006- 06/2010 **Main study period "Diplom-Biologie", Ludwig-Maximilians University Munich**

- Specialized subjects and final marks: Plant Physiology (1.0), Biochemistry (2.0), Cell biology (1.0)

10/2004 - 10/2006 **Intermediate studies "Diplom-Biologie", TU Darmstadt**

1995 - 2004 **Abitur, Secondary School, Lichtenbergschule Darmstadt**

1992 – 1995 **Primary school, Hirschbachschule, Reinheim/Georgenhausen**

SCIENTIFIC WORK EXPERIENCE

02/2011 **Scientific Visitor, Department of Plant Science, University of Oxford (with L. Sweetlove)**

- Microarray experiments: The effect on gene expression caused by the interrelation of organic acid and sugar signaling

06/2010 - 08/2010 **Student research assistant, Plant Physiology, Ludwig-Maximilians University Munich (AK Bolle)**

- DUPLO Projects: genotyping, crossing of *A.thaliana,* protein biochemical methods

11/2010 - 12/2010 **Student research assistant, Plant Physiology, Ludwig-Maximilians University Munich**

- Supervising tutor, practical course for Plant Science I

02/2010 - 03/2010 **Student research assistant, Plant Physiology, Ludwig-Maximilians University Munich**

- Supervising tutor, practical course for plant science II

09/2008 - 11/2008 **Student research assistant, Plant Physiology, Ludwig-Maximilians University Munich (AG Soll, K. Philippar)**

- Isolation of RNA, cDNA synthesis, light cycler, production of an antibody

04/2007 - 07/2007 **Student research assistant, Botany, Ludwig-Maximilians University Munich**

- Supervising tutor, practical course for botanic microscopy

ACHIEVEMENTS AND AWARDS

08/2012 **DAAD Travel Fund**

09/2011 **FEBS Youth Travel Fund**

09/2011 **Poster Price (Bayer Crop science)**

09/2007 **ERASMUS scholarship**

CONFERENCES

09/2011 **FEBS workshop 2011 –Plant Organellar Signaling- from algae to higher plants (August 31 – September, 2011) in Primosten, Croatia.**

- Poster presentation: The role of citrate in mitochondrial retrograde signaling.

08/2012 **Gordon Research Seminar 2012 -Mitochondria & Chloroplasts (July 28-29, 2012) in Bryant University, Smithfield, RI**

- Talk: The role of lysine acetylation in plant mitochondria

Gordon Research Conference 2012 –Mitochondria & Chloroplasts (July 29- August 03, 2012) in Bryant University, Smithfield, United States

- Poster presentation: The role of citrate in mitochondrial retrograde signaling.

05/2013 **8th International Conference for Plant Mitochondrial Biology (May 12-16, 2013) in Rosario, Argentina**

- Poster presentation: The role of citrate in mitochondrial retrograde signaling.

09/2013 **Deutsche Botanikertagung 2013 (September 29 – October 04), University of Tübingen in Germany**

- Poster presentation: Functional characterization of Arabidopsis class II sirtuin (SRT2)

10/2013 **International Closing Meeting of the Research Unit 804, Retrograde Signaling in Plants` (October 13-16, 2013), Ried in Germany**

11/2013 **Helped with organization of Symposium "The life of complex I", Center of advanced studies, LMU Munich**

05/2014 **German Mitochondrial Initiative Meeting (May 12-13, 2014) Bonn in Germany**

VIII. Eidesstattliche Erklärung

Ich versichere hiermit an Eides statt, dass die vorgelegte Dissertation von mir selbständig und ohne unerlaubte Hilfe angefertigt ist. Ich habe keine anderen als die angegebenen Quellen und Hilfsmittel benutzt. Textstellen, die wörtlich oder inhaltlich aus veröffentlichen Schriften entnommen wurden, sind als solche kenntlich gemacht. Ferner erkläre ich, dass die Dissertation nicht ganz oder in wesentlichen Teilen einer anderen Prüfungskommission vorgelegt worden ist. Ich habe mich nicht anderweitig einer Doktorprüfung ohne Erfolg unterzogen und ebenfalls habe ich nicht ohne Erfolg versucht eine Dissertation einzureichen oder mich der Doktorprüfung zu unterziehen.

München, den ....

(Unterschrift)

IX. Danksagung

An dieser Stelle möchte ich mich bei allen Bedanken, die mich die letzten Jahre bei meiner Promotion begleitet und unterstützt haben.

Ein besonderer Dank geht an meine Betreuerin Iris Finkemeier für die Möglichkeit als erste Doktorandin in ihrer Gruppe zu promovieren. Für das tolle Feedback, welches ich während dieser Zeit immer bekommen habe und für die vielen Möglichkeiten an Konferenzen teilzunehmen und mich wissenschaftlich weiterzubilden.

Des Weiteren möchte ich mich bei Dario Leister für die Aufnahme und Unterstützung der AK Finkemeier am Biozentrum Martinsried bedanken.

An nächster Stelle möchte ich Markus Hartl danken für alle Fragen die er mir beantworten musste, sowie für die Geduld mir Vieles zu erklären. Außerdem bedanke ich mich für die Diskussionen über wissenschaftliche, sowie andere wichtige Themen und für die großartigen Publikationen, die wir zusammen geschrieben haben.

Danke auch an Lena Füßl für den Spaß im Labor, aber vor allem auch die Unterstützung bei Experimenten und wissenschaftlichen Fragen, das Korrekturlesen meiner Doktorarbeit und die wilden Theorien über HDA f.

Außerdem geht ein ganz großes Dankeschön an meine Lieblings Ex-Mitbewohnerin Stephanie Otters, für das Korrekturlesen, das geduldige Zuhören wenn ein Vortrag bevorstand und vor allem für die immerzu aufbauenden Worte!

Für die gute und lange Zusammenarbeit im Labor und die vielen Theorien über die Citrat-Synthase möchte ich mich bei Elisabeth Schmidtmann bedanken.

Ein großes Dankeschön möchte ich auch an Anne Orwat richten für die großartige Hilfe bei jeglichen Experimenten (speziell für die immerzu intakten Mitos).

Ich möchte mich bei Hans-Peter Braun bedanken für die gute Zusammenarbeit und dafür, dass ich die Möglichkeit hatte bei den BN-PAGE Spezialisten zu lernen.

Ein Dank auch an alle meine ehemaligen und aktuellen Arbeitskollegen sowie an alle meine Freunde, besonders Hanne Gunnesch, Anja Kleinschmidt, Tine Mucha, Chiara Gandini, Francesca Paieri, Magdalena Plöchinger, Arianna Morosetti, Thomas Plunder, Salar Torabi, Vivien Ahrens, Rebekka Lemb und Stefania Viola.

Für die Hilfe bei der Formatierung meiner Doktorarbeit möchte ich mich bei Marcus Graßelt bedanken.

Bei Kristin Lucia möchte ich mich für das spontane Korrekturlesen meiner Arbeit bedanken!

Ein Dankeschön auch an meinen Freund, Francesco Dighera, für die Geduld beim Zuhören über für ihn höchstwahrscheinlich unverständliche biologische Probleme.

Und zu guter Letzt danke ich meiner Familie, insbesondere meinem Vater, der mir diesen Weg ermöglicht hat.

X. Publications 1-7

Publication 1

The impact of impaired mitochondrial function on retrograde signalling: a meta-analysis of transcriptomic responses.

Schwarzländer M, **König AC**, Sweetlove LJ, Finkemeier I.

(2012)

Journal of Experimental Botany 63(4):1735-50

Journal of Experimental Botany, Vol. 63, No. 4, pp. 1735–1750, 2012
doi:10.1093/jxb/err374 Advance Access publication 30 November, 2011

Journal of Experimental Botany
www.jxb.oxfordjournals.org

RESEARCH PAPER

The impact of impaired mitochondrial function on retrograde signalling: a meta-analysis of transcriptomic responses

Markus Schwarzländer[2,*], Ann-Christine König[1], Lee J. Sweetlove[2] and Iris Finkemeier[1,2,†]

[1] Department of Biology, Ludwig-Maximilians-University Munich, Grosshaderner Strasse 2, D-82152 Planegg-Martinsried, Germany
[2] Department of Plant Sciences, University of Oxford, South Parks Road, Oxford OX1 3RB, UK

* Present address: INRES, University of Bonn, Friedrich-Ebert-Allee 144, D- 53113 Bonn, Germany.
† To whom correspondence should be addressed. E-mail: i.finkemeier@lmu.de

Received 26 August 2011; Revised 18 October 2011; Accepted 25 October 2011

Abstract

Mitochondria occupy a central position in cellular metabolism. Their protein complement must therefore be dynamically adjusted to the metabolic demands of the cell. As >95% of mitochondrial proteins are encoded by nuclear DNA, regulation of the mitochondrial proteome requires signals that sense the status of the organelle and communicate it back to the nucleus. This is referred to as retrograde signalling. Mitochondria are tightly integrated into the network of cellular processes, and the output of mitochondrial retrograde signalling therefore not only feeds back to the mitochondrion, but also regulates functions across the cell. A number of transcriptomic studies have assessed the role of retrograde signalling in plants. However, single studies of a specific mitochondrial dysfunction may also measure secondary effects in addition to the specific transcriptomic output of mitochondrial signals. To gain an improved understanding of the output and role of mitochondrial retrograde signalling, a meta-analysis of 11 transcriptomic data sets from different models of plant mitochondrial dysfunction was performed. Comparing microarray data from stable mutants and short-term chemical treatments revealed unique features and commonalities in the responses that are under mitochondrial retrograde control. In particular, a common regulation of transcripts of the following functional categories was observed: plant–pathogen interactions, protein biosynthesis, and light reactions of photosynthesis. The possibility of a novel mode of interorganellar signalling, in which the mitochondrion influences processes in the plastid and other parts of the cell, is discussed.

Key words: *Arabidopsis*, electron transport chain, microarray, mitochondria, respiration, retrograde signalling, ROS.

Introduction

Plant mitochondria occupy a central role in sustaining cellular ATP supply as well as in a whole variety of other metabolic processes, many of which involve multiple subcellular compartments (reviewed in Sweetlove *et al.*, 2010; Millar *et al.*, 2011). In particular, the processes of respiration in the mitochondrion and photosynthesis in the chloroplast are intimately linked (Raghavendra and Padmasree, 2003; Matsuo and Obokata, 2006; Rasmusson and Escobar, 2007; Nunes-Nesi *et al.*, 2008, 2011). Alterations of mitochondrial respiratory metabolism can have dramatic effects on photosynthesis (Carrari *et al.*, 2003; Dutilleul *et al.*, 2003*a*, *b*; Nunes-Nesi *et al.*, 2005). The coordination of organellar functions requires dynamic adjustment of gene expression by retrograde signalling, during which organellar stimuli regulate nuclear-encoded genes (Butow and Avadhani, 2004; Leister, 2005; Rhoads and Subbaiah, 2007). Retrograde control is necessary as the nucleus encodes most organellar proteins and therefore initially controls most aspects of organellar biogenesis and function. Due to the multitude of organellar functions, a variety of interlinked retrograde pathways can be expected (Leister, 2005). The extent to which different signals can be integrated into common pathways is not clear (Ho *et al.*, 2008).

The first work on mitochondrial retrograde signalling was performed in yeast (Liao and Butow, 1993). Currently, different types of signalling molecules and pathways

(mTOR, RTG pathway, hypoxic signalling, and intergenomic signalling) are considered to play a role in transducing the physiological state of mitochondria to the nucleus in yeast (Butow and Avadhani, 2004; Liu and Butow, 2006; Ramanathan and Schreiber, 2009; Woo *et al.*, 2009). It is likely that the basic mitochondrial signalling strategies follow similar principles in plants.

Important progress has been made in the past two decades towards understanding plastid-to-nucleus signalling in plants (reviewed in Pesaresi *et al.*, 2007; Woodson and Chory, 2008; Kleine *et al.*, 2009). However, only little is known about the retrograde signalling pathway(s) from the mitochondria to the nucleus (Nott *et al.*, 2006; Rhoads and Subbaiah, 2007). Mitochondrial alternative oxidase 1 (AOX1a) was the first nuclear gene that was shown to be retrograde regulated and mainly in the context of the response to stress (Vanlerberghe and McIntosh, 1994, 1996; Djajanegara *et al.*, 2002; Gray *et al.*, 2004; Dojcinovic *et al.*, 2005). Recently, the transcription factor (TF) ABI4 was identified as a repressor of *AOX1a* which is de-repressed under rotenone treatment (Giraud *et al.*, 2009). ABI4 is also a regulator of plastid retrograde signalling to repress photosynthetic gene expression (Koussevitzky *et al.*, 2007; Woodson and Chory, 2008). Thus both retrograde signalling pathways may feed into the abscisic acid (ABA) signalling pathway which is intimately linked to carbohydrate signalling, and both organelles are hubs of energy and carbohydrate metabolism (Dekkers *et al.*, 2008). Although ABI4 represents one of the downstream components of a mitochondrial retrograde signalling pathway, the actual sensors within the organelle and second messengers of the signalling cascade are still unknown.

Several recent studies have compared publically available microarray data, to analyse the regulation of organellar genes (nuclear encoded or organellar encoded) under various stress conditions (Van Aken *et al.*, 2009; Leister *et al.*, 2011). However, organelles are tightly connected in the network of cellular processes, and changes in their biochemistry will have an impact at the whole-cell level. Therefore, not only nuclear-encoded organellar genes can be regulated in response to retrograde signals, but also genes associated with any cellular location and function. With the aim of unravelling common targets and pathways that are regulated by modulations in mitochondrial status, a meta-analysis of 11 transcriptomic data sets in which respiratory function was impaired in different ways has been performed.

Materials and methods

Plant materials

All *Arabidopsis thalina* lines used in this study were the Columbia ecotype. PrxII F-KO and pOpOFF2(kan)::MSD1 have been described previously (Finkemeier *et al.*, 2005; Schwarzländer *et al.*, 2011). For all experiments, surface-sterilized seeds were plated on 0.7% (w/v) agar plates supplemented with half-strength Murashige and Skoog (MS) medium.

Seedlings were grown in a controlled growth chamber with a 14/10 h day/night cycle (21/19 °C) at a light intensity of 50 μmol m^{-2} s^{-1}. Rosette tissue was used for the experiments at an age of 3 weeks.

Effector treatments

Antimycin A (AA) and dexamethasone were purchased from Sigma-Aldrich (Gillingham, Dorset, UK). Stock solutions were prepared in ethanol (EtOH; AA) or dimethylsulphoxide (DMSO; dexamethasone). For treatments, stocks were diluted in 0.01% Tween-20 to 20 μM (AA) and 10 μM (dexamethasone) final concentrations, respectively. Effectors were sprayed using an atomizer (AA) or painted (dexamethasone) onto plants. For AA treatments, controls were performed with 0.01% Tween-20 and the appropriate amount of solvent (EtOH). Seedlings were dark-adapted for 2 h prior to treatments and were kept in the dark for the duration of the AA treatment.

Microarray experiments

For microarray experiments, rosette material was harvested and flash-frozen in liquid nitrogen. Total RNA was extracted using TRIZOL reagent (Invitrogen Ltd, Paisley, UK). cDNA preparation and labelling was carried out using the 3DNA Array 50 kit (version 2, Genisphere Inc., Hatfield, USA) according to the manufacturer's instructions. Cy3- or Cy5-labelled cDNA probes were hybridized against 29k Arabidopsis Oligonucleotide Microarrays (http://ag.arizona.edu/microarray). Four biological replicates were analysed including two inversions of the labelling dye to avoid bias. Microarrays were scanned using an Affymetrix 428 Array scanner and acquisition software according to the manufacturer's instructions. After scanning, images were analysed in Genepix Pro Version 4.1 software (Molecular Devices, Sunnyvale, CA, USA) checking each spot individually. Raw data were saved as a.gpr-file and converted into a.mev-file using the Express Converter software (version 1.9, Dana Faber Cancer Institute, Boston, MA, USA). Data were normalized using the lowess (locfit) algorithm and block normalization in the MIDAS software (version 2.19, Dana Faber Cancer Institute, Boston, MA, USA). Normalized data were quality controlled in a spreadsheet file, and elements with median intensity <2 SDs from the mean of all median background values were discarded; in a case where one channel was discarded due to this criterion but the other was >10 SDs from the background, the element was retained; duplicates in the data set were removed by averaging intensity values, and ratio data were generated using the FiRe macro (Beckers and Conrath, 2006; Garcion *et al.*, 2006). The data sets were deposited at the EBI ArrayExpress database (accessions E-TABM-64, -1196, and -1197) according to the MIAME guidelines.

Microarray data of the published experiments were downloaded as processed files from the EBI ArrayExpress database (www.ebi.ac.uk) or the Gene Expression Omnibus database (GEO, http://www.ncbi.nlm.nih.gov). Experimental details and accession numbers can be found in the original publications as indicated in Table 1. Due to the heterogeneity of the experimental set-up of the different integrated experiments (such as sufficient numbers of replicates and microarray platforms), no careful statistical analysis could be performed. Instead microarrays were all analysed after the following criteria: only transcripts that were present in at least three replicates (two in cases where only two data sets were available) with a coefficient of variation <50% were used. Relative expression values were calculated and expressed as log2-transformed mean ratio. Hierarchical cluster analysis was performed using the algorithm for average linkage clustering with a Pearson correlation integrated in the MeV v.4.7.3 microarray software suite (Saeed *et al.*, 2006). Functional class scoring was implemented using MapMan software (Usadel *et al.*, 2005) applying the Hochberg correction. Co-expression networks were analysed using the Atted-II webinterface (Obayashi *et al.*, 2011).

Table 1. Overview of microarray experiments used in the meta-analysis: for each, the mitochondrial target is indicated. The numbers in parentheses indicate the type of mitochondrial impairment as shown in Fig. 1.Transgenic lines, tissues, treatments, microarray platforms, and source publications are indicated. n = number of replicates.

Experiment	Mitochondrial target	Genetic background	Plant tissue	Treatment	Time points	n	Microarray platform	Publication
Antimycin A	Inhibiton of complex III (3)	WT (Col)	Rosettes, 3 weeks	20 μM antimycin A	2 h	4	Galbraith 29k	This study
Antimycin A (*prxII F*)	Inhibiton of complex III (3)	*prxII F* (Col)	Rosettes, 3 weeks	20 μM antimycin A	2 h	4	Galbraith 29k	This study
aox1a	Loss of alternative oxidase (2)	*aox1a* (SALK_084897) (Col)	Leaves, 4 weeks	None	–	2	Affymetrix ATH1	Giraud *et al.* (2008)
uATPase9	Loss of mitochondrial ATP synthase (4)	*AP3:u-ATP9*, *A9:u-ATP9*	Flowers stage 12	None	–	4	Galbraith 29k	Busi *et al.* (2011)
msd1-RNAi	Loss of MSD1 protein (6)	pOpOFF2(kan)::*MSD1*, pOpOFF2(kan)::*LUC* (Col)	Rosettes, 3 weeks	None (10 μM dexamethasone for RNAi induction)	12 d	4	Galbraith 29k	This study
msh1×*recA*	Mitochondrial genome rearrangment (5)	*msh1*×*recA3* (Col)	Aboveground tissue, 8 weeks	None	–	2	Affymetrix ATH1	Shedge *et al.*, (2010)
Complex I	Loss of complex I (1)	*ndufs4*, *ndufa1* (Col)	Leaves, 6 weeks	None	–	3	Affymetrix ATH1	Meyer *et al.* (2009)
Oligomycin	Inhibition of ATP-synthase (4)	WT cell culture (Ler)	Cell culture, 4 d light	1.25 μM oligomycin	3 h	2	Affymetrix ATH1	Clifton *et al.* (2005)
Rotenone	Inhibition of complex I (1)	WT cell culture (Ler)	Cell culture, 4 d light	40 μM rotenone	3 h	2	Affymetrix ATH1	Clifton *et al.* (2005)

WT, wild type; Col, Columbia; Ler, Landsberg erecta; kan, kanamycin.

Results and Discussion

Mitochondrial dysfunction induces transcript changes in diverse transcriptome data sets

Eleven transcriptome data sets were selected that had been generated from various *Arabidopsis* tissues and ages (Table 1) in which either mitochondrial function was impaired genetically or the mitochondrial respiratory chain was inhibited at different points by short-term chemical treatment (Table 1, Fig. 1). Short-term application of respiratory inhibitors has the advantage of avoiding pleiotropic or acclimation responses which are observed in stable mutants. However, a possible drawback of using inhibitors is the degree of uncertainty about specificity of the agent, and special care must be taken in the design of experiments to use adequate concentrations, conditions, and controls. By analysing data sets from both types, the aim was to reveal commonalities and differences in transcriptional regulation triggered by mitochondrial dysfunction, and transcriptomic changes were interpreted as readout of mitochondrial signalling.

Eight of these transcriptomic studies have previously been published (oligomycin A and rotenone, Clifton *et al.*, 2005; *aox1a*, Giraud *et al.*, 2008; *ndufs4* and *ndufa1*, Meyer *et al.*, 2009; *msh1*×*recA*, Shedge *et al.*, 2010; *ap3:u-ATP9* and *ap9:u-ATP9*, Busi *et al.*, 2011). In addition, three unpublished data sets were included from the authors' own work (Table 1). A transcriptomic data set for an inducible RNA interference (RNAi) line against the mitochondrial manganese superoxide dismutase MSD1 was generated (Morgan *et al.*, 2008; Schwarzländer *et al.*, 2011) as well as two data sets for complex III inhibition by AA in the wild-type (WT) background and in the peroxiredoxinII F (*prxII F*) knockout mutant (Finkemeier *et al.*, 2005).

Because of the heterogeneity of the experimental systems/conditions and microarray platforms used, no valid statistical comparison of the array data sets could be performed (Gadjev *et al.*, 2006). Instead transcriptomic data sets were compared on the basis of the relative fold changes (mutant/WT or treatment/control). Comparable data sets were generated using stringent criteria on the coefficient of variation of replicates to calculate the fold changes (log2): transcript data were only included in the analysis if they were present in at least three biological replicates (two in cases where only two replicates were available) and if the coefficient of variance was <50% (Supplementary Table S1 available at *JXB* online). A cut-off value of ±0.5 (log2) was used to define a transcript as regulated. Higher cut-off values can give more robust results on single transcripts, but they can overlook milder but coordinated changes of functionally related transcript groups that are biologically highly relevant (e.g. Leakey *et al.*, 2009). Furthermore, for all data sets the same three-step strategy of analysis was used: (i) in a hierarchical cluster analysis unique transcripts were revealed as a measure for specificity of a certain mitochondrial dysfunction; (ii) the identified transcripts were analysed in a co-expression analysis with 1388 microarrays using the network drawer function of Atted-II to assess linked regulation of the selected transcripts and to extrapolate the functional output of the perturbed signalling pathway; and (iii) to reveal commonalities in the response of functional gene groups a class

scoring algorithm with Hochberg correction, as implemented in the MapMan software, was applied for whole data sets.

Table 2 shows the number of transcripts which changed >0.5-fold (log2 ratio) in all 11 data sets as well as the number of overlapping transcripts between two respective experiments. While six of the data sets (*aox1a*, *msh1*×*recA3*, *ndufa1*, *ndufs4*, oligomycin, and rotenone) contained ~3000–4000 transcripts passing the threshold of 0.5-fold regulation, five data sets contained <1000 including the authors' own three data sets [AA (WT), AA (*prxII F*), and *msd1*] with only 30–100 regulated transcripts. Even though the total number of overall detected transcripts from the authors' own data sets using the 29K Galbraith arrays was only about half of the amount of those detected on the Affymetrix chips, the percentage of regulated transcripts was still much less (0.5–1.6% of all detected transcripts regulated in comparison with 18–29%; see Table 2). Importantly, this was not due to an experimental artefact from using the 29K Galbraith array system, as ~9–14% of all transcripts were differentially regulated in the *u-ATP9* mutants which used the same array platform (Busi *et al.*, 2009). Furthermore, this array system was used in a previous study revealing drastic effects on transcript abundances after short-term menadione treatments which provoked oxidative stress in *Arabidopsis* roots (Lehmann *et al.*, 2009). The small transcript changes therefore represent a genuinely milder transcript response compared with the other systems, which most probably reflects the absence of a general stress or acclimation.

The 11 microarray data sets can be grouped according to their physiological effects on mitochondrial functions (Fig. 1).

(i) Complex I

Three data sets assessed defects of complex I on transcript levels. Complex I was affected in abundance in the *ndufs4*/*ndufa1* mutant leaves (Meyer *et al.*, 2009), and its activity was inhibited by 3 h short-term treatment of autotrophic cell cultures with 40 μM rotenone (Clifton *et al.*, 2005), respectively. Thus, similarities in transcriptional regulation observed in these studies which were not observed in the other studies may result from a retrograde signal connected with complex I activity. A total of 24 and 27 transcripts were up- and down-regulated, respectively, exclusively in this system (0.5-fold; Supplementary Table S1 at *JXB* online). The connection between these transcripts was analysed using the network drawer of Atted II. Interestingly, 14 of the up-regulated transcripts [including alternative NADPH dehydrogenase 2 (*NDA2*, At2g29990), S-locus lectin protein kinase (At1g11330, At1g61360), downy mildew resistant 6 (*DMR6*, At5g24530), nodulin MtN-21-related (At3g56620), chitinase (At4g01700), and resistant to *P. syringae* 4 (*RPS4*, At5g45250)] were co-expressed in a network together with 144 transcripts, many of which are related to plant–pathogen interactions such as WRKY33 (At2g38470), MKK2 (At4g29810), MEK1 (At4g26070), MPK4 (At4g01370), MAPKKK10 (At4g08470), BAK1 (At4g33430), NPR1 (At1g64280), and PAD4 (At3g52430) (Supplementary Fig. S1). NPR1 and PAD4 are known regulators of the salicylic acid (SA)-dependent defence pathway, and PAD4 was reported to be involved in *AOX1a*-dependent transcript regulation (Ho *et al.*, 2008). Twelve other up-regulated transcripts could be assigned to smaller co-expression networks that are closely linked to the large network and are related to biosynthesis of secondary metabolites, stilbenoid, diarylheptanoid, and gingerol biosynthesis, and glutathione metabolism, respectively. From 27 down-regulated transcripts, 18 [including phytochrome A (At1g09570), β-glucosidase 40 (At1g26560), WNK7 protein kinase (At1g49160), cellulose synthase 2 (*CESA2*, At4g39350), LRR-protein (At3g17640), VTC4 (At3g02870),

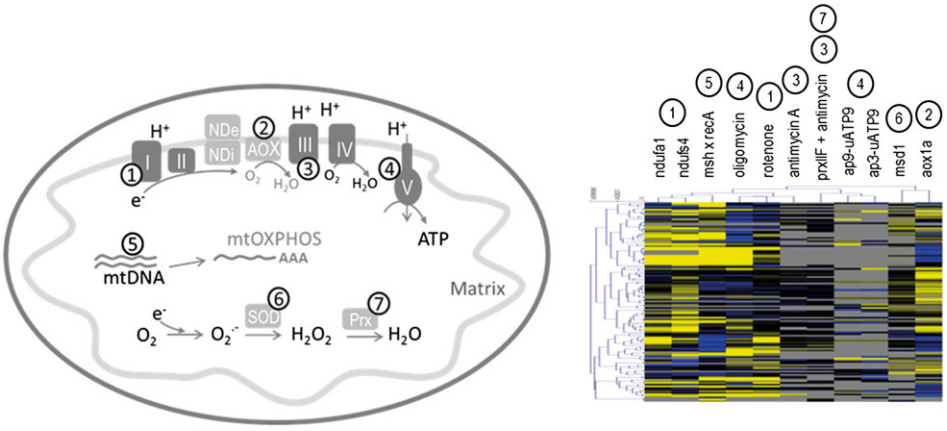

Fig. 1. Overview of microarray experiments dealing with mitochondrial impairments. Numbers depict treatments or mutations affecting mitochondrial targets. (1) Complex I: *ndufa1*, *ndufs4*, and rotenone. (2) AOX: *aox1a*. (3) Complex III: antimycin A. (4) Complex V: *AP3-uATP9*, *AP9-uATP9*, and oligomycin, (5) mtDNA: *msh1*×*recA*. (6) MnSOD: *msd1*. (7) PeroxiredoxinII F: *prxII F*. The corresponding publications are given in Table 1. The hierarchical cluster analysis of 122 transcripts coding for mitochondrial electron transport proteins was performed using the algorithm for average linkage clustering with a Pearson correlation integrated in the MeV v.4.7.3 microarray software suite (Saeed *et al.*, 2006). Yellow and blue indicate up- and down-regulated transcripts (more than ±0.5 log2 fold) in transgenic or treated plants in comparison with wild-type or untreated transgenic plants, respectively. Grey corresponds to missing values, and black indicates no regulation. The dendrogram on the top indicates the relationship of samples across the displayed transcripts.

Table 2. Overview of transcriptome changes in single data sets and overlaps between two experiments
Only transcripts that passed a ±0.5-fold (log2) threshold were included. Data were processed as described in the Materials and methods. Overlapping transcripts are not necessarily regulated in the same direction. For processed data, see Supplementary Table S1 at *JXB* online.

Experiment	Total no. greater than ±0.5-fold	% of total transcripts included in analysis	*msh1*×*recA3*	*ndufs4*	*ndufa1*	*AP3-uATP9*	*AP9-uATP9*	*aox1a*	*msd1*	*AA (prxII F)*	AA	Oligomycin	Rotenone
msh1×*recA3*	3878	18%		1355	1292	155	94	748	14	39	15	1049	899
ndufs4	3654	27%	1355		1892	154	97	639	8	22	8	815	745
ndufa1	3396	25%	1292	1892		151	98	670	10	16	5	807	741
AP3-uATP9	948	9%	155	154	151		261	120	2	5	2	148	111
AP9-uATP9	647	14%	94	97	98	261		81	1	7	1	108	98
aox1a	2944	22%	748	639	670	120	81		7	20	6	713	608
msd1	41	0.5%	14	8	10	2	1	7		0	0	12	8
AA (*prxII F*)	109	1.6%	39	22	16	5	7	20	0		18	36	32
AA	36	0.6%	15	8	5	2	1	6	0	18		9	7
Oligomycin	3947	29%	1049	815	807	148	108	713	12	36	9		1768
Rotenone	3280	24%	899	745	741	111	98	608	8	32	7	1768	

methyltransferase MTA-70 family protein (At1g19340), and an AP2-domain transcription factor (At1g21910) were part of a large co-expression network with 170 more genes that are related to light signalling, cold-regulated genes, plant–pathogen interactions, cyanoaminoacid metabolism, the cell wall, and cytoskeleton-related elements which are part of a phagosome (beta 6, 5, and 8-tubulin). The strong interaction of induced and repressed transcripts in large co-expression networks suggests a regulatory pathway related to biotic defence, which seemed to be triggered as a result of complex I dysfunction (for a review on the role of mitochondrion in biotic stress, see Amirsadeghi *et al.*, 2007).

A recent study by Gleason *et al.* (2011) provided genetic proof that complex II of the mitochondrial electron transport chain (ETC) is associated with mitochondrial reactive oxygen species (ROS) production and the propagation of plant stress and defence responses. A higher electron flux through complex II in the complex I mutant, which also showed increased ROS levels (Meyer *et al.*, 2009), may actually trigger the observed transcriptomic response. Furthermore, the early stress defence marker gene *GSTF8*, which was used in the study by Gleason *et al.* (2011), was strongly induced after rotenone treatment. As the transcriptomic data from the complex II mutant (Gleason *et al.*, 2011) were only available after completion of this analysis, they were not included here.

(ii) AOX

Giraud *et al.* (2008) used a knock-out mutant of the *AOX1a* gene which contained no immunodetectable AOX protein to generate a transcriptomic data set. AOX is part of an alternative respiratory pathway specific to plants as well as certain fungi and protists, and by-passes complex III as an electron acceptor from ubiquinol. It acts as an alternative terminal oxidase which reduces oxygen to water without the build up of a proton gradient (Vanlerberghe and McIntosh, 1997). AOX function is particularly important under stress conditions to avoid over-reduction of the ubiquinone pool and increased ROS generation (Maxwell *et al.*, 1999). However, even under non-stress conditions, the AOX makes up ~20–30% of the total cellular respiratory capacity (Gray *et al.*, 2004), and changes in transcript abundance could therefore result from a retrograde signal triggered by a higher flux through the cyanide-sensitive pathway of the ETC or increased coupling of respiration and ATP synthesis. Consequently, a loss of function in AOX may be expected to cause defects opposite to those of other dysfunctional respiratory complexes. In the *aox1a* mutant, 624 and 1179 transcripts were specifically up- or down-regulated, respectively (0.5-fold log2 threshold) (Supplementary Table S1 at *JXB* online). Those 1803 transcripts were from various functional gene classes, with a high representation of cell wall and lipid metabolism, biotic and abiotic stress, polyamine metabolism, degradation of xenobiotics, C1 metabolism, RNA regulation of transcription, and protein synthesis. Giraud *et al.* (2008) reported a significant change of 2985 transcripts for this mutant in comparison with the WT at a similar fold change level as used in this meta-analysis (2944 were detected based on the criteria used), which supports the validity of the analysis. Thus, the loss of AOX1a resulted in a specific transcript response that was mostly independent or even inversely regulated in comparison with the other data sets. This may suggest that the particular path of electron flow through the ETC is critical in mounting the underlying signal.

(iii) Complex III

Two transcriptomic data sets were generated assessing the effect of complex III inhibition. AA treatment for 2 h partly inhibited respiration, as measured by reduction of oxygen uptake by one-third (Schwarzländer *et al.*, 2009). AA inhibits complex III by binding to the 'N' site, strongly stimulating superoxide release (Murphy, 2009). To unravel

effects caused by ROS production, transcriptomic changes caused by AA treatment in a *prxII F* knock-out (*prxII F*) background were also analysed. The peroxidase PrxII F is located in the mitochondrial matrix, and is a key player in mitochondrial antioxidant defence (Finkemeier *et al.*, 2005). The rationale for including this data set was that responses to mitochondrial ROS (mtROS; specifically H_2O_2) are expected to be more pronounced in AA-treated *prxII F* plants than in AA-treated WT plants. In contrast, alteration of mitochondrial energy metabolism, as a result of AA treatment, can be expected to be similar in both AA-treated WT and *prxII F* mutants.

The transcriptomic changes detected in the *prxII F* mutant background (109 transcripts) relative to the WT (36 transcripts) were indeed in line with the expectation of a stronger response in the absence of PrxII F. However, both were relatively subtle compared with the other inhibitor experiments (Table 2). As AA is known to induce programmed cell death upon prolonged exposure, an early time point had been selected to generate the data sets, before major stress responses, such as electrolyte leakage, lipid peroxidation, and glutathione oxidation, were observed (in both the mutant and WT; unpublished data). The fact that more transcripts were regulated in the *prxII F* mutant background after AA treatment compared with the WT is consistent with ROS release upon AA treatment being responsible for the majority of transcriptomic changes rather than the inhibited flux through complex III (and the cyanide-sensitive pathway in general, see above, for AOX). Transcriptomic data of the response of *Arabidopsis* leaves to AA have been published previously by Yu *et al.* (2001), and selected data were published by Rhoads and Subbaiah (2007) using AA treatment for 6 h. Both studies identified ROS generation as the dominant effect of AA on transcript changes. However, Yu *et al.* (2001) described 621 transcripts which were doubled in abundance after 30 min of AA treatment, whereas in the authors' arrays none of the transcripts was increased by >2-fold. This most probably reflects the experimental design in the study of Yu *et al.* (2001) in which AA treatment was administered by floating detached leaves on an AA solution, while control leaves were sampled directly from the plant. Thus, many of the observed changes in transcripts could be a result of tissue wounding and reduced gas exchange during floating rather than due to AA.

In the AA data sets (*prxII F* and WT background), 45 transcripts were induced that were not regulated in any of the other nine data sets. Twenty-one of these 45 transcripts were found in the Atted-II co-expression database and 15 of those were connected with 174 more transcripts in a large co-expression network (again including PAD4, NPR1, BCS1, WRKY33, and WRKY 46) (Supplementary Fig. S1 at *JXB* online). Within this network, transcripts encoding proteins involved in secondary metabolism, plant–pathogen interaction, phenylalanine, tyrosine, and tryptophan biosynthesis, SNARE interactions in vesicular transport, cysteine and methionine metabolism, and ethylene and calcium signalling were detected.

(iv) Complex V

Three data sets included here dealt with the response to reduced mitochondrial ATP synthase (complex V) activity. Complex V activity was inhibited either by short-term oligomycin treatment (2 h) in autotrophic cell cultures (Clifton *et al.*, 2005), or by expression of the unedited form of the ATP synthase subunit 9 in *Arabidopsis* flowers under the control of APETALA 3 (AP3) and the A9 promoter, respectively (Busi *et al.*, 2011). While no effects on cellular respiration were observed after 24 h of oligomycin treatment, the respiration rate was decreased by 50–65% and ATP levels by 35% in flowers of the *u-ATP9* lines (Busi *et al.*, 2011). However, in a different study, short-term oligomycin treatment (1 h, 10 μM) also resulted in a lowered ATP content (by 30%) in tobacco suspension cultures (Wakamatsu *et al.*, 2010). Similar transcript changes between these three data sets thus might have been triggered by a lowered ATP content. Only five transcripts were exclusively regulated by complex V inhibition (four induced, one repressed) and not in the other data sets (Supplementary Table S1 at *JXB* online). Only two of these transcripts, one encoding an unknown protein (At5g47940) and one an armadillo/beta-catenin repeat family protein (At3g01400), were connected with 10 other transcripts [including MKP1 (At3g55270) and bHLH-TF (At5g46760)] in a co-expression network (Supplementary Fig. S1). The low number of transcripts exclusively regulated by complex V dysfunction may suggest that only a low number of transcripts was regulated by inhibition of complex V activity and thus compromised ATP levels. However, a more likely explanation is that the poor overlap resulted from the use of different tissues (cell cultures and flowers) in the two studies. Moreover, ATP levels were most probably perturbed in several of the other experiments as a result of impaired mitochondrial function, such as in the *ndufs4* mutant (Meyer *et al.*, 2009).

(v) mtDNA

One data set analysed in this study was generated from the double mutant *msh1×recA3* that shows severely compromised recombination surveillance of the mitochondrial genome (Shedge *et al.*, 2010). This mutant shows extensive rearrangements in its mitochondrial DNA (mtDNA) along with severely affected development and increased thermotolerance. As mitochondrial-encoded transcript levels were strongly up-regulated in the mutant and many of the recombination sites are within the open reading frames for mitochondrial genes, effects on mitochondrial oxidative phosphorylation (OXPHOS) can be expected (Shedge *et al.*, 2007; Arrieta-Montiel *et al.*, 2009). The *msh1×recA3* data set showed the strongest overlap in regulated transcript number with the other data sets (Table 2). This most probably reflects the fact that the *msh1×recA3* mutant has several defects in mitochondrial physiology that were shared with the other experiments. However, 860 and 537 transcripts were specifically up- and down-regulated, respectively, compared with the

other experiments (Supplementary Table S1 at *JXB* online). These included four strongly up-regulated TFs: two AP2-EREBP TFs (At1g22810; *RAP2.6*, At1g43160), a myb-domain protein (*MYB74*, At4g05100), and a WRKY-TF (*WRKY48*, At5g49520), which were connected in a co-expression network together with 192 transcripts of the categories biosynthesis of secondary metabolites, plant–pathogen interactions, cysteine and methionine metabolism, phenylalanine metabolism, and phenylpropanoid biosynthesis, as well as 30 more TFs of various classes (Supplementary Fig. S1). The *msh1*×*recA3* double mutant can be interpreted as an extreme case of mitochondrial dysfunction. In contrast to other experiments analysed here, drastic changes in growth, development, fertility, and stress resistance have been observed in this mutant (Shedge *et al.*, 2007). Due to the loss of MSH1 and RecA3, many mitochondrial-encoded genes are affected in their expression simultaneously. As most of the mitochondrial-encoded genes are components of the OXPHOS complexes, the integrity of the ETC may be destabilized at different locations simultaneously rather than just a single protein or complex, that usually allows functional bypass. It is therefore not surprising that this mutant also shows the strongest transcriptomic reprogramming compared with the other experiments. The overlap in regulated transcripts with other experiments suggests simultaneous activation of several retrograde signalling pathways, only some of which are activated in the other individual experiments. Interestingly, the strongest transcriptomic overlap was observed with experiments in which complex I was absent or dysfunctional. This provides an interesting correlation as complex I has the highest number of mitochondrial-encoded subunits of all ETC complexes (nine *NAD* genes in most plants including *Arabidopsis*; Rasmusson *et al.*, 1998). Complex I is therefore expected to be particularly prone to misexpression as an outcome of mitochondrial genome rearrangements.

(vi) mtROS

One data set dealt with the loss of the mitochondrial superoxide dismutase (SOD) MSD1 in 3-week-old rosettes of *Arabidopsis* plants. An inducible RNAi approach was chosen to manipulate specifically mtROS levels (Schwarzlander *et al.*, 2011) and to avoid pleiotropic effects that were observed in stable MSD1 antisense lines (Morgan *et al.*, 2008). As a result of induction, MSD1 protein became undetectable by immunoblotting in rosettes after 12 d of dexamethasone treatment in two independent *MSD1*-inducible RNAi lines (*msd1*, lines 1 and 12) compared with the control line [induced line with an RNAi-hairpin specific for luciferase; pOpOff2(kan)::LUC (Wielopolska *et al.*, 2005); data not shown; see Schwarzlander *et al.*, 2011]. In *Arabidopsis*, MSD1 is the only known SOD in the mitochondrial matrix (Kliebenstein *et al.*, 1998; Morgan *et al.*, 2008). Therefore, loss of MSD1 can be expected to cause perturbed $O_2{\cdot}^-$ detoxification. This was reflected in slightly decreased aconitase activity, a marker for superoxide levels (Gardner, 2002), after 12 d of RNAi induction (to 88±4% and 81±3% of the control, respectively). However, no signs of general oxidative stress or acclimatization were detectable in the inducible *msd1* lines, including unchanged electrolyte leakage from plant roots, no changes in the total proteome (except for MSD1 itself), no changes in other SOD protein levels, and an unaffected mitochondrial glutathione redox state (unpublished data). Only 41 transcripts were changed in the *msd1* line (Supplementary Table S1 at *JXB* online). The transcripts which showed the strongest regulation coded for a pathogen-related protein (1.2-fold, *PCC1*, At3g22231), and QQS, a potential regulator of starch biosynthesis (–1.7-fold, *QQS*, At3g30720) (Li *et al.*, 2009), respectively. Although only little is known about QQS function, similar repression has been demonstrated for a variety of biotic and abiotic conditions (Zimmermann *et al.*, 2004). Eight and 11 transcripts were exclusively up- and down-regulated, respectively, in the *msd1* line and were not regulated in the other 10 data sets. Six of the up-regulated transcripts [including three wall-associated kinases (At1g21230, At1g21270, At1g22710), an FKBP-binding protein (At2g14560), and late up-regulated in response to *Hyaloperonospora parasitica* (*LURP1*, At5g48580)] were detected in the AttedII co-expression database. Only two transcripts were connected in a co-expression network with 24 more transcripts. The other four subnetworks were lying in close proximity to these (Supplementary Fig. S1). Several of the co-expressed transcripts included disease resistance proteins (TIR-NBS-LRR class), AAA-ATPase transcripts, and PCC1. Eight of the 11 down-regulated transcripts [including ethylene-responsive AP2-EREBP TF (At5g43410), a MYB-TF (*transparent testa 2*, At5g35550), a transposable element gene (At2g11370), a maternal effect embryo arrest protein (*MEE38*, At3g43160), and damaged DNA-binding protein (*XRCC3*, At5g57450)] did not share a connected co-expression network. However, it was obvious from the functional categories of the transcripts that like in other data sets analysed here genes of pathogen defences were affected in particular. Interestingly, no overlap between the *msd1* and AA data was observed (Table 2), which might hint at distinct mtROS signals produced in these experiments. The relatively mild transcriptomic response to the complete removal of MSD1 protein probably reflects the very specific stimulus of this system. Different from the other studies, the absence of MSD1 does not directly disrupt the OXPHOS machinery and is therefore less likely to cause major respiratory defects. In addition, superoxide is membrane impermeable, which limits the ROS stimulus to the matrix. It is therefore expected that the changes observed in this system are, albeit mild, particularly specific and biologically meaningful.

Marker transcripts for mitochondrial dysfunction

From the above comparisons, a list of marker transcripts that were regulated in response to a specific mitochondrial impairment was generated (Table 3). Transcripts that reflected a general mitochondrial stress response were selected from a comparison of *msh1*×*recA3*, the complex I mutants, as well as oligomycin and rotenone treatments, as the highest overlaps with the strongest log fold changes were observed between those experiments. Transcripts that

Table 3. Marker transcripts for mitochondrial dysfunctions (targets) extracted from the comparison of data sets by hierarchical clustering.
Data were processed as described in the Materials and methods. Expression values are given as fold ratios (log2). Blue and red indicate up- and down-regulation of transcripts, respectively.

Target	AGI code	Description	Rotenone	*ndufs4*	*ndufa1*	AA (*prxII F*)	AA	*aox1a*	Oligomycin	*AP9-uATP9*	*AP3-uATP9*	*msd1*	*msh1xrecA3*
mt oxidative stress	At3g22370	AOX1A	2.3	0.2	0.6	-	0.4	-4.4	2.0	0.0	0.2	0.0	1.2
	At2g41730	Unknown protein	4.6	1.9	1.3	0.0	-	0.5	4.8	-0.2	0.1	0.2	3.8
	At4g37370	CYP81D8	3.8	1.0	0.9	-	-	0.2	4.0	-0.1		0.9	1.7
	At1g32870	ANAC13	1.6	1.0	1.2	-	-	-0.3	1.5	0.0	0.3	-	1.5
	At5g40690	Unknown protein	2.6	2.6	1.3	-	-	-0.3	2.5	0.1	0.3	-	1.0
	At5g59220	PP2C	3.2	1.5	1.4	-	-	-0.1	1.4	-	-	-	3.2
	At1g24090	RNase H domain-containing protein	1.0	1.0	1.0	-	-	-	1.1	-	-	-	1.3
	At2g41380	Embryo-abundant protein-related	1.6	1.5	0.8	-	-	-	1.3	-	-	-	1.1
Complex I	At1g68840	RAV2	2.1	-1.8	-1.3	0.2	-0.2	-0.9	1.6	-	-	0.5	-1.7
	At2g25200	Unknown protein	-2.0	-0.8	-0.8	0.0	0.0	0.3	1.2	-	-	-	-1.5
	At4g17340	TIP2;2	-2.0	-1.6	-1.0	0.0	-0.1	0.3	-1.7	-	-	-0.2	-1.2
	At5g62900	Unknown protein	1.3	1.2	0.9	0.0	-	0.0	0.5	-	-	0.0	-0.2
	At1g63840	C3HC4-type RING finger	3.4	1.4	1.1	-	-		0.4	-	0.1	0.1	0.5
	At4g01700	Chitinase, putative	1.2	1.8	1.9	-0.1	-0.3	0.0		-0.4	0.2	-	0.5
	At3g17640	Leucine-rich repeat	-1.1	-1.2	-1.1	-	-	-		0.1	0.4	-	0.0
	At5g54130	Calcium-binding EF hand	-1.7	-1.2	-1.0	-	-	-0.3	-0.4	-	-	-	-0.2
AOX	At4g15690	Glutaredoxin	-	-	-	0.0	-0.1	3.4	-	-	-	-0.3	-0.1
	At2g40860	PP2C	0.1	0.2	0.2	0.1	-	-2.8	0.3	-	0.2	-	-0.3
	At3g59420	Crinkly4	-	0.3	0.1	-	-	-2.1	-	-	-	-	-0.4
Complex V	At3g01400	Armadillo/beta-catenin repeat	-0.2	-0.3	0.2	-	-0.1	-0.5	0.6	1.0	0.5	0.1	0.0
	At2g22390	RABA4E	0.2	-0.3	-0.1	-	-	0.3	0.7	1.6	0.8	-	0.0
	At5g47940	Unknown protein	0.1	0.0	0.1	-	-	0.1	-0.8	-0.5	-0.7	-	0.3
	At4g30470	Cinnamoyl-CoA reductase-related	0.2	0.4	0.0	-0.1	-	-0.1	0.3	-0.1	-0.2	-	2.1
mtDNA	At1g24807	Anthranilate synthase beta subunit	0.0	0.0	-0.1	0.1	0.1	0.0	0.1	-	-	0.2	1.1
	At4g04340	ERD protein-related	-0.4	-0.4	-0.3	0.0	-0.1	-0.2	-0.1	-0.4	0.0	0.0	-1.0
	At2g31360	ADS2	-0.1	-0.3	-0.3	-0.1	0.0	0.2	0.2	0.1	0.1	0.0	-1.1
	At2g35470	Unknown protein	-0.2	-0.2	0.0	0.0	0.1	-0.1	0.2	0.0	0.0	-0.1	-1.1

were >1-fold (log2; either up- or down-) regulated in all these four experiments were searched. Ten transcripts that matched these criteria were detected: seven of these were up-regulated in all four experiments [RNase H domain-containing protein, At1g24090; NAC domain protein 13 transcription factor (*ANAC13*, At1g32870); embryo-abundant protein-related (At2g41380); CYP81D8 (At4g37370); unknown protein (At5g40690 and At2g41730); and protein phosphatase 2C (*PP2C*, At5g59220)], and one was down-regulated: tonoplast intrinsic protein 2;2 (*TIP2;2*, At4g17340) (Table 3). Those transcripts are considered general mitochondrial stress markers. The 'embryo-abundant protein-related' transcript was identified as a mitochondrial stress defence marker before, which could be confirmed here (Van Aken *et al.*, 2009). Four of the seven up-regulated marker transcripts, including the TF ANAC13, were detected in a co-expression network together with *AOX1a*, the most commonly used marker transcript for mitochondrial dysfunction (Supplementary Fig. S1 at *JXB* online). ANAC13 and both unknown proteins are generally regulated by hydrogen peroxide (Inzé *et al.*, 2011). PP2C was detected in a different co-expression network, and was reported to be highly induced by ABA treatment (Fujita *et al.*, 2009). It functions specifically in SRK2D/E/I-mediated ABA signalling in response to water stress in the vegetative stage of *Arabidopsis* (Fujita *et al.*, 2009). A general mitochondrial stress response appears, therefore, linked to ROS and ABA signalling.

Oxidative stress-related changes in gene expression

The *AOX1a* transcript, which is often used as a readout for mitochondrial retrograde signalling, was strongly [>1-fold (log2)] up-regulated in the *msh1*×*recA3* mutant and upon rotenone and oligomycin treatment as well as to a lesser extent in the complex I mutants and upon AA treatment (0.2o to 0.5-fold) (Table 3). *AOX1a* transcript induction is known to be suppressed by antioxidants, suggesting that ROS play a direct role in signal transduction (Maxwell *et al.*, 2002). Ho *et al.* (2008) identified 10 *cis*-acting regulatory elements (CAREs) in the promoter of the *AOX1a* gene. In a genome-wide search they identified 1141 genes that contained six or more of these CAREs. Most of these genes were regulated by oxidative, abiotic, and biotic stress (Ho *et al.*, 2008). Those genes were searched in the analysed array data sets. A total of 908 were present in at least one of the data sets and 148–165 transcripts of CARE genes were regulated >0.5-fold (log2) upon rotenone treatment and in the complex I and *msh1*×*recA3* mutants, respectively. Only 14 of these transcripts were regulated in *aox1a*; none of those was found to be regulated in the AA data sets, and only a minor number were regulated in the *u-ATP9* and *msd1* mutants (1–4 transcripts). This could hint at CARE gene regulation by a complex I-specific stimulus (complex I is likely to be impaired in *msh1*×*recA3* too, see above). Alternatively, oxidative stress, which is known to impact on CARE genes, was absent in the latter experiments, which is also reflected in a less pronounced transcriptomic response. Oxidative stress signalling is induced by increased ROS generation that leads to oxidative damage of cellular components. It is therefore important to distinguish between oxidative stress signalling and redox signalling, which occurs under non-stress conditions. In principle, there are three types of redox signals: the first derives from the redox state of the quinone pools in the photosynthetic and mitochondrial electron transport chain, the second from thiol-containing redox-active compounds, such as thioredoxins, and the third from ROS themselves (Pfannschmidt, 2003; Apel, 2004; Dietz, 2008). Redox signals of all three categories can be regarded as important candidates in mitochondrial retrograde signalling (Dutilleul *et al.*, 2003*b*). In this case, however, oxidative stress appeared to account for a significant proportion of the signalling stimuli that caused transcriptomic reprogramming in different systems of severe mitochondrial dysfunction.

Transcripts encoding ribosomal proteins and photosynthetic proteins are common targets of mitochondrial dysfunction

Individual marker transcripts are insufficient to get a picture of the actual functional output of mitochondrial signalling. Therefore, orchestrated transcript changes of functionally similar transcript groups were analysed across data sets. A functional class scoring algorithm with Hochberg correction was used, as implemented in the MapMan software (Usadel *et al.*, 2005). Interestingly, the categories 'protein synthesis' (eight data sets), 'photosynthetic light reactions' (eight data sets), 'protein targeting' (seven data sets), 'protein degradation' (five data sets), 'pentatricopeptide (PPR) repeat-containing proteins' (six data sets), and 'plasmamembrane intrinsic proteins (PIPs)' (five data sets) were significantly regulated in the data sets (Supplementary Table S2 at *JXB* online). Importantly, although only minor fold changes were observed in the AA and *msd1* microarrrays, they showed a significant co-regulation of transcripts in the above-mentioned categories (Table 4). Although ~600–900 transcripts were regulated in the *u-ATP9* lines, no significant functional categories were detected in the *AP3-uATP9* line (hence it was not listed in Table 4), and only a few subcategories from protein synthesis, targeting, the cell wall, and the tricarboxylic acid (TCA) cycle were significantly regulated in the *AP9-uATP9* line (Supplementary Table S2).

Although the functional category 'biotic stress' itself was not significantly regulated (except for *msh1*×*recA3*; Supplementary Table S2), a number of functional categories related to plant–pathogen interactions showed significant regulation in most experiments, including 'redox', 'protein degradation', 'MYB-related transcription factors' (five data sets each), 'cell wall', and 'hormone metabolism' (four data sets each) (Fig. S2; Supplementary Table S2 at *JXB* online). This, along with the high representation of individual regulated pathogen-related transcripts, points to plant–pathogen interaction as a general functional target of mitochondrial retrograde regulation.

Table 4. Overview of significantly affected functional classes of gene bins
Mean log2 fold ratios of transcripts were analysed by functional class scoring for each experiment using MapMan software and applying the Hochberg correction (Usadel *et al.*, 2005). Numbers of transcript elements of each bin are indicated and numbers below the experiments indicate significant *P*-values.

Bin	Name	Elements	*msh1×recA3*	*ndufs4*	*ndufa1*	*AP9-uATP9*	*aox1a*	*msd1*	AA (*prxII F*)	AA (WT)	Oligomycin	Rotenone
1	Photosynthesis (PS)	197		3.8E-38			0.0E+00	2.7E-02	7.6E-20	2.4E-08		
1.1	PS.lightreaction	141	2.5E-02	1.5E-34	1.4E-40		0.0E+00	4.3E-02	2.2E-15	1.5E-06		2.7E-02
1.3	PS.calvin cyle	34	2.3E-03	1.1E-02	3.7E-06		5.2E-09		2.0E-04			
29	Protein	3392	0.0E+00	1.8E-04	1.6E-10			4.5E-09	7.7E-11	6.4E-03	2.4E-11	
29.2	Protein.synthesis	559	0.0E+00	0.0E+00	0.0E+00		0.0E+00	0.0E+00	7.8E-45	1.2E-18		1.7E-06
29.2.1	Ribosomal protein	405	0.0E+00	0.0E+00	0.0E+00		0.0E+00	0.0E+00	7.3E-51	3.9E-21		9.0E-05
29.2.1.2	Ribosomal protein.eukaryotic	264	0.0E+00	0.0E+00	0.0E+00		0.0E+00	0.0E+00	2.9E-43	2.0E-13		2.1E-06
29.2.1.2.1	Ribosomal protein.eukaryotic.40S subunit	102	0.0E+00	4.1E-13	1.6E-10		0.0E+00	0.0E+00	7.6E-20	3.2E-03		5.6E-04
29.2.1.2.2	Ribosomal protein.eukaryotic.60S subunit	162	0.0E+00	0.0E+00	8.9E-13		0.0E+00	0.0E+00	7.3E-23	6.0E-10		9.1E-03
29.2.1.1	Ribosomal protein.prokaryotic	132	0.0E+00	1.1E-07			0.0E+00		1.6E-09	2.3E-07	9.4E-04	
29.2.1.1.1	Ribosomal protein.prokaryotic.chloroplast	72	3.0E-10		6.8E-04		0.0E+00		4.8E-08	1.6E-03	8.6E-04	
29.2.1.1.2	Ribosomal protein.prokaryotic.mitochondrion	12	1.1E-03	1.9E-05	1.6E-04							
29.2.1.1.3	Ribosomal protein.prokaryotic.unknown organellar	48	1.6E-09	7.9E-07	1.2E-07				4.2E-02	6.4E-03		
29.3	Protein.targeting	254	1.4E-07	1.7E-04	2.6E-06	4.8E-02	4.2E-02	3.8E-02			1.0E-02	
29.3.2	Protein.targeting.mitochondria	33	4.0E-04	1.4E-05	2.7E-03		3.0E-02					
29.5	Protein.degradation	1688	1.4E-07	4.0E-03		2.3E-12				0.0E+00	5.1E-08	
34.19.1	Transport.Major Intrinsic Proteins.PIP	15	2.3E-03		2.4E-02	4.7E-03	2.9E-05	3.3E-03				
35.1.5	Pentatricopeptide repeat-containing protein	431	0.0E+00	7.4E-13	3.9E-05	2.8E-03				4.7E-06	7.3E-13	

Mitochondrial control of biotic stress responses is consistent with previous findings based on the study of marker genes (reviewed in Amirsadeghi *et al.*, 2007). As mitochondrial electron transport is highly sensitive to external stimuli and controls mtROS release and cell death programmes (Scott and Logan 2008), the mitochondrion satisfies the requirements to act as an intracellular relay station of cellular pathogen defence. Candidate mechanisms for linking pathogen attack and mitochondrial impairment include ETC inhibition by SA (Xie and Chen, 1999). Cross-talk between ROS generation by NADPH oxidases at the plasma membrane and by the ETC in mitochondria in animal systems may suggest a similar connection in plants (Daiber, 2010). Mounting an appropriate defence response may therefore depend on retrograde signalling. In turn, genetic or pharmacological impairment of mitochondrial respiration may activate mitochondrially controlled pathogen-related gene expression via the same pathways.

For the functional category 'protein synthesis', changes for individual transcripts were mostly subtle but highly orchestrated for a large number of cytosolic, plastidic, and mitochondrial ribosomal proteins (Fig. 2). Interestingly, two groups of responses were revealed. While the transcripts coding for cytosolic ribosomal proteins were co-ordinately up-regulated in the *ndufs4*, *ndufa1*, *msh1×recA3*, *msd1*, and *aox1a* mutants, they were mostly down-regulated in the short-term inhibitor experiments (AA, rotenone, and oligomycin) (Fig. 2). This most probably reflects the fact that acclimation responses had occurred in the stable transgenic lines which were absent in the inhibitor treatments. This suggests that acute mitochondrial dysfunction leads to a repression of the cytosolic protein synthesis machinery, while chronic dysfunction triggers compensation and an induction. Transcripts encoding organellar ribosomal proteins responded differently from their cytosolic counterparts. In the complex I mutants (*ndufa1* and *ndufs4*), inverse changes were observed for transcripts encoding mitochondrial (up-regulated) or plastidic ribosomal proteins (down-regulated), whereas in *msh1×recA3* and *aox1a* mutants as well as upon oligomycin treatment, all transcripts of organellar ribosomal proteins were largely up-regulated (Fig. 2).

The transcripts coding for photosynthetic light reactions were also significantly regulated in eight data sets. While an orchestrated down-regulation was observed in seven data sets [*msh1×recA3*, *ndufa1*, *ndufs4*, rotenone, AA (WT), AA (*prxII F*), and *msd1*] for photosystem I (PSI)- and PSII-encoding transcripts, a significant up-regulation was observed in the *aox1a* mutant under control conditions. This opposite response in a mutant with a defect in the alternative respiratory pathway strengthens once more the suggestion that retrograde control can be modulated by the route of electron flow. However, the down-regulation of transcripts encoding light reaction components is not necessarily dependent on the presence of the AOX protein, as a strong down-regulation of these transcripts was also observed in the *aox1a* mutant subjected to light and drought stress (Giraud *et al.*, 2008), showing that there are other regulatory pathways controlling

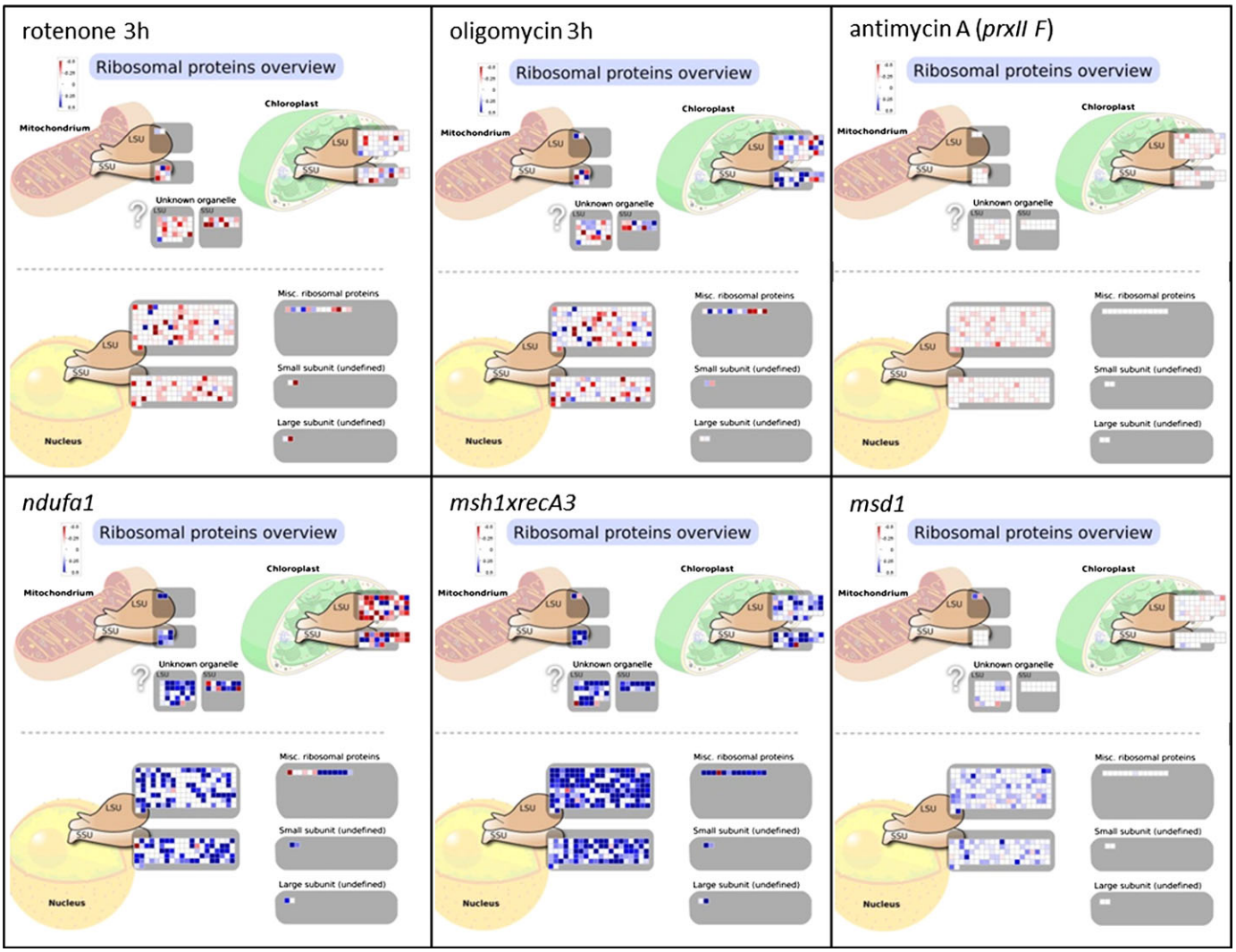

Fig. 2. Regulated transcripts of the functional group 'ribosomal proteins' in response to mitochondrial impairments. The bin 'protein synthesis.ribosomal proteins' was significantly regulated in the experiments of the displayed data sets (rotenone 3 h, oligomycin 3 h, AA (*prxIIF*), *ndufa1*, *msh1*×*recA3*, and *msd1*) (compare Table 4). Two additional data sets in which this functional class is regulated (AA and *ndufs4*) are not shown (compare Table 4). The display has been adopted from the MapMan software. Boxes represent individual transcripts, and blue and red indicate up- and down-regulation, respectively (log2 ratios).

these transcripts under more severe stress. The expression of genes encoding photosynthetic and ribosomal proteins is, for example, also regulated by the cytosolic energy-sensing kinase SnRK1 which mediates general cellular starvation and sugar responses (Baena-González and Sheen, 2008; Smeekens *et al.*, 2010). It will be interesting to see in the future whether a mitochondrial-derived retrograde signal also feeds into this pathway (Fig. 3).

A connection between organellar protein synthesis and retrograde signalling was also observed in *Arabidopsis* mutants that are defective in organellar protein biosynthesis due to down-regulation of the prolyl-tRNA synthetase gene (*prors1*, At5g52520) which is targeted to both chloroplast and mitochondria (Pesaresi *et al.*, 2006). Only the combination of decreased translation rates in both organelles, due to defective *prors1* expression, caused a down-regulation of photosynthesis-related transcripts (Pesaresi *et al.*, 2006). However, a direct connection between the *prors1* transcript level and photosynthetic gene expression was not observed in the present analysis. The *msh1*×*recA3* mutant showed even a slightly increased *prors1* transcript level while at the same time a strong repression of photosynthetic gene products was observed (Supplementary Table S2 at JXB online). In contrast, the *aox1a* mutant showed a strong and significant up-regulation of transcripts coding for photosynthetic proteins under control conditions, while transcripts coding for ribosomal proteins were strongly increased as in the *msh1*×*recA3* mutant. This leads to two important conclusions: Changes in transcript levels encoding photosynthetic proteins (i) can be caused by mitochondrial-specific dysfunction and (ii) are not necessarily co-regulated with transcripts encoding proteins involved in organellar protein biosynthesis.

Experiments on *Chlamydomonas reinhardtii* have revealed a link between mitochondrial electron transport function and the expression of nuclear genes encoding photosynthetic

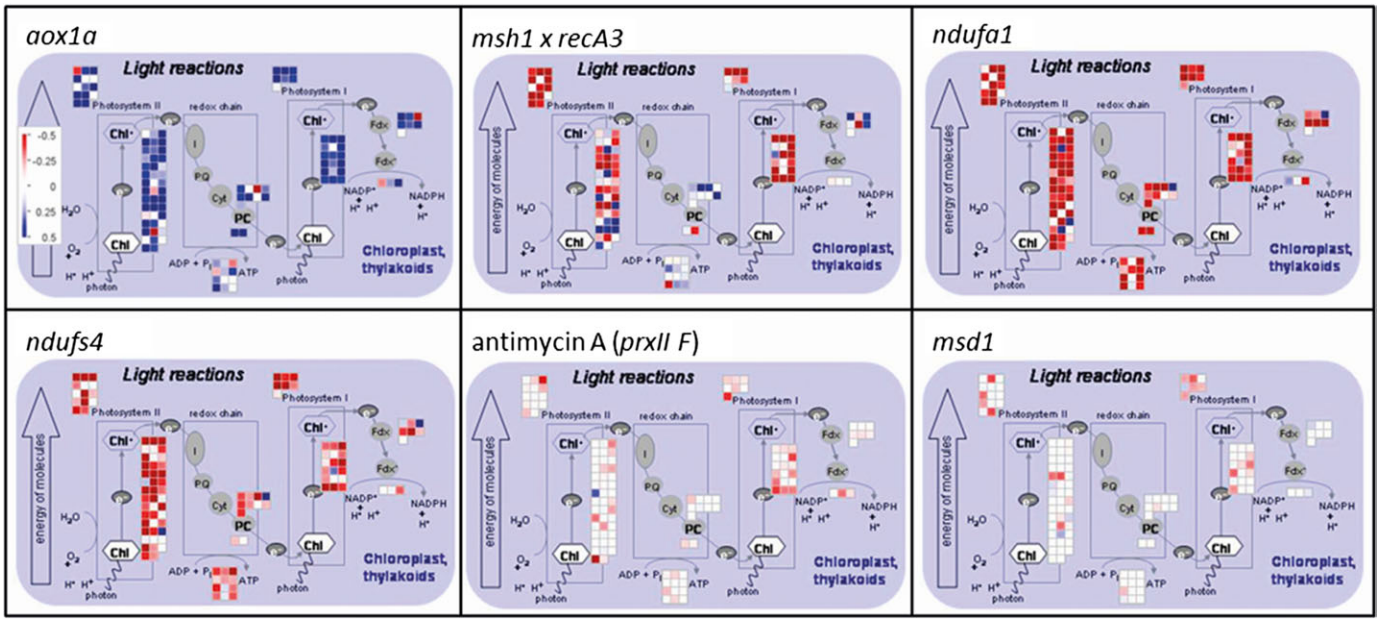

Fig. 3. Regulated transcripts of the functional group 'photosynthetic light reactions' in response to mitochondrial impairments. The bin 'photosynthesis.light reactions' was significantly regulated in the experiments of the displayed data sets [*aox1a*, *msh1*×*recA3*, *ndufa1*, *ndufs4*, A A (*prxIIF*), and *msd1*]. Two additional data sets in which this functional class is regulated (AA and rotenone) are not shown (compare Table 4). The display has been adopted from the MapMan software. Boxes represent individual transcripts, and blue and red indicate up- and down-regulation, respectively (log2 ratios).

proteins (Matsuo and Obokata, 2006; Matsuo *et al.*, 2011). It was found that active mitochondrial respiration induced photosynthetic transcripts and that this induction was blocked in mitochondrial respiratory mutants, as well as by the application of AA. Although the nature of the retrograde signal was not identified, it seems justified to consider mitochondrial electron transport an upstream stimulus for regulation of nuclear gene expression.

The findings presented here for *Arabidopsis* are in agreement with a general mitochondrial control of nuclear-encoded photosynthetic genes. It needs to be pointed out that all systems which rely on photosynthesis as their main energy source show this response consistently (eight out of 11 data sets). The remaining three data sets were gathered from overall heterotrophic systems, such as flowers and cultured cells. Complete consistency between systems provides strong evidence for mitochondrial control of photosynthesis on a transcriptional level. Although the effect has already been observed in individual systems (Dutilleul *et al.*, 2003*a*; Garmier *et al.*, 2008; Meyer *et al.*, 2009), unambiguous interpretation has been difficult due to the possibility of a unique effect of the respective mitochondrial dysfunction or direct experimental impacts on plastidic status. For example, AA can also inhibit the cytochrome b_6f complex in plastids (although treatments were performed in dark-adapted plants), and there is new evidence for dual targeting of MSH1 (but not RecA3) to mitochondria and plastids (Xu *et al.*, 2011). The risk of inappropriate interpretation is minimized in this meta-analysis due to the consistent regulation of photosynthetic transcripts in all autotrophic systems analysed here, independent of the treatment or mitochondrial defect. It is unlikely that in all systems the plastid was directly affected (although indirect effects via altered mitochondrial status are a possibility). The present data therefore strongly suggest that mitochondrial status can determine the expression of nuclear-encoded photosynthetic transcripts. Such interorganellar cross-talk between both bioenergetic organelles via the nucleus complements the well-studied metabolic interaction between mitochondria and chloroplasts (Raghavendra and Padmasree, 2003). It could provide an important level of regulation to synchronize both organelles and guarantee efficient collaboration under changing conditions.

Conclusions and perspectives

Three main functional targets of mitochondrial retrograde signalling were identified: (i) protein synthesis; (ii) photosynthetic light reactions; and (iii) plant–pathogen interactions. Transcripts from these groups were affected by mild mitochondrial impairments as well as by severe mitochondrial and respiratory dysfunctions. Similar observations have been made in the individual studies already; however, this comprehensive meta-analysis reveals them as general and robust targets of mitochondrial signalling. Figure 4 summarizes a working model of retrograde signalling as discussed in this study. The key components of the retrograde signalling pathway(s) regulating the transcription factor ABI4 are still unknown and might include components of known ABA, ROS, and energy signalling pathways (Fig. 4).

The differential regulation of photosynthetic light reactions depending on the precise type of mitochondrial dysfunction

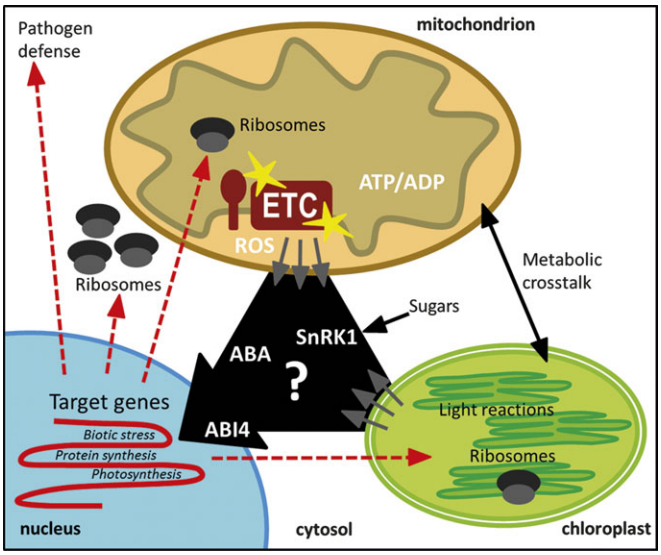

Fig. 4. Schematic representation of the working model for mitochondrial retrograde signalling triggered by various respiratory impairments. An orchestrated regulation of transcriptional read-out markers was found for the functional categories 'light reactions', 'protein synthesis', and 'plant–pathogen interactions' (depicted in red). The actual key players and components in the mitochondrial retrograde signalling pathway are still unknown and might involve known ABA, ROS, and energy signalling pathways (depicted in white). The transcription factor ABI4 is a known target of retrograde signalling from mitochondria and plastids (Giraud *et al.*, 2009).

reveals a new layer of complexity of mitochondria–chloroplast interaction and raises questions about the nature of signalling between them. Future research also needs to clarify the role of the coordinated transcript changes of ribosomal proteins which raises the possibility that mitochondrial retrograde control might not only influence the expression of genes at the promoter level, but could also act directly on the level of translation (Ho *et al.*, 2008).

The outcomes of several forward genetic screens on mitochondrial retrograde signalling mutants are anticipated in the next years, and raise high hopes that the molecular components responsible for mitochondrial retrograde signalling in plants might be finally identified.

Supplementary data

Supplementary data are available at *JXB* online.

Figure S1. Co-expression networks identified by Atted-II for transcripts which are solely regulated in the individual experiments.

Figure S2. MapMan display of regulated transcripts involved in the plant–pathogen response in individual experiments.

Table S1. Data table with log fold changes from all transcripts of the 11 analysed microarray experiments which were used in the meta-analysis, and lists of transcripts which were specifically regulated by a certain mitochondrial impairment.

Table S2. Functional class scoring results with Hochberg correction from individual experiments using the MapMan software. Functional bins with *P*-values are indicated.

Acknowledgements

We would like to thank the authors of the published data sets that were used in this work. MS was supported by The Gatsby Charitable Foundation and a Weston Junior Research Fellowship (New College, University of Oxford, UK). IF was supported by a Junior Research Fellowship (Christ Church College, University of Oxford, UK) and by a Feodor Lynen Research Fellowship (Alexander von Humboldt foundation, Germany). This work was supported by the Deutsche Forschungsgemeinschaft, Germany (Emmy Noether Programme FI-1655/1-1 and Research Unit 804).

References

Amirsadeghi S, Robson CA, Vanlerberghe. 2007. The role of the mitochondrion in plant response to biotic stress. *Physiologia Plantarum* **129,** 256–266.

Apel K, Hirt H. 2004. Reactive oxygen species: metabolism, oxidative stress, and signal transduction. *Annual Reviews in Plant Biology* **55,** 373–399.

Arrieta-Montiel MP, Shedge V, Davila J, Christensen AC, Mackenzie SA. 2009. Diversity of the Arabidopsis mitochondrial genome occurs via nuclear-controlled recombination activity. *Genetics* **183,** 1261–1268.

Baena-González E, Sheen J. 2008. Convergent energy and stress signaling. *Trends in Plant Science* **13,** 474–482.

Beckers GJ, Conrath U. 2006. Microarray data analysis made easy. *Trends in Plant Science* **11,** 322–323.

Busi MV, Gomez-Lobato ME, Rius SP, Turowski VR, Casati P, Zabaleta EJ, Gomez-Casati DF, Araya A. 2011. Effect of mitochondrial dysfunction on carbon metabolism and gene expression in flower tissues of Arabidopsis thaliana. *Molecular Plant* **4,** 127–143.

Butow RA, Avadhani NG. 2004. Mitochondrial signaling: the retrograde response. *Molecular Cell* **14,** 1–15.

Carrari F, Nunes-Nesi A, Gibon Y, Lytovchenko A, Ehlers Loureiro M, Fernie AF. 2003. Reduced expression of aconitase results in an enhanced rate of photosynthesis and marked shifts in carbon partitioning in illuminated leaves of wild species tomato. *Plant Physiology* **133,** 1322–1335.

Clifton R, Lister R, Parker KL, Sappl PG, Elhafez D, Millar AH, Day DA, Whelan J. 2005. Stress-induced co-expression of alternative respiratory chain components in Arabidopsis thaliana. *Plant Molecular Biology* **58,** 193–212.

Daiber A. 2010. Redox signaling (cross-talk) from and to mitochondria involves mitochondrial pores and reactive oxygen species. *Biochimica et Biophysica Acta* **1797,** 897–906.

Dekkers BJ, Schuurmans JA, Smeekens SC. 2008. Interaction between sugar and abscisic acid signalling during early seedling development in Arabidopsis. *Plant Molecular Biology* **67,** 151–167.

Dietz KJ. 2008. Redox signal integration: from stimulus to networks and genes. *Physiologia Plantarum* **133,** 459–468.

Djajanegara I, Finnegan PM, Mathieu C, McCabe T, Whelan J, Day DA. 2002. Regulation of alternative oxidase gene expression in soybean. *Plant Molecular Biology* **50,** 735–742.

Dojcinovic D, Krosting J, Harris AJ, Wagner DJ, Rhoads DM. 2005. Identification of a region of the Arabidopsis AtAOX1a promoter necessary for mitochondrial retrograde regulation of expression. *Plant Molecular Biology* **58,** 159–175.

Dutilleul C, Driscoll S, Cornic G, De Paepe R, Foyer CH, Noctor G. 2003*a*. Functional mitochondrial complex I is required by tobacco leaves for optimal photosynthetic performance in photorespiratory conditions and during transients. *Plant Physiology* **131,** 264–275.

Dutilleul C, Garmier M, Noctor G, Mathieu C, Chetrit P, Foyer CH, de Paepe R. 2003*b*. Leaf mitochondria modulate whole cell redox homeostasis, set antioxidant capacity, and determine stress resistance through altered signaling and diurnal regulation. *The Plant Cell* **15,** 1212–1226.

Finkemeier I, Goodman M, Lamkemeyer P, Kandlbinder A, Sweetlove LJ, Dietz KJ. 2005. The mitochondrial type II peroxiredoxin F is essential for redox homeostasis and root growth of Arabidopsis thaliana under stress. *Journal of Biological Chemistry* **280,** 12168–12180.

Fujita Y, Nakashima K, Yoshida T, *et al*. 2009. Three SnRK2 protein kinases are the main positive regulators of abscisic acid signaling in response to water stress in Arabidopsis. *Plant and Cell Physiology* **50,** 2123–2132.

Gadjev I, Vanderauwera S, Gechev TS, Laloi C, Minkov IN, Shulaev V, Apel K, Inzé D, Mittler R, Van Breusegem F. 2006. Transcriptomic footprints disclose specificity of reactive oxygen species signaling in Arabidopsis. *Plant Physiology* **141,** 436–445.

Garcion C, Baltensperger R, Fournier T, Pasquier J, Schnetzer MA, Gabriel JP, Métraux JP. 2006. FiRe and microarrays: a fast answer to burning questions. *Trends in Plant Science* **11,** 320–322.

Gardner PR. 2002. Aconitase: sensitive target and measure of superoxide. *Methods in Enzymology* **349,** 9–23.

Garmier M, Carroll AJ, Delannoy E, Vallet C, Day DA, Small ID, Millar AH. 2008. Complex I dysfunction redirects cellular and mitochondrial metabolism in Arabidopsis. *Plant Physiology* **148,** 1324–1341.

Giraud E, Ho LH, Clifton R, *et al*. 2008. The absence of ALTERNATIVE OXIDASE1a in Arabidopsis results in acute sensitivity to combined light and drought stress. *Plant Physiology* **147,** 595–610.

Giraud E, Van Aken O, Ho LH, Whelan J. 2009. The transcription factor ABI4 is a regulator of mitochondrial retrograde expression of ALTERNATIVE OXIDASE1a. *Plant Physiology* **150,** 1286–1296.

Gleason C, Huang S, Thatcher LF, Foley RC, Anderson CR, Carroll AJ, Millar AH, Singh KB. 2011. Mitochondrial complex II has a key role in mitochondrial-derived reactive oxygen species influence on plant stress gene regulation and defense. *Proceedings of the National Academy of Sciences, USA* **108,** 10768–10773.

Gray GR, Maxwell DP, Villarimo AR, McIntosh L. 2004. Mitochondria/nuclear signaling of alternative oxidase gene expression occurs through distinct pathways involving organic acids and reactive oxygen species. *Plant Cell Reports* **23,** 497–503.

Ho LH, Giraud E, Uggalla V, Lister R, Clifton R, Glen A, Thirkettle-Watts D, Van Aken O, Whelan J. 2008. Identification of regulatory pathways controlling gene expression of stress-responsive mitochondrial proteins in Arabidopsis. *Plant Physiology* **147,** 1858–73.

Inzé A, Vanderauwera S, Hoeberichts FA, Vandorpe M, Van Gaever T, Van Breusegem F. 2012. A subcellular localization compendium of hydrogen peroxide-induced proteins. *Plant Cell and Environment* **35,** 308–20.

Kliebenstein DJ, Monde RA, Last RL. 1998. Superoxide dismutase in Arabidopsis: an eclectic enzyme family with disparate regulation and protein localization. *Plant Physiology* **118,** 637–650.

Kleine T, Voigt C, Leister D. 2009. Plastid signalling to the nucleus: messengers still lost in the mists? *Trends in Genetics* **25,** 185–192.

Koussevitzky S, Nott A, Mockler TC, Hong F, Sachetto-Martins G, Surpin M, Lim J, Mittler R, Chory J. 2007. Signals from chloroplasts converge to regulate nuclear gene expression. *Science* **4,** 715–719.

Leakey AD, Xu F, Gillespie KM, McGrath JM, Ainsworth EA, Ort DR. 2009. Genomic basis for stimulated respiration by plants growing under elevated carbon dioxide. *Proceedings of the National Academy of Sciences, USA* **106,** 3597–602.

Lehmann M, Schwarzländer M, Obata T, *et al*. 2009. The metabolic response of Arabidopsis roots to oxidative stress is distinct from that of heterotrophic cells in culture and highlights a complex relationship between the levels of transcripts, metabolites, and flux. *Molecular Plant* **2,** 390–406.

Leister D. 2005. Genomics-based dissection of the cross-talk of chloroplasts with the nucleus and mitochondria in Arabidopsis. *Gene* **354,** 110–116.

Leister D, Wang X, Haberer G, Mayer KF, Kleine T. 2011. Intra- and intercompartmental transcriptional networks coordinate the expression of genes for organellar functions. *Plant Physiology* **157,** 386–404.

Li L, Foster CM, Gan Q, Nettleton D, James MG, Myers AM, Wurtele ES. 2009. Identification of the novel protein QQS as a component of the starch metabolic network in Arabidopsis leaves. *The Plant Journal* **58,** 485–498.

Liao X, Butow RA. 1993. *RTG1* and *RTG2*: two yeast genes required for a novel path of communication from mitochondria to the nucleus. *Cell* **72,** 61–71.

Liu Z, Butow RA. 2006. Mitochondrial retrograde signaling. *Annual Review of Genetics* **40,** 159–185.

Matsuo M, Obokata J. 2006. Remote control of photosynthetic genes by the mitochondrial respiratory chain. *The Plant Journal* **47,** 873–882.

Matsuo M, Hachisu R, Tabata S, Fukuzawa H, Obokata J. 2011. Transcriptome analysis of respiration-responsive genes in Chlamydomonas reinhardtii: mitochondrial retrograde signalling coordinates the genes for cell proliferation with energy-producing metabolism. *Plant Cell Physiology* **52,** 333–343.

Maxwell DP, Nickels R, McIntosh L. 2002. Evidence of mitochondrial involvement in the transduction of signals required for the induction of genes associated with pathogen attack and senescence. *The Plant Journal* **29,** 269–279.

Maxwell DP, Wang Y, McIntosh L. 1999. The alternative oxidase lowers mitochondrial reactive oxygen production in plant cells. *Proceedings of the National Academy of Sciences, USA* **96,** 8271–8276.

Meyer EH, Tomaz T, Carroll AJ, Estavillo G, Delannoy E, Tanz SK, Small ID, Pogson BJ, Millar AH. 2009. Remodeled respiration in ndufs4 with low phosphorylation efficiency suppresses Arabidopsis germination and growth and alters control of metabolism at night. *Plant Physiology* **151,** 603–619.

Millar AH, Whelan J, Soole KL, Day DA. 2011. Organization and regulation of mitochondrial respiration in plants. *Annual Reviews in Plant Biology* **62,** 79–104.

Morgan MJ, Lehmann M, Schwarzländer M, *et al*. 2008. Decrease in manganese superoxide dismutase leads to reduced root growth and affects tricarboxylic acid cycle flux and mitochondrial redox homeostasis. *Plant Physiology* **147,** 101–114.

Murphy MP. 2009. How mitochondria produce reactive oxygen species. *Biochemical Journal* **417,** 1–13.

Nott A, Jung HS, Koussevitzky S, Chory J. 2006. Plastid-to-nucleus retrograde signaling. *Annual Reviews in Plant Biology* **57,** 739–759.

Nunes-Nesi A, Araújo WL, Fernie AR. 2011. Targeting mitochondrial metabolism and machinery as a means to enhance photosynthesis. *Plant Physiology* **155,** 101–107.

Nunes-Nesi A, Carrari F, Lytovchenko A, Smith AMO, Ehlers Loureiro M, Ratcliffe RG, Sweetlove LJ, Fernie AF. 2005. Enhanced photosynthetic performance and growth as a consequence of decreasing mitochondrial malate dehydrogenase acttivity in transgenic tomato plants. *Plant Physiology* **137,** 611–622.

Nunes-Nesi A, Sulpice R, Gibon Y, Fernie AR. 2008. The enigmatic contribution of mitochondrial function in photosynthesis. *Journal of Experimental Botany* **59,** 1675–1684.

Obayashi T, Nishida K, Kasahara K, Kinoshita K. 2011. ATTED-II updates: condition-specific gene coexpression to extend coexpression analyses and applications to a broad range of flowering plants. *Plant and Cell Physiology* **52,** 213–219.

Pesaresi P, Masiero S, Eubel H, Braun HP, Bhushan S, Glaser E, Salamini F, Leister D. 2006. Nuclear photosynthetic gene expression is synergistically modulated by rates of protein synthesis in chloroplasts and mitochondria. *The Plant Cell* **18,** 970–991.

Pesaresi P, Schneider A, Kleine T, Leister D. 2007. Interorganellar communication. *Current Opinion in Plant Biology* **10,** 600–606.

Pfannschmidt T. 2003. Chloroplast redox signals: how photosynthesis controls its own genes. *Trends in Plant Science* **8,** 33–41.

Raghavendra AS, Padmasree K. 2003. Beneficial interactions of mitochondrial metabolism with photosynthetic carbon assimilation. *Trends in Plant Science* **8,** 546–553.

Ramanathan A, Schreiber SL. 2009. Direct control of mitochondrial function by mTOR. *Proceedings of the National Academy of Sciences, USA* **106,** 22229–22232.

Rasmusson AG, Escobar MA. 2007. Light and diurnal regulation of plant respiratory gene expression. *Physiologia Plantarum* **129,** 57–67.

Rasmusson AG, Heiser VV, Zabaleta E, Brennicke A, Grohmann L. 1998. Physiological, biochemical and molecular aspects of mitochondrial complex I in plants. *Biochimica et Biophysica Acta* **1364,** 101–111.

Rhoads DM, Subbaiah CC. 2007. Mitochondrial retrograde regulation in plants. *Mitochondrion* **7,** 177–194.

Saeed AI, Bhagabati NK, Braisted JC, Liang W, Sharov V, Howe EA, Li J, Thiagarajan M, White JA, Quackenbush J. 2006. TM4 microarray software suite. *Methods in Enzymology* **411,** 134–193.

Schwarzländer M, Fricker MD, Sweetlove LJ. 2009. Monitoring the *in vivo* redox state of plant mitochondria: effect of respiratory inhibitors, abiotic stress and assessment of recovery from oxidative challenge. *Biochimica et Biophysica Acta* **1787,** 468–475.

Schwarzländer M, Logan DC, Fricker MD, Sweetlove LJ. 2011. The circularly permuted yellow fluorescent protein cpYFP that has been used as a superoxide probe is highly responsive to pH but not superoxide in mitochondria: implications for the existence of superoxide 'flashes'. *Biochemical Journal* **437,** 381–387.

Scott I, Logan DC. 2008. Mitochondria and cell death pathways in plants: actions speak louder than words. *Plant Signaling Behaviour* **3,** 475–477.

Shedge V, Arrieta-Montiel M, Christensen AC, Mackenzie SA. 2007. Plant mitochondrial recombination surveillance requires unusual RecA and MutS homologs. *The Plant Cell* **19,** 1251–1264.

Shedge V, Davila J, Arrieta-Montiel MP, Mohammed S, Mackenzie SA. 2010. Extensive rearrangement of the Arabidopsis mitochondrial genome elicits cellular conditions for thermotolerance. *Plant Physiology* **152,** 1960–1970.

Smeekens S, Ma J, Hanson J, Rolland F. 2010. Sugar signals and molecular networks controlling plant growth. *Current Opinion in Plant Biology* **13,** 274–279.

Sweetlove LJ, Beard KF, Nunes-Nesi A, Fernie AR, Ratcliffe RG. 2010. Not just a circle: flux modes in the plant TCA cycle. *Trends in Plant Science* **15,** 462–470.

Usadel B, Nagel A, Thimm O, *et al*. 2005. Extension of the visualization tool MapMan to allow statistical analysis of arrays, display of corresponding genes, and comparison with known responses. *Plant Physiology* **138,** 1195–1204.

Van Aken O, Zhang B, Carrie C, Uggalla V, Paynter E, Giraud E, Whelan J. 2009. Defining the mitochondrial stress response in Arabidopsis thaliana. *Molecular Plant* **2,** 1310–1324.

Vanlerberghe GC, McIntosh L. 1994. Mitochondrial electron transport regulation of nuclear gene expression. Studies with the alternative oxidase gene of tobacco. *Plant Physiology* **105,** 867–874.

Vanlerberghe GC, McIntosh L. 1996. Signals regulating the expression of the nuclear gene encoding alternative oxidase of plant mitochondria. *Plant Physiology* **111,** 589–595.

Vanlerberghe GC, McIntosh L. 1997. ALTERNATIVE OXIDASE: from gene to function. *Annual Review of Plant Physiology and Plant Molecular Biology* **48,** 703–734.

Wakamatsu K, Fujimoto M, Nakazono M, Arimura S, Tsutsumi N. 2010. Fusion of mitochondria in tobacco suspension cultured cells is dependent on the cellular ATP level but not on actin polymerization. *Plant Cell Reports* **29,** 1139–1145.

Wielopolska A, Townley H, Moore I, Waterhouse P, Helliwell C. 2005. A high-throughput inducible RNAi vector for plants. *Plant Biotechnology Journal* **3,** 583–590.

Woo DK, Phang TL, Trawick JD, Poyton RO. 2009. Multiple pathways of mitochondrial–nuclear communication in yeast: intergenomic signaling involves ABF1 and affects a different set of genes than retrograde regulation. *Biochimica et Biophysica Acta* **1789,** 135–145.

Woodson JD, Chory J. 2008. Coordination of gene expression between organellar and nuclear genomes. *Nature Reviews Genetics* **9,** 383–95.

Xie Z, Chen Z. 1999. Salicylic acid induces rapid inhibition of mitochondrial electron transport and oxidative phosphorylation in tobacco cells. *Plant Physiology* **120,** 217–226.

Xu YZ, Arrieta-Montiel MP, Virdi KS, *et al*. 2011. MutS HOMOLOG1 is a nucleoid protein that alters mitochondrial and plastid properties and plant response to high light. *Plant Cell* **23,** 3428–41.

Yu J, Nickels R, McIntosh L. 2001. A genome approach to mitochondrial–nuclear communication in Arabidopsis. *Plant Physiology and Biochemistry* **39,** 345–353.

Zimmermann P, Hirsch-Hoffmann M, Hennig L, Gruissem W. 2004. GENEVESTIGATOR. Arabidopsis microarray database and analysis toolbox. *Plant Physiology* **136,** 2621–2632.

Publication 2

Transcriptomic analysis of the role of carboxylic acids in metabolite signaling in Arabidopsis leaves.

Finkemeier I, **König AC**, Heard W, Nunes-Nesi A, Pham PA, Leister D, Fernie AR, Sweetlove LJ.

(2013)

Plant Physiology 162(1): 239-53

Transcriptomic Analysis of the Role of Carboxylic Acids in Metabolite Signaling in Arabidopsis Leaves[1][W][OA]

Iris Finkemeier*, Ann-Christine König, William Heard[2], Adriano Nunes-Nesi[3], Phuong Anh Pham, Dario Leister, Alisdair R. Fernie, and Lee J. Sweetlove

Department of Plant Sciences, University of Oxford, Oxford OX1 3RB, United Kingdom (I.F., W.H., L.J.S.); Department of Biology, Ludwig-Maximilians-University Munich, 82152 Planegg-Martinsried, Germany (I.F., A.-C.K., D.L.); and Max-Planck-Institute of Molecular Plant Physiology, 14476 Potsdam-Golm, Germany (A.N.-N., P.A.P., A.R.F.)

The transcriptional response to metabolites is an important mechanism by which plants integrate information about cellular energy and nutrient status. Although some carboxylic acids have been implicated in the regulation of gene expression for select transcripts, it is unclear whether all carboxylic acids have the same effect, how many transcripts are affected, and how carboxylic acid signaling is integrated with other metabolite signals. In this study, we demonstrate that perturbations in cellular concentrations of citrate, and to a lesser extent malate, have a major impact on nucleus-encoded transcript abundance. Functional categories of transcripts that were targeted by both organic acids included photosynthesis, cell wall, biotic stress, and protein synthesis. Specific functional categories that were only regulated by citrate included tricarboxylic acid cycle, nitrogen metabolism, sulfur metabolism, and DNA synthesis. Further quantitative real-time polymerase chain reaction analysis of specific citrate-responsive transcripts demonstrated that the transcript response to citrate is time and concentration dependent and distinct from other organic acids and sugars. Feeding of isocitrate as well as the nonmetabolizable citrate analog tricarballylate revealed that the abundance of selected marker transcripts is responsive to citrate and not downstream metabolites. Interestingly, the transcriptome response to citrate feeding was most similar to those observed after biotic stress treatments and the gibberellin biosynthesis inhibitor paclobutrazol. Feeding of citrate to mutants with defects in plant hormone signaling pathways did not completely abolish the transcript response but hinted at a link with jasmonic acid and gibberellin signaling pathways. Our results suggest that changes in carboxylic acid abundances can be perceived and signaled in Arabidopsis (*Arabidopsis thaliana*) by as yet unknown signaling pathways.

Several types of metabolites have been shown to act as regulators of gene expression in various prokaryotic and eukaryotic organisms (Sellick and Reece, 2005). More than 20 years ago, it was demonstrated that the promoter activities of selected photosynthetic genes are repressed by sugars and acetate while they are induced by nitrate and several amino acids and carboxylic acids (Sheen, 1990). Since then, a large number of metabolic genes whose expression is regulated by altered concentrations of key nutrient metabolites such as sugars and nitrate have been reported (Stitt, 1999; Coruzzi and Zhou, 2001; Price et al., 2004; Usadel et al., 2008).

Sheen and coworkers demonstrated that, in addition to its enzymatic role, hexokinase also functions as a key enzyme in sugar signaling, acting as a direct metabolite sensor in plants that senses hexose concentrations in order to control sugar-regulated gene expression (Jang et al., 1997; Moore et al., 2003).

Intracellular kinases, such as the evolutionarily conserved SUCROSE NONFERMENTING1-related kinases, regulate transcription under energy or nutrient deficiency to restore metabolic homeostasis. However, the identity of the signal that is perceived by these kinases still remains to be elucidated (Baena-González and Sheen, 2008). Indeed, it is increasingly apparent that there may be many more metabolites that are able to initiate transcriptomic changes in plants (Sheen, 1990; Templeton and Moorhead, 2004; Lancien and Roberts, 2006; van Schooten et al., 2006).

Recently, signaling functions were discovered for different tricarboxylic acid (TCA) cycle intermediates such as citrate, succinate, fumarate, 2-oxoglutarate (2-OG),

[1] This work was supported by a Junior Research Fellowship of Christ Church College, University of Oxford (to I.F.), a Feodor Lynen Research Fellowship of the Alexander von Humboldt Foundation, Germany (to I.F.), the Oxford Centre for Integrative Systems Biology (to I.F. and L.J.S.), the Max Planck Gesellschaft (to A.N.-N., P.A.P., and A.R.F.), and the Deutsche Forschungsgemeinschaft (Emmy Noether Programme grant no. FI–1655/1–1, Research Unit 804, to I.F., A.-C.K., and D.L.).

[2] Present address: Sainsbury Laboratory, Norwich Research Park, Norwich NR4 7UH, UK.

[3] Present address: Departamento de Biologia Vegetal, Universidade Federal de Viçosa, 36570–000 Viçosa, Minas Gerais, Brazil.

* Corresponding author; e-mail i.finkemeier@lmu.de.

The author responsible for distribution of materials integral to the findings presented in this article in accordance with the policy described in the Instructions for Authors (www.plantphysiol.org) is: Iris Finkemeier (i.finkemeier@lmu.de).

[W] The online version of this article contains Web-only data.

[OA] Open Access articles can be viewed online without a subscription.

www.plantphysiol.org/cgi/doi/10.1104/pp.113.214114

and the closely related metabolite 2-hydroxyglutarate (in its reduced form) in human cells (Hewitson et al., 2007; Wellen et al., 2009; Gomez et al., 2010; Yang et al., 2012). While succinate, fumarate, and 2-hydroxyglutarate were shown to inhibit several chromatin modifiers and consequently affect transcription (Yang et al., 2012), citrate has been discussed to be of particular importance for histone acetylation via cleavage to acetyl-CoA by ATP-citrate lyase to regulate the expression of glycolytic genes in liver cells (Wellen et al., 2009). Furthermore, iron citrate was shown to competitively inhibit the activities of protein Tyr phosphatases and thereby to enhance mitogen-activated protein kinase (MAPK) signaling (Gomez et al., 2010).

Evidence that TCA cycle intermediates themselves (as opposed to other downstream metabolites) act in regulating transcript abundances first came from a genome-wide expression analysis of yeast mutants with TCA cycle defects (McCammon et al., 2003). Stepwise inactivation of 15 genes encoding the eight TCA cycle enzymes in yeast revealed changes in expression patterns of genes responding to the TCA cycle defects, which correlated with altered levels of citrate, 2-OG, succinate, and malate (McCammon et al., 2003). In plants, supply of exogenous TCA cycle organic acids, such as citrate, led to a strong accumulation of *ALTERNATIVE OXIDASE1* (*AOX1*) transcripts in tobacco (*Nicotiana tabacum*) as well as in Arabidopsis (*Arabidopsis thaliana*) cell suspension cultures, while *AOX2* transcript abundance was decreased (Gray et al., 2004; Clifton et al., 2005). Moreover, Muller et al. (2001) reported that the *NITRATE REDUCTASE* transcript (*NIA*) was decreased in abundance after 4 h of feeding tobacco leaves with 40 mM malate or citrate but highly induced by 40 mM 2-OG. As these are unlikely to be the only gene products regulated by the abundance of TCA cycle organic acids, we speculated that the induction of *AOX1* and repression of the *NIA* transcript belong to a general response of a certain set of nucleus-encoded genes to a changed abundance in organic acid levels. Intermediates of the TCA cycle are good candidate signaling molecules, as they reflect both the metabolic and redox status of the cell and are known to be transported between compartments. The aim of this study was to establish the role of carboxylic acids in regulating nuclear gene expression in plants.

RESULTS

Citrate Has a Stronger Effect on Transcript Abundances Than Malate

To establish whether carboxylic acids have a general role in the regulation of transcript abundances, the influence of exogenously supplied malate and citrate on the Arabidopsis transcriptome was analyzed in leaf slices. The leaf slice system has been used for gene expression analysis in several previous studies (Raven and Farquhar, 1981; Horling et al., 2003). It allows a fast and homogenous application of effector solutions. Often, cell cultures or protoplasts are also used to allow homogenous application of metabolites to cells (Sheen, 1990; Clifton et al., 2005; Baxter et al., 2007; Ho et al., 2008); however, they have the disadvantage that they contain high amounts of sugars that can also have strong effects on the expression of metabolic genes.

Based on published data on the organic acid-dependent induction of the *AOX1* gene of tobacco (Gray et al., 2004), 1 mM citrate and 1 mM malate were chosen for initial treatments of 2, 4, and 8 h. Reverse transcriptase PCR analysis revealed that the *AOX1a* (At3g22370) transcript of Arabidopsis was increased to a peak level after an 8-h treatment with 1 mM citrate and malate (Fig. 1A). Thus, these two treatments were selected for further microarray analysis (Arabidopsis 29k Oligonucleotide Microarrays, Galbraith laboratory; Zhang et al., 2008). From about 14,000 to 16,000 transcripts that were detected in each of four independent biological replicates, 1,876 transcripts showed a significant change in abundance after citrate treatment in comparison with leaf slices infiltrated with control buffers only. After malate treatment, only 327 transcripts were significantly differentially regulated (Fig. 1B; Cyber-T test, Bayes $P < 0.05$). A nearly equal number of up- and down-regulated transcripts were found in both treatments (Supplemental Table S1). Although a large number of transcripts were changed by more than 10% after citrate treatment, only 21 transcripts were increased by more than 2-fold (Table I). Six of the these transcripts, *ATPase AHA2* (At4g30190), *EXORDIUM* (*EXO*; At4g08950), *SAM-DEPENDENT METHYLTRANSFERASE* (*SAM-MT*; At2g41380), *LEUCINE-RICH REPEAT PROTEIN KINASE* (At1g51850), *PEROXIDASE* (At5g39580), and *MERISTEM5* (At4g30270), as well as three of the down-regulated transcripts, two *UNKNOWN PROTEINs* (At1g76960 and

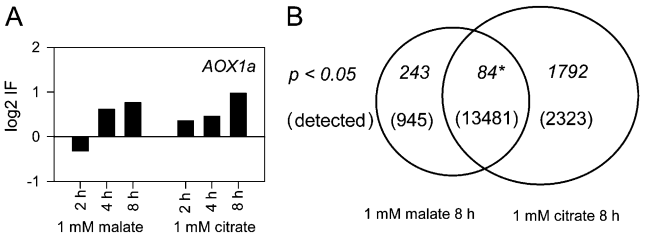

Figure 1. Effect of 1 mM malate and 1 mM citrate on transcriptome changes in Arabidopsis leaf slices. A, Time-dependent effect of the exogenous application of malate and citrate on *AOX1a* transcript abundance as analyzed by reverse transcriptase PCR. Expression levels were normalized according to *UBQ10* and *ACTIN2* expression levels. Relative expression values (treatment/control) are expressed as log2IF. B, Venn diagram of transcripts detected in the malate and citrate microarrays. Leaf slices from 4-week-old plants were infiltrated and incubated for 8 h with 1 mM malate or 1 mM citrate (both in 1 mM MES, pH 5.5) or 1 mM MES buffer (pH 5.5) only (control). A total of 327 and 1,876 transcripts were significantly regulated by 8-h malate and citrate treatment, respectively ($n = 4$; Cyber-T test, Bayes $P < 0.05$; Supplemental Table S1). A significant overlap of 84 transcripts was detected under both conditions (χ^2 test), of which 36 transcripts were inversely regulated with citrate or malate.

Table I. *List of transcripts altered more than 2-fold by 1 mM citrate treatment for 8 h*

Transcript induction factors following 1 mM malate treatment for 8 h are included for comparison. The complete microarray data set is provided in Supplemental Table S1. Fold changes are calculated as mean log2IF (treatment/control; $n = 4$). Asterisks and crosses indicate significant differences by Cyber-T (Baldi and Long, 2001) as follows: ***$P < 0.001$, **$P < 0.01$, *$P < 0.05$, $^{+}P < 0.1$. n.d., Not detected. Significant values ($P < 0.05$) appear in boldface.

Identifier	Description	1 mM Malate	1 mM Citrate
At1g73120	Unknown protein	n.d.	**1.98*** **
At2g43660	Glycosyl hydrolase family protein17	n.d.	**1.51** **
At4g08950	Exordium	0.38^{+}	**1.34*** **
At2g23150	*NRAMP3*	0.01	**1.30*** **
At5g17330	Glu decarboxylase1	n.d.	**1.27*** **
At2g41380	SAM-dependent methyltransferase	−0.08	**1.17*** **
At5g01600	Ferritin1	−0.10	**1.10*** **
At4g30270	Xyloglucan:xyloglucosyl transferase *SEN4*	0.31	**1.05*** **
At4g30670	Putative membrane lipoprotein	−0.01	**1.05*** **
At1g51850	Putative Leu-rich repeat protein kinase	**0.29***	**1.01*** **
At4g30190	Hydrogen-exporting ATPase *AHA2*	0.09	**1.01*** **
At5g39580	Putative peroxidase	n.d.	**1.01** **
At2g47280	Pectinesterase	n.d.	**1.00*** **
At1g19960	Putative transmembrane receptor	0.04	**−1.01*** **
At2g34430	*LHCB1.4*	−0.03	**−1.03*** **
At5g44430	Plant defensin1.2c	−0.10	**−1.06*** **
At1g76960	Unknown protein	0.00	**−1.08*** **
At2g26010	Plant defensin1.3	−0.24^{+}	**−1.29*** **
At1g75830	Plant defensin1.1	−0.24^{+}	**−1.45*** **
At5g44420	Plant defensin1.2a	−0.20	**−1.48*** **
At2g26020	Plant defensin1.2b	−0.16	**−1.50*** **

At1g19960) and *LIGHT-HARVESTING CHLOROPHYLL PROTEIN-COMPLEXII SUBUNIT B1* (*LHCB1.4*; At2g34430), were also changed in the same directions after treatment of Arabidopsis with an avirulent *Pseudomonas syringae* strain (Supplemental Fig. S1A; $P < 0.05$, Genevestigator database; Zimmermann et al., 2004).

The strongest up-regulated transcript after citrate treatment was At1g73120 (about 4-fold increased), which encodes a protein of unknown function that we refer to here as *CITRATE-INDUCED1* (*CI1*). *CI1* was also more than 3-fold up-regulated in iron-deficient roots as well as by a 3-h abscisic acid (ABA) treatment and an 8-d treatment with brassinolide and boric acid ($P < 0.05$, Genevestigator database; Supplemental Fig. S1B). Two more genes that are involved in iron homeostasis, *FERRITIN1* (*FER1*; At5g01600) and *NATURAL RESISTANCE ASSOCIATED MACROPHAGE PROTEIN3* (*NRAMP3*; At2g23150), were also more than 2-fold up-regulated after citrate treatment and strongly induced by ABA treatment but, on the contrary, not by iron deficiency (Supplemental Fig. S1B; $P < 0.05$, Genevestigator database).

When comparing the lists of significant genes from the malate and citrate experiment, a significant overlap of 84 transcripts (compared with an expected 36 transcripts if the overlap is random) was found that changed under both conditions (Fig. 1B). Among these 84 transcripts, 33 and 15 were up- and down-regulated in both treatments, respectively, and 36 transcripts were inversely regulated (Supplemental Table S1). The group of transcripts that showed a similar response to an increased citrate and malate availability most likely responded to the same signal produced under both conditions, which could be a response to a general increase in carbon availability. This is supported by the observation that many of these genes are also regulated by known sugar signaling pathways (Baena-González and Sheen, 2008). However, given that the transcriptional responses to increased malate or citrate availability were generally very different from one another, the overlap of inversely regulated transcripts most likely responded specifically to either citrate or malate availability and included transcripts coding for the glucan-water dikinase *STARCH EXCESS1* (*SEX1*; At1g10760), *OUTER-ENVELOPE PROTEIN16-1* (*OEP16-1*; At2g28900), *ALTERNATIVE NAD(P)H DEHYDROGENASE2* (*NDA2*; At2g29990), *PHOTOSYSTEM I LIGHT HARVESTING PROTEIN COMPLEX GENE3* (*LHCA3*; At1g61520), *DREB SUBFAMILY A4* of *ETHYLENE RESPONSE FACTOR/APETALA2 TRANSCRIPTION FACTOR* (*DREBA4-TF*; At2g44940), and several stress-responsive proteins, such as *DEHYDROASCORBATE REDUCTASE1* (*DHAR1*; At1g19570), *TRYPSIN INHIBITOR* (At1g73260), and *PLANT DEFENSIN1.2B* (*PDF1.2B*; At2g26020; Supplemental Table S1).

Functional Gene Categories Affected by Citrate and Malate Treatment

To identify significantly changed functional classes rather than single transcripts that responded specifically

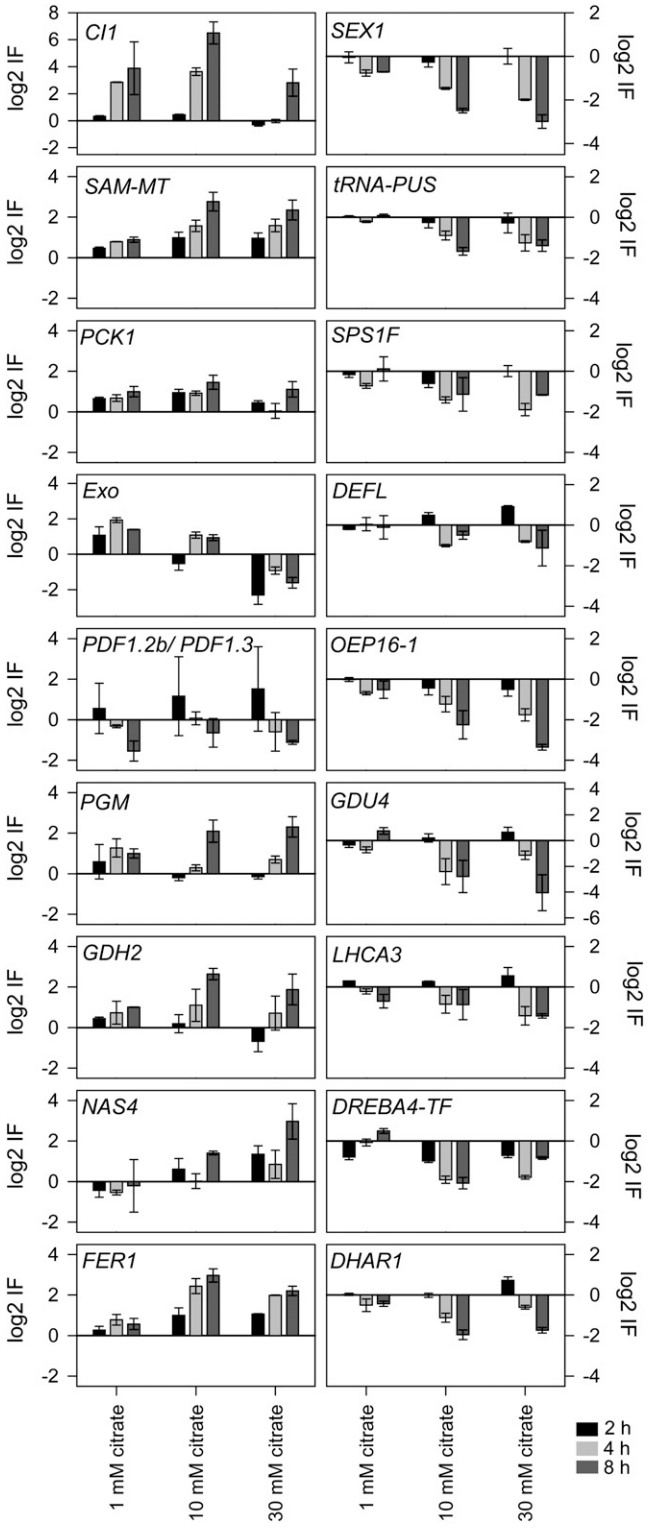

Figure 2. Concentration- and time-dependent effects of externally applied citrate on the abundance of 18 transcripts selected from the microarray analysis. Arabidopsis leaf slices were incubated in 0, 1, 10, and 30 mM citrate for 2 h (black bars), 4 h (gray bars), and 8 h (dark gray bars) as described in "Materials and Methods." QRT-PCR analysis was carried out in triplicate (technical and biological) using SYBR Green PCR Master Mix. Expression levels were normalized to the *UBQ10* and *ACTIN2* transcripts for each treatment and time point. Relative expression values (treatment/control) are expressed as log2IF (mean values ± SE; $n = 3$). Accession numbers of the transcripts are as follows: *CI1*, At1g73120; *DEFL*, At2g43550; *DHAR1*, At1g19570; *DREBA4-TF*, At2g44940; *EXO*, At4g08950; *FER1*, At5g01600; *GDH2*, At5g07440; *GDU4*, At2g24762; *LHCA3*, At1g61520; *NAS4*, At1g56430; *OEP16-1*, At2g28900; *PCK1*, At4g37870; *PDF1.2b/PDF1.3*, At2g26020/At2g26010; *PGM*, At3g60420.1/0.2; *SAM-MT*, At2g41380; *SEX1*, At1g10760; *SPS1F*, At5g20280; *tRNA-PUS*, At2g30320. Full names of transcripts and primer sequences are given in Supplemental Table S4.

to malate and citrate availability, the microarray data were analyzed using a Wilcoxon rank-sum test (Benjamini-Hochberg corrected) integrated within the MapMan software (Thimm et al., 2004). Categories that were revealed to be significantly regulated under both conditions were photosynthesis (PSI), cell wall, biotic stress, and protein synthesis (Supplemental Table S2). However, most of the functional categories were specific to one or the other treatment, such as the TCA cycle, nitrogen metabolism, sulfur assimilation, and DNA synthesis and signaling for citrate as well as glycolysis and abiotic stress for malate (Supplemental Table S2). In summary, the results from the array experiments revealed that citrate feeding leads to widespread changes in transcript abundances that are distinct from those identified after malate feeding. These findings support the hypothesis that different organic acids might have unique roles in metabolite signaling.

Citrate-Dependent Transcript Regulation Is Time and Concentration Dependent

To confirm the expression data from the microarray analysis and also to investigate whether citrate has a concentration-dependent effect, the abundances of 18 transcripts selected from the microarray analysis were analyzed by quantitative real-time (QRT)-PCR. Citrate-regulated transcripts were selected on the basis that they showed a significant induction (*CI1*, *EXO*, *FER1*, *PHOSPHOENOLPYRUVATE CARBOXYKINASE1* [*PCK1*; At4g37870], *GLUTAMATE DEHYDROGENASE2* [*GDH2*; At5g07440], and *PHOSPHOGLYCERATE MUTASE* [*PGM*; At3g60420]) or suppression (*PDF1.2b* and *TRANSFER RNA-PSEUDOURIDINE SYNTHASE* [*tRNA-PUS*; At2g30320]) following citrate treatment or in the case that they showed an inverse regulation by malate and citrate (*LHCA3*, *SEX1*, *DEFENSIN-LIKE FAMILY PROTEIN* [*DEFL*; At2g43550], *OEP16-1*, *DREBA4-TF*, and *DHAR1*). *NICOTIANAMINE SYNTHASE4* (*NAS4*; At1g56430), *SUCROSE PHOSPHATE SYNTHASE1* (*SPS1*; At5g20280), and *GLUTAMINE DUMPER4* (*GDU4*; At2g24762) showed no significant regulation in the microarray experiments with low levels of citrate. A concentration series of 0, 1, 10, and 30 mM citrate was selected and incubated with the leaf slices for 2, 4, and 8 h. Relative transcript abundances were calculated

for all 18 transcripts relative to the respective control treatment from the same time points (Fig. 2). The expression data from the microarray analysis was confirmed for 17 of the marker transcripts by QRT-PCR at the 8-h time point with 1 mM citrate. The transcript level of *CI1* was increased to a much greater extent than detected on the microarray (about 15-fold [$\log_2$ = 3.89] induced in the QRT-PCR analysis and only 4-fold in the microarray analysis). All transcripts showed a qualitatively similar response to the microarray except for *DREBA4-TF*, which did not respond to low concentrations of citrate, but similar to the array it was altered in abundance in response to higher concentrations of citrate (10 and 30 mM; Fig. 2). For most transcripts, the expression levels were most strongly regulated by 10 mM citrate at the 4- and 8-h time points. Changes in most transcripts could also be detected as early as 2 h (Fig. 2). Treatment with 30 mM citrate did not lead to a further induction for most of the transcripts, and for *CI1*, *DREBA4-TF*, *FER1*, and *PCK1*, the induction was actually less than with 10 mM citrate (Fig. 2). In summary, the kinetic analysis of the citrate marker transcripts clearly showed a time- and concentration-dependent effect of citrate on gene expression level.

Metabolic Perturbations Resulting from Feeding of Malate and Citrate

Feeding malate and citrate to Arabidopsis leaves led to a substantial perturbation in the transcriptome. However, it cannot be concluded that this is a direct response, since these metabolites will affect related metabolic pathways in various subcellular compartments. To gain a better insight into the metabolic perturbations that might have been caused by citrate and malate feeding, a gas chromatography-mass spectrometry (GC-MS)-based metabolite profile analysis from leaf slices treated for 2, 4, and 8 h was performed (Fig. 3; Supplemental Table S3).

The metabolite profile from malate-treated leaf slices was not significantly different from control leaf slices at the time points 2 and 4 h. Only after 8 h were a marginally significant increase in malate content (P = 0.058) and slight decreases in benzoic acid, glycerol, and Gly content detected (Supplemental Table S3). More changes in metabolite contents were observed after citrate feeding, especially after 4 and 8 h, with significant increases in sugars (Suc, Glc, Fru, and Gal), amino acids (Glu, Tyr, and Phe), and organic acids (citrate and succinate) contents (Fig. 3). However, since gene expression changes were already apparent after 2 h (Fig. 2), the number of other possible candidate metabolites involved in signaling remains low. It cannot be ruled out that some of the alterations in gene expression relate to local subcellular changes in metabolite concentrations that were not detected by the GC-MS method employed here.

The Effect of Sugars and Other Organic Acids on Citrate Marker Transcripts

The repression of transcripts involved in photosynthesis as observed after citrate feeding is also known to occur after sugar or acetate feeding (Sheen, 1990). As feeding of citrate also resulted in increased sugar levels, it is possible that at least part of the observed transcript response is related to increased sugar levels. To compare the effects of sugars (Suc and Glc) and other carboxylic acids (acetate, pyruvate, isocitrate, 2-OG, succinate, fumarate, malate, and oxaloacetate) with the response to citrate treatment, a comparative QRT-PCR analysis for selected marker transcripts was performed. The above-mentioned metabolites (10 mM each) were fed to Arabidopsis leaf slices for 4 h in order to obtain a maximal transcript response at an early time point. Similar concentrations of various organic acids (5 mM) were used by Sheen (1990) to study the expression of the pyruvate phosphodikinase in maize (*Zea mays*) protoplasts. As citrate and malate are the most abundant carboxylic acids in plant cells, with concentrations of about 1 to 5 mM in the cytosol (Martinoia and Rentsch, 1994), external feeding of 10 mM carboxylic acid should also be high enough for the other selected carboxylic acids.

The transcript of *LHCA3* was selected as a down-regulated marker transcript for citrate (Fig. 2) but also for Suc ($P < 0.05$, Genevestigator database), and *AOX1a* was selected as an up-regulated marker transcript for organic acids in general (Gray et al., 2004). Furthermore, four genes were selected that showed a strong regulation on transcript level even with low levels of citrate: *CI1*, *FER1*, *OEP16-1*, and *SAM-MT* (Fig. 2). In the QRT-PCR analysis, *LHCA3* was down-regulated by the following metabolites with decreasing strength: acetate > Suc > isocitrate > citrate (Fig. 4). No regulation of the *LHCA3* transcript was observed after Glc treatment (Fig. 4), which is consistent with the data from the Genevestigator database, where no transcript regulation occurred after treatment of seedlings for 4 h with 3% Glc (Li et al., 2006).

A slight but significant up-regulation of *LHCA3* transcript was observed for pyruvate ($P < 0.05$), and a marginally significant up-regulation was also observed for 2-OG treatment ($P < 0.1$). An up-regulation of *LHCA3* transcript is also known to occur after nitrate treatment, while nitrate starvation led to a strong decrease in *LHCA3* transcript level ($P < 0.05$, Genevestigator database; data not shown). As organic acid metabolism is ultimately linked to nitrate assimilation, a connection of organic acid and nitrate signaling is conceivable.

The up-regulation of *AOX1a* transcript and protein levels is known to occur as a general response to increased levels of TCA cycle organic acids (Gray et al., 2004). In the QRT-PCR analysis, *AOX1a* transcript level was strongly induced after incubation of leaf slices with acetate (11-fold) and to a slightly lesser extent with citrate, Glc, oxaloacetate, and pyruvate

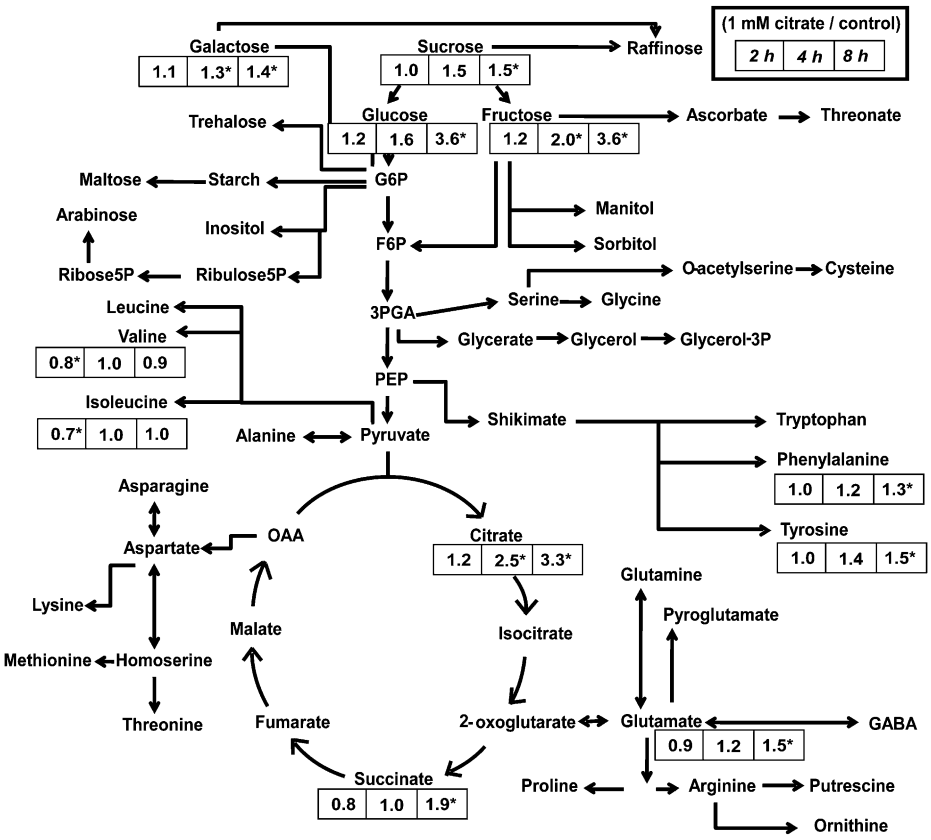

Figure 3. Metabolic map showing relative metabolite changes after 2, 4, and 8 h of 1 mM citrate in comparison with the respective control treatment. Arabidopsis leaf slices were incubated in 0 and 1 mM citrate for 2, 4, and 8 h as described in "Materials and Methods." Relative fold changes in metabolite contents (1 mM citrate/control) are shown for each time point in boxes as indicated (mean values; $n = 5$). Only metabolite levels with significant fold changes at least at one time point are shown. Asterisks indicate significant differences from control treatments (buffer only; $P < 0.05$, Student's t test). GABA, γ-Aminobutyrate; PEP, phospho*enol*-pyruvate; G6P, Glu-6-P; F6P, Fru-6-P; 3PGA, 3-phosphoglycerate; OAA, oxaloacetate.

(around 2-fold; Fig. 4). Up-regulation of *AOX1a* after incubation with malate and Suc was only marginally significant after 4 h.

OEP16-1 was selected as a citrate-specific down-regulated marker transcript (Fig. 2; Supplemental Table S1). The *OEP16-1* transcript level was also significantly decreased by acetate, malate, and oxaloacetate and only marginally significantly decreased by isocitrate and 2-OG treatments. However, a significant up-regulation of *OEP16-1* was observed for Suc, Glc, and pyruvate treatments (Fig. 4). Gonzali et al. (2006) also observed a strong and concentration-dependent up-regulation of *OEP16-1* by Suc and Glc, while Fru and turanose had no such strong effect.

Interestingly, two of the citrate marker transcripts, *CI1* and *FER1*, only responded to citrate with a significant up-regulation in transcript level but not to isocitrate or any other organic acid or sugar treatment. On the contrary, both transcripts were significantly down-regulated by most of the other treatments (Fig. 4).

The transcript of *SAM-MT* was also significantly up-regulated by citrate and to a lesser extent by Glc and isocitrate. A significant down-regulation in *SAM-MT* transcript level was observed for pyruvate, 2-OG, succinate, malate, and oxaloacetate (Fig. 4). These results indicate that the transcript response to citrate is specific for selected transcripts and that citrate can be distinguished from isocitrate by the cell.

Tricarballylate Feeding Resembles the Citrate Response of Marker Transcripts

To get a better insight into the discrimination between isocitrate and citrate on marker gene expression, the effect of feeding the nonmetabolizable citrate analog tricarballylate (Wolffram et al., 1993) was also tested. Tricarballylate can be transported into cells and mitochondria via citrate transporters. The molecular structure of tricarballylate is very similar to that of citrate and isocitrate, but the hydroxyl group at the C3 atom of citrate and at the C2 atom of isocitrate is missing. However, tricarballylate and citrate are structurally distinct from the chiral isocitrate molecule, which will ultimately impact their binding affinities to protein recognition sites.

Similar to citrate, and in contrast to isocitrate, tricarballylate was also able to induce (with slightly less efficiency) the transcript levels of the solely citrate-induced genes *CI1* and *FER1* (Figs. 4 and 5). Tricarballylate also displayed a comparable effect to citrate on the transcript levels of *OEP16-1* and *SAM-MT*, which were also regulated by isocitrate, albeit to a lesser extent (Figs. 4 and 5). Tricarballylate might partially interfere with citrate sensing, as the transcript induction was slightly less efficient than after citrate feeding (Fig. 5).

To compare the effects of tricarballylate and citrate on metabolite abundances, a GC-MS-based metabolite

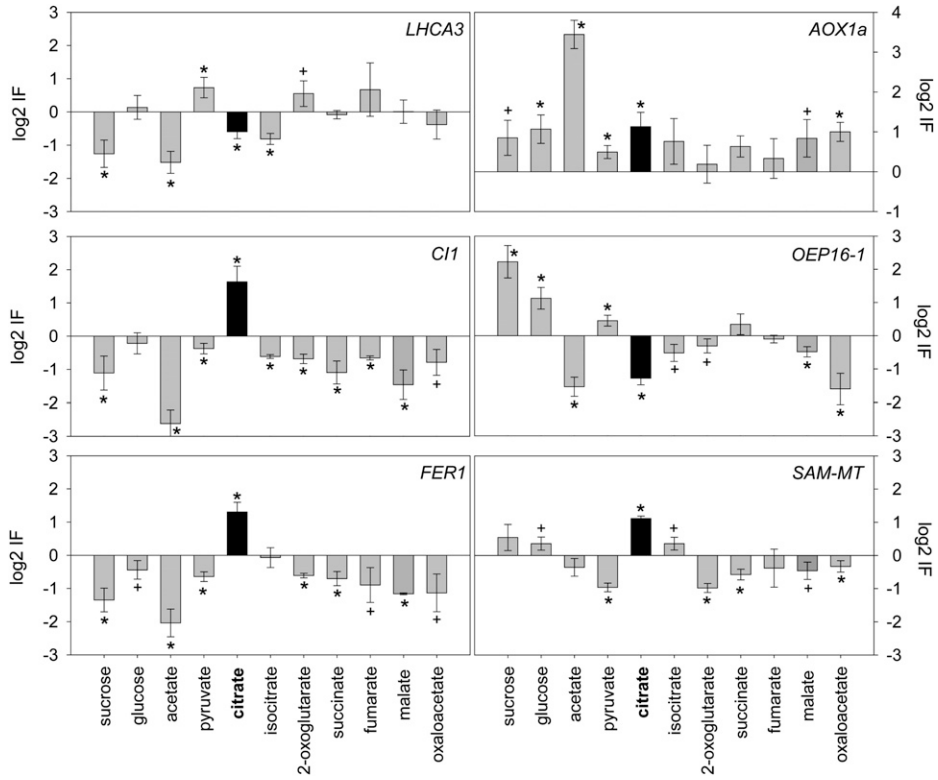

Figure 4. Comparison of the effects of different sugars and organic acids on the abundance of *LHCA3*, *AOX1a*, *CI1*, *OEP16-1*, *FER1*, and *SAM-MT* transcripts. Arabidopsis leaf slices were incubated in 0 or 10 mM of each metabolite for 4 h as described in "Materials and Methods." For a better overview, changes in transcript abundances after citrate treatment are marked in black. QRT-PCR analysis was carried out in triplicate (technical and biological) using SYBR Green PCR Master Mix. Expression levels were normalized to the *UBQ10* and *ACTIN2* transcripts. Relative expression values (treatment/control) are expressed as log2IF (mean values ± SE; $n = 3$). Crosses and asterisks indicate significant differences from control treatments (buffer only; $^{*}P < 0.05$, $^{+}P < 0.1$, Student's *t* test). Accession numbers of transcripts are as follows: *AOX1a*, At3g22370; *CI1*, At1g73120; *FER1*, At5g01600; *LHCA3*, At1g61520; *OEP16-1*, At2g28900; *SAM-MT*, At2g41380.

profiling analysis was performed (Supplemental Table S4). Again, levels of Fru and Suc were significantly increased after feeding of 10 mM citrate (as with 1 mM citrate; Fig. 3) but not after feeding with tricarballylate. The only metabolite that was changed significantly in the same direction in both treatments was citrate itself. Increases in cellular citrate levels following tricarballylate feeding are most likely due to a competitive inhibition of aconitase (Gawron and Jones, 1977). Together, these results strongly indicate that citrate itself rather than a downstream product is sensed by the plant cell.

The Transcriptome Response to Citrate Is Most Similar to Biotic Stress Treatments

To identify physiological conditions or treatments that most closely resemble the transcriptome response to citrate, a comparative data analysis was performed between all highly significantly citrate-regulated transcripts ($P < 0.001$; 38 transcripts up- and down-regulated greater than 1.5-fold) and all publicly available Affymetrix microarray data sets dealing with environmental perturbations (5,178 data sets) using the Signature tool in Genevestigator (data not shown). The highest similarity was revealed between citrate and three microarray experiments dealing with *Pseudomonas syringae* infection for 24 h compared with mock-treated leaf samples for 24 h (Wang et al., 2008) as well as leaf samples treated with bacterial flagellin22 (flg22) and leaf samples treated with the GA biosynthesis inhibitor paclobutrazol (PBZ; both Gene Expression Omnibus accession no. GSE17464).

To further analyze this similarity in more detail, a cluster analysis was performed on all significant transcripts after 1 mM citrate feeding ($P < 0.05$) and the experiments dealing with biotic stress, GA, and sugar signaling. For this, the following microarray data sets were selected: 2-h treatment with flg22 or PBZ (GSE17464), 2-h treatment with Glc (E-MEXP-475), 4-h treatment with Suc (NASCARRAYS-315), KIN10 overexpressors versus the wild type (Baena-González et al., 2007), and 1 mM malate for 8 h (this study). The hierarchical cluster analysis confirmed the similarity between the transcript response to citrate and biotic stress, as citrate was most similar to flg22 and *P. syringae* treatment in five out of 10 clusters (Fig. 6, clusters 2, 3, 5, 6, and 7). In three of 10 clusters, each transcript altered after citrate treatment behaved most similarly to PBZ (clusters 4, 5, and 7) and Glc (clusters 1, 2, and 5). Interestingly, transcripts were mostly regulated in opposite directions in KIN10 mutants in comparison with citrate (Fig. 6).

Citrate-Dependent Transcript Regulation Is Modulated in the Plant Hormone Signaling Mutants

As many of the citrate-regulated transcripts were identified to respond to biotic stresses as well as nutrient and hormone-dependent signaling pathways, 11 Arabidopsis mutants with defects in nutrient and hormonal signaling pathways were selected to elucidate

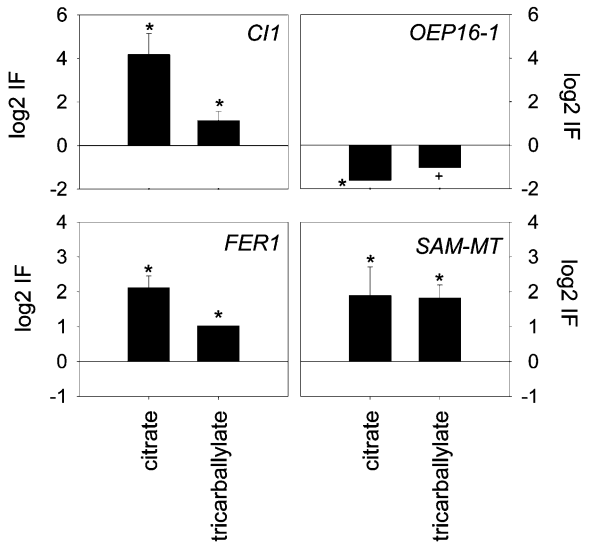

Figure 5. Effects of the citrate analog tricarballylate on the transcript levels of citrate marker transcripts *CI1*, *OEP16-1*, *FER1*, and *SAM-MT*. Arabidopsis leaf slices were incubated in 0 or 10 mM citrate and tricarballylate for 4 h as described in "Materials and Methods." QRT-PCR analysis was carried out in triplicate (technical and biological) using SYBR Green PCR Master Mix. Expression levels were normalized to the *UBQ10* and *ACTIN2* transcripts. Relative expression values (treatment/control) are expressed as log2IF (mean values ± SE; $n = 3$). Crosses and asterisks indicate significant differences from control treatments (buffer only; $^{*}P < 0.05$, $^{+}P < 0.1$, Student's *t* test). Accession numbers of transcripts are as follows: *CI1*, At1g73120; *FER1*, At5g01600; *OEP16-1*, At2g28900; *SAM-MT*, At2g41380.

whether one of these pathways is interlinked with citrate-dependent gene expression: (1) *pII* (defect in carbon/nitrogen balance; Ferrario-Méry et al., 2005); (2) *abi4* (ABA insensitive; Finkelstein et al., 1998); (3) *bak1* (*elg*; brassinosteroid [BR] hypersensitive; Whippo and Hangarter, 2005); (4) *coi1* (jasmonic acid [JA] insensitive; Xie et al., 1998); (5) *mlo2-11 NahG* (*mlo2-11*; powdery mildew resistant; Consonni et al., 2006); *NahG* (suppressed salicylic acid [SA] accumulation; Gaffney et al., 1993); (6) *npr1* (for *nonexpressor of pathogenesis-related genes1*; blocked SA signal transduction; Cao et al., 1997); (7) *pad4-1* (inhibited SA signaling; Glazebrook et al., 1997); (8) *ctr1* (constitutive ethylene signaling; Kieber et al., 1993); (9) *ein2-1 pad4-1* (*ein2-1*; ethylene insensitive; Guzmán and Ecker, 1990); (10) *quadruple DELLA* (*qDELLA*; relief of growth repression, methyl jasmonate, and GA insensitive; Cheng et al., 2004; Navarro et al., 2008); and (11) *gai* (for GA insensitive; Lee et al., 2002).

The PII protein presented a likely candidate for a carboxylic acid-dependent signaling pathway, as it is an evolutionarily conserved carboxylic acid sensor protein that is localized in chloroplasts in plants (Ferrario-Méry et al., 2005). However, the *pII* mutant did not show an altered response to citrate in comparison with the wild type for the selected citrate-regulated marker transcripts *CI-1*, *OEP16-1*, *FER1*, and *SAM-MT* (Fig. 7). The transcript abundance response to citrate was also not completely abolished in any other of the hormone signaling mutants (Fig. 7). However, a significant attenuation in citrate induction of *CI-1*, *FER1*, and *SAM-MT* transcripts was observed in the *bak1* (*elg*) mutant. BAK1 (for BRI1-associated kinase), the coreceptor of BRI1 (a BR receptor) and FLS2 (a flg22 receptor), is a Leu-rich repeat receptor kinase and is involved in restricting programmed cell death in response to pathogen challenge (Chinchilla et al., 2009). The other mutant that also showed an attenuated citrate induction of *FER1* and *SAM-MT* transcripts was *qDELLA* (Fig. 7). The *qDELLA* mutant is deficient in four of the five DELLA proteins involved in GA signaling and is insensitive to methyl jasmonate (Navarro et al., 2008). However, a constitutively active DELLA mutant that stabilizes DELLA proteins (*gai*) was not overall significantly differentially affected by citrate treatment in comparison with the wild type (Fig. 7). Only the *SAM-MT* transcript was more strongly induced by citrate in the *gai* mutant. In contrast, the down-regulation of transcripts after citrate treatment might involve different signaling pathways, as another set of mutants showed an altered response toward citrate on the down-regulated marker transcript *OEP16-1*. Repression of *OEP16-1* by citrate was attenuated again in the *qDELLA* mutant as well as in the SA defense signaling lines *NahG* and *pad4-1*, while the *npr1* mutant showed a significantly increased repression of *OEP16-1* transcript in the presence of citrate in comparison with the wild type (Fig. 7). A slightly increased repression of *OEP16-1* was also observed in the *coi1* mutant in the presence of citrate (Fig. 7). Thus, our results indicate that BAK1 and possibly also DELLA proteins might play a role in the amplification of the signal that leads to an accumulation of transcripts after citrate treatment. However, overall, our results do not clearly imply that citrate impacts a single plant hormone signaling pathway, which could be due to the fact that signaling pathways are usually not linear, and often, an extensive cross talk branch between different signaling pathways is observed to enable plants to integrate different signals (Genoud et al., 2001).

DISCUSSION

Besides their conserved function as TCA cycle intermediates, carboxylic acids such as citrate have been identified as important players in metabolite signaling in yeast and animal cells (McCammon et al., 2003; Wellen et al., 2009; Yang et al., 2012). Similar functions can also be expected for malate and citrate in plants, as both carboxylic acids can be exported from or imported into mitochondria, plastids, and other subcellular compartments (Fernie et al., 2004; Meyer et al., 2010a). Therefore, they are linked to various metabolic pathways in different compartments, making them ideally placed to function as reporter molecules of metabolic states. The aim of this study was to assess whether malate and citrate have general roles in the regulation

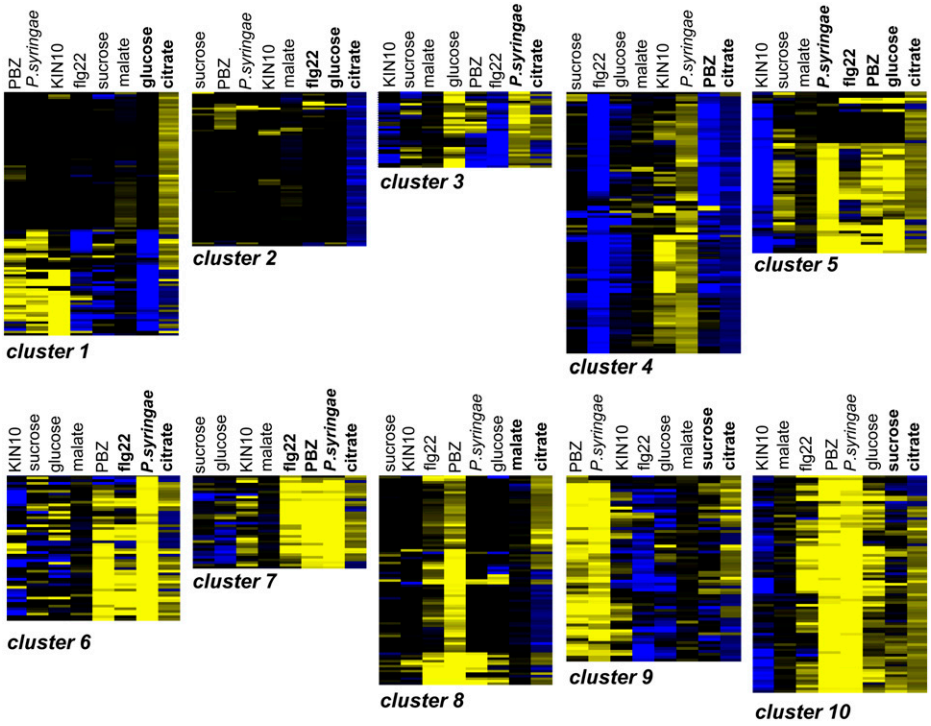

Figure 6. Comparison of transcripts regulated after citrate feeding with transcriptomic changes related to biotic stress and energy signaling. A hierarchical cluster analysis with 10 clusters was performed on all transcripts significantly regulated in abundance after citrate treatment ($P < 0.05$) using the algorithm for average linkage clustering with a Pearson correlation integrated in the MeV version 4.7.3 microarray software suite. The following microarray data sets were used for comparison: 2-h treatment with flg22 or PBZ (GSE17464), 2-h treatment with Glc (E-MEXP-475), 4-h treatment with Suc (NASCARRAYS-315), KIN10 overexpressors (Baena-González et al., 2007), and 1 mM malate for 8 h. The heat map depicts down-regulated transcripts in blue and up-regulated transcripts in yellow, and most closely related experiments to citrate are highlighted in boldface.

of transcript abundances of nuclear genes and to elucidate whether there exist a general organic acid response to altered levels of TCA cycle metabolites or whether different organic acids might convey a different signal to the cell.

Alterations in Citrate and Malate Levels Result in Unique Transcriptome Responses

To investigate the transcript response to alterations in organic acid levels, an established leaf slice system was applied (Raven and Farquhar, 1981; Muller et al., 2001; Horling et al., 2003) that allows quick and efficient feeding of organic acids and other effector solutions to leaves. The microarray experiments from feeding low levels of citrate and malate (1 mM each) revealed that both organic acids convey an overall very different transcriptome response and that only a small set of transcripts such as *AOX1a* is regulated by both organic acids (Fig. 1). Even at a higher concentration of 10 mM, which lies well above the usual apoplastic malate concentrations under low and high

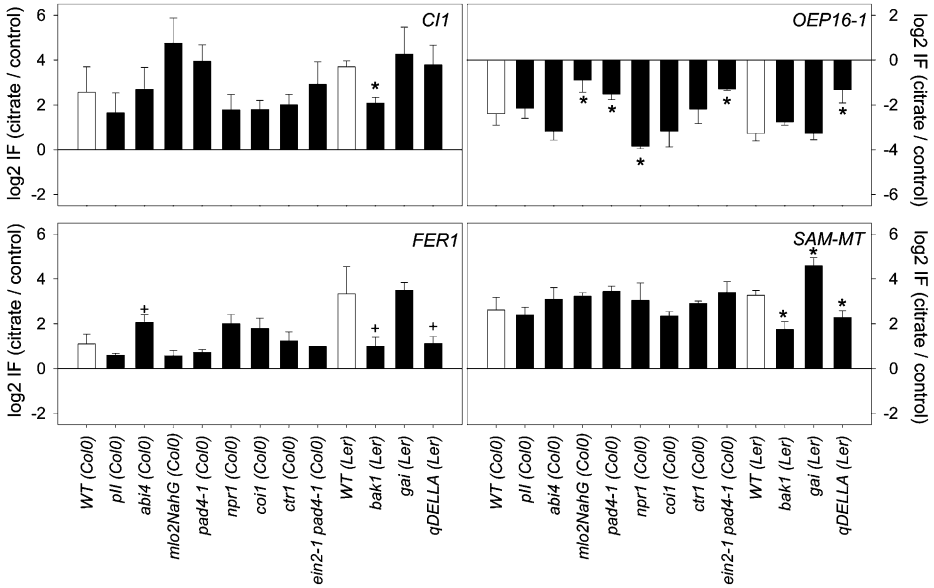

Figure 7. Transcript abundances of citrate marker transcripts *CI-1*, *OEP16-1*, *FER1*, and *SAM-MT* after citrate treatment (10 mM, 4 h) in diverse energy and hormone signaling mutants (black bars) and wild-type (WT; white bars) Arabidopsis accessions. Significant differences between the wild type and mutants are indicated (*$P < 0.05$, $^{+}P < 0.1$, Student's t test). QRT-PCR analysis was carried out in triplicate (technical and biological) using SYBR Green PCR Master Mix. Expression levels were normalized to the *UBQ10* and *ACTIN2* transcripts. Relative expression values (citrate/control) are expressed as log2IF (mean values ± SE; $n = 3$). Accession numbers of transcripts are as follows: *CI1*, At1g73120; *FER1*, At5g01600; *OEP16-1*, At2g28900; *SAM-MT*, At2g41380.

CO_2 concentrations (0.4–3 mM; Hedrich et al., 1994), the transcript response to malate and citrate was overall very different for selected marker transcripts (Fig. 4). Hence, from these results, we conclude that there is only a small general cellular response to low levels of weak acids and that most of the transcript response is specific to one or the other carboxylic acid. In addition to citrate being the stronger effector of transcript abundances, several transcripts from different functional categories were regulated in opposite directions to malate and citrate in comparison with control treatments (Supplemental Table S1). Many of the regulated transcripts encoded metabolism-associated proteins, demonstrating that there is metabolite-signaled feedback regulation of enzyme abundance. Distinct effects on gene expression have also been recently reported for the phosphonate analogs of 2-OG, which inhibit the 2-OG complex (Araújo et al., 2012). Seventy-six transcripts were significantly regulated after treatment of leaf samples with succinyl phosphonate for 4 h, which are mostly different from those observed after citrate and malate feeding (data not shown).

Citrate and Malate Have Unique Roles in Cellular Metabolism That Might Be Responsible for the Observed Transcriptome Response

Despite the fact that malate and citrate are both TCA cycle intermediates, they have different chemical properties and also partially different cellular functions. In contrast to malate, citrate acts as a chelator of apoplastic Fe^{3+} in plants to maintain cellular iron homeostasis (Haydon and Cobbett, 2007). Thus, alterations in citrate levels might convey information about cellular iron homeostasis, and 11 transcripts coding for proteins involved in metal handling and transport were significantly up-regulated with increased citrate abundance (Supplemental Table S1). A specific role for iron citrate in cellular signaling was recently demonstrated in macrophage cells, where the mononuclear dicitrate-iron complex specifically inhibits protein Tyr phosphatases in vitro as well as in vivo and stimulates MAPK signaling (Gomez et al., 2010).

Different functions for malate and citrate also concern the redox status of cells, as malate that is converted to oxaloacetate produces either NADH or NADPH through malate dehydrogenases, which are localized in cytosol, mitochondria, peroxisomes, and chloroplasts. Malate derived from chloroplasts has often been discussed in the context of redox signaling, since excess reducing equivalents produced by the photosynthetic electron transport chain can be exported as malate: the so-called "malate valve" (Scheibe, 2004). An increase in apoplastic malate concentration was recently demonstrated to regulate the closure of stomata via the guard cell-specific R-type anion channel AtALMT12 (Meyer et al., 2010b). Thus, a feedback response of changes in malate levels of photosynthetic gene expression is plausible, and changes in photosynthetic rates are often observed in TCA cycle mutants (Carrari et al., 2003; Nunes-Nesi et al., 2005, 2007; Sienkiewicz-Porzucek et al., 2010; Sulpice et al., 2010; Araújo et al., 2011). The observation that citrate had a generally repressive effect on the abundance of photosynthetic transcripts while malate feeding resulted in a slight accumulation of these transcripts is interesting in this context (Supplemental Tables S1 and S2). Similar observations of a coordinated transcript response on photosynthetic transcripts were also made under diverse conditions where mitochondrial functions were impaired (Schwarzländer et al., 2012). Perturbation of mitochondrial function often leads to an oxidative inhibition of the mitochondrial aconitase, which is followed by a rise in cellular citrate levels (Vanlerberghe and McIntosh, 1994; Morgan et al., 2008; Lehmann et al., 2009; Gupta et al., 2012). Mitochondrial citrate was discussed as a possible mediator of mitochondrial retrograde signals in plants as well as in yeast cells, but an in-depth transcriptome study was lacking so far (Vanlerberghe and McIntosh, 1994; Mackenzie and McIntosh, 1999; McCammon et al., 2003; Clifton et al., 2005; Schwarzländer and Finkemeier, 2013). Vanlerberghe and McIntosh (1996) already reported that the *AOX1* transcript level responded to increased levels of citrate that were supplied externally or were increased internally through the inhibition of aconitase using monofluroacetate. While isocitrate could also induce *AOX1* (although to a lesser extent than citrate), malate, 2-OG, succinate, pyruvate, or Gly showed no such effect (Vanlerberghe and McIntosh, 1996). *AOX1a*, *SAM-MT,* and *NDA2*, which are marker transcripts of the mitochondrial retrograde response (Schwarzländer et al., 2012; Van Aken and Whelan, 2012), were also induced by citrate in this study. Recently, it was demonstrated in Arabidopsis roots that citrate but not nitric oxide mediates the induction of *AOX* (transcript as well as activity) upon hypoxia after the inhibition of aconitase (Gupta et al., 2012). However, the induction of *AOX1a* in our study was not specific to citrate, as it was induced most strongly after acetate treatment as well as after pyruvate, malate, oxaloacetate, and sugar feeding (Fig. 4). High carboxylic acid levels as well as sugar levels are known to report an energy-rich situation regulating glycolysis and nitrogen metabolism by inhibiting phosphofructokinase and phospho*enol*pyruvate carboxylase activities, respectively (Plaxton, 1996). In these situations, the risk of overreduction of the mitochondrial and chloroplastic electron transport chain must be decreased by reprogramming metabolism to use the excess energy for biosynthetic reactions and to avoid oxidative damage.

The Relationship of the Transcriptome Response to Citrate and Biotic Stress

In our array experiment, 50 transcripts, which belong to the functional category biotic stress and plant defense, were significantly altered in abundance after

citrate treatment (Supplemental Table S1). Furthermore, the cluster analysis revealed a high similarity of the transcript response to citrate in experiments dealing with biotic stress, such as after *P. syringae* infection or flg22 treatment (Fig. 6). Several of the transcripts related to pathogen defense were decreased in expression, such as the *PATHOGENESIS-RELATED5* (*PR5*) transcript (At1g75040), which is known to be induced by Glc via the catalytic activity of hexokinase (Xiao et al., 2000). Citrate is known to have an inhibitory effect on the growth of gram-negative bacteria due to its action as a chelator of Ca^{2+} and Mg^{2+} ions, which destabilizes the plasma membrane of bacteria (Vaara, 1992; Boziaris and Adams, 1999). Hence, an increased production of citrate could act as a defense mechanism to pathogens in plants. Interestingly, an enhanced resistance to *P. syringae* infection and expression of SA-linked *PR* genes was observed in knockout lines of the cytosolic NADP-isocitrate dehydrogenase, which accumulated citrate (2-fold) while sugars such as Fru were decreased in abundance and SA levels were not increased (Mhamdi et al., 2010). In contrast to the external citrate treatment, the *PR5* transcript level was significantly up-regulated in the *icdh* lines (2-fold) while it was significantly down-regulated (log_2-transformed relative induction factor [log2IF] = −0.41) after citrate treatment (Supplemental Table S1). Differences in transcript regulation between short-term chemical treatments and constitutive knockout lines, however, are not surprising, as mutant plants often adapt their signaling state to changes in metabolism (Schwarzländer et al., 2012). Furthermore, in this study, it was shown that most transcript abundances are regulated depending on citrate concentration and incubation time (Fig. 2). To mimic the same dynamic conditions in a transgenic plant, and thus a one-to-one comparison, will be nearly impossible to achieve, especially as metabolic cross talk in signaling can also be expected (e.g. sugar levels were down-regulated in *icdh* mutants while they were up-regulated with citrate feeding).

A link between mitochondrial function and pathogen defense was recently demonstrated in the *noxy* mutants, which have a defect in mitochondrial physiology and are affected in mitochondrial retrograde signaling (Vellosillo et al., 2013). Whether the *noxy* mutations also affect mitochondrial TCA cycle activities, and thus citrate export, is currently unknown and will be interesting to investigate.

The Interaction of Citrate with Plant Hormone Signaling Pathways

The comparison with Genevestigator data sets also revealed a similarity of the transcriptome response to citrate and PBZ treatment that inhibits GA biosynthesis and thus affects GA signaling (Fig. 6). To further investigate the interaction of citrate with plant hormone signaling, several mutants with defects in hormone signaling pathways that convey signals derived from GA, JA, SA, and BR were tested (Fig. 7). The *bak1* mutant, which is hypersensitive to BR (Whippo and Hangarter, 2005), as well as *qDELLA*, which is constitutively derepressed in GA signaling, showed the strongest attenuation in the transcript accumulation after citrate treatment. Both proteins play a role in plant hormone signaling pathways involved in the plant response to biotic stress. Thus, citrate might partially repress the GA signaling pathway, which could also explain the similarity to the transcriptome response to pathogens, as GA not only regulates important plant growth responses but also interacts with other plant hormone signaling pathways and, for example, stimulates the production of SA (Alonso-Ramírez et al., 2009). Furthermore, BRs also inhibit flg22 responses and promote the susceptibility of Arabidopsis to *P. syringae* (Albrecht et al., 2012; Belkhadir et al., 2012), which may explain why the BR-hypersensitive *bak1* mutant has reduced citrate responses.

Interestingly the repression of *OEP16-1* after citrate treatment was elevated in the *npr1* mutant, which is derepressed in JA signaling. The redox-regulated NPR1 protein usually acts as suppressor of JA-dependent signaling by transcriptional suppression of JA-induced genes and by blocking signaling via the E3 ubiquitin ligase-containing complex SCF^{COI1} containing COI1 (Spoel et al., 2003). Besides its SA-dependent regulation, NPR1 also acts independently and integrates JA and ethylene signals (Feys and Parker, 2000). This was demonstrated by Reuber et al. (1998), who reported that *PR1* induction was abolished in the *NahG* transgenic line upon pathogen infection with *Erysiphe orontii* but was only partially compromised in the *npr1* mutant background. In the case of *OEP16-1*, the *npr1* mutant even showed an opposite effect to the *NahG* transgenic line (Fig. 7), indicating that NPR1 might act as a suppressor of citrate-mediated gene repression. Hence, citrate feeding might impact the interaction of these different plant hormone signaling pathways, and it will be important to further dissect this interaction in the future.

Is Citrate Affecting the Transcriptome Directly?

Here, we have demonstrated that feeding of citrate to Arabidopsis leaves induced a mild but widespread reprogramming of gene expression. Although some of the observed transcriptome changes might result from an induced accumulation of sugars, some of the transcriptome changes were different from those observed after Glc and Suc feeding (Fig. 6) or even unique to citrate feeding, such as the response of the selected marker transcripts, *CI1* and *FER1*, which were solely regulated in abundance with increased citrate and not with other sugars or carboxylic acids (Fig. 4). Only feeding with the nonmetabolizable citrate analog tricarballylate also resulted in an induced accumulation of these marker transcripts (Fig. 5). The extent of

induction of *CI1* and *FER1* marker transcripts, however, was slightly less than after citrate feeding, while internal citrate levels were increased to a similar extent than after citrate feeding. One explanation for the difference in induction could be that citrate is directly sensed at the plasma membrane, and thus the subcellular location of citrate would be important for signaling. However, an alternative explanation could be that tricarballylate competes with citrate for binding sites at putative receptor proteins or enzymes involved in signaling. Despite the structural similarity of citrate and tricarballylate, tricarballylate is much less inhibitory to isocitrate dehydrogenase activity than citrate at high concentrations (Coultate and Dennis, 1969). Another example is the bacterial tricarboxylate chemoreceptor McpS (for methyl-accepting chemotaxis receptor protein), which has much higher binding affinities to citrate than to isocitrate and no binding affinities to tricarballylate, indicating an essential role for the hydroxy group in protein binding and recognition in this case (Lacal et al., 2010). Our results demonstrate that the regulation of transcript abundance by altered citrate level was very much time and concentration dependent (Fig. 2). Taken together, these results strongly indicate that plants cells can specifically recognize the abundance of citrate.

In mammalian cells, different carboxylic acids have been shown to have specific effects on the activity of 2-OG-dependent 2-oxygenases, such as the hypoxia-inducible factor prolyl hydroxylases, JmjC family Lys demethylases, and 5-methylcytosine hydroxylases, and thus affect transcription (for review, see Yang et al., 2012). While fumarate, succinate, and isocitrate were shown to competitively inhibit the PHD2 hypoxia-inducible factor hydroxylase, citrate was also able to bind to the active site of PHD2 but had no inhibitory effect. Furthermore, citrate was the only carboxylic acid to induce the PHD2 apocomplex formation and protected PHD2 activity from inactivation by actively removing iron (Hewitson et al., 2007). Another specific role for citrate in metabolite signaling was shown for iron dicitrate, which competitively inhibits the SHP1 protein Tyr phosphatase in macrophage cells to regulate MAPK signaling (Gomez et al., 2010). Furthermore, citrate exported from mitochondria and metabolized through the cytosolic ATP-citrate lyase was shown to mediate histone acetylation in liver cells to specifically regulate the expression of glycolysis-related genes (Wellen et al., 2009). Hence, citrate might indeed have specific roles in signaling that differ from other carboxylic acids, especially due to its high affinity to binding divalent cations such as iron or even calcium (for review, see Schwarzländer and Finkemeier, 2013). It will be interesting to investigate whether such specific signaling mechanisms also exist in plants, and the major challenge in future research will be to understand how the abundance of key metabolites such as citrate and other carboxylic acids is perceived and signaled within the plant cell.

MATERIALS AND METHODS

Plant Material and Growth Conditions

Arabidopsis (*Arabidopsis thaliana*) plants were grown on soil for 4 weeks on compost supplemented with vermiculite at 22°C with a photoperiod of 16 h and a light intensity of 100 to 150 μmol m^{-2} s^{-1}. The following mutant lines were obtained from the Nottingham Arabidopsis Stock Center: *coi1* (N663405), *bak1* (N159), *npr1-1* (N3726), *abi4-1* (N8104), *pad4-1* (N3806), *ein2-1/pad4-1* (N66000), and *mlo2-11/NahG* (N9726). The *pII* mutant seeds were kindly provided by Sylvie Ferrario-Mery (INRA) and Michael Hodges (Université Paris Sud-XI); *qDELLA*, *gai*, and *ctr1* mutant seeds were kindly provided by Nicholas Harberd (University of Oxford).

Effector Treatments

Ten to 20 fully expanded leaves from 4-week-old Arabidopsis plants were pooled and cut into 2-mm-diameter leaf slices using a razor blade (for each biological replicate). After vacuum infiltration in effector solutions (three times for 5 min each), the leaf slices were incubated at a light intensity of 100 μmol m^{-2} s^{-1} for the indicated time periods. All solutions used for infiltrations were made in 1 mM MES, and pH was adjusted afterward to 5.5 (KOH). All chemicals were purchased from Sigma-Aldrich. At the end of the incubations, leaf material was briefly blotted dry on tissue paper and flash frozen in liquid nitrogen.

RNA Isolation, cDNA Synthesis, and QRT-PCR

RNA was extracted using Trizol Reagent (Invitrogen) followed by chloroform extraction, isopropanol precipitation, and subsequent $LiCl_2$ precipitation. The quality and quantity of RNA were confirmed on agarose gels and by spectrophotometric quantitation. Complementary DNA (cDNA) was synthesized from DNase-treated RNA with SuperScriptII reverse transcriptase (Invitrogen) after the manufacturer's protocol. QRT-PCR was carried out in triplicate in an ABI Prism 3700 using SYBR Green Master Mix (ABI) and gene-specific primers. Levels of selected transcripts in each sample were calculated using the standard curve method (Applied Biosystems; McWatters et al., 2007). Expression levels of each transcript were normalized to *ACTIN2* (At3g18780) and *POLYUBIQUITIN10* (At4g05320) transcripts as housekeeping genes. The amount of transcript in each control treatment (for each time point) was set to 1, and changes in treated samples are expressed as log2IFs (treatment/control). Primer sequences are listed in Supplemental Table S5.

Microarray Experiments

cDNA labeling was carried out using the 3DNA Array 50 kit (version 2; Genisphere) according to the manufacturer's instructions. Cy3- or Cy5-labeled cDNA probes were hybridized against the Arabidopsis 29k Oligonucleotide Microarrays (http://ag.arizona.edu/microarray). Microarray hybridization and data analysis were performed as described (Schwarzländer et al., 2012). Significantly regulated transcripts were detected by a Cyber-T test analysis (Baldi and Long, 2001; Bayes $P < 0.05$). The data sets were deposited at the European Bioinformatics Institute ArrayExpress database (accession no. E-MEXP-3110) according to the Minimum Information About Microarray Experiments guidelines. Functional class scoring was implemented using MapMan software (Thimm et al., 2004) applying the Benjamini-Hochberg correction. The Genevestigator database was used to analyze the expression of selected marker genes under various stress treatments as well as to perform a similarity analysis with citrate-regulated transcripts against all available microarray data sets in the database (Zimmermann et al., 2004). Hierarchical cluster analysis was performed using the algorithm for average linkage clustering with a Pearson correlation integrated in the MeV version 4.7.3 microarray software suite (Saeed et al., 2006). Transcript data for the cluster analysis were extracted from the following microarray data sets: flg22 and PBZ (GSE17464), Glc (E-MEXP-475), Suc (NASCARRAYS-315), and KIN10 overexpressors (Baena-González et al., 2007).

Determination of Metabolite Levels

For metabolite extraction, 100 mg of leaf material was briefly washed, dried, and flash frozen in liquid nitrogen. Metabolites were extracted and analyzed by GC-MS as described (Roessner et al., 2001), and relative quantification was performed using the TagFinder software package (Luedemann et al., 2008).

Statistical Analysis

Student's t and χ^2 tests were performed using Microsoft Excel. Significant differences ($P < 0.05$) are highlighted with asterisks and marginal significant differences ($P < 0.1$) with crosses in the figures. Cyber-T analysis was performed using the online platform http://cybert.ics.uci.edu (Baldi and Long, 2001).

Supplemental Data

The following materials are available in the online version of this article.

Supplemental Figure S1. Differential expression of selected citrate-regulated transcripts under biotic and abiotic stress treatments.

Supplemental Table S1. Data table with mean $\log_2$ fold changes and P values from Cyber-T analysis from malate and citrate microarray analysis.

Supplemental Table S2. Functional class scoring results with Hochberg correction from malate and citrate microarray experiments using MapMan software.

Supplemental Table S3. List of regulated metabolites after 1 mM citrate and malate feeding for 2, 4, and 8 h identified by GC-MS analysis.

Supplemental Table S4. List of regulated metabolites after feeding of 10 mM citrate or 10 mM tricarballylate for 4 h identified by GC-MS analysis.

Supplemental Table S5. List of primers used in QRT-PCR experiments.

ACKNOWLEDGMENTS

We gratefully thank James Whelan and Estelle Giraud (University of Western Australia, Perth) for help with the "significance of overlaps" analysis, Sylvie Ferrario-Mery (Institut Jean-Pierre Bourgin, Institut National de la Recherche Agronomique, Versailles) and Michael Hodges (Université Paris Sud XI) for the *pII* seeds, Nicholas Harberd (University of Oxford) for the *qDELLA*, *gai*, and *ctr1* seeds. Technical assistance by Marcel Strüwe (Rudolf-Rempel-Berufskolleg, Bielefeld) is gratefully acknowledged.

Received January 10, 2013; accepted March 13, 2013; published March 13, 2013.

LITERATURE CITED

Albrecht C, Boutrot F, Segonzac C, Schwessinger B, Gimenez-Ibanez S, Chinchilla D, Rathjen JP, de Vries SC, Zipfel C (2012) Brassinosteroids inhibit pathogen-associated molecular pattern-triggered immune signaling independent of the receptor kinase BAK1. Proc Natl Acad Sci USA **109:** 303–308

Alonso-Ramírez A, Rodríguez D, Reyes D, Jiménez JA, Nicolás G, López-Climent M, Gómez-Cadenas A, Nicolás C (2009) Evidence for a role of gibberellins in salicylic acid-modulated early plant responses to abiotic stress in Arabidopsis seeds. Plant Physiol **150:** 1335–1344

Araújo WL, Nunes-Nesi A, Osorio S, Usadel B, Fuentes D, Nagy R, Balbo I, Lehmann M, Studart-Witkowski C, Tohge T, et al (2011) Antisense inhibition of the iron-sulphur subunit of succinate dehydrogenase enhances photosynthesis and growth in tomato via an organic acid-mediated effect on stomatal aperture. Plant Cell **23:** 600–627

Araújo WL, Tohge T, Nunes-Nesi A, Daloso DM, Nimick M, Krahnert I, Bunik VI, Moorhead GB, Fernie AR (2012) Phosphonate analogs of 2-oxoglutarate perturb metabolism and gene expression in illuminated Arabidopsis leaves. Front Plant Sci **3:** 114

Baena-González E, Rolland F, Thevelein JM, Sheen J (2007) A central integrator of transcription networks in plant stress and energy signalling. Nature **448:** 938–942

Baena-González E, Sheen J (2008) Convergent energy and stress signaling. Trends Plant Sci **13:** 474–482

Baldi P, Long AD (2001) A Bayesian framework for the analysis of microarray expression data: regularized t-test and statistical inferences of gene changes. Bioinformatics **17:** 509–519

Baxter CJ, Redestig H, Schauer N, Repsilber D, Patil KR, Nielsen J, Selbig J, Liu J, Fernie AR, Sweetlove LJ (2007) The metabolic response of heterotrophic Arabidopsis cells to oxidative stress. Plant Physiol **143:** 312–325

Belkhadir Y, Jaillais Y, Epple P, Balsemão-Pires E, Dangl JL, Chory J (2012) Brassinosteroids modulate the efficiency of plant immune responses to microbe-associated molecular patterns. Proc Natl Acad Sci USA **109:** 297–302

Boziaris IS, Adams MR (1999) Effect of chelators and nisin produced in situ on inhibition and inactivation of gram negatives. Int J Food Microbiol **53:** 105–113

Cao H, Glazebrook J, Clarke JD, Volko S, Dong X (1997) The Arabidopsis NPR1 gene that controls systemic acquired resistance encodes a novel protein containing ankyrin repeats. Cell **88:** 57–63

Carrari F, Nunes-Nesi A, Gibon Y, Lytovchenko A, Loureiro ME, Fernie AR (2003) Reduced expression of aconitase results in an enhanced rate of photosynthesis and marked shifts in carbon partitioning in illuminated leaves of wild species tomato. Plant Physiol **133:** 1322–1335

Cheng H, Qin L, Lee S, Fu X, Richards DE, Cao D, Luo D, Harberd NP, Peng J (2004) Gibberellin regulates Arabidopsis floral development via suppression of DELLA protein function. Development **131:** 1055–1064

Chinchilla D, Shan L, He P, de Vries S, Kemmerling B (2009) One for all: the receptor-associated kinase BAK1. Trends Plant Sci **14:** 535–541

Clifton R, Lister R, Parker KL, Sappl PG, Elhafez D, Millar AH, Day DA, Whelan J (2005) Stress-induced co-expression of alternative respiratory chain components in *Arabidopsis thaliana*. Plant Mol Biol **58:** 193–212

Consonni C, Humphry ME, Hartmann HA, Livaja M, Durner J, Westphal L, Vogel J, Lipka V, Kemmerling B, Schulze-Lefert P, et al (2006) Conserved requirement for a plant host cell protein in powdery mildew pathogenesis. Nat Genet **38:** 716–720

Coruzzi GM, Zhou L (2001) Carbon and nitrogen sensing and signaling in plants: emerging 'matrix effects.' Curr Opin Plant Biol **4:** 247–253

Coultate TP, Dennis DT (1969) Regulatory properties of a plant NAD:isocitrate dehydrogenase: the effect of inorganic ions. Eur J Biochem **7:** 153–158

Fernie AR, Carrari F, Sweetlove LJ (2004) Respiratory metabolism: glycolysis, the TCA cycle and mitochondrial electron transport. Curr Opin Plant Biol **7:** 254–261

Ferrario-Méry S, Bouvet M, Leleu O, Savino G, Hodges M, Meyer C (2005) Physiological characterisation of Arabidopsis mutants affected in the expression of the putative regulatory protein PII. Planta **223:** 28–39

Feys BJ, Parker JE (2000) Interplay of signaling pathways in plant disease resistance. Trends Genet **16:** 449–455

Finkelstein RR, Wang ML, Lynch TJ, Rao S, Goodman HM (1998) The *Arabidopsis* abscisic acid response locus ABI4 encodes an APETALA 2 domain protein. Plant Cell **10:** 1043–1054

Gaffney T, Friedrich L, Vernooij B, Negrotto D, Nye G, Uknes S, Ward E, Kessmann H, Ryals J (1993) Requirement of salicylic acid for the induction of systemic acquired resistance. Science **261:** 754–756

Gawron O, Jones L (1977) Structural basis for aconitase activity inactivation by butanedione and binding of substrates and inhibitors. Biochim Biophys Acta **484:** 453–464

Genoud T, Trevino Santa Cruz MB, Métraux JP (2001) Numeric simulation of plant signaling networks. Plant Physiol **126:** 1430–1437

Glazebrook J, Zook M, Mert F, Kagan I, Rogers EE, Crute IR, Holub EB, Hammerschmidt R, Ausubel FM (1997) Phytoalexin-deficient mutants of Arabidopsis reveal that PAD4 encodes a regulatory factor and that four PAD genes contribute to downy mildew resistance. Genetics **146:** 381–392

Gomez MA, Alisaraie L, Shio MT, Berghuis AM, Lebrun C, Gautier-Luneau I, Olivier M (2010) Protein tyrosine phosphatases are regulated by mononuclear iron dicitrate. J Biol Chem **285:** 24620–24628

Gonzali S, Loreti E, Solfanelli C, Novi G, Alpi A, Perata P (2006) Identification of sugar-modulated genes and evidence for *in vivo* sugar sensing in Arabidopsis. J Plant Res **119:** 115–123

Gray GR, Maxwell DP, Villarimo AR, McIntosh L (2004) Mitochondria/nuclear signaling of alternative oxidase gene expression occurs through distinct pathways involving organic acids and reactive oxygen species. Plant Cell Rep **23:** 497–503

Gupta KJ, Shah JK, Brotman Y, Jahnke K, Willmitzer L, Kaiser WM, Bauwe H, Igamberdiev AU (2012) Inhibition of aconitase by nitric oxide leads to induction of the alternative oxidase and to a shift of metabolism towards biosynthesis of amino acids. J Exp Bot **63:** 1773–1784

Guzmán P, Ecker JR (1990) Exploiting the triple response of *Arabidopsis* to identify ethylene-related mutants. Plant Cell **2:** 513–523

Haydon MJ, Cobbett CS (2007) Transporters of ligands for essential metal ions in plants. New Phytol **174:** 499–506

Hedrich R, Marten I, Lohse G, Dietrich P, Winter H, Lohaus G, Heldt HW (1994) Malate-sensitive anion channels enable guard-cells to sense changes in the ambient CO_2 concentration. Plant J **6:** 741–748

Hewitson KS, Liénard BM, McDonough MA, Clifton IJ, Butler D, Soares AS, Oldham NJ, McNeill LA, Schofield CJ (2007) Structural and mechanistic studies on the inhibition of the hypoxia-inducible transcription factor hydroxylases by tricarboxylic acid cycle intermediates. J Biol Chem **282:** 3293–3301

Ho LH, Giraud E, Uggalla V, Lister R, Clifton R, Glen A, Thirkettle-Watts D, Van Aken O, Whelan J (2008) Identification of regulatory pathways controlling gene expression of stress-responsive mitochondrial proteins in Arabidopsis. Plant Physiol **147:** 1858–1873

Horling F, Lamkemeyer P, König J, Finkemeier I, Kandlbinder A, Baier M, Dietz KJ (2003) Divergent light-, ascorbate-, and oxidative stress-dependent regulation of expression of the peroxiredoxin gene family in Arabidopsis. Plant Physiol **131:** 317–325

Jang JC, León P, Zhou L, Sheen J (1997) Hexokinase as a sugar sensor in higher plants. Plant Cell **9:** 5–19

Kieber JJ, Rothenberg M, Roman G, Feldmann KA, Ecker JR (1993) CTR1, a negative regulator of the ethylene response pathway in Arabidopsis, encodes a member of the raf family of protein kinases. Cell **72:** 427–441

Lacal J, Alfonso C, Liu X, Parales RE, Morel B, Conejero-Lara F, Rivas G, Duque E, Ramos JL, Krell T (2010) Identification of a chemoreceptor for tricarboxylic acid cycle intermediates: differential chemotactic response towards receptor ligands. J Biol Chem **285:** 23126–23136

Lancien M, Roberts MR (2006) Regulation of *Arabidopsis thaliana* 14-3-3 gene expression by gamma-aminobutyric acid. Plant Cell Environ **29:** 1430–1436

Lee S, Cheng H, King KE, Wang W, He Y, Hussain A, Lo J, Harberd NP, Peng J (2002) Gibberellin regulates Arabidopsis seed germination via RGL2, a GAI/RGA-like gene whose expression is up-regulated following imbibition. Genes Dev **16:** 646–658

Lehmann M, Schwarzländer M, Obata T, Sirikantaramas S, Burow M, Olsen CE, Tohge T, Fricker MD, Møller BL, Fernie AR, et al (2009) The metabolic response of Arabidopsis roots to oxidative stress is distinct from that of heterotrophic cells in culture and highlights a complex relationship between the levels of transcripts, metabolites, and flux. Mol Plant **2:** 390–406

Li Y, Lee KK, Walsh S, Smith C, Hadingham S, Sorefan K, Cawley G, Bevan MW (2006) Establishing glucose- and ABA-regulated transcription networks in Arabidopsis by microarray analysis and promoter classification using a relevance vector machine. Genome Res **16:** 414–427

Luedemann A, Strassburg K, Erban A, Kopka J (2008) TagFinder for the quantitative analysis of gas chromatography-mass spectrometry (GC-MS)-based metabolite profiling experiments. Bioinformatics **24:** 732–737

Mackenzie S, McIntosh L (1999) Higher plant mitochondria. Plant Cell **11:** 571–586

Martinoia E, Rentsch D (1994) Malate compartmentation: responses to a complex metabolism. Annu Rev Plant Physiol Plant Mol Biol **45:** 447–467

McCammon MT, Epstein CB, Przybyla-Zawislak B, McAlister-Henn L, Butow RA (2003) Global transcription analysis of Krebs tricarboxylic acid cycle mutants reveals an alternating pattern of gene expression and effects on hypoxic and oxidative genes. Mol Biol Cell **14:** 958–972

McWatters HG, Kolmos E, Hall A, Doyle MR, Amasino RM, Gyula P, Nagy F, Millar AJ, Davis SJ (2007) ELF4 is required for oscillatory properties of the circadian clock. Plant Physiol **144:** 391–401

Meyer S, De Angeli A, Fernie AR, Martinoia E (2010a) Intra- and extracellular excretion of carboxylates. Trends Plant Sci **15:** 40–47

Meyer S, Mumm P, Imes D, Endler A, Weder B, Al-Rasheid KA, Geiger D, Marten I, Martinoia E, Hedrich R (2010b) AtALMT12 represents an R-type anion channel required for stomatal movement in Arabidopsis guard cells. Plant J **63:** 1054–1062

Mhamdi A, Mauve C, Gouia H, Saindrenan P, Hodges M, Noctor G (2010) Cytosolic NADP-dependent isocitrate dehydrogenase contributes to redox homeostasis and the regulation of pathogen responses in Arabidopsis leaves. Plant Cell Environ **33:** 1112–1123

Moore B, Zhou L, Rolland F, Hall Q, Cheng WH, Liu YX, Hwang I, Jones T, Sheen J (2003) Role of the Arabidopsis glucose sensor HXK1 in nutrient, light, and hormonal signaling. Science **300:** 332–336

Morgan MJ, Lehmann M, Schwarzländer M, Baxter CJ, Sienkiewicz-Porzucek A, Williams TC, Schauer N, Fernie AR, Fricker MD, Ratcliffe RG, et al (2008) Decrease in manganese superoxide dismutase leads to reduced root growth and affects tricarboxylic acid cycle flux and mitochondrial redox homeostasis. Plant Physiol **147:** 101–114

Muller C, Scheible WR, Stitt M, Krapp A (2001) Influence of malate and 2-oxoglutarate on the NIA transcript level and nitrate reductase activity in tobacco leaves. Plant Cell Environ **24:** 191–203

Navarro L, Bari R, Achard P, Lisón P, Nemri A, Harberd NP, Jones JD (2008) DELLAs control plant immune responses by modulating the balance of jasmonic acid and salicylic acid signaling. Curr Biol **18:** 650–655

Nunes-Nesi A, Carrari F, Gibon Y, Sulpice R, Lytovchenko A, Fisahn J, Graham J, Ratcliffe RG, Sweetlove LJ, Fernie AR (2007) Deficiency of mitochondrial fumarase activity in tomato plants impairs photosynthesis via an effect on stomatal function. Plant J **50:** 1093–1106

Nunes-Nesi A, Carrari F, Lytovchenko A, Smith AM, Loureiro ME, Ratcliffe RG, Sweetlove LJ, Fernie AR (2005) Enhanced photosynthetic performance and growth as a consequence of decreasing mitochondrial malate dehydrogenase activity in transgenic tomato plants. Plant Physiol **137:** 611–622

Plaxton WC (1996) The organization and regulation of plant glycolysis. Annu Rev Plant Physiol Plant Mol Biol **47:** 185–214

Price J, Laxmi A, St Martin SK, Jang JC (2004) Global transcription profiling reveals multiple sugar signal transduction mechanisms in *Arabidopsis*. Plant Cell **16:** 2128–2150

Raven JA, Farquhar GD (1981) Methylammonium transport in *Phaseolus vulgaris* leaf slices. Plant Physiol **67:** 859–863

Reuber TL, Plotnikova JM, Dewdney J, Rogers EE, Wood W, Ausubel FM (1998) Correlation of defense gene induction defects with powdery mildew susceptibility in Arabidopsis enhanced disease susceptibility mutants. Plant J **16:** 473–485

Roessner U, Luedemann A, Brust D, Fiehn O, Linke T, Willmitzer L, Fernie A (2001) Metabolic profiling allows comprehensive phenotyping of genetically or environmentally modified plant systems. Plant Cell **13:** 11–29

Saeed AI, Bhagabati NK, Braisted JC, Liang W, Sharov V, Howe EA, Li J, Thiagarajan M, White JA, Quackenbush J (2006) TM4 microarray software suite. Methods Enzymol **411:** 134–193

Scheibe R (2004) Malate valves to balance cellular energy supply. Physiol Plant **120:** 21–26

Schwarzländer M, Finkemeier I (2013) Mitochondrial energy and redox signaling in plants. Antioxid Redox Signal (in press)

Schwarzländer M, König AC, Sweetlove LJ, Finkemeier I (2012) The impact of impaired mitochondrial function on retrograde signalling: a meta-analysis of transcriptomic responses. J Exp Bot **63:** 1735–1750

Sellick CA, Reece RJ (2005) Eukaryotic transcription factors as direct nutrient sensors. Trends Biochem Sci **30:** 405–412

Sheen J (1990) Metabolic repression of transcription in higher plants. Plant Cell **2:** 1027–1038

Sienkiewicz-Porzucek A, Sulpice R, Osorio S, Krahnert I, Leisse A, Urbanczyk-Wochniak E, Hodges M, Fernie AR, Nunes-Nesi A (2010) Mild reductions in mitochondrial NAD-dependent isocitrate dehydrogenase activity result in altered nitrate assimilation and pigmentation but do not impact growth. Mol Plant **3:** 156–173

Spoel SH, Koornneef A, Claessens SMC, Korzelius JP, Van Pelt JA, Mueller MJ, Buchala AJ, Métraux JP, Brown R, Kazan K, et al (2003) NPR1 modulates cross-talk between salicylate- and jasmonate-dependent defense pathways through a novel function in the cytosol. Plant Cell **15:** 760–770

Stitt M (1999) Nitrate regulation of metabolism and growth. Curr Opin Plant Biol **2:** 178–186

Sulpice R, Sienkiewicz-Porzucek A, Osorio S, Krahnert I, Stitt M, Fernie AR, Nunes-Nesi A (2010) Mild reductions in cytosolic NADP-dependent isocitrate dehydrogenase activity result in lower amino acid contents and pigmentation without impacting growth. Amino Acids **39:** 1055–1066

Templeton GW, Moorhead GB (2004) A renaissance of metabolite sensing and signaling: from modular domains to riboswitches. Plant Cell **16:** 2252–2257

Thimm O, Bläsing O, Gibon Y, Nagel A, Meyer S, Krüger P, Selbig J, Müller LA, Rhee SY, Stitt M (2004) MAPMAN: a user-driven tool to display genomics data sets onto diagrams of metabolic pathways and other biological processes. Plant J **37:** 914–939

Usadel B, Bläsing OE, Gibon Y, Retzlaff K, Höhne M, Günther M, Stitt M (2008) Global transcript levels respond to small changes of the carbon status during progressive exhaustion of carbohydrates in Arabidopsis rosettes. Plant Physiol **146:** 1834–1861

Vaara M (1992) Agents that increase the permeability of the outer membrane. Microbiol Rev **56:** 395–411

Van Aken O, Whelan J (2012) Comparison of transcriptional changes to chloroplast and mitochondrial perturbations reveals common and specific responses in Arabidopsis. Front Plant Sci **3:** 281

Vanlerberghe GC, McIntosh L (1994) Mitochondrial electron transport regulation of nuclear gene expression: studies with the alternative oxidase gene of tobacco. Plant Physiol **105:** 867–874

Vanlerberghe GC, McIntosh L (1996) Signals regulating the expression of the nuclear gene encoding alternative oxidase of plant mitochondria. Plant Physiol **111:** 589–595

van Schooten B, Testerink C, Munnik T (2006) Signalling diacylglycerol pyrophosphate, a new phosphatidic acid metabolite. Biochim Biophys Acta **1761:** 151–159

Vellosillo T, Aguilera V, Marcos R, Bartsch M, Vicente J, Cascón T, Hamberg M, Castresana C (2013) Defense activated by 9-lipoxygenase-derived oxylipins requires specific mitochondrial proteins. Plant Physiol **161:** 617–627

Wang L, Mitra RM, Hasselmann KD, Sato M, Lenarz-Wyatt L, Cohen JD, Katagiri F, Glazebrook J (2008) The genetic network controlling the Arabidopsis transcriptional response to *Pseudomonas syringae* pv. *maculicola*: roles of major regulators and the phytotoxin coronatine. Mol Plant Microbe Interact **21:** 1408–1420

Wellen KE, Hatzivassiliou G, Sachdeva UM, Bui TV, Cross JR, Thompson CB (2009) ATP-citrate lyase links cellular metabolism to histone acetylation. Science **324:** 1076–1080

Whippo CW, Hangarter RP (2005) A brassinosteroid-hypersensitive mutant of BAK1 indicates that a convergence of photomorphogenic and hormonal signaling modulates phototropism. Plant Physiol **139:** 448–457

Wolffram S, Zimmermann W, Scharrer E (1993) Transport of tricarballylate by intestinal brush-border membrane vesicles from steers. Exp Physiol **78:** 473–484

Xiao W, Sheen J, Jang JC (2000) The role of hexokinase in plant sugar signal transduction and growth and development. Plant Mol Biol **44:** 451–461

Xie DX, Feys BF, James S, Nieto-Rostro M, Turner JG (1998) COI1: an Arabidopsis gene required for jasmonate-regulated defense and fertility. Science **280:** 1091–1094

Yang MS, Soga T, Pollard PJ, Adam J (2012) The emerging role of fumarate as an oncometabolite. Front Oncol **2:** 85

Zhang C, Barthelson RA, Lambert GM, Galbraith DW (2008) Global characterization of cell-specific gene expression through fluorescence-activated sorting of nuclei. Plant Physiol **147:** 30–40

Zimmermann P, Hirsch-Hoffmann M, Hennig L, Gruissem W (2004) GENEVESTIGATOR: Arabidopsis microarray database and analysis toolbox. Plant Physiol **136:** 2621–2632

Publication 3

Redox regulation of Arabidopsis mitochondrial citrate synthase.

Schmidtmann E[1], **König AC**, Orwat A, Leister D, Hartl M, Finkemeier I

(2014)

Molecular Plant 7(1): 156-69

Molecular Plant • Volume 7 • Number 1 • Pages 156–169 • January 2014 RESEARCH ARTICLE

Redox Regulation of *Arabidopsis* Mitochondrial Citrate Synthase

Elisabeth Schmidtmann, Ann-Christine König, Anne Orwat, Dario Leister, Markus Hartl and **Iris Finkemeier**[1]

Botany, Department I of Biology, Ludwig-Maximilians-University Munich, Grosshaderner Strasse 2, 82152 Planegg-Martinsried, Germany

ABSTRACT Citrate synthase has a key role in the tricarboxylic (TCA) cycle of mitochondria of all organisms, as it catalyzes the first committed step which is the fusion of a carbon–carbon bond between oxaloacetate and acetyl CoA. The regulation of TCA cycle function is especially important in plants, since mitochondrial activities have to be coordinated with photosynthesis. The posttranslational regulation of TCA cycle activity in plants is thus far almost entirely unexplored. Although several TCA cycle enzymes have been identified as thioredoxin targets *in vitro*, the existence of any thioredoxin-dependent regulation as known for the Calvin cycle, yet remains to be demonstrated. Here we have investigated the redox regulation of the *Arabidopsis* citrate synthase enzyme by site-directed mutagenesis of its six cysteine residues. Our results indicate that oxidation inhibits the enzyme activity by the formation of mixed disulfides, as the partially oxidized citrate synthase enzyme forms large redox-dependent aggregates. Furthermore, we were able to demonstrate that thioredoxin can cleave diverse intra- as well as intermolecular disulfide bridges, which strongly enhances the activity of the enzyme. Activity measurements with the cysteine variants of the enzyme revealed important cysteine residues affecting total enzyme activity as well as the redox sensitivity of the enzyme.

Key words: citrate synthase; mitochondria; cysteine residues; redox regulation; thioredoxin; TCA cycle; *Arabidopsis*.

INTRODUCTION

The mitochondrial tricarboxylic acid cycle (TCA cycle) plays an important role in energy metabolism of all aerobic organisms. Different carbon fuels are metabolized to acetyl CoA and organic acids in aerobic cells which are subsequently oxidized in the TCA cycle to deliver reduction equivalents for oxidation and ATP production in the mitochondrial electron transport chain. Furthermore, the TCA cycle delivers precursors for other biosynthetic processes such as the synthesis of aspartate. In plants, the regulation of TCA cycle and respiration is more complex than in heterotrophic organisms, as the plant mitochondrial metabolism has to be orchestrated with photosynthetic processes such as carbon assimilation in the Calvin cycle, photorespiration, nitrogen assimilation, and the dissipation of excess energy (Araujo et al., 2012; Schwarzlander and Finkemeier, 2013). The coordination of mitochondrial and chloroplastic functions was previously demonstrated in tomato mutants of different mitochondrial TCA cycle enzymes (Nunes-Nesi et al., 2011). However, not much is known yet about the mechanisms that posttranslationally regulate mitochondrial TCA cycle enzymes, and thus might coordinate the activities of chloroplasts and mitochondria (Nunes-Nesi et al., 2013).

The cellular redox milieu is one of the most important determinants that affect the catalytic activity of many metabolic enzymes by altering the redox state of cysteine residues (Scheibe and Dietz, 2012). In chloroplasts, several metabolic processes, such as the Calvin cycle and starch synthesis, for example, are regulated by NADPH-dependent thioredoxin (TRX) activation through the reduction of inter- or intramolecular disulfide bridges in enzymes (Buchanan, 1984; Schürmann and Buchanan, 2008; Michalska et al., 2009). TRXs are thiol-oxidoreductases and they generally function in redox regulation of diverse cellular processes in most organisms (Meyer et al., 2012). Their catalytic activity is based on two redox-active cysteine residues embedded in a conserved active site (Cys–Gly–Pro–Cys) (König et al., 2012). The redox-active cysteine residues of TRXs are activated by reduction which is usually mediated by NADPH-dependent thioredoxin reductases (NTR). The plant mitochondrion also contains a functional TRX/NTR-system (Laloi et al., 2001), and more than 100 *in vitro* TRX-targets have been identified in plant mitochondria from different species including several enzymes of the TCA cycle such as citrate synthase in

[1] To whom correspondence should be addressed. E-mail i.finkemeier@lmu.de, tel. +49(0)89-2180-74672.

doi:10.1093/mp/sst144, Advance Access publication 6 November 2013

Received 11 August 2013; accepted 11 October 2013

Arabidopsis mitochondria (Balmer et al., 2004; Yoshida et al., 2013). Citrate synthase catalyzes the first committed step in the TCA cycle, which is the condensation of an acetyl group (from acetyl CoA) and oxaloacetate (OAA) to citryl CoA, and requires no co-factor or metal ion for its activity. Citryl CoA is subsequently hydrolyzed by water, and citrate and CoA are released from the enzyme. In contrast to other TCA cycle enzymes, citrate synthase is exclusively localized in mitochondria in green tissues and thus the TCA cycle cannot be bypassed via cytosolic isoforms. Only in tissues with an active glyoxylate cycle are the peroxisomal isoforms of citrate synthase expressed (Pracharoenwattana et al., 2005). This is important in the context that the activity of *Arabidopsis* citrate synthase was previously shown to be inhibited by oxidation (Stevens et al., 1997) and thus cannot be instantly bypassed by the peroxisomal isoforms. Furthermore, alterations in cellular citrate contents were recently demonstrated to cause major changes in the transcriptome (Finkemeier et al., 2013). A controlled regulation of citrate synthase activity could therefore be an important regulatory mechanism for mitochondria-to-nucleus signaling. Hence, the redox regulation of *Arabidopsis* mitochondrial citrate synthase deserves further investigation, and the functional significance of the TRX interaction for its enzymatic function has not been demonstrated so far. In this study, we investigated the redox-dependent regulation of CS4 which is the major mitochondrial isoform of *Arabidopsis* citrate synthase.

RESULTS

CS4 Is the Major Mitochondrial Citrate Synthase Isoform in *Arabidopsis*

Arabidopsis mitochondria possess two predicted citrate synthase isoforms: CS4 (At2g44350) and CS5 (At3g60100), encoded by two separate nuclear genes. Although CS4 is the main isoform and much more abundant than CS5, both isoforms have previously been identified in *Arabidopsis* mitochondria in different proteomic approaches (Heazlewood et al., 2004; Klodmann et al., 2011). Not only is the protein of CS4 more abundant than CS5, but also the CS4 transcript is present at much higher levels during all growth stages in *Arabidopsis*, while the CS5 transcript is only present at fairly low levels (Genevestigator database; Zimmermann et al., 2004) (Supplemental Figure 1).

CS4 Contains Six Cysteine Residues of which Cys364 Is the Most Conserved

The mitochondrial citrate synthase sequences from plants and animals are overall highly similar in primary structure. The best characterized enzyme is the porcine citrate synthase (Larson et al., 2009), which shares 63% and 61% sequence identity with *Arabidopsis* CS4 and CS5, respectively (Figure 1), and several sites involved in coenzyme binding, the dimer–dimer interphase, as well as the amino acids of the catalytic triade (His–His–Asp) are conserved between these species (Supplemental Figure 2).

CS4 shares about 85% sequence identity with CS5 on amino acid level and, although both sequences are highly similar, they differ in their number of cysteine residues. While CS4 contains six cysteine residues, CS5 contains only four (Figure 1). The six cysteine residues of CS4 are referred to as Cys108, Cys209, Cys325, Cys365, Cys439, and Cys467 in the following and as depicted in Figure 1. The two cysteine residues, Cys209 and Cys467, which are missing in CS5 are conserved in the protein sequence of citrate synthase of rice (*Oryza sativa*), while Cys209 but not Cys467 is also conserved in the porcine (*Sus scrofa*) but not in the human citrate synthase sequence. While Cys365 seems to be conserved in most organisms, Cys325 and Cys439 are plant-specific. Hence, we selected *Arabidopsis* CS4 for further analysis, since it is the main mitochondrial isoform and it was previously identified as target of the mitochondrial TRX-o1 by TRX-affinity chromatography (Yoshida et al., 2013).

The Recombinant 6xHis-CS4 Protein Is an Active Citrate Synthase Enzyme

As the function of *Arabidopsis* CS4 is only inferred by sequence homology, we first characterized the enzyme function using a recombinant CS4 protein, which we expressed and purified with an N-terminal 6xHis-tag from *Escherichia coli*. Pettersson et al. (2000) used an N-terminal His-tag for isolation of a related recombinant citrate synthase protein from yeast and showed that it had no inhibitory effect on the enzyme activity. For the basic enzymatic characterization, we purified the recombinant CS4 protein under native conditions and kept a cysteine-reducing environment throughout all purification and dialysis steps (Figure 2A). The purified protein was highly active and showed the typical acetyl CoA- and OAA-dependent citrate synthase enzyme activity (Figure 2B–2D). Maximal citrate synthase activity was observed at 20°C and pH 8, although nearly 50% of the activity was still retained at 35°C, as well as at physiological high (pH 9) or low pH (pH 5) (Figure 2B and 2C). The K_m-values of CS4 for acetyl CoA and OAA were determined by keeping one substrate concentration constant (200 μM) and by varying the amount of the other (2.5–120 μM) (Figure 2D). While the K_m-values for acetyl CoA and OAA were with 16.5 and 49.4 μM, respectively, in the range of the K_m-value observed for pea (31 and 16 μM) and tomato (18 and 19 μM), they were slightly higher than those observed for porcine mitochondrial citrate synthase (5 and 5.9 μM) (Iredale, 1979; Jeffery et al., 1988; Kurz et al., 1995). By comparing the K_m-values as well as the specificity constants (k_{cat}/K_m) for OAA and acetyl CoA, it becomes clear that CS4 has a higher affinity for acetyl CoA than OAA (Table 1). From pig heart citrate synthase, it is known that, during catalysis, OAA is bound first, which increases the binding constant for acetyl CoA (Johansson and Pettersson, 1977). The turnover number (K_{cat}) of CS4 for acetyl CoA (72 s^{-1}) and

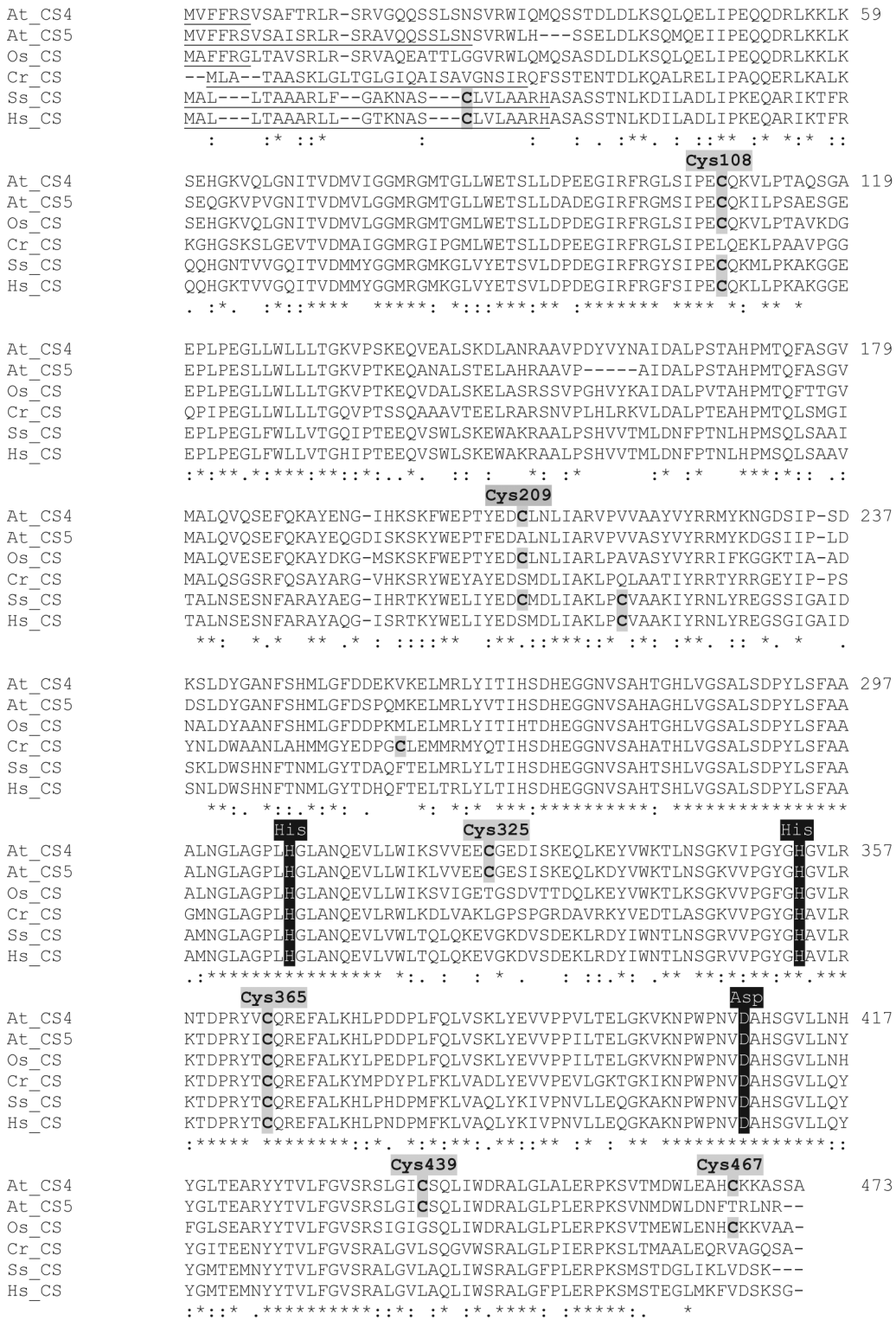

Figure 1. Amino Acid Sequence Alignment of Putative Mitochondrial Citrate Synthases from Selected Species.

Arabidopsis thaliana (At_CS4: At2g44350.1, At_CS5: At3g60100), *Oryza sativa* (Os_CS: AF302906_1), *Chlamydomonas reinhardtii* (Cr_CS: XP_001702983), *Sus scrofa* (Ss_CS: NP_999441.1), and *Homo sapiens* (Hs_CS: NM_004077.2). The alignment was performed using Clustal O version 1.2.0. Highlighted in black are the amino acids of the catalytic triade which is conserved in all species. Cysteine residues are highlighted in gray. The position of cysteine residues from AT_CS4 are indicated on top of the sequence. Putative mitochondrial presequences are underlined as predicted with TargetP (Nielsen et al., 1997; Emanuelsson et al., 2000).

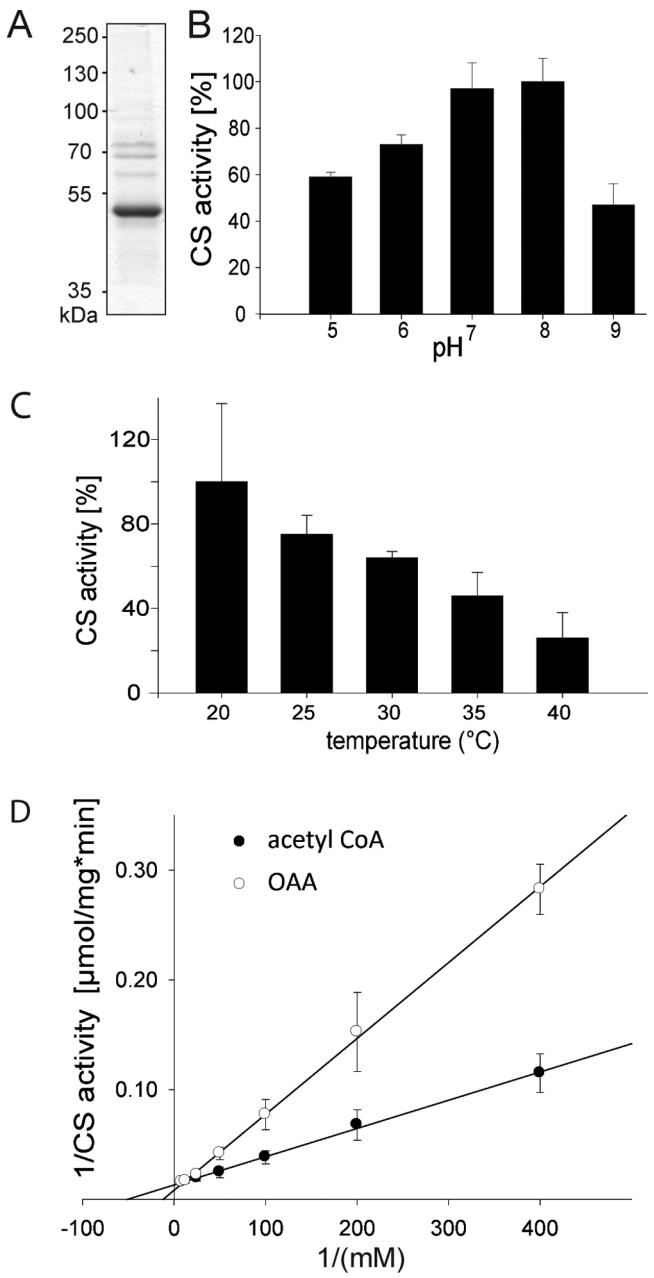

Figure 2. The Recombinant CS4 Protein Is an Active Citrate Synthase Enzyme.

(A) Coomassie-stained SDS–PAGE of the Ni-NTA purified 6xHis-CS4 protein.
(B) Enzyme activity of CS4 in dependence on pH. 100% are equal to the mean activity at pH 8 (mean ± SE, $n = 3$).
(C) Enzyme activity of CS4 in dependence on temperature. 100% are equal to the mean activity at 20°C (mean ± SE, $n = 3$).
(D) Lineweaver–Burk plot of CS4 activities depending on substrate concentrations at pH 8 and 20°C. Either oxaloacetate (OAA, white dots) or acetyl CoA (black dots) concentrations were varied while the other substrate was kept at a constant concentration of 200 µM (mean ± SE, $n = 3$).

OAA (90 s^{-1}) was not significantly different but about half of that previously reported for porcine citrate synthase (169 s^{-1}) (Kurz et al., 1995).

The *Arabidopsis* CS4 Protein Is Not Only Present as Dimer but Also as High-Molecular-Weight Oligomer under Native Conditions

Eukaryotic citrate synthase enzymes from plants and animals have generally been purified as dimers of around 100 kDa (Remington, 1992). The analysis of the crystal structure of pig heart citrate synthase revealed that two identical subunits form a non-disulfide-dependent dimer (Wiegand et al., 1979; Larson et al., 2009). To study the quaternary structure of the endogenous *Arabidopsis* citrate synthase from isolated mitochondria, we produced an antiserum against gel-purified recombinant CS4 protein. In a Western blot analysis of a Blue-Native (BN)–PAGE of membrane-solubilized mitochondrial protein complexes, we observed that citrate synthase is not only present as a dimer of around 100 kDa, but that it can also be detected in higher-molecular-weight complexes of up to 1000 kDa (Figure 3A). Hence, the detection of higher-molecular-weight complexes could indicate either that citrate synthase interacts with different mitochondrial electron chain complexes or that it forms large oligomeric complexes by itself. To further study the quaternary structure of the citrate synthase, we performed a gel-filtration chromatography with soluble proteins of *Arabidopsis* mitochondria and analyzed the eluted fractions by Western blot analysis (Figure 3B). In the gel-filtration analysis of mitochondrial extract, the protein eluted mainly as dimer but was partly also present as monomer as well as tetramer and a faint band was detected for the oligomeric form (Figure 3B, mitochondria). The recombinant protein showed a similar elution profile, although it was shifted to the higher-molecular-weight fractions (Figure 3B, CS4). Hence, *Arabidopsis* citrate synthase forms not only dimers, but also oligomeric complexes by itself.

Hydrogen Peroxide Sensitivity of CS4 Activity

In a previous study, the activity of citrate synthase from *Arabidopsis* whole-plant extracts was shown to be inactivated by 25% by oxidation using diamide, while reduction with DTT resulted in an increased enzyme activity (Stevens et al., 1997). Similarly, the recombinant CS4 protein in our study is sensitive to oxidation by hydrogen peroxide, as its activity was decreased by 54% (Figure 4). Hence, we were interested to see whether one of the six cysteine residues of CS4 is redox-sensitive and responsible for the inactivation upon oxidative stress. To test this, we produced site-directed mutants for each cysteine of CS4. The cysteine residues were exchanged to serine, to keep an amino acid of similar size and charge that is able to perform hydrogen bond interactions, but not disulfide bridge formations. The proteins were again overexpressed and purified under reducing conditions as described above. Interestingly, all cysteine mutants were able to convert acetyl CoA and oxaloacetate to citrate but with decreased efficiencies compared to CS4 (Figure 4, black bars). Cys108Ser and Cys325Ser were nearly inactive under control conditions, as their activities were decreased by 98% compared to CS4.

Table 1. Substrate-Dependent Enzymatic Characteristics of Recombinant 6xHis-Citrate Synthase 4 (CS4) of *Arabidopsis thaliana*.

Arabidopsis CS4	Oxaloacetate	Acetyl CoA
K_m (μM)	49.4	16.5
k_{cat} (s^{-1})	90.3	71.6
k_{cat}/K_m (s^{-1} M^{-1})	1 827 935	4 339 394

K_m and V_{max} values (for k_{cat}) were calculated by non-linear least squares fitting of data (Kemmer and Keller, 2010).

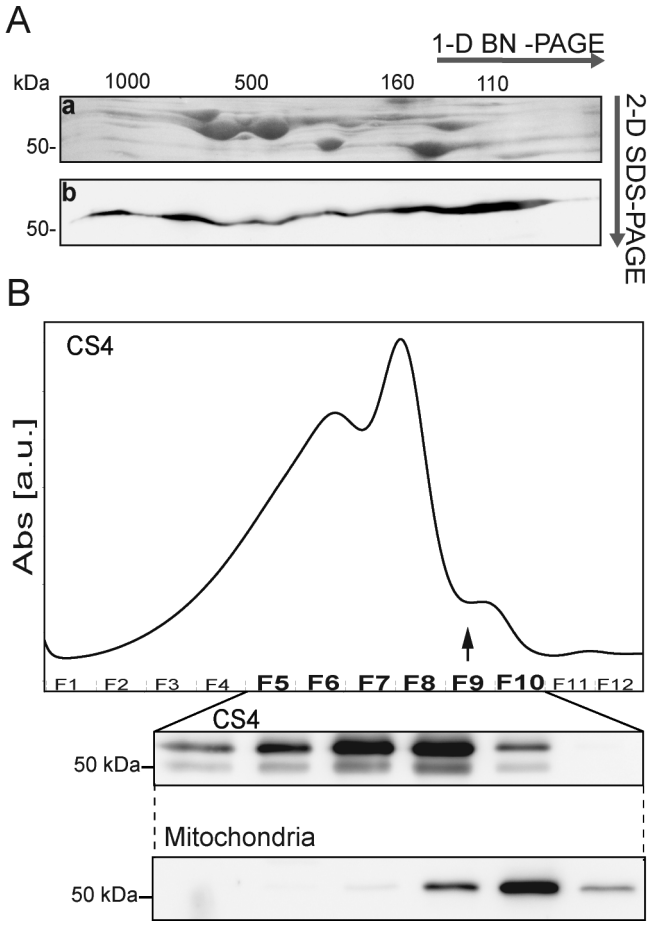

Figure 3. *Arabidopsis* Mitochondrial Citrate Synthase Forms High-Molecular-Weight Complexes *In Vivo* as well as *In Vitro*.

(A) 2D-BN–PAGE of mitochondrial protein complexes solubilized with digitonin. (a) PonceauS staining after transfer of 2D-BN–PAGE onto a nitrocellulose membrane, (b) Western blot analysis using α-CS4 antibody.

(B) Analysis of citrate synthase via size exclusion chromatography. The elution profile of the recombinant CS4 protein is shown as recorded at 280 nm. Recombinant CS4 (100 μg) and isolated mitochondria (180 μg) from *Arabidopsis* plants, respectively, were loaded onto a Superose 6 column. The eluted 1-ml fractions of recombinant CS4 or mitochondrial proteins (below) were analyzed via Western blot using αCS4-antibody (F5–F10). The arrow indicates the fraction containing the citrate synthase dimer. F5: >950 kDa, F6: 460–950 kDa, F7: 230–460 kDa, F8: 110–230 kDa, F9: 54–110 kDa, F10: 26–54 kDa.

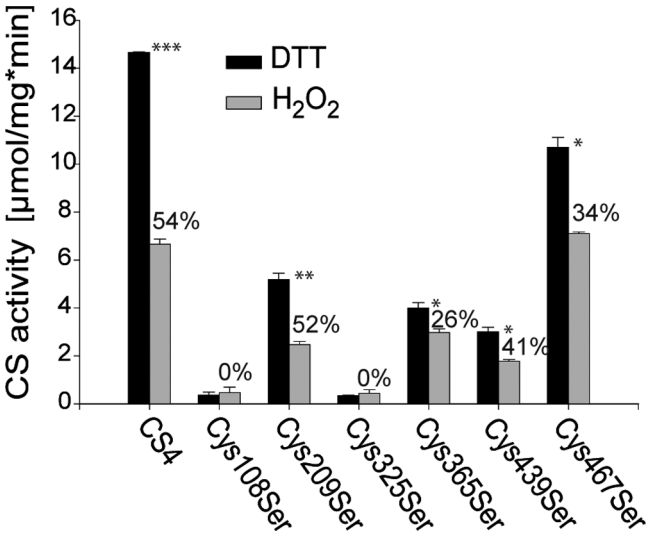

Figure 4. Cys108 and Cys325 Are Important for the Overall Citrate Synthase Activity.

Activities of recombinant CS4 variants after incubation with (gray bars) or without (black bars) hydrogen peroxide. Recombinant proteins were purified under reducing conditions (+DTT). Citrate synthase activity was measured 30 min after incubation with 400 μM H_2O_2 at room temperature (mean ± SE, n = 3). The percentage of inhibition after hydrogen peroxide treatment is indicated above the bars. Asterisks indicate significant differences (* $p < 0.05$, ** $p < 0.005$, *** $p < 0.001$).

Under control conditions, a 60%–80% decrease in activity was observed for Cys209Ser, Cys365Ser, and Cys439Ser, respectively, while Cys467Ser was only slightly affected in activity (Figure 4A). The sensitivity of the mutant proteins towards hydrogen peroxide was also very different compared to CS4 (Figure 4, gray bars). Interestingly, both nearly inactive forms Cys108Ser and Cys325Ser were not further decreased in activity by hydrogen peroxide treatment and also Cys365Ser and Cys467Ser were only decreased by 25%–30% in activity. Only Cys209Ser and Cys439Ser showed a similar extent of inhibition to hydrogen peroxide as CS4 (Figure 4). Hence, Cys108 and Cys325 are indispensable for normal citrate synthase activity and might also partly contribute to the redox sensitivity of the enzyme. Cys365 and Cys467 are not as important for the overall activity, but are also responsible for the redox sensitivity of citrate synthase.

Citrate Synthase Is Activated by Thioredoxin-Dependent Reduction

As oxidation resulted in a decrease in CS4 activity but affected the Cys mutants very differentially (Figure 4), we were interested to find out whether the enzyme can be reduced by TRX and to identify cysteine residues responsible for the interaction with TRX. To test this, we purified the recombinant CS4 variants under non-disulfide-reducing conditions. A strong and more than eight-fold activation of enzyme activity was observed for CS4, Cys108Ser, Cys210Ser, Cys439Ser, as well as Cys467Ser with *E. coli* TRX coupled to reduction by NTR and

NADPH (Figure 5A). Despite the little overall citrate synthase activity of Cys325Ser, TRX was still able to increase its activity by four-fold. The least activation was observed for Cys365Ser, where treatment with TRX only resulted in a 1.4-fold activation of the enzyme activity. Instead, the activity of Cys365Ser was three times higher than that of the CS4 protein when purified under non-disulfide-reducing conditions (Figure 5A). Furthermore, there was no significant difference in the activity of Cys365Ser purified under reducing or non-disulfide-reducing conditions (Figures 4 and 5A). Hence, Cys365 seems to be a major TRX-target and mutation of Cys365 to serine confers a resistance towards oxidation of citrate synthase.

To confirm the interaction of TRX with the CS4 variants, we mutated the second cysteine of TRX to serine (TRX–Cys36S) to alter the catalytic site of TRX to 'CGPS'. The N-terminal cysteine (Cys32) in this mutant is still able to form a mixed-disulfide with the cysteine residues of its target proteins. However, this bond is not broken anymore, as the second cysteine is missing which usually performs the nucleophilic attack (Verdoucq et al., 1999). Such mutants are commonly used to identify TRX-interaction proteins by TRX chromatography (Motohashi et al., 2001; Balmer et al., 2004; Yoshida et al., 2013). Hence, if TRXCys36Ser interacts with CS4, a more or less stable covalent bond is formed and a size shift of 14 kDa can be observed. This was indeed the case when we incubated TRXCys36S with CS4 and analyzed the interaction by SDS–PAGE and Western blot analysis using the α-CS4 antibody (Figure 5B). To distinguish the hybrid TRX–CS4 proteins from other higher-molecular-weight CS4 aggregates, we compared the reduced protein (+DTT) with the non-reduced protein and the non-reduced protein after reaction with TRXCys36Ser (TRXi) (Figure 5B). A clear TRX–CS4 fusion protein was observed for the unmutated CS4 protein, Cys108Ser and Cys325Ser, but not for Cys365Ser (Figure 5B), which confirms that Cys365 is the major target for interaction with TRX as already inferred from the citrate synthase activity assay in the presence of TRX (Figure 5A).

CS4 Forms Inter- as well as Intramolecular Disulfide Bridges that Can Be Reduced by DTT and Thioredoxin

Since the *Arabidopsis* citrate synthase can be activated by TRX and is sensitive towards oxidation, it is most likely that either intra- or intermolecular disulfide bridges are formed which affect the activity of the enzyme. A previous study investigating the plant mitochondrial disulphide proteome indeed identified intra- as well as intermolecular disulfides on *Arabidopsis* citrate synthase after oxidation with diamide (Winger et al., 2007). Similarly to the spots of around 100 kDa (intermolecular disulfide) and 60 kDa (intramolecular disulphide) identified for the mitochondrial citrate synthase detected in mitochondria treated with diamide (Winger et al., 2007), we also identified several mixed disulfides for *Arabidopsis* citrate synthase in a diagonal PAGE using isolated mitochondria from seedlings (Figure 6A). Hence, even without excessive oxidative stress, the protein can be partially oxidized. However, we cannot exclude that the oxidation occurred during the mitochondrial preparation, as it was previously observed for the alternative oxidase (Umbach and Siedow, 1997). For the recombinant CS4 protein

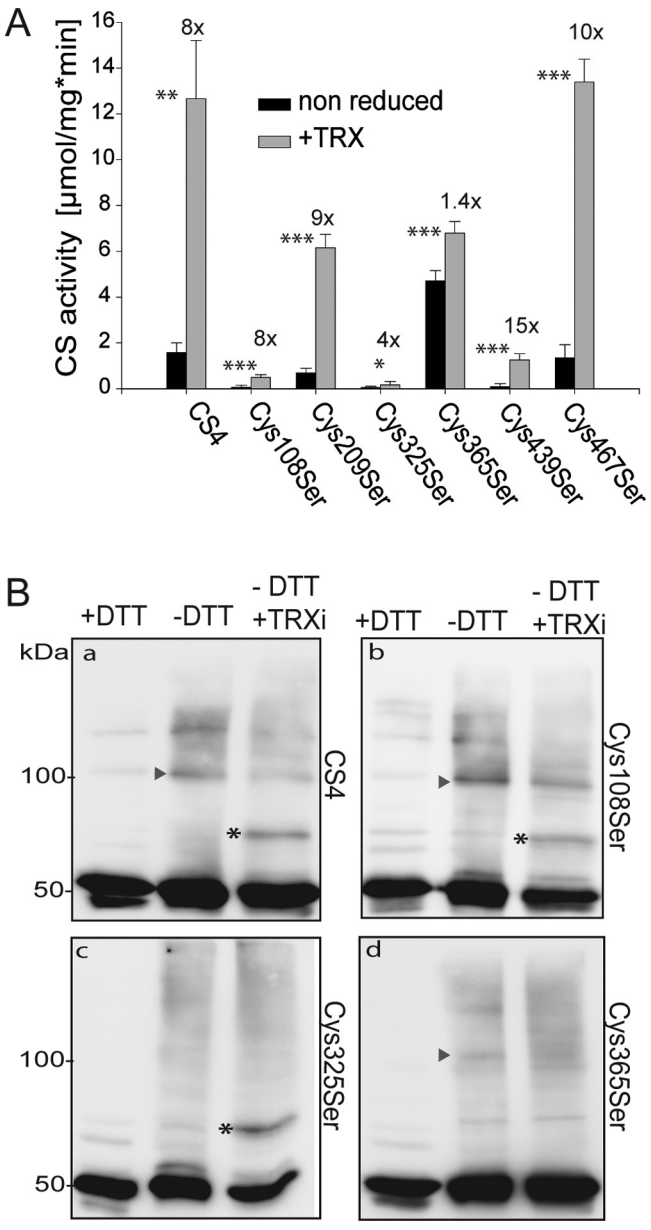

Figure 5. Thioredoxin (TRX)-Dependent Reduction of CS4.

(A) TRX-dependent activation of recombinant citrate synthase variants. Recombinant proteins were purified under non-reducing conditions. Activity of citrate synthase was measured in the absence (black bars) or presence (gray bars) of *E. coli* TRX, NTR, and NADPH (mean ± SE, $n = 6$). The fold-change of activation after TRX treatment is indicated above the bars. Asterisks indicate significant differences (* $p < 0.05$, ** $p < 0.005$, *** $p < 0.001$).

(B) *In vitro* interaction of mutated and inactive recombinant *E. coli* TRXi (TRX-Cys36Ser, mutated active site: CGPS) with CS4 variants. (a) CS4, (b) Cys108Ser, (c) Cys325Ser, (d) Cys365Ser. First lane without DTT (–DTT), second lane with DTT (+DTT), and third lane without DTT but with TRX–Cys36Ser (–DTT, +TRXi). Triangles indicate size of citrate synthase dimer. Asterisk indicates covalent interaction between CS4 variant with TRXi.

that was purified from *E. coli* under non-disulfide-reducing conditions, a redox-dependent dimer as well as intramolecular disulfides were also detected (Figure 6B). Indeed, most of the oxidized protein was not detected in discrete spots but rather as a smear, indicating that there are several mixed disulfides formed during oxidation of CS4 (Figure 6B, b). All of the higher-molecular-weight spots were removed upon reduction with DTT, resulting in all CS4 protein spots migrating exactly on the diagonal as their redox state is not altered by reduction with DTT in the first and second dimension of the gel (Figure 6B, a). Immune-reactive spots smaller than 50 kDa in size that were detected on the reducing diagonal PAGE most likely represent CS4 forms that possess intramolecular disulfide bridges that cannot be reduced by DTT and thus probably migrate faster due to a less bulky structure (Figure 6B, a, c, e, g). Next we tested whether the two nearly inactive mutants Cys108Ser and Cys325Ser as well the less redox-sensitive form Cys365Ser showed a cysteine-dependent dimerization. While under non-reducing conditions, Cys108Ser behaved more like the CS4 protein on the diagonal PAGE (or even showed a stronger intermolecular disulfide formation) (Figure 6B, d), Cys325Ser showed nearly no dimerization, but a stronger intramolecular disulfide formation (Figure 6B, f). Interestingly, the less redox-sensitive form Cys365Ser was able to form a well-defined intermolecular dimer as well as intramolecular disulfide bridges (Figure 6B, h). Our results indicate that the intermolecular disulfide bridge is dependent on Cys325, but no single cysteine could be identified that is mainly responsible for the intramolecular disulfide bridge formation.

To find out whether TRX is able to reduce either the intra- or intermolecular disulfide bridges of CS4, we analyzed the non-reduced CS4 protein after reduction with *E. coli* TRX coupled to NTR and NADPH on the diagonal 2D-PAGE. TRX was not only able to fully reduce the intermolecular but also the intramolecular disulfide bridges of CS4 and thus was nearly as efficient in reduction of the protein as DTT (Figure 6C). Hence, in plant mitochondria, TRXs will be the most likely *in vivo* reduction partners of CS4.

Different Combinations of Inter- and Intramolecular Mixed Disulfides Are Found in the Non-Reduced CS4 Protein

As no single cysteine was identified that was solely responsible for the formation of intramolecular disulfides, we performed an LC–MS-based mass spectrometry analysis of the purified CS4 protein from non-cysteine-reducing conditions to identify disulfide bonds within the protein. Prior to digestion with trypsin, the purified CS4 protein was either carbamidomethylated with iodoacetamide, to label only free cysteines, or fully reduced with DTT before carbamidomethylation, to label all cysteine residues. After measurement of both samples, the calculated masses of doubly or triply charged ions corresponding to theoretical di-peptide masses for all possible disulfide-linked peptides of CS4 were used (Supplemental

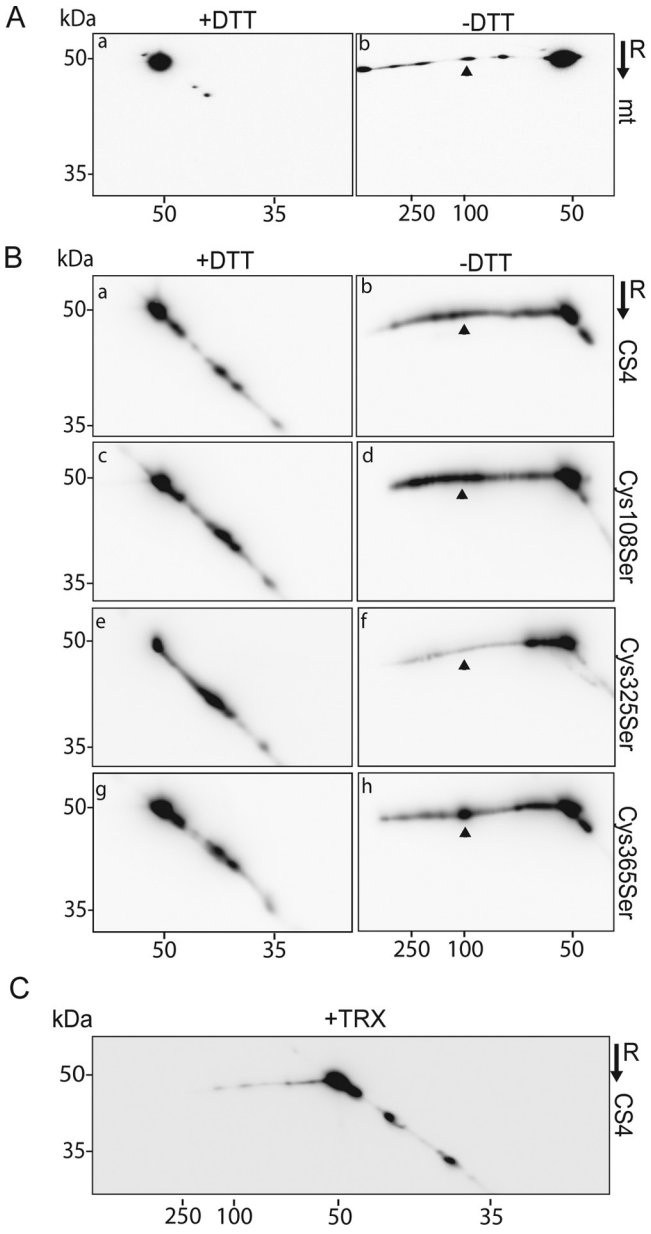

Figure 6. Diagonal Redox 2D-SDS–PAGE to Analyze Disulfide Formation in Recombinant CS4 Protein and Cys-Variants.

(A) Western blots of diagonal 2D-SDS–PAGE of citrate synthase from *Arabidopsis* mitochondria (mt) with (a) and without (b) prior DTT treatment (100 mM) in the first dimension.

(B) Western blots of diagonal 2D-SDS–PAGE of recombinant CS4 proteins treated with (+DTT) or without (–DTT) prior DTT treatment (100 mM) in the first dimension.

(a, b) recombinant protein of CS4, (c, d) recombinant protein of Cys108Ser, (e, f) recombinant protein of Cys325Ser, (g, h) recombinant protein of Cys365Ser.

(C) Western blots of diagonal 2D-SDS–PAGE of the non-reduced recombinant CS4 protein treated with *E. coli* TRX, NTR, and NADPH prior to the diagonal 2D-SDS–PAGE. For clarity of the identity of proteins, all gels were analyzed by Western blot using αCS4-antibody. The gel lanes were subjected to an SDS-gel electrophoresis in the second dimension under reducing conditions (R, 100 mM DTT).Triangles indicate dimers of citrate synthase.

Tables 1 and 2). Only if an ion matched the selected mass window of 3 p.p.m., displayed the expected charge state with the corresponding isotopic envelope, and was present in the unreduced but not in the reduced sample was it considered to be the corresponding di-peptide (Table 2). All cysteine-containing peptides showed stronger intensities after reduction with DTT, which suggests that a considerable number of the Cys residues formed disulfide bonds in the non-reduced sample (Supplemental Table 1). Interestingly, multiple disulfides for every cysteine were detected, which indicates that the non-reduced protein is most likely not correctly folded, as intramolecular disulfides were only predicted from structural modeling for the pairs of Cys108 and Cys365 as well as for Cys209 and Cys439 (Figure 7A) (Stevens et al., 1997). Although a disulfide bridge was detected for Cys108 and Cys365 as predicted from structural modeling, no disulfide bridge was detected for Cys209 and Cys439 in our analysis. Intermolecular disulfide bridges between the same cysteines were only detected for Cys108 and Cys325 (Table 2). However, only the mutant which lacked Cys325 (but not Cys108) showed no dimer formation anymore. This indicates that the bond between 'Cys325-Cys325' is the preferentially formed dimer.

DISCUSSION

Although many mitochondrial proteins with diverse metabolic functions have been identified as TRX-targets (Balmer et al., 2004; Yoshida et al., 2013), the functional significance of these interactions has not been investigated in detail for most of the proteins. So far, the best examined example for a plant mitochondrial TRX-target is the alternative oxidase (AOX). For several plant species, it was demonstrated that *in vitro* TRX is able to reduce a disulfide in the AOX dimer, which is crucial for AOX activation (Gelhaye et al., 2004; Marti et al., 2009; Yoshida et al., 2013). Furthermore, TRXo1 was shown to serve as an *in vitro* electron donor to the mitochondrial peroxiredoxin IIF of *Arabidopsis* and pea (Finkemeier et al., 2005; Barranco-Medina et al., 2008). Here, we provide evidence that the activity of a key enzyme in the TCA cycle is also regulated by TRX. Citrate synthase was recently identified as *in vitro* TRX-target in *Arabidopsis* in an affinity chromatography approach (Yoshida et al., 2013). Similarly to the other TCA cycle enzymes which have been identified in this and other approaches, citrate synthase has conserved cysteine residues which are either plant-specific or conserved in most higher eukaryotic organisms (Figure 1).

Different crystal structures of either the monomeric (open; 1CTS, 3enj) or dimeric form (closed; 4CTS) of the pig heart citrate synthase have been published (Remington et al., 1982; Wiegand et al., 1984; Larson et al., 2009). It is generally assumed that the active citrate synthase enzyme of higher organisms consists of a dimer composed of two identical subunits, and each of the subunit contributes functional groups to the active site (Remington, 1992). Each subunit contains a large and small domain with the substrate-binding site lying in the cleft between these two domains. When OAA binds to the enzyme the two domains perform a large conformational change of about 19 degrees relative to each other, and the acetyl CoA binding site is formed (Remington, 1992). Thus, as monomeric protein, citrate synthase is inactive. We fitted the structure of pig heart citrate synthase to the amino acid sequence of *Arabidopsis* (Figure 7A). The position of the studied cysteine residues here are indicated in the model. If the model is correct for *Arabidopsis*, none of the cysteine residues is lying at the dimer interface of the active enzyme. From our analysis, we can conclude that, in *Arabidopsis* mitochondria, citrate synthase is present not only as a dimer, although this is the most abundant form (Figure 3A and 3B). Next to the monomeric form, we also identified multimeric aggregates which are mainly formed due to non-covalent interactions between subunits as the protein runs mainly as monomer on a non-reducing SDS–PAGE (Figures 3A and 5 (–DTT)). However, citrate synthase also forms covalently bound dimeric and oligomeric structures due to the formation of mixed inter- and intramolecular disulfides (Figures 5, 6A, and 6B, and Table 2). Stevens et al. (1997) already compared the conservation of cysteine residues in plant and animal citrate synthase enzymes, and they also analyzed the redox sensitivity of these enzymes by treating total protein extracts with either diamide or DTT.

Table 2. Overview of Disulfide-Linked Di-Peptides in the Non-Reduced CS4 Protein.

CS4	Cys108	Cys209	Cys325	Cys365	Cys439	Cys467
Cys108	+++	+++	++	+++	+	+
Cys209	+++			+		
Cys325	++			+	+	
Cys365	+++	+	+	+	+	++
Cys439	+		+	+		+
Cys467	+			++	+	

The peptide masses and integrated peak areas from three replicates are listed in Supplemental Table 3. Prior to digestion with trypsin, the purified CS4 protein was either carbamidomethylated with iodoacetamide, preserving existing disulfide bridges, or fully reduced with DTT before carbamidomethylation, to break all disulfide bonds. Only if a matched ion was present in the unreduced but missing or at least five-fold decreased in the reduced sample was it considered to be very likely the corresponding di-peptide. The presence of these putative di-sulfides is marked with '+' for each replicate. Combinations between different cysteine residues could represent both intra- and intermolecular bonds.

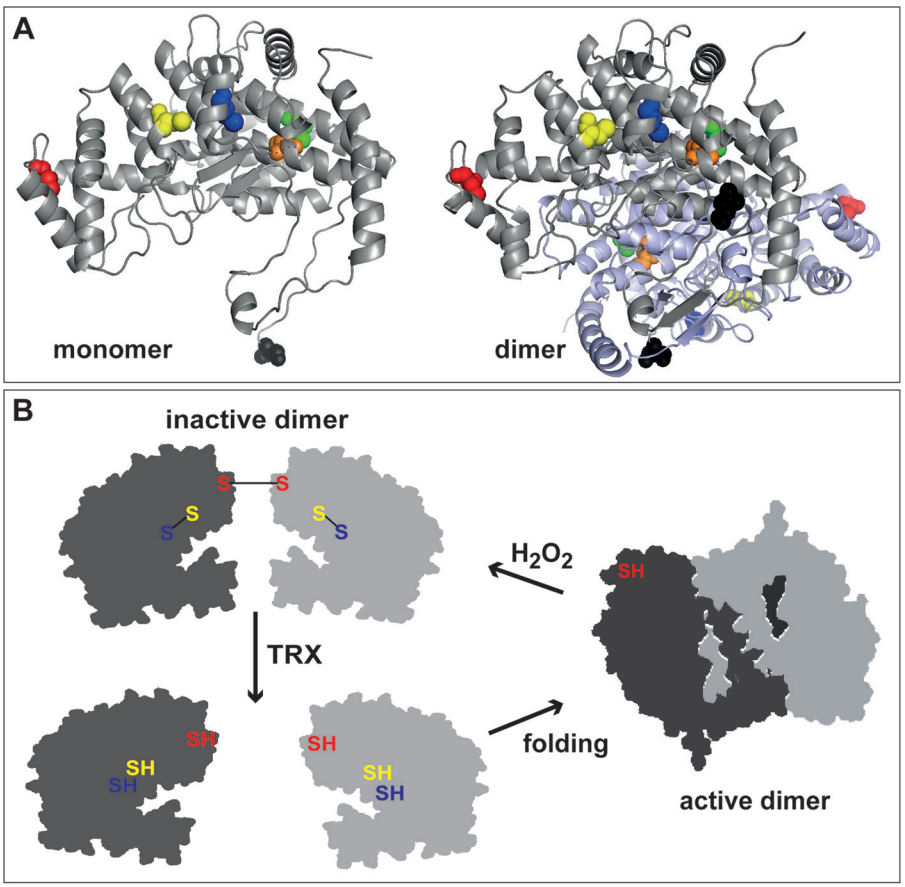

Figure 7. Hypothetical Model on Redox Regulation of *Arabidopsis* Citrate Synthase.

(A) Ribbon diagram of the predicted tertiary structure and positions of cysteine residues (spacefill) in *Arabidopsis* citrate synthase. The 3D structures were modeled with a Swiss PDB Viewer 4.0 and modified with Pymol Version 1.6. CS4 (At2g44350) was fitted to pig heart citrate synthase (3ENJ (left), 4CTS (right)). The cysteine residues are color-coded as follows: Cys108 (blue), Cys209 (green), Cys325 (red), Cys365 (yellow), Cys439 (orange), Asp461 for Cys467 (gray).

(B) Scheme on redox regulation of *Arabidopsis* citrate synthase. The oxidized form of citrate synthase forms mixed disulfides. An intermolecular disulfide bridge between Cys325 (red) is formed. Additionally, Cys108 (blue) and Cys365 (yellow) can form an intramolecular disulfide bridge next to others. In the presence of TRX, the disulfide bonds are reduced and the active dimer which is independent on disulfides can be formed. Oxidants like hydrogen peroxide can again lead to an inactivation of citrate synthase enzyme.

Interestingly, they found that only plant citrate synthase enzymes seem to be redox-regulated by diamide and DTT treatment in contrast to citrate synthase enzymes from pig heart or *Caenorhabditis elegans*, although two of the cysteine residues are conserved in the analyzed species that are potentially able to form a disulfide bond. These two conserved cysteine residues refer to *Arabidopsis* Cys108 and Cys365 in our study. When looking at the structural model, it is conceivable that these two cysteine residues (blue and yellow colored) can form a disulfide bridge as well as Cys209 and Cys439 (green and orange colored) (Figure 7A). Although we identified a disulfide bond between Cys108 and Cys365 by mass spectrometry, no bond was detected for Cys209 and Cys439. However, we cannot exclude that the latter bond is still present but that the peptide is not be accessible by the applied LC–MS-based method. Stevens et al. (1997) argued that the difference in redox sensitivity of the plant and animal enzymes is caused by a difference in charge distribution as predicted from *in silico* structural simulations (Stevens et al., 1997). However, caution has to be taken from interpretation of the modeling done by Stevens et al. (1997) on the *Arabidopsis* citrate synthase, as the annotation of the amino acid sequence was not entirely correct at that time. An additional cysteine close to Cys108 was present in the annotation of the *Arabidopsis* protein sequence used by Stevens et al. (1997) (GenBank P20115), which is not present in the current genome annotation (TAIR10) anymore and which was confirmed by mass spectrometry.

The goal of this study was to analyze the redox sensitivity of *Arabidopsis* CS4 by site-directed mutagenesis of each of its six cysteine residues. Three of these cysteine residues are conserved in the very well characterized porcine citrate synthase (Figure 1). First of all, we confirmed that the annotated CS4 gene of *Arabidopsis* actually functions as citrate synthase enzyme. The recombinant CS4 protein containing

an N-terminal 6xHis-tag was highly active with acetyl CoA and oxaloacetate as substrates and showed very similar catalytic properties to those previously reported for citrate synthase enzymes from other organisms, proving the validity of our approach (Figure 2 and Table 1) (Jeffery et al., 1988; Kurz et al., 1995). Oxidation with hydrogen peroxide resulted in a decreased enzyme activity of the recombinant protein (Figure 4A), which has also been reported by Stevens et al. (1997) for citrate synthase in *Arabidopsis* leaf extracts.

The active site of citrate synthase is formed by a highly conserved catalytic triade consisting of His307, His353, and Asp408 (numbers for *Arabidopsis* CS4). Thus far, the importance of cysteine residues for the catalytic activity of eukaryotic citrate synthase enzymes has not been studied by site-directed mutagenesis, although Cys108 and Cys365 have been reported as the most conserved cysteine residues that have the potential to form disulfide bonds (Stevens et al., 1997). Here, we demonstrated that CS4 variants which either lack Cys108 or Cys325 (the latter of which is only conserved in plants) have only a very little catalytic activity compared to the unmodified form or the other cysteine variants (Figure 4). Whether these cysteine residues are involved in the actual catalytic activity of *Arabidopsis* citrate synthase is unclear and it is maybe more likely that they are important for the correct folding of the enzyme. Interestingly, both variants are not further inactivated by oxidation but their activity can be increased by TRX-dependent reduction (Figure 5A). Hence, Cys108 and Cys325 seem to be especially important for the function of *Arabidopsis* citrate synthase. Strikingly, only very few redox-dependent dimers and oligomers can be observed when Cys325 is mutated to serine (Figure 6B).

We also made some remarkable observations for Cys365, which is the only cysteine that is highly conserved in all organisms. When Cys365 is mutated, the enzyme is not as active as CS4 in its reduced state, but the really interesting observation was that Cys365Ser is not overly sensitive to oxidative inactivation any longer. Furthermore, Cys365Ser was also the variant, which showed the least activation by TRX (Figures 4 and 5). This was also confirmed by the fact that the mutated TRX–Cys36Ser was not able to bind to Cys365Ser (Figure 5B). Thus, Cys365 has a key role in the oxidative inactivation of *Arabidopsis* citrate synthase and it is most likely the most important target cysteine that is reduced by TRX *in vivo*. However, we demonstrated that TRX not only reduces disulfide bonds formed by Cys365, as all inter- and intramolecular mixed-disulfide bridges in CS4 and variants were removed by TRX or DTT (Figure 6B and 6C). Thus, a TRX-dependent activation of CS4 is most likely an important regulatory mechanism for the regulation of the TCA cycle *in vivo* (Figure 7B).

Plants can adapt to phosphorous deficiency or aluminum toxicity in soils by secreting citrate into the rhizosphere (Ligaba et al., 2004). When citrate synthase was overexpressed in different plant species, generally an increased tolerance towards aluminum toxicity can be observed (de la Fuente et al., 1997; Anoop et al., 2003; Deng et al., 2009; Han et al., 2009). Hence, the flux through the TCA cycle is somehow limited by citrate synthase in wild-type plants under these conditions. It will be interesting to see in future experiments whether a mutated version of CS4–Cys365 expressed in plants could even further increase the tolerance of plants towards aluminum stress, as oxidative stress is an often observed side effect of metal toxicity. Engineering of the redox sensitivity of citrate synthase could therefore be a possible way to optimize growth of crop plants under stress conditions.

METHODS

Cloning of Constructs, Heterologous Expression, and Purification of Proteins

The CS4 open reading frame was amplified from *Arabidopsis* cDNA by RT–PCR using the Phusion High Fidelity Polymerase (Thermo Scientific) excluding the coding region of the mitochondrial presequence (first 18 nucleotides after the ATG). The following primer combination was used for amplification: CS4-F 5′-GTATCGGCCTTTACTAGGCT-3′, CS4-R 5′-GACTTAAGCAGATGAAGCTTTC-3′. The CS4 PCR product was cloned into pEXP1–DEST vector by Gateway technology (Invitrogen) for expression and purification of the recombinant N-terminally 6xHis-tagged protein. All vector constructs were verified by sequencing. Expression of the recombinant proteins were performed in BL21* cells (Invitrogen) and purification on Ni-NTA columns as described in detail by Horling et al. (2003). For cysteine-reducing conditions, 20 mM β-mercaptoethanol was added to each buffer during purification, and eluted proteins were dialyzed overnight at 4°C against a 25-fold volume of dialysis buffer (50 mM Tris–HCl (pH 8), 50 mM NaCl, 10% glycerol) containing 0.2 mM DTT. The dialysis buffer was exchanged twice. For cysteine-non-reducing conditions, 20 mM ascorbate was added to each buffer during purification to prevent overoxidation of cysteines. Eluted proteins were dialyzed against dialysis buffer without DTT. *E. coli* TRX and NTR were cloned into pET16-b overexpressed and purified as described by Yamamoto et al. (1999). The protein concentrations of dialyzed proteins were determined in a Bradford assay using the Coomassie Plus Protein Assay (Thermo Scientific) and bovine serum albumin as a reference. The dialyzed proteins were snap frozen in liquid nitrogen and stored at –80°C until further use.

Site-Directed Mutagenesis

Site-directed mutagenesis of plasmids was performed using the QuikChange Lightning Multi Site-Directed Mutagenesis Kit (Agilent Technologies) according to the manufacturer's protocol. The following oligonucleotides were used to obtain the recombinant CS4 variants with each one cysteine residues replaced by serine (Ser): Cys108Ser: 5′-gtcgattcctgagagccagaaagtattacc-3′, Cys210Ser: 5′-caacatatgaggatagcctcaacctgattgc-3′, Cys325Ser: 5′-cagtcgtagaggaaagtggagaagatatatc-3′, Cys365Ser: 5′-gatccaagatatgtaagccaaagagaatttgcc-3′, Cys439Ser: 5′-gagtcttggcatcagctctcagcttatatgg-3′, Cys467Ser:

5′-ttaagcagatgaagctttcttagaatgg-3′. To replace the second cysteine (Cys36) of *E. coli* TRX by serine, the oligonucleotide 5′-tggtgcggtccgagcaaaatgatcg-3′ was used.

Citrate Synthase Activity Assay

Citrate synthase activity was measured spectrophotometrically as described previously (Srere et al., 1963; Anoop et al., 2003) in an assay based on the absorbance of DTNB after reaction with CoA at 412 nm. 75 ng recombinant protein was incubated with 0.2 mM acetyl–CoA (Roche) in 1 mM DTNB (in 100 mM Tris–HCl pH 8.0) and the reaction was started after addition of 0.2 mM oxaloacetate.

For activity measurements with TRX, citrate synthase was purified under non-reducing conditions (see above). For TRX-dependent reduction, 0.25 µg recombinant citrate synthase was incubated with 35 µg recombinant *E. coli* TRX, 0.8 µg recombinant *E. coli* thioredoxin-reductase (NTR), and 1.5 mM NADPH for 15 min at room temperature. A volume equivalent to 75 ng citrate synthase was used for activity measurements. K_m and V_{max} values were calculated by non-linear least squares data fitting (Kemmer and Keller, 2010).

In Vitro Interaction-Assay of CS4 with Mutated Recombinant Bacterial TRX

1 µg of recombinant CS4 was incubated with 5 µg of recombinant TRX–Cys36Ser, 0.8 µg Trx-Red, and 1.5 mM NAPDH for 30 min at room temperature, then SDS sample buffer (11.5% SDS, 313 mM Tris/HCl pH 6.8, 50% glycerol, 0.01% bromophenol blue) was added and denatured for 5 min at 95°C before loading onto a 12% non-reducing SDS–PAGE.

Isolation of Mitochondria and 2D BN/SDS–PAGE

Mitochondria were isolated from 10-day-old *Arabidopsis* seedlings grown in liquid cultures as described in detail by Morgan et al. (2008). 750 µg protein of freshly isolated mitochondria were sedimented by centrifugation for 10 min at 23 700 *g*. The pellet was re-suspended in 75 µl of digitonin solubilization buffer. BN-gel electrophoresis and second gel dimension was carried out in a standard dual cooled gel electrophoresis chamber (Hoefer) with a gel dimension of 18 × 16 cm as described by Klodmann et al. (2011).

Antiserum Production and Western Blot Analysis

For antiserum production, a rabbit was immunized with 850 µg heterologously expressed and gel-purified CS4 protein (Pineda, Berlin). The antiserum was affinity-purified against CS protein after the protocol described by Tran et al. (2012). For Western blot analysis, SDS-gels were transferred to nitrocellulose membranes and incubated overnight in a dilution of 1:5000 of CS4-antibody. Secondary goat-anti-rabbit HRP antibody (Thermo Scientific) was used in a 1:2000 dilution and detection followed by SuperSignal West Dura enhanced chemiluminescent substrate (Thermo Scientific). The chemiluminescent signal was detected using an ECL-reader (PEQlab).

Diagonal Gel Electrophoresis

Purified heterologous CS4 proteins were used to study disulfide-dependent complex formation by diagonal gel electrophoresis. 1.5 µg of protein was treated either with 20 mM DTT or without DTT for 30 min at room temperature. 100 mM iodoacetamide was added and incubated for 30 min in the dark and then diluted with SDS-buffer without DTT. The gel electrophoresis was performed as described by Winger et al. (2007).

Size Exclusion Chromatography

The aggregation state of citrate synthase was analyzed by gel-filtration using a Superose 6 10/300 GL column coupled to an ÄKTA purifier chromatographic system (GE Healthcare). The column was calibrated with a Low Molecular Weight Calibration Kit (GE Healthcare) and equilibrated with Tris-buffer (50 mM Tris–HCl pH 8, 150 mM NaCl) at a flow rate of 0.5 ml min^{-1}. 100 µg of protein were loaded onto the column. The elution profile of recombinant proteins was monitored at 280 nm. After chromatography, 1-ml fractions were collected and analyzed by Western blot.

Mass Spectrometry and Data Analysis

About 2 µg CS4 protein was denatured in 8 M urea in 100 mM Tris–HCl pH 8, 1 mM $CaCl_2$, and either reduced with 5 mM DTT and alkylated with 14 mM iodoacetamide or only alkylated without prior reduction. Proteins were digested overnight using 400 ng mass-spec grade trypsin (Roche) at 37°C. Digestion was stopped with 0.3% trifluoroacetic acid, peptides were desalted using custom-made C18 StageTips (Rappsilber et al., 2007), and peptide-containing eluates were evaporated using a speed-vac. Dried peptides were re-dissolved in 2% acetonitrile, 0.1% trifluoroacetic acid, before analysis. Samples were analyzed using a Rheos Allegro UPLC (Flux Instruments) coupled to an LTQ-Orbitrap classic (Thermo Fisher). The peptides were separated on frit-less, self-pulled fused silica emitters (10 cm × 100 µm), packed in-house with reversed-phase ProntoSIL C18 ace-EPS 5 µm resin (Bischoff Analysentechnik und -geräte GmbH). Approximately 0.2 µg peptides were loaded onto the column and eluted for 60 min using a segmented linear gradient of 3%–95% solvent B (80% acetonitrile, 0.5% acetic acid) at a flow rate of 250 nl min^{-1}. Survey full-scan mass spectra were acquired in the Orbitrap analyzer. The scanned mass range was 300–1800 m/z, at a resolution of 60 000 at 400 m/z and the seven most intense ions were sequentially isolated, fragmented (CID at 35 eV), and measured in the linear ion trap. Peptides with a charge of +1 or with unassigned charge state were excluded from fragmentation for MS2; dynamic exclusion of maximum 500 m/z values prevented repeated selection of selected masses for 90 s. Ions were accumulated to a target value of 10^6 for full FT–MS in the Orbitrap and of 10^4 for MS2 in the linear ion trap. Raw data were processed using MaxQuant software (version 1.4.1.2, www.maxquant.org/) (Cox and Mann, 2008) and searched against The Arabidopsis Information Resource protein

database (build TAIR10_pep_20101214, ftp://ftp.Arabidopsis.org/home/tair/Proteins/TAIR10_protein_lists/), with trypsin specificity and a maximum of two missed cleavages at a protein and peptide false discovery rate of 1%. Carbamidomethylation of cysteine residues and oxidation of methionine were set as variable modifications. For the analysis of linked disulfides in CS4, masses of doubly or triply charged ions corresponding to theoretical di-peptide masses for all possible linked peptides of CS4 (see Supplemental Tables 1 and 2) were used to produce extracted ion chromatograms with a mass window of 3 p.p.m. In the case of doubly and triply charged ions being present for a specific di-peptide, the peaks of both charge states had to co-elute to be considered the same peptide.

Structure Models of Citrate Synthase

For modeling of *Arabidopsis* citrate synthase structures, the software Swiss PDB Viewer (http://spdbv.vital-it.ch/) and RasWin were used. The amino acid sequence of CS4 (At2g44350.1) was fitted to the crystal structures of porcine citrate synthase (PDB-ID: 4CTS (closed form dimer) and 3ENJ (open form monomer)).

Statistical Analysis

Student's *t*-tests were performed using Microsoft Excel (Microsoft, USA).

Accession Numbers

Sequence data for the gene presented in this study can be found in the GenBank data libraries under the following accession numbers: CS4 (At2g44350.1).

SUPPLEMENTARY DATA

Supplementary Data are available at *Molecular Plant Online.*

FUNDING

E.S. was funded by an award of Lehre@LMU of the Ludwig-Maximilians University Munich. This work was supported by the Deutsche Forschungsgemeinschaft, Germany (Emmy Noether Programme FI-1655/1-1). No conflict of interest declared.

REFERENCES

Anoop, V.M., Basu, U., McCammon, M.T., McAlister-Henn, L., and Taylor, G.J. (2003). Modulation of citrate metabolism alters aluminum tolerance in yeast and transgenic canola overexpressing a mitochondrial citrate synthase. Plant Physiol. **132**, 2205–2217.

Araujo, W.L., Nunes-Nesi, A., Nikoloski, Z., Sweetlove, L.J., and Fernie, A.R. (2012). Metabolic control and regulation of the tricarboxylic acid cycle in photosynthetic and heterotrophic plant tissues. Plant Cell Environ. **35**, 1–21.

Balmer, Y., Vensel, W.H., Tanaka, C.K., Hurkman, W.J., Gelhaye, E., Rouhier, N., Jacquot, J.P., Manieri, W., Schurmann, P., Droux, M., et al. (2004). Thioredoxin links redox to the regulation of fundamental processes of plant mitochondria. Proc. Natl Acad. Sci. U S A. **101**, 2642–2647.

Barranco-Medina, S., Krell, T., Bernier-Villamor, L., Sevilla, F., Lazaro, J.J., and Dietz, K.J. (2008). Hexameric oligomerization of mitochondrial peroxiredoxin PrxIIF and formation of an ultrahigh affinity complex with its electron donor thioredoxin Trx-o. J. Exp. Bot. **59**, 3259–3269.

Buchanan, B.B. (1984).The ferredoxin/thioredoxin system: a key element in the regulatory function of light in photosynthesis. Bioscience. **34**, 378–383.

Cox, J., and Mann, M. (2008). MaxQuant enables high peptide identification rates, individualized p.p.b.-range mass accuracies and proteome-wide protein quantification. Nat. Biotech. **26**, 1367–1372.

de la Fuente, J.M., Ramirez-Rodriguez, V., Cabrera-Ponce, J.L., and Herrera-Estrella, L. (1997). Aluminum tolerance in transgenic plants by alteration of citrate synthesis. Science. **276**, 1566–1568.

Deng, W., Luo, K., Li, Z., Yang, Y., Hu, N., and Wu, Y. (2009). Overexpression of *Citrus junos* mitochondrial citrate synthase gene in *Nicotiana benthamiana* confers aluminum tolerance. Planta. **230**, 355–365.

Emanuelsson, O., Nielsen, H., Brunak, S., and von Heijne, G. (2000). Predicting subcellular localization of proteins based on their N-terminal amino acid sequence. J. Mol. Biol. **300**, 1005–1016.

Finkemeier, I., Goodman, M., Lamkemeyer, P., Kandlbinder, A., Sweetlove, L.J., and Dietz, K.J. (2005). The mitochondrial type II peroxiredoxin F is essential for redox homeostasis and root growth of *Arabidopsis thaliana* under stress. J. Biol. Chem. **280**, 12168–12180.

Finkemeier, I., Konig, A.C., Heard, W., Nunes-Nesi, A., Pham, P.A., Leister, D., Fernie, A.R., and Sweetlove, L.J. (2013). Transcriptomic analysis of the role of carboxylic acids in metabolite signaling in *Arabidopsis* leaves. Plant Physiol. **162**, 239–253.

Gelhaye, E., Rouhier, N., Gerard, J., Jolivet, Y., Gualberto, J., Navrot, N., Ohlsson, P.I., Wingsle, G., Hirasawa, M., Knaff, D.B., et al. (2004). A specific form of thioredoxin h occurs in plant mitochondria and regulates the alternative oxidase. Proc. Natl Acad. Sci. U S A. **101**, 14545–14550.

Han, Y., Zhang, W., Zhang, B., Zhang, S., Wang, W., and Ming, F. (2009). One novel mitochondrial citrate synthase from *Oryza sativa* L. can enhance aluminum tolerance in transgenic tobacco. Mol. Biotech. **42**, 299–305.

Heazlewood, J.L., Tonti-Filippini, J.S., Gout, A.M., Day, D.A., Whelan, J., and Millar, A.H. (2004). Experimental analysis of the *Arabidopsis* mitochondrial proteome highlights signaling and regulatory components, provides assessment of targeting prediction programs, and indicates plant-specific mitochondrial proteins. Plant Cell. **16**, 241–256.

Horling, F., Lamkemeyer, P., Konig, J., Finkemeier, I., Kandlbinder, A., Baier, M., and Dietz, K.J. (2003). Divergent light-, ascorbate-, and oxidative stress-dependent regulation of expression of the peroxiredoxin gene family in *Arabidopsis*. Plant Physiol. **131**, 317–325.

Iredale, S.E. (1979). Properties of citrate synthase from *Pisum sativum* mitochondria. Phytochemistry. **18**, 1057–1057.

Jeffery, D., Goodenough, P.W., and Weitzman, P.D.J. (1988). Citrate synthase and malate dehydrogenase from tomato fruit. Phytochemistry. **27**, 41–44.

Johansson, C.J., and Pettersson, G. (1977). Substrate-inhibition by acetyl-CoA in condensation reaction between oxaloacetate and acetyl–CoA catalyzed by citrate synthase from pig heart. Biochim. Biophys. Acta. **484**, 208–215.

Kemmer, G., and Keller, S. (2010). Nonlinear least-squares data fitting in Excel spreadsheets. Nat. Protoc. **5**, 267–281.

Klodmann, J., Senkler, M., Rode, C., and Braun, H.P. (2011). Defining the protein complex proteome of plant mitochondria. Plant Physiol. **157**, 587–598.

König, J., Muthuramalingam, M., and Dietz, K.J. (2012). Mechanisms and dynamics in the thiol/disulfide redox regulatory network: transmitters, sensors and targets. Curr. Opin. Plant Biol. **15**, 261–268.

Kurz, L.C., Shah, S., Frieden, C., Nakra, T., Stein, R.E., Drysdale, G.R., Evans, C.T., and Srere, P.A. (1995). Catalytic strategy of citrate synthase–subunit interactions revealed as a consequence of a single amino-acid change in the oxaloacetate binding-site. Biochemistry. **34**, 13278–13288.

Laloi, C., Rayapuram, N., Chartier, Y., Grienenberger, J.M., Bonnard, G., and Meyer, Y. (2001). Identification and characterization of a mitochondrial thioredoxin system in plants. Proc. Natl Acad. Sci. U S A. **98**, 14144–14149.

Larson, S.B., Day, J.S., Nguyen, C., Cudney, R., and McPherson, A. (2009). Structure of pig heart citrate synthase at 1.78 angstrom resolution. Acta Crystallogr. F. **65**, 430–434.

Ligaba, A., Shen, H., Shibata, K., Yamamoto, Y., Tanakamaru, S., and Matsumoto, H. (2004). The role of phosphorus in aluminium-induced citrate and malate exudation from rape (*Brassica napus*). Physiol. Plant. **120**, 575–584.

Marti, M.C., Olmos, E., Calvete, J.J., Diaz, I., Barranco-Medina, S., Whelan, J., Lazaro, J.J., Sevilla, F., and Jimenez, A. (2009). Mitochondrial and nuclear localization of a novel pea thioredoxin: identification of its mitochondrial target proteins. Plant Physiol. **150**, 646–657.

Meyer, Y., Belin, C., Delorme-Hinoux, V., Reichheld, J.P., and Riondet, C. (2012). Thioredoxin and glutaredoxin systems in plants: molecular mechanisms, crosstalks, and functional significance. Antioxidants & Redox Signaling. **17**, 1124–1160.

Michalska, J., Zauber, H., Buchanan, B.B., Cejudo, F.J., and Geigenberger, P. (2009). NTRC links built-in thioredoxin to light and sucrose in regulating starch synthesis in chloroplasts and amyloplasts. Proc. Natl Acad. Sci. U S A. **106**, 9908–9913.

Morgan, M.J., Lehmann, M., Schwarzlander, M., Baxter, C.J., Sienkiewicz-Porzucek, A., Williams, T.C., Schauer, N., Fernie, A.R., Fricker, M.D., Ratcliffe, R.G., et al. (2008). Decrease in manganese superoxide dismutase leads to reduced root growth and affects tricarboxylic acid cycle flux and mitochondrial redox homeostasis. Plant Physiol. **147**, 101–114.

Motohashi, K., Kondoh, A., Stumpp, M.T., and Hisabori, T. (2001). Comprehensive survey of proteins targeted by chloroplast thioredoxin. Proc. Natl Acad. Sci. U S A. **98**, 11224–11229.

Nielsen, H., Engelbrecht, J., Brunak, S., and von Heijne, G. (1997). Identification of prokaryotic and eukaryotic signal peptides and prediction of their cleavage sites. Protein Eng. **10**, 1–6.

Nunes-Nesi, A., Araujo, W.L., and Fernie, A.R. (2011). Targeting mitochondrial metabolism and machinery as a means to enhance photosynthesis. Plant Physiol. **155**, 101–107.

Nunes-Nesi, A., Araujo, W.L., Obata, T., and Fernie, A.R. (2013). Regulation of the mitochondrial tricarboxylic acid cycle. Curr. Opin. Plant Biol. **16**, 335–343.

Pettersson, H., Olsson, P., Bülow, L., and Pettersson, G. (2000) Kinetics of the coupled reaction catalysed by a fusion protein of yeast mitochondrial malate dehydrogenase and citrate synthase. Eur. J. Biochem. **267**, 5041–5046.

Pracharoenwattana, I., Cornah, J.E., and Smith, S.M. (2005). *Arabidopsis* peroxisomal citrate synthase is required for fatty acid respiration and seed germination. Plant Cell. **17**, 2037–2048.

Rappsilber, J., Mann, M., and Ishihama, Y. (2007). Protocol for micro-purification, enrichment, pre-fractionation and storage of peptides for proteomics using StageTips. Nat. Protoc. **2**, 1896–1906.

Remington, S., Wiegand, G., and Huber, R. (1982). Crystallographic refinement and atomic models of two different forms of citrate synthase at 2.7 and 1.7 Å resolution. J. Mol. Biol. **158**, 111–152.

Remington, S.J. (1992). Structure and mechanism of citrate synthase. Curr. Top. Cell. Regul. **33**, 209–229.

Scheibe, R., and Dietz, K.J. (2012). Reduction–oxidation network for flexible adjustment of cellular metabolism in photoautotrophic cells. Plant Cell Environ. **35**, 202–216.

Schürmann, P., and Buchanan, B.B. (2008). The ferredoxin/thioredoxin system of oxygenic photosynthesis. Antioxidants & Redox Signaling. **10**, 1235–1274.

Schwarzlander, M., and Finkemeier, I. (2013). Mitochondrial energy and redox signaling in plants. Antioxidants & Redox Signaling. **18**, 2122–2144.

Srere, P.A., Gonen, L., and Brazil, H. (1963). Citrate condensing enzyme of pigeon breast muscle and moth flight muscle. Acta Chem. Scand. **17**, 129–134.

Stevens, F.J., Li, A.D., Lateef, S.S., and Anderson, L.E. (1997). Identification of potential inter-domain disulfides in three higher plant mitochondrial citrate synthases: paradoxical differences in redox-sensitivity as compared with the animal enzyme. Photosynthesis Research. **54**, 185–197.

Tran, H.T., Nimick, M., Uhrig, R.G., Templeton, G., Morrice, N., Gourlay, R., DeLong, A., and Moorhead, G.B. (2012). *Arabidopsis thaliana* histone deacetylase 14 (HDA14) is an alpha-tubulin deacetylase that associates with PP2A and enriches in the microtubule fraction with the putative histone acetyltransferase ELP3. Plant J. **71**, 263–272.

Umbach, A.L., Siedow, J.N. (1997). Changes in the redox state of the alternative oxidase regulatory sulfhydryl/disulfide system during mitochondrial isolation: implications for inferences of activity *in vivo*. Plant Science. **123**, 19–28.

Verdoucq, L., Vignols, F., Jacquot, J.P., Chartier, Y., and Meyer, Y. (1999). *In vivo* characterization of a thioredoxin h target protein defines a new peroxiredoxin family. J. Biol. Chem. **274**, 19714–19722.

Wiegand, G., Kukla, D., Scholze, H., Jones, T.A., and Huber, R. (1979). Crystal-structure analysis of the tetragonal crystal form

and preliminary molecular model of pig-heart citrate synthase. Eur. J. Biochem. **93**, 41–50.

Wiegand, G., Remington, S., Deisenhofer, J., and Huber, R. (1984). Crystal structure analysis and molecular model of a complex of citrate synthase with oxaloacetate and S-acetonyl-coenzyme A. J. Mol. Biol. **174**, 205–219.

Winger, A.M., Taylor, N.L., Heazlewood, J.L., Day, D.A., and Millar, A.H. (2007). Identification of intra- and intermolecular disulphide bonding in the plant mitochondrial proteome by diagonal gel electrophoresis. Proteomics. **7**, 4158–4170.

Yamamoto, H., Miyake, C., Dietz, K.J., Tomizawa, K.I., Murata, N., and Yokota, A. (1999). Thioredoxin peroxidase in the Cyanobacterium Synechocystis sp. PCC 6803. FEBS Lett. **447**, 269–273.

Yoshida, K., Noguchi, K., Motohashi, K., and Hisabori, T. (2013). Systematic exploration of thioredoxin target proteins in plant mitochondria. Plant Cell Physiol. **54**, 875–892.

Zimmermann, P., Hirsch-Hoffmann, M., Hennig, L., and Gruissem, W. (2004). GENEVESTIGATOR. *Arabidopsis* microarray database and analysis toolbox. Plant Physiol. **136**, 2621–2632.

Publication 4

The life of plant mitochondrial complex I.

Braun HP, Binder S, Brennicke A, Eubel H, Fernie AR, Finkemeier I, Klodmann J, **König AC**, Kühn K, Meyer E, Obata T, Schwarzländer M, Takenaka M, Zehrmann A.

(2014)

Mitochondrion. pii: S1567-7249(14)00020-8

Mitochondrion xxx (2014) xxx–xxx

Contents lists available at ScienceDirect

Mitochondrion

journal homepage: www.elsevier.com/locate/mito

The life of plant mitochondrial complex I

Hans-Peter Braun [a,*], Stefan Binder [b], Axel Brennicke [b], Holger Eubel [a], Alisdair R. Fernie [c], Iris Finkemeier [d], Jennifer Klodmann [a], Ann-Christine König [d], Kristina Kühn [e], Etienne Meyer [c], Toshihiro Obata [c], Markus Schwarzländer [f], Mizuki Takenaka [b], Anja Zehrmann [b]

[a] Institut für Pflanzengenetik, Leibniz Universität Hannover, Herrenhäuser Str. 2, 30419 Hannover, Germany
[b] Molekulare Botanik, Universität Ulm, Albert-Einstein-Allee 11, 89069 Ulm, Germany
[c] Max Planck Institute of Molecular Plant Physiology, Am Mühlenberg 1, 14476 Potsdam, Germany
[d] Plant Sciences, Ludwig Maximilians Universität München, Grosshadernerstr. 2-4, 82152 Planegg-Martinsried, Germany
[e] Institut für Biologie/Molekulare Zellbiologie der Pflanzen, Humboldt Universität zu Berlin, Philippstraße 13, 10115 Berlin, Germany
[f] INRES — Chemical Signalling, Rheinische Friedrich-Wilhelms-Universität Bonn, Friedrich-Ebert-Allee 144, D-53113 Bonn, Germany

ARTICLE INFO

Article history:
Received 27 November 2013
Received in revised form 28 January 2014
Accepted 12 February 2014
Available online xxxx

Keywords:
Plant mitochondria
Oxidative phosphorylation
Oxidoreductase
Carbonic anhydrase
RNA editing
Reactive oxygen species

ABSTRACT

The mitochondrial NADH dehydrogenase complex (complex I) of the respiratory chain has several remarkable features in plants: (i) particularly many of its subunits are encoded by the mitochondrial genome, (ii) its mitochondrial transcripts undergo extensive maturation processes (*e.g.* RNA editing, *trans*-splicing), (iii) its assembly follows unique routes, (iv) it includes an additional functional domain which contains carbonic anhydrases and (v) it is, indirectly, involved in photosynthesis. Comprising about 50 distinct protein subunits, complex I of plants is very large. However, an even larger number of proteins are required to synthesize these subunits and assemble the enzyme complex. This review aims to follow the complete "life cycle" of plant complex I from various molecular perspectives. We provide arguments that complex I represents an ideal model system for studying the interplay of respiration and photosynthesis, the cooperation of mitochondria and the nucleus during organelle biogenesis and the evolution of the mitochondrial oxidative phosphorylation system.

1. Introduction

The NADH dehydrogenase complex was first characterized in bovine mitochondria (Hatefi et al., 1962). Over 50 years ago, Hatefi and co-workers systematically studied the structural basis of "cellular respiration" — the transfer of electrons from mitochondrial substrates to molecular oxygen. Using biochemical fractionation procedures they could show that respiration can be subdivided into four segments (reviewed in Hatefi, 1985). Upon their re-constitution, respiration was re-established. In contrast, further fractionation of the individual segments caused irreversible loss of respiratory activity. Therefore, the segments were considered to represent the smallest physiological units of respiration. Physically, all of them represent protein complexes: the NADH dehydrogenase complex (complex I), the succinate dehydrogenase complex (complex II), the cytochrome c reductase complex (complex III) and the cytochrome c oxidase complex (complex IV). Together, the complexes I to IV form the respiratory electron transfer chain, which catalyzes electron transfer from NADH or $FADH_2$ to molecular oxygen.

The respiratory chain is linked to synthesis of ATP by an indirect mechanism first suggested by Peter Mitchell (1961): respiratory electron transport causes formation of a proton gradient across the inner mitochondrial membrane which is subsequently used by another protein complex, the ATP synthase (also known as complex V), to catalyze phosphorylation of ADP. Indeed, complexes I, III and IV of the respiratory chain are not only oxidoreductases but also proton translocators. In most eukaryotes, ATP synthesis coupled to oxygen reduction by the respiratory chain ("oxidative phosphorylation") is of central importance. It has been calculated that about 65 kg ATP are produced by this process per day in an average human (Rich, 2003). Approximately 40% of the protons needed for ATP synthesis by oxidative phosphorylation are supplied by mitochondrial complex I (Watt et al., 2010).

Complex I is a major entry site for electrons into the respiratory chain. It transfers electrons from NADH to ubiquinone. Complex I was already present in the ancestors of mitochondria, the proteobacteria, and as such is considered to have arisen early in evolution (Gray, 2012). Bacterial complex I has a comparatively simple subunit composition and has been studied extensively. Very recently, the structure of complex I from the eubacterium *Thermus thermophilus* was resolved by X-ray crystallography (Baradaran et al., 2013; Sazanov et al., 2013). Complex I is an L-shaped particle (Fig. 1). It is composed of two elongate

* Corresponding author.
E-mail address: braun@genetik.uni-hannover.de (H.-P. Braun).

http://dx.doi.org/10.1016/j.mito.2014.02.006
1567-7249/

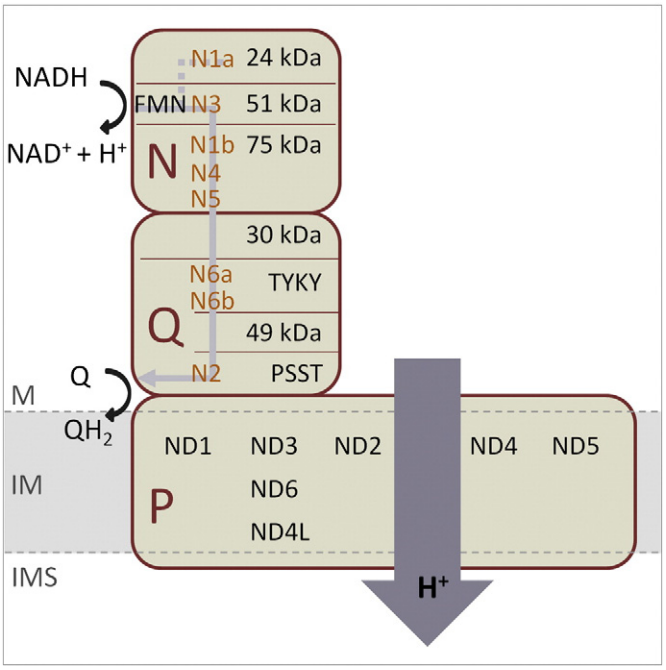

Fig. 1. Modular design of complex I. N = NADH oxidation module, Q = quinone reduction module, P = proton translocation module. Core subunits of each module are indicated (black) as well as respective FeS cluster(s) (orange). The NADH oxidation site (FMN) is located at the 51 kDa subunit. Electron flow through the peripheral arm and proton translocation across the membrane arm are indicated by gray arrows. M: matrix, IM: inner membrane, IMS: inter-membrane space. (For interpretation of the references to color in this figure legend, the reader is referred to the web version of this article.)

domains, also termed 'arms': the membrane arm, which is inserted into the inner mitochondrial membrane, and the peripheral arm, which protrudes into the mitochondrial matrix. Physiologically, complex I can be divided into three functional modules: the NADH oxidation and the quinone reduction modules (N and Q modules), both localized in the peripheral arm, and the proton transfer module (P module) which equals the membrane arm. Based on the crystal structure of bacterial complex I a mechanism for the coupling of electron transfer and proton translocation has been postulated (see Section 3.1; Baradaran et al., 2013; Brandt, 2013).

Like its prokaryote counterpart, mitochondrial complex I is also L-like shaped as revealed by electron microscopy (EM) analyses (Grigorieff, 1998; Guénebaut et al., 1997; Leonard et al., 1987). However, its composition is more complex. While the minimal bacterial complex I consists of 14 subunits, the eukaryotic enzyme is composed of more than 40 different proteins, *e.g.* 44 subunits in bovine mitochondria (Balsa et al., 2012; Carroll et al., 2006). Most of the complex I subunits present in other eukaryotes represent homologs of the bovine subunits (Cardol, 2011) but nomenclature of subunits unfortunately varies in different species. In this review, the bovine nomenclature is adopted since complex I subunits have been studied extensively in this species. In addition, commonly used alternative nomenclatures are provided in the appendix of our article (Supp. Tables 1 and 2).

In plants, complex I biology is particularly intriguing. Besides oxidative phosphorylation, plants generate large amounts of ATP in their chloroplasts during photosynthesis by photophosphorylation (light dependent phosphorylation of ADP). Mechanistically, this process resembles oxidative phosphorylation as it is based on a proton gradient (across the thylakoid membrane) exploited by an ATP synthase complex. However, generation of the proton gradient is driven by electrons coming from the two photosystems. Chloroplasts also include an NAD(P)H dehydrogenase complex. This complex is low in abundance as compared to mitochondrial complex I and is functionally involved in a cyclic electron transport around photosystem I (Shikanai, 2007). It therefore has a distinct physiological role and is outside of the focus of this review.

In plants, the biology of mitochondrial complex I takes place at the functional interface between respiration and photosynthesis. In addition, and this is relevant for complex I in all eukaryotes, it takes place at the functional interface of the mitochondria and the cell nucleus. In bovine mitochondria, seven out of the 44 complex I subunits are encoded by the mitochondrial genome, while the other 37 subunits are nuclear encoded, synthesized on cytosolic ribosomes and transported into the organelle (Balsa et al., 2012; Carroll et al., 2006). In most plants, two additional complex I subunits are encoded on the mitochondrial genome (Unseld et al., 1997). Furthermore, mitochondrial complex I transcripts undergo extensive maturation processes such as RNA editing or *trans*-splicing, which do not occur in any animal system studied so far. These processes are mainly catalyzed by nuclear encoded proteins which additionally have to be imported from the cytosol. How is protein biosynthesis in the mitochondrial matrix regulated by the nucleus of the plant cell?

Plant complex I represents an ideal model system for studying the nuclear–mitochondrial cooperation as well as for analyzing the molecular interplay of respiration and photosynthesis. It is of limited complexity with about 50 protein constituents, but further proteins are involved in its biosynthesis and assembly. Several aspects of its biology have been extensively studied from various angles. In this review we aim to integrate different lines of research by following "the life cycle of plant complex I" from the biosynthesis of its parts, over its assembly and its function to its dis-assembly and degradation.

2. Biosynthesis and assembly ("birth and childhood")

Complex I follows a long and remarkably intricate route to become functionally active: approximately fifty genes have to be transcribed in a coordinated manner in two different cellular compartments, the nucleus and the mitochondrion, these transcripts have to be translated in the cytosol or in the mitochondrial matrix, products of cytosolic translation have to be transported into mitochondria and their presequences have to be removed, subunits have to fold correctly and become equipped with the prosthetic groups necessary for enzymatic activity and, finally, subunits have to assemble to form the active holo-complex. To make things even more complex, mitochondrial transcripts undergo extensive maturation processes and translation products require posttranslational modifications. The following sections describe the extraordinary route by which complex I becomes a functionally active protein complex.

2.1. Genes

2.1.1. Mitochondrial genes

The first coding sequences for complex I subunits in the mitochondrial genome of plants were identified about 25 years ago by similarity to their homologs in Mammalia and Fungi. In watermelon, sequences with features of ND1 (Stern et al., 1986) and in *Oenothera berteriana* similarities to ND5 were first observed (Wissinger et al., 1988). However, both initial gene models turned out to be incomplete. It took several more years to unravel the respective complete genes: they are fragmented with exons spread through the genome. In fact, the three open reading frames of the nad1, nad2 and nad5 genes need to be assembled by *trans*-splicing from genomically unconnected mRNAs. The connection between the adjacent exons is made *via* assembly of the intervening halves of group II introns which somehow find their fitting counterparts in the other RNA molecule and form the secondary (and tertiary) structure to join the two exons (Binder et al., 1992; Chapdelaine and Bonen, 1991; Knoop et al., 1991; Wissinger et al., 1991).

These complex arrangements were ultimately proven by cDNA sequence analyses of the respective mature mRNAs. From these the complete open reading frames were deduced even though identifying similarity with homologs in animals and fungi is usually restricted to

Please cite this article as: Braun, H.-P., et al., The life of plant mitochondrial complex I, Mitochondrion (2014), http://dx.doi.org/10.1016/j.mito.2014.02.006

certain domains of the proteins. While in animals seven subunits (ND1–ND6 plus ND4L) are encoded in the mitochondrial genomes, plant mitochondrial DNA usually codes for nine subunits, ND1–7, ND4L and ND9. 'Usually encoded in the mitochondrial genome' means that in some plant species one or the other of these genes has moved to the nuclear genome. For example, in the liverwort *Marchantia polymorpha*, the nad7 gene is present in the mitochondrial genome only as a pseudogene while a functional copy of nad7 is located in the nuclear genome (Kobayashi et al., 1997).

Some of the smaller complex I subunit genes are continuous reading frames, but most of the larger mitochondrially encoded complex I subunits are interrupted by group II introns in *trans*- as well as in *cis*-configurations. In fact, most of the mitochondrial introns are found in these genes (Bonen, 2008; Unseld et al., 1997). It has been speculated that this concentration of introns in complex I genes may be connected to a regulatory mechanism which controls respiratory functions in plant mitochondria from the nucleus–cytosol compartment. Through this pathway expression of the mitochondrially encoded subunits could be collectively coordinated with the nuclear encoded polypeptides during development and/or in reply to stress situations (Bonen, 2008). Part of this as yet hypothetical pathway could be the nuclear encoded freestanding maturase genes which are required for splicing of the mitochondrial complex I introns. However, the functional and evolutionary assembly of this concentration of introns presently merely remains as an observation which needs to be substantiated through further experimental investigation.

2.1.2. Nuclear genes

According to the most recent proteomic analysis, complex I from *Arabidopsis* consists of at least 49 different subunits (see Section 2.7.; Peters et al., 2013), nine of which are encoded by the mitochondrial genome. The genes encoding the remaining 40 subunits are localized in the nucleus. Seven of the 40 subunits occur in pairs of isoforms. This adds up to 47 currently known complex I genes in the nucleus in *Arabidopsis thaliana* (Supp. Table 1). These genes are spread across the genome in *Arabidopsis*: eleven genes are localized on chromosome I, ten on chromosomes II and III, respectively, five on chromosome IV and eleven on chromosome V. Besides the nine mitochondrially encoded subunits, five of the nuclear encoded complex I subunits belong to the minimal set of 14 complex I proteins present in bacteria (the 75 kDa, 51 kDa, 24 kDa, TYKY and PSST subunits). During evolution, genes encoding these proteins were transferred from the ancestral mitochondrial genome to the nuclear DNA. The remaining genes encode subunits which most likely became part of mitochondrial complex I after the development of the eukaryotic cell. This probably occurred early in evolution because the set of nuclear encoded complex I subunits is largely identical in animal and plant mitochondria (Cardol, 2011). In fact, homologs of 40 of the 49 complex I subunits of *Arabidopsis* likewise form part of bovine complex I (Peters et al., 2013). The seven pairs of complex I isoforms probably arose by gene duplication events. The two copies of the pairs are localized on different chromosomes in all but one case.

2.2. Transcription

2.2.1. Nuclear transcription

Nuclear genes for complex I subunits show only minor variations in transcript levels between photosynthetic and non-photosynthetic tissues (Lee et al., 2008). Together with the finding that transcripts for mitochondrial proteins and transcripts required for energy metabolism have relatively long half-lives (Narsai et al., 2007), this implies that transcription of nuclear complex I subunit genes is relatively stable. Enhanced transcript levels seen in meristematic and reproductive tissues for mitochondrial proteins have been attributed to an overall stimulation of mitochondrial biogenesis due to increased energy demands (Brennicke et al., 1999). The constitutive nature of complex I gene transcription contrasts with the light- and stress-induced transcription of genes for alternative NAD(P)H dehydrogenases (see Section 3.1.; Millar et al., 2011).

Preliminary data suggest the response regulator ARR2 controls transcription of genes encoding complex I subunits (Lohrmann et al., 2001). Expression of nuclear genes for complex I subunits also likely involves transcription factors of the TCP family. An *in silico* survey revealed that specific *cis*-acting regulatory elements recognized by these factors were over-represented in the promoter regions of nuclear genes for the mitochondrial oxidative phosphorylation (OXPHOS) system in *Arabidopsis* (Welchen and Gonzalez, 2006). These elements, which are referred to as site II, were shown to control transcription of several genes for mitochondrial proteins (Giraud et al., 2010). Site II elements were also detected in promoters of numerous complex I genes in both *Arabidopsis* and rice (Welchen and Gonzalez, 2006). Their role in controling complex I biogenesis has, however, not yet been experimentally explored.

Besides genes for complex I subunits, complex I biogenesis requires hundreds of genes for mitochondrial protein import, mitochondrial gene expression and other steps of OXPHOS biogenesis. The modes of transcriptional control of these genes, whose expression mostly peaks during germination (Law et al., 2012; Narsai et al., 2011), will have to be discussed elsewhere.

2.2.2. Mitochondrial transcription

In addition to genes for nine complex I subunits, plant mitochondrial genomes contain genes for subunits of several other OXPHOS complexes, proteins required for cytochrome maturation and a few components of the mitochondrial translational apparatus (Unseld et al., 1997). For complex I biogenesis, correct expression of the latter is also necessary. As for nuclear complex I genes, transcript levels for complex I genes in mitochondria have been described as stable. Interestingly, diurnal changes in the transcription of all mitochondrial genes, including complex I genes, have been reported but were found to not affect steady-state mitochondrial transcript levels (Okada and Brennicke, 2006).

Complex I genes are generally not clustered in plant mitochondrial genomes. Only in a few cases can neighboring complex I genes be co-transcribed. Moreover, nad1, nad2 and nad5 each have five exons that are located in different genomic regions and joined through *trans*-splicing following their separate transcription (see above). Earlier studies of mitochondrial transcription and potential regulatory mechanisms controling this process mostly focused on the architecture and distribution of mitochondrial promoters (Dombrowski et al., 1999; Fey and Marechal-Drouard, 1999; Forner et al., 2007; Kühn et al., 2005). These studies revealed that in most cases, each mitochondrial gene is transcribed from multiple promoters. Mitochondrial promoter sequences, which extend over approximately 20 nucleotides comprising the transcription start site, are only moderately conserved. Importantly, no promoter elements have been identified that are specific for subsets of mitochondrial genes, such as complex I genes. Therefore, mitochondrial promoters are likely to predominantly facilitate transcription initiation rather than transcriptional regulation of mitochondrial gene subsets. This is in agreement with the observation that plant mitochondrial genomes frequently recombine and thus evolve structurally with high rate, resulting in divergent upstream sequences and promoters of mitochondrial genes in different species (Choi et al., 2012).

Mitochondrial genomes are transcribed by nucleus-encoded bacteriophage-type RNA polymerases (Liere et al., 2011). Cereals and other monocots have one mitochondrial RNA polymerase named RPOTm whereas eudicot mitochondria have acquired a second RNA polymerase named RPOTmp. This enzyme is also present in plastids. Distinct roles of these enzymes in species with multiple mitochondrial RNA polymerases have so far been investigated in the model plant *Arabidopsis* through *in vitro* transcription assays with recombinant RPOTm and RPOTmp enzymes (Kühn et al., 2007) or reverse-genetic

Please cite this article as: Braun, H.-P., et al., The life of plant mitochondrial complex I, Mitochondrion (2014), http://dx.doi.org/10.1016/j.mito.2014.02.006

approaches (Kühn et al., 2009). RPOTm recognizes diverse mitochondrial promoter sequences *in vitro* and has been proposed to be involved in transcription of most, if not all, mitochondrial genes. Inactivation of the RPOTm gene is lethal, substantiating a central role for this enzyme in mitochondrial transcription and OXPHOS biogenesis. *Arabidopsis* plants lacking a functional RPOTmp gene show reduced, but not completely disrupted, transcription of distinct mitochondrial genes, including complex I subunit genes nad1, nad2, nad4, nad5, nad6 and nad9. In contrast, transcription of nad3, nad4L and nad7 is entirely maintained through RPOTm. Together with the complex IV subunit gene cox1, nad6 depends most strongly on RPOTmp, causing severely reduced levels of complexes I and IV in *rpoTmp* mutants. It was therefore proposed that while RPOTm transcribes all mitochondrial genes, RPOTmp additionally transcribes a subset of mitochondrial genes and specifically affects complex I and IV biogenesis. Mapping of promoters for RPOTmp-dependent genes did not identify RPOTmp-specific promoter sequences, raising the question of how gene specificity of mitochondrial RNA polymerases is controlled. Remarkably, independently transcribed nad1, nad2 or nad5 exons also depend on RPOTmp to varying extent. Therefore, different transcriptional mechanisms participate in transcribing these genes, which adds to the complexity of mitochondrial complex I gene transcription. Different transcriptional mechanisms in complex I gene expression are supported by a recent transcriptomic study of mitochondrial biogenesis during seed germination (Law et al., 2012) and an earlier mitochondrial genome-wide transcriptional survey (Giegé et al., 2000). The latter study used run-on transcription assays and found significantly different transcription rates for individual genes encoding subunits of the same protein complex, with nad4L strongly exceeding transcription of other complex I genes. Steady-state transcript levels were considerably more homogeneous, presumably due to transcript stability effects.

Central questions emerging from these observations are: i) How are activity and gene specificity of mitochondrial RNA polymerases controlled? ii) Does the RNA polymerase RPOTmp present a mechanism for specifically regulating the biogenesis of complexes I and IV in response to developmental or environmental cues? High-resolution RPOTm- and RPOTmp-specific transcriptomes, which can be generated using resources available for the dicot model species *Arabidopsis*, will help in addressing these questions. For future research targeting different modes of complex I gene transcription in dicot *versus* monocot mitochondria, comparisons of high-resolution mitochondrial transcriptomes and promoters between monocot and dicot species would provide important groundwork.

2.3. Transcript maturation

2.3.1. Splicing of mitochondrial nad mRNAs

Evidence for effective regulation of mitochondrial gene expression is still relatively weak and to date it remains unclear as to whether there are regulatory mechanisms influencing expression of mitochondrial genes. That said the importance of the various post-transcriptional processes for the formation of mature RNAs is unquestionable and processes such as splicing, RNA editing and transcript end maturation provide options for regulation. In seed plants, the nad4 gene contains three introns (nad4i1 to i3), while the nad1, nad2, nad5 and nad7 genes are split by four introns (i1 to i4). These intervening sequences are classified as group II introns, which are spliced by a two-step transesterification pathway (Bonen, 2008). Typically this ribozymic intron class encodes factors required for splicing, but in seed mitochondria a matR gene encoding a reverse transcriptase like protein (maturase) is found only in nad1i4 (Bonen, 2008). A secondary structure with six helical domains (I to VI) has been proposed for group II introns, but many plant mitochondrial introns lack classical characteristics of this intron type (Bonen, 2008). Fragmentation of the nad1, nad2 and nad5 genes into different pieces is one of the most exceptional features of mitochondrial-encoded genes. Translatable transcripts of these genes have to be assembled by trans-splicing of independently transcribed RNAs encoded at distant genomic locations. Trans-spliced introns fold into group II intron structures that are disrupted in domain IV (Bonen, 2008). Several RNA editing sites have been identified in intron sequences, a few of them correcting non-canonical base pairs into classical A-U pairs as for instance in nad1i1 and nad7i4. *In vitro* experiments with a yeast autocatalytic intron containing domain VI of the *Oenothera* nad1i3 and *in organello* studies of trans-spliced nad1i4 and nad5i2 of wheat demonstrated that RNA editing has to precede splicing (Bonen, 2008; Farré et al., 2012). However, it has also been found that excised introns are only partially edited. Thus it seems that RNA editing of particular sites is a prerequisite for splicing while in other cases C to U exchanges may merely increase splicing efficiency (Bonen, 2008).

In *Arabidopsis*, several proteins were found to be involved in mitochondrial splicing (Table 1). The DEAD-box RNA helicase PMH2 has a general supporting role in splicing of various transcripts including nad mRNAs (Köhler et al., 2010). Similarly, a relaxed substrate spectrum was reported for mCSF1, an RNA binding protein required for efficient splicing of various introns (Zmudjak et al., 2013). Broad substrate specificity has also been reported for DEXH-box RNA helicase ABO6 identified in a screen for abscisic acid (ABA) overly-sensitive mutants. In the absence of this protein, splicing efficiency of several introns of different nad transcripts is severely impaired (He et al., 2012). Nuclear-encoded factors homologous to the mitochondrial-encoded MATR are involved in the intron removal from various nad mRNAs (nMAT1 for nad1i1, nad2i1 and nad4i2; nMAT2 for nad1i2 and nad7i2) (Keren et al., 2012). Likewise, RUG3, a protein related to human guanine nucleotide exchange factor, is an important but not essential factor for splicing of nad2i3 (Kühn et al., 2011). Besides these factors, three PPR proteins were found to be involved in splicing of different nad transcripts. OTP43 is essential for splicing of the trans-spliced nad1i1 (Falcon de Longevialle et al., 2007). BIR6, found in a mutant screen for root growth in the presence of the glutathione synthesis inhibitor buthionine sulfoximine, is a splicing factor involved in the removal of nad7i1 (Koprivova et al., 2010). ABO5, identified in the same screen as ABO6, participates in splicing of the nad2i3. Many mutants with defects in splicing of nad transcripts exhibit severely impaired complex I assembly and activity and show visual phenotypes such as retarded growth or curled leaves. Several of the proteins described above are involved in both *cis*- and *trans*-splicing events suggesting that there is no fundamental difference between the splicing mechanisms of these introns. Most of these factors may directly bind to RNA, but their exact molecular functions in the splicing process are unclear. Remarkably, the identification of two splicing factors in a screen for ABA overly-sensitive mutants suggests a link between mitochondrial gene expression and ABA signaling.

2.3.2. Processing of mitochondrial transcript extremities

Another major step toward the formation of mature mitochondrial RNA is the post-transcriptional generation of 5′ and 3′ ends. In *Arabidopsis*, two mitochondrial 3′ to 5′ exoribonucleases (polynucleotide phosphorylase (PNPase) and RNase R homolog 1 (RNR1)) have been identified which appear to be required for the generation of 3′ termini of the majority of mitochondrial-encoded RNAs including nad transcripts (Perrin et al., 2004) (Table 1). Additionally, MTSF1, a PPR protein involved in the generation of the +30 3′ terminus of nad4 mRNA has been characterized. Similar to a mechanism found in chloroplasts, this protein binds to the 3′ terminal region of the nad4 mRNA, thereby protecting the transcript from degradation by the mitochondrial PNPase (and RNR1) and concomitantly defining the 3′ end of the mRNA (Haili et al., 2013). Interestingly, this protein is also involved in splicing of nad2 RNAs. In contrast, several factors, exclusively P-class PPR proteins, are required for the generation of mature 5′ termini (Table 1). RNA PROCESSING FACTOR1 (RPF1) and the not yet identified RPF7 seem to be exclusively involved in processing for nad4 and nad2 5′ termini, respectively, while RPF2 and RPF5 are required not only for formation of mature nad9 and nad6 5′ ends, but also for cox3, atp9 and rrn26

Please cite this article as: Braun, H.-P., et al., The life of plant mitochondrial complex I, Mitochondrion (2014), http://dx.doi.org/10.1016/j.mito.2014.02.006

Table 1
Proteins involved in complex I gene transcription, transcript splicing and transcript end maturation in plant mitochondria.

Functional category	Gene family	Gene[a]	AGI	Target transcript (CI)	Reference
Transcription	Phage-type RNA polymerase	*RPOTm*	At1g68990	nad1, nad2, nad3, nad4, nad4L, nad5, nad6, nad7, nad9	Kühn et al. (2009)
Transcription	Phage-type RNA polymerase	*RPOTmp*	At5g15700	nad1, nad2, nad4, nad4L, nad5, nad6, nad9	Kühn et al. (2009)
Splicing	PPR family	*OTP43*	At1g74900	nad1	Falcon de Longevialle et al. (2007)
Splicing	PPR family	*BIR6*	At3g48250	nad7	Koprivova et al. (2010)
Splicing	PPR family	*ABO5*	At1g51965	nad2	Liu et al. (2010)
Splicing	RNA helicase	*PMH2*	At3g22330	nad1, nad2, nad4, nad5, nad7, others	Köhler et al. (2010)
Splicing	RNA helicase	*ABO6*	At5g04895	nad1, nad2, nad4, nad5	He et al. (2012)
Splicing	RCC1-like	*RUG3*	At5g60870	nad2	Kühn et al. (2011)
Splicing	Gene not identified	*NMS1*		nad4	Brangeon et al. (2000)
Splicing	RNA maturase	*MAT1*	At1g30010	nad1, nad2, nad4	Keren et al. (2012)
Splicing	RNA maturase	*MAT2*	At5g46920	nad1, nad7	Keren et al. (2009)
Splicing	CRM-domain family	*mCSF1*	At4g31010	nad1, nad2, nad4, nad5, nad7, others	Zmudjak et al. (2013)
Splicing	PPR family	*MTSF1*	At1g06710	nad2	Haili et al. (2013)
End maturation	PPR family	*MTSF1*	At1g06710	nad4	Haili et al. (2013)
End maturation	PPR family, P-class	*RPF1*	At1g12700	nad4	Hölzle et al. (2011)
End maturation	PPR family, P-class	*RPF2*	At1g62670	nad9, cox2	Jonietz et al. (2010)
End maturation	PPR family, P-class	*RPF5*	At4g28010	nad6, atp9, 26S rRNA	Hauler et al. (2013)
End maturation	Gene not identified	*RPF7*		nad2	Stoll et al. (2013)

[a] Excepting *NMS1* described in *Nicotiana sylvestris*, all listed genes were identified in *Arabidopsis thaliana*.

RNAs (Hauler et al., 2013; Hölzle et al., 2011; Jonietz et al., 2010). As for the proteins involved in RNA splicing the precise molecular function of the RPF is unknown. It is assumed that they bind to the target RNA in a sequence-specific manner thereby recruiting a potential endonuclease to the cleavage site. In general, plant lines (mutant or accessions) with defective RPFs are indistinguishable from wild type or show reduced seed germination capacity like the rpf5-1 knockout mutant (Hauler et al., 2013). How mitochondrial 5′ processing influences seed germination will be subject of future studies that might bring up deeper insights into the importance of this post-transcriptional maturation step in the regulation of plant mitochondrial functions.

2.3.3. RNA editing of mitochondrial transcripts

Expression of the complex I subunit genes in the mitochondrial genome is not only complicated by the interruption by group II introns in *trans*- as well as in *cis*-configurations, but also their coding sequences are modified post-transcriptionally by RNA editing (For a review: Takenaka et al., 2008, 2014). In the model plant *A. thaliana* a total of about 500 RNA editing events alter coding sequences in the mitochondria. Nearly 200 editing events occur in the RNAs for complex I subunits (Table 2). Some RNA editing events in intron sequences are required for correct folding and splicing of these introns (Börner et al., 1995). However, most RNA editing events occur in exons and alter the triplet identity to code for a different amino acid than the one predicted by the genomic DNA.

The extent of RNA editing in the mitochondrial complex I genes is in the intermediate range as compared to other mitochondrial genes. The group of genes coding for heme-cluster biosynthesis factors are much more extensively edited while the mRNAs for subunits of complex III or of the ATPase are usually less altered by the C to U RNA editing process. Again, why the mRNAs for individual subunits of a certain complex are treated to a similar, yet unique, extent by splicing or editing remains unanswered. Speculations such as a common control of half-life and/or translational speed with associated similar time spans remain to be investigated.

Numerous nuclear genes are required for processing the RNA editing events, most notably a number of PPR protein coding genes have been identified to be required for individual or very few editing sites. Up to now, 19 editing factors could be assigned to editing events in complex I transcripts (Table 3). Whether any of these proteins is used by the nucleus–cytosol compartment to exert control over gene expression in mitochondria remains an open question. It is unlikely that many of the PPR proteins are involved as their expression levels are very low. However, this feature could also allow fine tuning of these limiting factors. Here only those few at crucial editing sites could function in any sort of control since many editing events will not yield a gross phenotypic effect. Such potential fine tuning does not extend to a variation in polypeptide composition since *e.g.* the protein sequence of ND9 of complex I contains only the protein corresponding to fully edited mRNA although at one of the non-silent sites only about half of the steady state mRNA is actually edited.

2.3.4. Maturation of transcripts of nuclear-encoded subunits of the NADH dehydrogenase

Expression of nuclear genes encoding subunits of the NADH dehydrogenase complex is controlled at the transcriptional level. Whether there is any substantial contribution of post-transcriptional processes like intron splicing or polyadenylation to the expression regulation of nuclear complex I genes has not yet been specifically addressed in plants. Likewise, it is unknown whether any of the small RNA pathways control such genes but data mining of genome wide studies might shed some light on the post-transcriptional maturation or nuclear-encoded complex I transcripts.

2.4. Translation

Basically nothing is known about common features and control of translation events specific to complex I genes in both mitochondria and the cytosol. The absence of a mitochondrial *in vitro* translation system has hampered such analyses in this compartment. A recent study of a silenced nuclear gene for a mitochondrial ribosomal protein suggests that there may be a regulatory feedback from translational activity to mitochondrial mRNA abundance (Kwasniak et al., 2013).

Table 2
Total numbers of RNA editing sites in coding regions of complex I mRNAs in mitochondria of *Arabidopsis thaliana*.

Mt gene	No. of editing sites
nad1	22
nad2	29
nad3	11
nad4	35
nad4L	9
nad5	31
nad6	11
nad7	29
nad9	7
matR	10
Total	194

Please cite this article as: Braun, H.-P., et al., The life of plant mitochondrial complex I, Mitochondrion (2014), http://dx.doi.org/10.1016/j.mito.2014.02.006

Here differential mRNA levels were observed between the respiratory chain complexes with complex I and complex IV subunit mRNAs being stronger elevated than that of complex III for example.

In the nucleus/cytosol so far no specific investigations of complex I mRNAs and their transport to the vicinity of the mitochondrial outer membranes have been initiated. It will be interesting to see whether polysomes with mRNAs specifying complex I subunits associate at similar regions at the mitochondrial surface and if their translational progress is in any way controlled and coordinated.

2.5. Import of nuclear encoded subunits

All nuclear-encoded mitochondrial proteins have to be imported into mitochondria after the precursor proteins have been synthesized on cytosolic ribosomes and guided by chaperones to the organelle surface for import. So far 47 nuclear-encoded complex I proteins have been identified by mass spectrometry in *Arabidopsis* mitochondria (Suppl. Table 1) and five of them were also confirmed to be targeted to mitochondria by C-terminal GFP fusions (Abu-Abied et al., 2009; Lee et al., 2002; Murcha et al., 2007; Tanz et al., 2013; Tian et al., 2004; Wang et al., 2012a). Depending on the intra-organellar localization, mitochondrially targeted proteins contain either N-terminal presequences or internal non-cleavable signal sequences which are recognized by the protein import receptor TOM20 at the surface of the outer mitochondrial membrane (Rimmer et al., 2011; Schleiff and Becker, 2011). Proteins containing a presequence are usually destined to the mitochondrial matrix, while proteins to be inserted into the inner mitochondrial membrane contain an internal presequence-like signal (reviewed in Schleiff and Becker, 2011).

Upon *in silico* analysis of the 47 nuclear encoded proteins using TargetP (Emanuelsson et al., 2000), 29 proteins are predicted to comprise a cleavable mitochondrial presequence (data not shown). However, presequence definition by TargetP was reported to be largely incorrect if applied to mitochondrial proteins from plants (error rate of 70%, Huang et al., 2009). In another approach to define the presequences of complex I subunits, we determined the apparent molecular masses of all 47 nuclear encoded subunits of *Arabidopsis* by use of 2D Blue native/SDS PAGE (as displayed at the GelMap portal www.gelmap.de) and compared them with their calculated molecular masses (Supp. Table 3). Since most plant mitochondrial presequences comprise 20–70 amino acids (Zhang and Glaser, 2001), which corresponds to about 2–8 kDa in mass, we defined the presence of a mitochondrial presequence if the apparent molecular mass of a complex I subunit was reduced by at least 2 kDa in relation to its calculated molecular mass. Using this criterion, 12 of the 47 nuclear encoded complex I proteins comprise a cleavable presequence (Supp. Table 3). Interestingly, only 3 of the 28 nuclear encoded proteins of the membrane arm seem to possess a presequence (10%), while 9 of the 19 proteins constituting the peripheral arm or the carbonic anhydrase domain are equipped with one (50%). However, one has to keep in mind that although the gel-based protein size determination already gives some good indication on the actual size of the mature complex I proteins, we cannot rule out that some of the proteins analyzed here are processed or modified at other positions than the N-terminus and thus an experimental validation of their presequences is still needed. Indeed, N-terminal sequences of complex I subunits from either *Arabidopsis*, rice or potato have already been experimentally defined by mass spectrometry or Edman degradation for overall 16 subunits: the B13 subunit (Kruft et al., 2001), the B14, B14.5, B18, B22, CAL1, CAL2, 18 kDa, 75 kDa, PSST and TYKY subunits (Huang et al., 2009; Jänsch et al., 1996), the CA1, CA2 and CA3 subunits (Klodmann et al., 2010) and the AGGG and B12 subunits (Salvato et al., 2014) (Supp. Table 3). Nine of these subunits lack a cleavable presequence, while seven comprise one. In 14 of 16 cases (88%), these results are in line with our GelMap-based prediction (Supp. Table 3).

Analyses of experimentally defined presequences of complex I subunits in *Arabidopsis* (5 proteins) rice (7 proteins) reveals the following properties (Supp. Table 4): (i) presequence length varies between 11 amino acids (B13 subunit of *Arabidopsis*) and 46 amino acids (PSST subunit of *Arabidopsis*); (ii) amino acid composition of the presequences is much enriched in alanine (21%), arginine (15%), leucine (14%) and serine (12%); (iii) presequences completely lack glutamate and aspartate; (iv) the presequences have a disposition to form amphiphilic α–helices and (v) an arginine residue is located at position −2 or −3 with respect to the cleavage site in nearly all presequences of complex I subunits. These presequence properties are in line with the general properties defined for mitochondrial presequences in plants (Zhang and Glaser, 2001). The arginine at position −2/−3 is known to be a prerequisite for presequence cleavage by the mitochondrial processing peptidase. Due to the very limited number of defined presequences for complex I subunits in plants, it currently cannot be determined whether complex I subunits share common presequence properties which significantly differ from the properties of presequences of other mitochondrial proteins not forming part of complex I.

We conclude that more than half of the complex I subunits and nearly all of the subunits of its membrane arm seem to lack a cleavable presequence in plants. These proteins might contain internal presequence-like signals which are difficult to detect. Hence, more experimental evidence is needed to dissect the import pathways of complex I subunits into plant mitochondria, which will be crucial for the understanding of the sophisticated assembly of this protein complex.

2.6. Assembly, assembly factors

2.6.1. Assembly of complex I

To date, the assembly of complex I has been mainly studied in fungi and mammals. Complex I is assembled in a modular way in which building blocks, each containing a few subunits, are joined together to establish a functional complex I (Mimaki et al., 2012; Vogel et al., 2007b). These building blocks have been identified in mutants lacking a subunit (Antonicka et al., 2003; Nehls et al., 1992) or by following the insertion of labeled subunits into the growing complex (Lazarou et al., 2007; Ugalde et al., 2004; Vogel et al., 2007a). Compared with mammals, considerably fewer complex I mutations have been studied

Table 3
RNA editing sites in complex I mRNAs to which PPR type RNA editing factors have been assigned in mitochondria of *Arabidopsis thaliana*.

Mt gene	Position from ATG	Editing factor	AGI acc.	PPR type
nad1	308	MEF25	At3g25060	E
nad1	571	MEF32	At4g14170	E
nad2	558	REME1	At2g03880	DYW
nad2	842	MEF10	At3g11460	DYW
nad2	1160	MEF1	At5g52630	DYW
nad2	1433	MEF7	At5g09950	DYW
nad3	149	MEF22	At3g12770	DYW
nad3	250	SLG1	At5g08490	E
nad4	124	MEF11	At4g14850	DYW
nad4	376	AHG11	At2g44880	E
nad4	449	SLO1	At2g22410	E
nad4	1355	MEF18	At5g19020	E
nad4L	41	MEF7	At5g09950	DYW
nad4L	110	SLO2	At2g13600	E
nad5	374	MEF12	At3g09040	E
nad5	676	MEF8	At2g25580	DYW
nad5	1550	MEF29	At4g30700	DYW
nad6	95	MEF8	At2g25580	DYW
nad7	24	OTP87	At1g74600	E
nad7	200	MEF9	At1g62260	E
nad7	739	SLO2	At2g13600	E
nad7	963	MEF1	At5g52630	DYW
nad9	328	SLO1	At2g22410	E
matR	1730	MEF11	At4g14850	DYW
matR	1895	MEF14	At3g26780	DYW

Please cite this article as: Braun, H.-P., et al., The life of plant mitochondrial complex I, Mitochondrion (2014), http://dx.doi.org/10.1016/j.mito.2014.02.006

in plants and little data on complex I assembly is available. Nevertheless, a similar modular assembly pathway has been suggested (Vogel et al., 2007b). Recently, several *Arabidopsis* mutants each lacking a different subunit have been investigated for accumulating assembly intermediates, and a first model for the assembly of the membrane arm of complex I in plants was proposed (Meyer et al., 2011). This work showed that in plants, like in all other organisms studied to date, the assembly of the membrane arm involves joining together of an intermediate containing ND1 with an intermediate containing ND2, followed by the addition of a module containing ND4 and ND5. In addition, the study highlighted a major difference between the plant and mammalian pathways: the plant-specific subunit CA2 is essential for the initial step of the membrane arm assembly (Meyer et al., 2011). Two of the intermediates described by Meyer et al. (2011) have been identified as having a higher turnover than complex I, confirming these intermediates as assembly subcomplexes (Li et al., 2013). In addition, import of several plant-specific subunits into isolated mitochondria lead to their rapid incorporation in complexes with sizes in accordance with the membrane arm intermediates (Carrie et al., 2010; Li et al., 2013). On the other hand, no assembly intermediates of the peripheral arm have so far been detected in plants. Hence, the joining of the matrix and membrane arms in plant mitochondria has not yet been elucidated. Additional work involving the analysis of new mutants and the utilization of alternative strategies, such as the labeling techniques recently developed in the plant system (Li et al., 2013), will be required to better characterize the complex I assembly pathway in plants.

2.6.2. Assembly factors

Analyses of molecular defects responsible for complex I deficiency in human mitochondria defined three classes of mutations: mutations in complex I subunits, mutations in proteins involved in mitochondrial gene expression and mutations in assembly factors (Hoefs et al., 2012). Assembly factors are proteins essential for the assembly of complex I which are absent from the mature complex. Proteins involved in mitochondrial protein import or mitochondrial gene expression are not considered assembly factors. Assembly factors are often associated with assembly intermediates which they stabilize thus aiding the progress of assembly. In mammals, several such factors have been identified (for review see Mimaki et al., 2012; Pagniez-Mammeri et al., 2012). Orthologs of different mammalian assembly factors are also present in the *Arabidopsis* genome (E.H. Meyer, unpublished data), however, the potential roles of these candidates in complex I assembly are yet to be investigated. To date, only one potential plant complex I assembly factor has been described in the model organism *A. thaliana*. This factor is the last enzyme of the ascorbate biosynthesis pathway, the L-galactono-1,4-lactone dehydrogenase (GLDH). GLDH is absent from mature complex I but has been shown to be associated with a smaller version of the complex (Heazlewood et al., 2003) and with smaller complexes likely representing complex I assembly intermediates (Schertl et al., 2012). As the knock-out mutant of GLDH does not accumulate complex I (Pineau et al., 2008), GLDH can be considered the first complex I assembly factor described for plants. The role of GLDH during complex I assembly remains to be resolved. Given that complex I assembly in plants differs from the mammalian pathway, further plant-specific assembly factors might be involved. The determination of the composition of previously identified assembly intermediates will almost certainly identify new candidate assembly factors in plants.

2.7. Architecture and internal subunit arrangement

Proteome projects have been carried out to systematically investigate the subunit composition of complex I in plants (Cardol et al., 2004; Heazlewood et al., 2003; Klodmann and Braun, 2011; Klodmann et al., 2010; Li et al., 2013; Meyer et al., 2008; Peters et al., 2013; Sunderhaus et al., 2006; Meyer, 2012). According to the most recent investigation, complex I of the model plant *A. thaliana* consists of at least 49 types of subunits (Peters et al., 2013, Supp. Table 1). As mentioned above, 40 of these subunits are present as homologs in complex I particles of bovine mitochondria. The remaining nine subunits are considered to be special constituents of mitochondrial complex I in plants. Seven of the 49 subunits occur in pairs of isoforms in *Arabidopsis*. Therefore, overall 56 genes encode complex I proteins in *Arabidopsis*, nine of which are localized on the mitochondrial genome and 47 on the nuclear genome. This number may even rise further in the future because additional proteins were identified representing potential complex I subunits (Peters et al., 2013, Supp Table 2).

Electron microscopy analyses revealed that plant complex I has a unique structure which includes an additional domain (Fig. 2). This domain has a spherical shape and is attached to the membrane arm at a central position on its matrix exposed side (Dudkina et al., 2005). It also has been described for complex I of potato, maize, and the alga *Polytomella* (Bultema et al., 2009; Peters et al., 2008; Sunderhaus et al., 2006). The domain includes a set of subunits which occur in plants as well as in some protist lineages and which resemble gamma-type carbonic anhydrases (Gawryluk and Gray, 2010; Perales et al., 2004). Three of these proteins have a conserved active site and are termed carbonic anhydrases 1, 2 and 3 (CA1, CA2 and CA3) while the other two proteins show less similarity and are designated "carbonic anhydrase-like" proteins 1 and 2 (CAL1 and CAL2) (Perales et al., 2004, 2005). As mentioned above another plant specific protein associated with complex I is the L-galactono-1,4-lactone dehydrogenase which catalyzes the terminal step of ascorbic acid biosynthesis. It most likely does not form part of mature complex I but evidence has been presented that it aids assembly of complex I in plants (Pineau et al., 2008; Schertl et al., 2012). Some further plant specific complex I subunits have low molecular masses and are of unknown function.

To facilitate complex I research in plants, two 2D gel-based reference maps were recently generated which are freely accessible *via* the GelMap portal (http://www.gelmap.de; Senkler and Braun, 2012). Information on all identified complex I spots is retrievable from interactive spot maps. One of the maps has been constructed from the disassembled complex I of *Arabidopsis* (http://www.gelmap.de/complex-i/). On the basis of a systematic analysis of the protein compositions of defined complex I subcomplexes a rough internal architecture of complex I has been resolved (Klodmann et al., 2010). The second map (http://www.gelmap.de/arabidopsis-3d-complex-i/) visualizes complex I subunits upon separation by three dimensional BN/SDS/SDS

Fig. 2. Averaged strucure of mitochondrial complex I from *Arabidopsis thaliana*. Isolated complex I was stained by uranyl acetate and images were taken by transmission electron microscopy.
From: Sunderhaus et al., 2006, J. Biol. Chem. 281, 6482–6488, with permission.

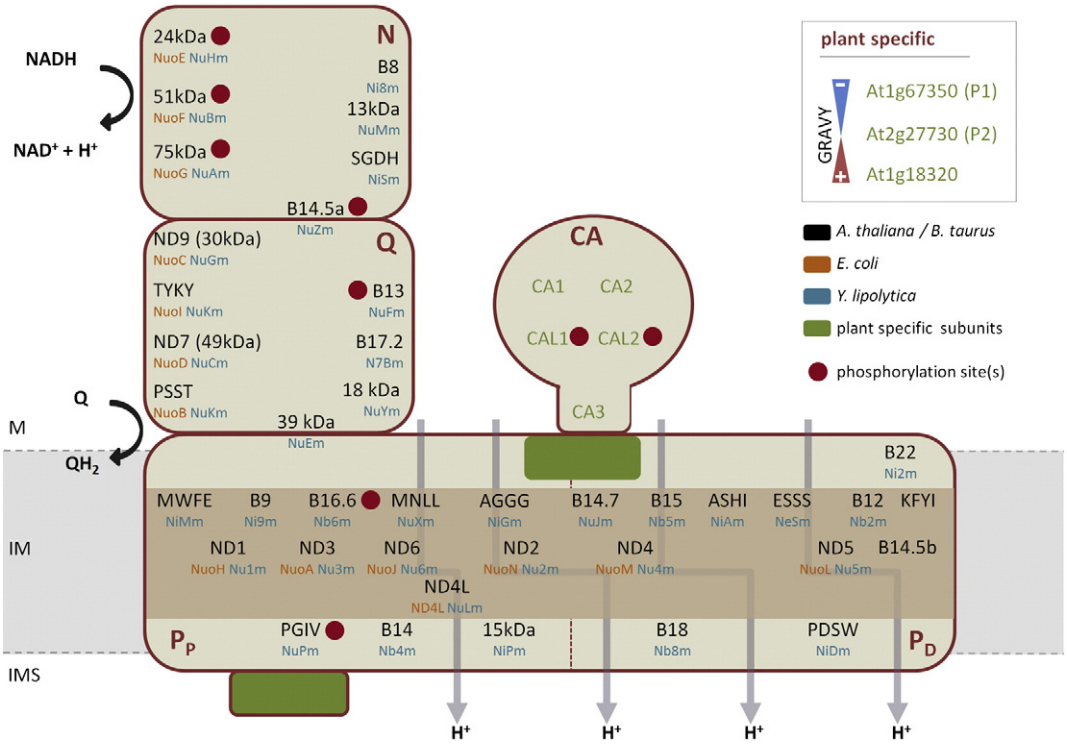

Fig. 3. Model of the internal subunit arrangement of plant complex I. The P-module contains two domains: one proximal to the peripheral arm (P_P), the other one on distal side (P_D) (Angerer et al., 2011). Subunits are named according to the bovine nomenclature (black), which also has been used for *Arabidopsis* (see Supp. Table 1). Furthermore, names of homologs in *Escherichia coli* (orange) and *Yarrowia lipolytica* (blue) are indicated. Besides the carbonic anhydrases subunits (CA domain), positions of plant specific subunits are not clear so far. Therefore, these subunits are listed in the box above the scheme according to their GRAVY scores (which indicates tendencies for peripheral [negative scores] or integral positions [positive score]). In the model, possible locations of these subunits are indicated in green. Membrane-spanning subunits of the membrane arm are given in the center of this domain, and subunits localized more peripherally within the membrane are given above and below (beige background). Phosphorylated subunits are marked by red dots (for details see Supp. Table 5). M: matrix, IM: inner membrane, IMS: inter membrane space. (For interpretation of the references to color in this figure legend, the reader is referred to the web version of this article.)

PAGE (Peters et al., 2013). Besides subunit ND4L it includes a complete set of currently known complex I subunits in *Arabidopsis*. Fig. 3 summarizes the current knowledge on the internal subunit arrangement of complex I in plants.

3. Function and regulation (adulthood/maturity)

Biosynthesis and assembly of functional complex I follow a long route and include several complicated and energy-costly biochemical processes. What is the benefit of all this major investment for the cell? What is the physiological role of mitochondrial complex I, especially in the context of photosynthesis, in the plant cell? The following sections summarize its activities, its physiological roles, its partners and its integration into metabolic networks.

3.1. Physiological roles of complex I

3.1.1. Oxidoreductase and proton translocation functions

The crystal structure of the bacterial complex I has provided first insights into the coupling mechanism of oxidoreduction and proton translocation. NADH is oxidized by a flavine mononucleotide (FMN) attached to the 51 kDa subunit (Fig. 1). A chain of seven iron–sulfur (FeS) clusters coordinated by subunits of the N- and Q modules passes electrons from the 51 kDa subunit to PSST. The latter subunit includes FeS cluster N2 which transfers the electrons to quinone. This takes place at a quinone binding pocket close to the interface between the two arms of complex I. Another FeS cluster, N1a, is located in close proximity to FMN. As NADH transfers two electrons to complex I but only one electron can be forwarded by FMN, the cluster N1a keeps one electron until the first has passed through the chain. Hence, FMN in complex I is also called "two-to-one electron converter" (Brandt, 2006). Reduction of ubiquinone triggers an electrostatic chain reaction in the membrane arm which drives proton translocation across the bacterial or mitochondrial membrane. Based on the bacterial crystal structure the following mechanism has been proposed (Baradaran et al., 2013): upon quinone reduction (conversion of quinone to quinol), four proton half channels formed by ND2, ND4, ND5 and ND3/6/4L simultaneously open at the matrix side of the membrane arm. Protons then bind to charged amino acid residues in the center of the inner mitochondrial membrane. Upon exchange of the quinol by quinone, the four half channels close and four half channels on the other side of the inner mitochondrial membrane open, allowing the four protons to be released into the mitochondrial intermembrane space. As a consequence, four protons are translocated across the inner mitochondrial membrane per oxidized NADH. Due to the similarities in the basic structure of complex I across different lineages, this reaction mechanism can also be anticipated for complex I of plants.

3.1.2. Role of complex I function in respiration and photorespiration

The respiratory chain is estimated to translocate 10 protons from the mitochondrial matrix to the mitochondrial intermembrane space per oxidized NADH (Watt et al., 2010). Four of these protons are translocated by complex I. Re-entry of three protons from the mitochondrial intermembrane space into the mitochondrial matrix at the ATP synthase complex is necessary to synthesize one molecule of ATP (Rich, 2003). Consequently, complex I makes a major contribution to oxidative phosphorylation. However, mitochondria of plants also contain alternative NAD(P)H dehydrogenases (Millar et al., 2011; Rasmusson et al., 2004). Genes encoding these enzymes are light-regulated and contribute to NADH oxidation at daytime. The necessity to increase NADH oxidation capacity in plants at daytime is a consequence of photosynthesis. In most plants, photosynthesis is coupled to

photorespiration which includes glycine-serine conversion in mitochondria. The decarboxylation of glycine is linked to NAD^+ reduction and generates additional NADH with high rate, which requires efficient re-oxidation by mitochondrial NADH dehydrogenases. However, deletion of complex I by knocking-out a gene encoding one of its subunits is not always lethal. Hence, most likely due to the presence of the alternative NAD(P)H oxidoreductases, plants have a particularly flexible OXPHOS system.

3.1.3. Role of complex I function in photosynthesis

Indication that complex I plays an important role in photosynthesis comes from various experimental findings. First, complex I is more abundant in green tissues than in non-green tissues. This has been shown by comparing the mitochondrial proteome in roots and shoots (Lee et al., 2011) but also by estimating the relative abundance and activities of respiratory complexes in different tissues (Peters et al., 2012). Furthermore, characterization of mutants has revealed clear effects of down-regulation or deletion of complex I on photosynthesis (Noctor et al., 2004). While the capacity of the photosynthetic apparatus does not seem to be affected by the reduced complex I activity (Dutilleul et al., 2003b; Meyer et al., 2009), the photosynthetic activity measured as the efficiency of photosystem II or as chloroplastic electron transfer is reduced (Juszczuk et al., 2007; Meyer et al., 2009; Sabar et al., 2000). This reduction of photosynthetic activity is more pronounced under high light conditions or under conditions that favor photorespiration, suggesting that complex I is playing a particularly important role for this metabolic pathway (Dutilleul et al., 2003b) (see above). As a consequence, the growth phenotype and the lower photosynthetic activity of complex I mutants can be overcome when plants are grown under high CO_2 conditions to prevent photorespiration (Priault et al., 2006). Therefore the reduced photosynthetic activity of complex I mutants could be explained by limited CO_2 supply for photosynthesis. Alternatively, it may be caused by a change in cellular redox homeostasis. Indeed, under high light or photorespiratory conditions, an over-reduction of the plant cell is expected to happen (increased NAD(P)H/$NAD(P)^+$ ratio). In the context of a complex I mutation, the total NADH concentration and the NAD(P)H/$NAD(P)^+$ ratio are increased (Hager et al., 2010). These observations suggest that in addition to its role in oxidative phosphorylation, the respiratory chain plays a key role in maintaining the redox system of the plant cell in a balance. Complex I, together with the alternative NAD(P)H dehydrogenases, probably forms part in this over-reduction protection mechanism by controling cellular NADH concentrations. Another interaction between respiratory chain and photosynthesis has been evidenced in *Chlamydomonas reinhardtii*: the activity of the cytochrome pathway controls the expression of photosynthetic genes (Matsuo and Obokata, 2006). Similar regulation may occur in land plants as transcripts encoding the light reaction of photosynthesis are significantly down-regulated in complex I mutants (Meyer et al., 2009; Pellny et al., 2008). In summary, the extensive characterization of complex I mutants indicates that there are several potential levels for the control of photosynthesis by complex I but the mechanisms involved remain unknown. However, findings on complex I mutants at the same time have to be taken with caution because in general it is difficult to discriminate between direct complex I effects and indirect effects caused by modified primary metabolism. Understanding complex I function in green tissues is essential to unravel the interactions between mitochondria and chloroplasts.

3.1.4. Carbonic anhydrase function

The physiological role of the five CA/CAL subunits present in *Arabidopsis* complex I remains elusive. Based on several indirect experimental findings, CO_2–bicarbonate conversion at complex I was proposed to be part of a CO_2 transport mechanism between mitochondria and chloroplasts (Braun and Zabaleta, 2007; Zabaleta et al., 2012). The proposed mechanism resembles the cyanobacterial carbon-concentration mechanism (CCM). Furthermore, it has been suggested that complex I might represent a bicarbonate translocase in the context of the proposed transport system (Zabaleta et al., 2012). Besides their proposed role for carbon fixation, the CA/CAL subunits are essential for assembly of plant complex I (Li et al., 2013; Meyer et al., 2011; Perales et al., 2005).

3.1.5. Other functions

Complex I includes several subunits resembling proteins of known function which exhibit activities in the context of other biochemical processes. For instance, subunits resembling proteins of the pre-protein translocase of the inner mitochondrial membrane (the TIM complex) form part of complex I (Klodmann et al., 2011; Wang et al., 2012b). The B16.6 subunit resembles the GRIM19 protein which participates in an apoptotic signal transduction pathway (Remacle et al., 2008). Finally, complex I in fungi and mammals includes an acyl carrier protein and it has been shown that fatty acid biosynthesis can take place at the surface of fungal complex I (Zensen et al., 1992). However, this subunit is not present in complex I from plants (Meyer et al., 2007).

In summary, complex I is not only an oxidoreductase but rather should be considered a multi-functional platform that hosts a range of biochemical processes (Fig. 4). Future research will need to explore how exactly the different functions of complex I are interconnected.

3.2. Posttranslational modifications

Since complex I is a major pacemaker of oxidative phosphorylation and a hotspot for mitochondrial reactive oxygen species (ROS) production (see Section 3.4.), it can be expected that its activity is regulated in response to cellular demand for oxidation of NADH generated from respiratory and photorespiratory substrates. Both transcriptional and posttranscriptional regulatory mechanisms could play a role in the regulation of complex I activity. However, in contrast to the mitochondrial alternative dehydrogenase transcripts, most of the nuclear-encoded complex I transcripts are only mildly regulated in dependence on abiotic and biotic stresses (reviewed in Schwarzländer and Finkemeier, 2013). Furthermore, most of the complex I subunits have been estimated to have a relatively slow protein turnover [see below and (Nelson et al., 2013)]. Hence, posttranslational modifications would be an efficient means to promptly regulate complex I activities as required by cellular metabolism. Nevertheless not many plant mitochondrial proteins have been found to carry post-translational modifications thus far (Hartl and Finkemeier, 2012).

3.2.1. Phosphorylation

None of the complex I subunits have been identified in any of two different targeted phosphoproteomic approaches on isolated mitochondria of *Arabidopsis* cell cultures or potato tubers (Bykova et al., 2003; Ito et al., 2009). The lack of identified phosphorylated complex I subunits in these two studies, however, could be due to the loss of phosphorylation during the long mitochondrial isolation procedures rather than to the actual lack of complex I phosphorylation in plants. Indeed, in three different shotgun phosphoproteomic approaches of whole *Arabidopsis* protein extracts, 11 phosphosites on either serine, threonine or tyrosine residues have been identified on 9 different complex I subunits (Suppl. Table 5; Heazlewood et al., 2008; Reiland et al., 2009, 2011; Engelsberger and Schulze, 2012). Seven of these proteins (24 kDa, 51 kDa, 75 kDa, PGIV, B13, CAL1, and CAL2) are protruding into the mitochondrial matrix, while the other two are more integral to the membrane arm according to the latest complex I model for plants (Fig. 3). Hence, the complex I subunits which are facing the matrix side are potential targets of one of the 10 protein kinases identified in the *Arabidopsis* mitochondrial proteome (Heazlewood et al., 2004). Intriguingly more than half of the identified proteins are phosphorylated at tyrosine residues. Tyrosine (Tyr) phosphorylation of mitochondrial proteins was previously shown to be tightly connected to the

Please cite this article as: Braun, H.-P., et al., The life of plant mitochondrial complex I, Mitochondrion (2014), http://dx.doi.org/10.1016/j.mito.2014.02.006

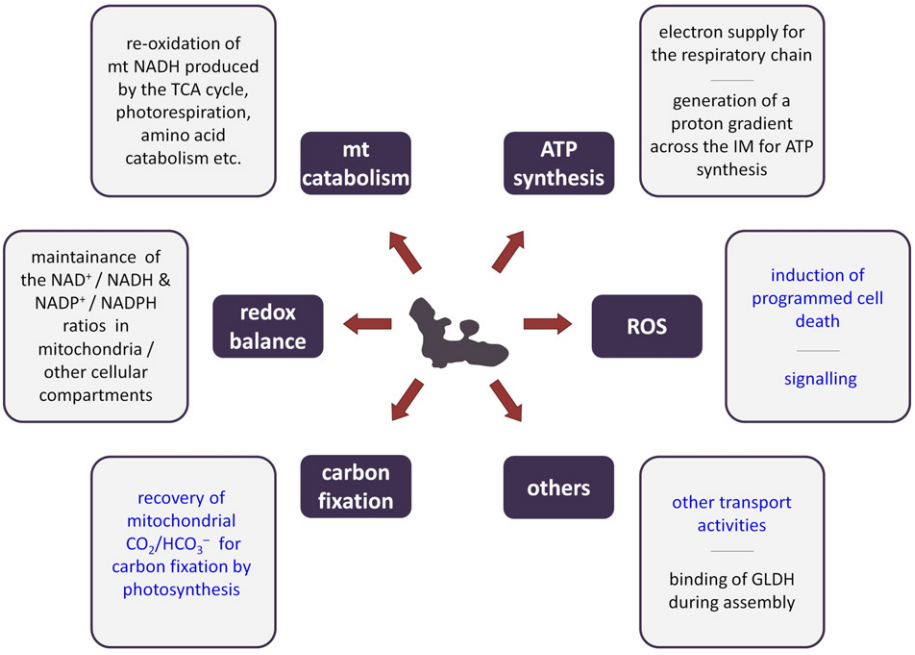

Fig. 4. Functions (black) and putative functions (blue) of mitochondrial complex I in plants. mt: mitochondrial, IM: inner mitochondrial membrane, GLDH: L-galactono-1,4-lactone dehydrogenase. (For interpretation of the references to color in this figure legend, the reader is referred to the web version of this article.)

mitochondrial redox state and thus could have an important regulatory role in the regulation of the electron transport chain (Håkansson and Allen, 1995; Salvi et al., 2005). Furthermore, in mammalian mitochondria Tyr phosphorylation of respiratory complexes was shown to be of great importance for the regulation of respiration (reviewed in Cesaro and Salvi, 2010). Recently, it was demonstrated that phosphorylation of Tyr193 of NDUFV2, the human homolog to the *Arabidopsis* 24 kDa subunit, is a requirement for complex I activity in T98G cells (Ogura et al., 2012). Serine and threonine phosphorylation have also been shown to be important for the regulation of complex I activity in mammalian mitochondria. The cAMP-dependent phosphorylation of NDUFS4 (18 kDa subunit), for example, enhances the import of this subunit into mitochondria in human fibroblasts. This was shown to be important for the exchange of the oxidatively damaged subunit with the *de novo* synthesized subunits in the mature complex (De Rasmo et al., 2012). Oxidatively damaged complex I subunits were also detected in mitochondria isolated from potato tubers (Møller and Kristensen, 2006), and thus it remains to be explored whether similar phosphorylation-dependent repair mechanisms do exist in plant mitochondria.

3.2.2. Thiol-related posttranslational modifications

Several subunits of complex I contain cysteine residues that may act as targets of oxidative thiol modification. Using protein extracts of different plant species, trapping experiments have identified most subunits of the peripheral arm (including the 24 kDa, 75 kDa, 30 kDa, 49 kDa, B13 and TYKY-1 subunits), as well as some of the membrane arm (including B22, PDSW-2, MNLL) as potential targets of glutaredoxins and thioredoxins (Balmer et al., 2004; Rouhier et al., 2005; Yoshida et al., 2013). This suggests that several thiols are available for redox-modification in principle. If those cysteines are also sterically available on the surface of the intact complex, if their modification can occur under *in vivo* redox conditions and what mechanistic impact that may have on complex I is currently unclear, however. Also the nature of modification remains unclear, with protein–protein disulfide formation, glutathionylation and S-nitrosation as good candidates. While mammalian complex I can be S-nitrosated as well as S-glutathionylated, analogous information is currently still lacking for plants (Dahm et al., 2006; Kang et al., 2012; Palmieri et al., 2010). S-Glutathionylation was shown to occur even under mild oxidative stress and correlated with an inactivation of complex I (Hurd et al., 2008). Only recently glutathionylation of the conserved Cys-226 of the 75 kDa subunit was identified as primary mechanism for complex I inactivation, which occurs upon depletion of reduced glutathione (Kang et al., 2012). Of particular interest for regulation of complex I activity is a cysteine in the mitochondrial encoded ND3 subunit of the complex I membrane arm, that is highly conserved in eukaryotes, including plants. This thiol (Cys-39 and Cys-45 in bovine and plant ND3, respectively) is located in a matrix loop adjacent to the peripheral arm (Galkin et al., 2008). For mammals the cysteine has been shown to be available to S-nitrosation in the inactive state of complex I only (Galkin and Moncada, 2007; Galkin et al., 2008). The active/inactive (A/D) transition is a well conserved feature of complex I in eukaryotes and provides a potential regulatory switch for complex I activity (Vinogradov, 1998). For plants a similar transition is expected, but remains to be characterized in detail (indications for two different functional states of complex I in plants indeed come from early biochemical work on matrix NADH oxidation, Møller and Palmer, 1982; Soole et al., 1990). The inactive state is favored by lack of substrate and hypoxia both *in vitro* and *in vivo* (Galkin et al., 2009). Instead of dehydrogenase activity the inactive state of complex I can mediate H^+/Na^+ exchange (Roberts and Hirst, 2012). The transition back to the active state can be triggered by re-supply of substrate or oxygen, but is inhibited by S-nitrosation of the ND3 cysteine (Galkin et al., 2009). S-Nitrosation of ND3 is of particular importance during reperfusion of ischemic tissue to prevent ROS production and damage to complex I. This thiol switching mechanism has recently been shown to operate *in vivo* were it can mediate cardioprotection (Chouchani et al., 2013). Similar principles could also help keeping complex I inactive during assembly or repair. The S-nitrosation of ND3 is fully reversible and can be removed by glutathione and thioredoxin to reactivate complex I (Chouchani et al., 2013). That makes redox modification of this critical cysteine an intriguing potential target for redox dependent regulation of complex I activity in response to changing physiological conditions. Such level of regulation is particularly interesting in plants, where the requirement for reduction of matrix NADH may vary strongly between

light and dark, and where alternative dehydrogenases need to work in concert with complex I.

3.2.3. Lysine acetylation

The reversible acetylation of lysine residues was recently shown to be of major importance for the regulation of mitochondrial functions (Masri et al., 2013), including the regulation of complex I activities in mouse mitochondria (Ahn et al., 2008). Similar to protein phosphorylation, lysine acetylation is fully reversible and regulated by the antagonistic action of lysine acetyltransferases and deacetylases. Although not much is known yet about the identity of mitochondrial acetyltransferases, lysine deacetylation in mitochondria of plants and animals is regulated by sirtuin-type proteins (reviewed in Sauve, 2010; König et al., 2014). Sirtuins (Sirt) are of great interest with regard to the regulation of metabolism as their activity is dependent on NAD^+ and usually increases during starvation. Mice with deficiency in Sirt3 showed decreased complex I activity due to increased acetylation of the complex I subunit NDUFA9 (39 kDa) (Ahn et al., 2008). Recently several additional lysine acetylation sites on complex I subunits NDUFB3 (B12), NDUFB11 (ESSS), NDUFS7 (PSST) and NDUFS8 (TYKY) were identified and showed an increase in acetylation in Sirt3-deficient mice or human cell lines (Rardin et al., 2013; Sol et al., 2012). However, the functional relevance of each individual site has not yet been investigated in detail. Lysine acetylation can also be detected by Western-blot analysis on complex I subunits in *Arabidopsis*, albeit the identity of the actual lysine acetylation sites have not been confirmed by mass spectrometry thus far (Finkemeier et al., 2011; Wu et al., 2011; I. Finkemeier and A. König, unpublished results). Hence, it remains to be determined whether lysine acetylation is also an important regulatory mechanism for complex I activity in plants.

3.3. Protein and lipid interactions of complex I

Apart from its enzymatic substrates (NADH, ubiquinone, and, (potentially) CO_2 for the CAs and CALs), complex I also interacts with other molecules such as proteins and lipids. Proteins associate with complex I either in their monomeric forms or in the form of protein complexes. Being a membrane-localized enzyme, complex I also interacts with lipids, some of which have the potential to influence its interactions with other proteins. Since data on plant complex I interactions is scarce, data from phylogenetically distant species are also presented here and discussed in terms of their validity for plants.

3.3.1. Protein interactions

Complex I is well known for its association with the dimeric cytochrome c reductase complex (complex III_2) and the resulting formation of a respiratory supercomplex in bacteria, mammals and plants (Dudkina et al., 2005; Eubel et al., 2003; Schägger, 2002). Given that plant complex III_2 also associates with the cytochrome c oxidase (complex IV, Eubel et al., 2004; Krause et al., 2004), it indirectly connects complex IV to complex I as well. Stoichiometric associations of these three complexes are referred to as respirasomes (Schägger and Pfeiffer, 2000) since, in the presence of the mobile electron carriers ubiquinone and cytochrome c, they are capable of transferring electrons from NADH all the way to molecular oxygen. Moreover, even higher organizations of respiratory complexes (including complex I) have been suggested on the basis of electron microscopy and blue-native (BN) PAGE analyses (Allen et al., 1989; Bultema et al., 2009; Wittig et al., 2006).

Upon solubilization of plant mitochondria with the non-ionic detergent digitonin, the supercomplex consisting of complexes I and III_2 (termed 'SC I/III_2' in the following) is the most prominent supercomplex on BN gels. Complex IV containing supercomplexes either are not strong enough to survive solubilization quantitatively or do not play major roles in respiratory electron transfer. In any case, the physiological benefits inherent to the interaction of complexes I and III are speculative and remain the subject of ongoing discussion. Amongst others, they include regulation of electron flow through the branched plant mitochondrial chain, reduction in the generation of reactive oxygen species (ROS) and an increased capacity of the cristae membranes to accommodate proteins (Dudkina et al., 2005, 2010). Apart from the latter, most of these processes rely heavily on substrate channeling *i.e.* the rapid sequestration of reaction products within the complex. However, true substrate channeling within pSC I/III_2 would require the presence of two separate ubiquinone pools within the inner mitochondrial membrane. The first pool would be free to accept electrons from complex I monomers, the alternative NADH dehydrogenases, complex II, and other enzymes feeding electrons into the respiratory chain. In addition, the second, independent pool of ubiquinone would be incorporated into the SC I/III_2 and only uses the electrons delivered from complex I within the supercomplex. Current data do not explicitly contradict the notion of two separate pools but evidence in favor of their existence is also lacking. The most profound argument against the existence of substrate channeling with pSC I/III_2 is the location of the ubiquinone binding site within complex I. Structural data on *T. thermophilus* complex I locate it at the end of a cavity on the far side of the contact area with complex III. In addition, the entrance of this cavity is also pointing away from the cytochrome c reductase (Baradaran et al., 2013), resulting in the longest possible diffusion path for ubiquinone within the complex. In the light of these findings, substrate channeling cannot be considered as the most likely explanation for SC I/III_2 formation. However, compared to evenly-distributed singular respiratory complexes the close proximity of complexes I and III_2 will allow for faster electron transfer due to reduced diffusion distances. Therefore, the association of complex I with other members of the respiratory chain is expected to have an impact on mitochondrial electron transfer even in the absence of true substrate channeling.

Apart from complex III_2, recent analysis of members of the Preprotein and Amino acid Transporter (PrAT) family revealed the presence of two of its members in respiratory complex I as well as in the preprotein translocase of the inner mitochondrial membrane, the TIM17/23 protein complex (Wang et al., 2012b). Overexpression of one of these proteins (TIM23-2) leads to reduced complex I abundance. By contrast, knockout mutants of complex I subunits or proteins which affect assembly of the protein complex are characterized by increased levels of TIM23-2. Interestingly, plants overexpressing TIM23-2 also phenocopy complex I knock-out plants, suggesting functional interaction between these protein complexes. It remains to be seen if this also includes physical association of the two complexes. For baker's yeast (lacking complex I) physical interactions between protein import components and respiratory protein complexes have been reported (van der Laan et al., 2006).

In addition to protein complexes and excluding assembly factors, also individual proteins were found to interact with complex I or its subunits. *In vitro* binding assays of purified pig heart complex I with matrix NAD-coupled dehydrogenases (Sumegi and Srere, 1984) suggested interactions between these enzymes but similar data on plant complex I are missing. However, using the list of complex I subunits as shown in Supp. Table 1 to query the *Arabidopsis* subcellular database (SUBA, queried 17.06.2013; Tanz et al., 2013) yielded a broad spectrum of potential complex interacting proteins. The subcellular localizations of these proteins are diverse and, after subtracting other complex I subunits, only those proteins unambiguously assigned to mitochondria are considered here.

The most prominent group among these proteins is composed of members of the prohibitin family (Atphb1, At4g28510; Atphb2, At1g03860, Atphb3, At5g40770; Atphb4, At3g27280; Atphb6, At2g20530; Atphb7, At5g44140). The reported interactions between prohibitins and complex I are inferred from 3D BN/dSDS gels (Meyer et al., 2008). Since the prohibitin complex runs close to complex I in the first dimension BN-PAGE, it is most likely that the presence of prohibitins within the complex I dSDS gel is not due to physical association of the two complexes but rather due to the presence of small amounts of the prohibitin complex during the excision of the complex

Please cite this article as: Braun, H.-P., et al., The life of plant mitochondrial complex I, Mitochondrion (2014), http://dx.doi.org/10.1016/j.mito.2014.02.006

I band from the BN-PAGE. Prohibitins therefore cannot be considered bona fide complex I interactors.

Using a yeast two-hybrid (Y2H) approach, the majority (five) of the remaining six proteins was found to interact with the γ-type carbonic anhydrase 3 (At5g66510) while a single protein interacts with a member of the LYR family of Fe/S cluster biogenesis protein (At4g34700, *Arabidopsis* Interactome Mapping Consortium, 2011). This group of complex I interacting proteins spans a wide functional range and includes a 2Fe–2S ferredoxin (At3g07480), a protein involved in the assembly of iron–sulfur clusters destined to remain in mitochondria or to be exported to the cytosol (Nfu4, At3g20970, Leon et al., 2003), a small heat-shock protein (At4g25200), a co-chaperone (At5g55200) as well as a putative thiol-disulfide oxidoreductase (At5g50100) and a tetratricopeptide repeat protein (At5g09450). However, the high percentage of non-mitochondrial interactors found by the Y2H approach implies the presence of a considerable percentage of false positively identified proteins among the data set of putative complex I interacting proteins. It is also worth mentioning that these data do not allow discrimination between interactions with individual or interfaces of complex I as a whole. Their physical connection with complex I function therefore remains unclear. Interestingly, no complex III subunits are among the potential interactors although the interaction between the two complexes is stable enough to withstand solubilization and electrophoresis. Several reasons for the lack of those established interactions seem feasible. First, complex I and complex III subunits are part of large (0.5–1.0 MDa) complexes and for the majority of the theoretically calculable interactions between the subunits of the complexes distances between the two complexes may simply be too long in order to trigger a response. Moreover, large reporter groups on subunits may prevent their integration into the complexes, which would prevent a signal even if those subunits sit in close proximity within the supercomplex. However, such a scenario would also prevent signals from associations of subunits within the same complex, which have clearly been picked up by the approach. An additional reason for the lack of complex I/complex III interactions with the Y2H method might be due to the presence of other molecules within the supercomplex structure preventing immediate contact of the subunits of one complex with those of the other. Such molecules may, for example, be lipids.

3.3.2. Lipid interactions

Mitochondrial protein complexes not only depend on the provision of protein subunits for proper function but also require the presence of phospholipids (Fleischer et al., 1962). Most of these lipids are easily detachable following treatment with organic solvents or detergents and have no or little influence on the activity of the enzymes. By contrast, the dimeric phospholipid cardiolipin (CL) behaves differently in requiring more stringent conditions for its removal from mitochondrial protein complexes. Within mammalian cells appreciable amounts of CL are only present in the mitochondrial membrane systems, with the bulk of it located in the inner membrane (Gebert et al., 2009). While in most cases CL is not essential for the function of mitochondrial protein complexes, their respective performances are markedly increased in the presence of CL (for a review on cardiolipin interaction with mitochondrial proteins and protein complexes see Schlame et al., 2000). For complex I isolated from beef heart mitochondria Fry and Green (1981) demonstrated that it contains tightly bound CL and that its removal from the complex is accompanied by a loss of function. No interaction of cardiolipin with plant complex I has yet been reported. However, plants are capable of synthesizing CL and the last enzyme in the pathway of its synthesis, CL synthase, is located in the mitochondria of plants (Katayama et al., 2004). From this and the data on mammalian complex I it may be predicted that CL is also part of plant respiratory chain complexes, including complex I.

Apart from being an integral part of individual inner membrane protein complexes, cardiolipin also promotes formation of respiratory supercomplexes. While the integrity of respiratory complexes II, III, and IV (baker's yeast does not possess complex I) in cardiolipin deficient yeast remains unchanged, the abundances of complex III and complex IV containing supercomplexes is reduced (Zhang et al., 2005). Disturbances in acyl chain remodeling of CL in Barth syndrome patients mainly affect complex III: IV interactions but, to a lesser extent, also those between complexes I and III (McKenzie et al., 2006). Cardiolipin is therefore either involved in the formation of such supercomplexes or in maintaining their stability. In either case, as a result, the respiratory capacity of CL deficient mitochondria is markedly reduced. Similar to the role of cardiolipin in individual mitochondrial complexes, little is known about the utilization of cardiolipin for plant mitochondrial supercomplexes. The common ancestral origin and the elementary similarities between the plant, yeast and mammalian respiratory chain strongly suggest that CL is likely to also have an impact on the respiratory supercomplexes in plants. *Arabidopsis* knock-out mutant lines for CL synthase are now available and recently gave first insights into the role of CL in plant respiratory electron transport (Katayama and Wada, 2012; Pineau et al., 2013).

3.4. ROS formation at complex I

Complex I is a major contributor toward mitochondrial ROS production. This assumption is largely based on results from isolated mammalian mitochondria and has been extrapolated to plants. While this leap appears justified based on overall conservation of complex I structure and function, it exemplifies a more general shortage of rigorous ROS measurements in plant mitochondria. Due to the specialized role of complex I in respect to photosynthesis plant specific modes of mitochondrial ROS generation remain a possibility and deserve specific research attention.

In mammalian mitochondria the NADH binding site within the 51 kDa subunit of complex I can generate superoxide by a single electron reduction step from reduced flavin mononucleotide (FMN) to molecular oxygen. That site is structurally and functionally conserved between mammals and plants, which implies similar properties in superoxide production. Oxygen reduction by single electron transfer is thermodynamically and kinetically possible due first to a steric accessibility of FMN for oxygen and secondly to a highly negative redox potential of the FMN redox couple. While the first possibility follows from the requirement of the site to accommodate NADH as substrate, the second depends on the bioenergetic situation and there are two extreme scenarios under which high rates of superoxide generation can occur (reviewed by Murphy, 2009). On the one hand, a high NADH/NAD^+ ratio in the matrix leads to overreduction, an extended lifetime and a more negative redox potential of the reduced FMN site. Inhibition of the electron transport chain can contribute to this mode, by causing electrons to back up. On the other hand, when a highly reduced ubiquinone pool (due to sources of electrons other than NADH) coincides with a high proton motive force, superoxide can be produced at complex I by 'reverse electron transport' (Lambert and Brand, 2004). Under such conditions superoxide production is more sensitive to the pH gradient across the inner mitochondrial membrane than to the membrane potential. This observation suggests an intimate connection with the proton pumping mechanism of complex I and hints at a contribution of the Q-site to superoxide production (Murphy, 2009). It is not clear if reverse electron transport can occur *in vivo*, and for plant tissues expressing alternative oxidase such a situation may be particularly unlikely, as the ubiquinone pool may be effectively oxidized before the critical threshold of ubiquinone reduction is reached. The total rate of superoxide production increases with the number of contributing complexes, *i.e.* complex I abundance, and the regulation thereof on the different levels described above. Mutant plants that lack complex I are therefore in principal expected to produce less superoxide in their mitochondria. Measurements of ROS and redox indicators in several different complex I mutants have suggested unchanged or even increased oxidative loads on the tissue level (Dutilleul et al., 2003a;

Please cite this article as: Braun, H.-P., et al., The life of plant mitochondrial complex I, Mitochondrion (2014), http://dx.doi.org/10.1016/j.mito.2014.02.006

He et al., 2012; Koprivova et al., 2010; Lee et al., 2002; Liu et al., 2010; Meyer et al., 2009). Those results may suggest increased rates of superoxide generation by other electron transfer chain complexes (such as complex III) due to the imbalance in electron flow in the absence of complex I. More importantly it is unclear, however, to which extent those data can be validly interpreted with respect to mitochondrial superoxide production due to very limited chemical or subcellular specificity of the employed methods. In principle complex I mediated superoxide production could increase dramatically, if fragments of the peripheral arm accumulate in a mutant and redox active sites that are normally embedded inside the complex are exposed. While partially assembled complex I fragments of the membrane arm have been detected in several mutants, none of the redox-active peripheral arm have been found thus far (Meyer et al., 2011). This could indicate that such a fragment has detrimental effects on plant viability and excessive ROS generation may contribute to lethality.

Superoxide generated at the FMN site of complex I will be released into the matrix and is unlikely to pass the inner membrane due to its negative charge at the alkaline pH of the matrix. In the matrix superoxide can undergo different fates: dismutation to H_2O_2 and O_2, either spontaneously or catalyzed by Mn-superoxide dismutase, reaction with other radicals such as NO (to give rise to $ONOO^-$) or transition metal compounds, such as Fe–S clusters. By contrast, superoxide itself is not particularly reactive with proteins or DNA. Its mutagenic potential can therefore largely be ascribed to its downstream products. Other mitochondrial sites of superoxide generation include complex III, which can be a particularly stimulated by inhibition with antimycin A. Although that mode has been exploited extensively as model for mitochondrial ROS production, it is unclear to which extent complex III contributes to mitochondrial superoxide generation *in vivo*. Thus on the basis of the current, albeit sketchy picture, complex I is likely to be the main producer of matrix ROS *in vivo* under a wide range of conditions. The potential of complex I derived ROS to mediate transcriptional reprogramming has been assessed in plants using the inhibitor rotenone as well as genetic mutants (Dutilleul et al., 2003a; Garmier et al., 2008; Meyer et al., 2009; Schwarzländer et al., 2012). To separate out ROS-specific effects from other physiological changes remains a major challenge, however, one which has not yet been overcome. Combining the available resources of genetic complex I lines with novel *in vivo* ROS sensing techniques (Cocheme et al., 2011; Gutscher et al., 2009) and the structural models of complex I architecture (Baradaran et al., 2013; Klodmann et al., 2010) now provides the unique opportunity to dissect both the mechanisms and the physiological significance of ROS production by complex I in plants.

4. Turnover, dis-assembly and degradation of complex I ("old age and death")

Relatively little information is available on the degradation of complex I. It is clear that oxidoreductases such as complex I can get damaged easily due to the presence of reactive oxygen and nitrogen species or other reactive compounds which can arise during cellular respiration and further biochemical functions in the mitochondria. This raises the question if the entire complex I is degraded in case of damage of a single subunit, or if individual subunits can be replaced by functionally intact copies. Both mechanisms are known to occur in other protein complexes. Recent experiments using tagged complex I subunits have indicated that many but not all complex I subunits can be inserted into pre-existing complex I particles in human cell lines (Dieteren et al., 2012). However, for more extensively damaged complex I particles a complete degradation pathway is likely to exist. Based on isotope labeling experiments the half-life of OXPHOS complexes in plants is estimated to lie in the range of several days (Li et al., 2012; Nelson et al., 2013). Large protease complexes of the AAA family are known to specifically degrade protein complexes of the inner mitochondrial membrane. Complete protein degradation in mitochondria subsequently involves a set of different organelle-specific proteases including ATP-dependent proteases, processing peptidases, and oligopeptidases (for a recent review see Kwasniak et al., 2012). Since complex I is 1 MDa in molecular mass, its complete degradation substantially affects the amino acid pool sizes of the mitochondria (the currently known 49 subunits of *Arabidopsis* complex I sum up to about 9500 amino acids/complex I particle). The degradation products of a complex I that has been taken out of service thus replenish the amino acid pools that are required for a new life cycle of complex I to begin.

5. Outlook

Complex I of plants is of central importance for oxidative phosphorylation, is indirectly involved in both photorespiration and photosynthesis and includes additional auxiliary activities not directly related to energy metabolism. Its biogenesis is exceptionally complicated and sophisticated in plants (Fig. 5). Mitochondrial phage-type polymerases are the first players to generate primary transcripts. Several nuclear encoded factors are required to remove numerous introns, including maturases which are partially encoded by the introns themselves. Nearly 200 nucleotide sites have to be edited which requires several additional factors, many of which belong to the large group of PPR proteins. Why is the generation of mature transcripts so amazingly complex in mitochondria of plants? Does this offer additional levels of regulation in assembly of plant complex I? Next, subunits of complex I are synthesized in two different cellular compartments, the mitochondria and the cytosol. Transport of polypeptides from the cytosol is particularly difficult in plants because strict discrimination between mitochondrial and chloroplastic import has to occur for all nuclear encoded complex I constituents. Finally, complex I assembly follows unique routes in plants and, at an early stage, requires carbonic anhydrase-related proteins which even form part of the holo-enzyme and contribute to its unique shape: an L-shaped particle with an additional central element (finally looking like a "lying F-shaped particle"). What is the significance of a protein of the ascorbate biosynthesis pathway to contribute to complex I assembly in plants? Complex I appears to act as a true multi-functional platform hosting and integrating a multitude of physiological processes of the plant cell.

Despite considerable efforts in research, many aspects of the biology of plant complex I are far from being understood. A broad and integrative research approach will be required if we are to tackle the most intriguing questions, some of which are outlined in the following paragraphs:

5.1. In vivo role of plant complex I

Future exploration of the versatility of complex I will be aided by the technical development of *in vivo* sensing techniques in mitochondria. Given its role as central hub of mitochondrial physiology, complex I regulation is likely to have direct impact on mitochondrial homeostasis. Redox state of the matrix NAD-pool, the proton motive force or ROS production depend directly on complex I characteristics, but also ATP/ADP ratio or redox status of the glutathione and ascorbate pools in the matrix are closely linked with complex I properties.

Matrix physiology can be expected to react particularly sensitively to changes in complex I characteristics, due to its relatively small volume as compared to the cytosol and its direct interaction with the complex. It is therefore of particular interest to measure changes in matrix physiology separately from those in other subcellular compartments. Current developments in quantitative imaging and a careful application of genetically-encoded fluorescent protein sensors will allow dissecting changes in physiology with subcellular resolution. Recently, fluorescent protein sensors for several key parameters of mitochondrial physiology have become available, covering ATP, NAD^+, H_2O_2, pH, calcium, and glutathione levels, some of which have already been adopted for measurements *in planta* (see recent summary by Gjetting et al., 2013).

Please cite this article as: Braun, H.-P., et al., The life of plant mitochondrial complex I, Mitochondrion (2014), http://dx.doi.org/10.1016/j.mito.2014.02.006

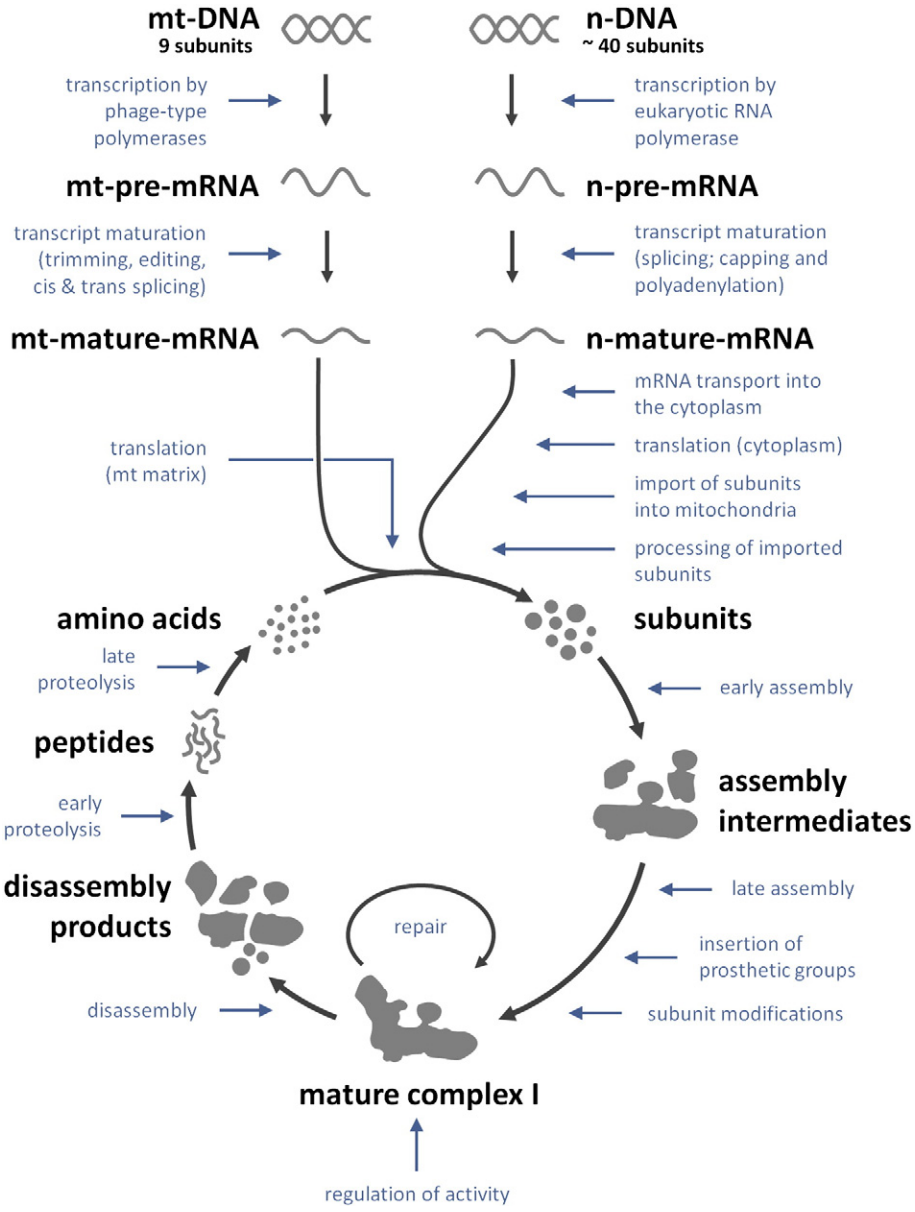

Fig. 5. Life cycle of mitochondrial complex I in plants. mt: mitochondrial, n: nuclear.

Applying such *in vivo* sensing techniques to the spectra of available complex I mutants holds the potential to resolve the exact place of complex I in the physiological network of plant mitochondria. While major consequences on whole cell physiology have been documented in mutants with severely reduced complex I abundance (Dutilleul et al., 2003a; Meyer et al., 2009), mitochondria-specific *in vivo* sensing techniques will allow measuring milder, yet physiologically meaningful, alterations, that would otherwise be obscured by effects from other parts of the cell. Being able to measure physiological parameters specifically and dynamically in the living cell and with subcellular resolution holds the opportunity to eventually unravel the exact functional impact that complex I regulation has *in vivo* (such as reversible supercomplex formation) on mitochondrial and cellular physiology.

5.2. Complex I as a site for metabolic channeling

Complex I in mammals binds several mitochondrial NAD-coupled dehydrogenase complexes including pyruvate dehydrogenase, α-ketoglutarate dehydrogenase, the mitochondrial malate dehydrogenase (mMDH) and β-hydroxyacyl-CoA dehydrogenase (Sumegi and Srere, 1984). It has been proven that in the complex I–mMDH complex the NADH which is produced by mMDH is channeled to the binding site of complex I thereby avoiding diffusion *via* the bulk phase (Fukushima et al., 1989). Such channeling not only ensures an efficient traffic of NADH to the electron transport chain but additionally prevents both the consumption of NADH by competing enzymes and the inhibition of enzymes, for example the TCA cycle, by NADH. Intriguingly, the complex I–mMDH interaction of mammals is abolished by the addition of NADH *in vitro* (Fukushima et al., 1989) suggesting the possibility of regulating NADH metabolism by the transient binding of mMDH to complex I. To date studies on the association/disassociation of proteins to complexes of the mitochondrial electron transport chain in plants have largely been restricted to the interaction with L-galactono-1, 4-lactone dehydrogenase (GLDH, Pineau et al., 2008) and the formation of supercomplexes (Eubel et al., 2004). As described above, the interaction with GLDH had variously been reported to occur (Hervás et al., 2013; Schertl et al., 2012). By contrast, consensus has been reached regarding supercomplex formation in plants with several possible composition stoichiometries present and reports suggesting that these are responsive to environmental conditions (Ramírez-Aguilar et al., 2011).

Please cite this article as: Braun, H.-P., et al., The life of plant mitochondrial complex I, Mitochondrion (2014), http://dx.doi.org/10.1016/j.mito.2014.02.006

In addition, results of a recent study using BN/SDS-PAGE suggest that several mitochondrial enzymes including NAD^+-dependent malic enzyme and monodehydroascorbate reductase preferentially associate/disassociate to protein complexes under oxidative stress (Obata et al., 2011). Furthermore, clear evidence has been provided that the majority of NADH in plant mitochondria is bound to proteins (Kasimova et al., 2006). One possible explanation for this could potentially be the result of NADH channeling between complex I and mitochondrial dehydrogenases or even between different mitochondrial dehydrogenases. Indirect evidence for this hypothesis comes from complex I activity measurements in isolated mitochondria/inside out vesicles of submitochondrial particles in the presence of the channel-forming antibiotic alamethicin (Johansson et al., 2004). It seems likely that application of currently used experimental techniques such as co-purification and BN PAGE (used recently in characterizing the plant glycolytic metabolome; Giegé et al., 2003; Graham et al., 2007) in addition to newly emerging techniques such as bimolecular complementation assays and structural prediction of protein binding surfaces as well as ever increasing spatial resolution of metabolic studies (Aharoni and Brandizzi, 2012; Steinhauser et al., 2012; Zhang et al., 2012) will prove highly informative in detecting protein association and metabolite channeling in and around complex I in plants.

From our perspective, complex I lends itself as a highly suitable model system to study various molecular aspects of the plant cell: the maintenance of organelle homeostasis and the channeling of metabolites as outlined above, the interplay of respiration, photorespiration and photosynthesis and the coordination of protein biosynthesis machineries in the nuclear and the mitochondrial compartment.

Acknowledgments

This article summarizes contributions related to plant mitochondrial complex I presented at the 8th International Conference on Plant Mitochondrial Biology (ICPMB) which was held from May 12 to 16, 2013 in Rosario, Argentina. The authors wish to thank the organizing committee for arranging a wonderful conference. Furthermore, the authors thank the Center for Advanced Studies (CAS) of the Ludwig-Maximilians-University Munich for supporting the Symposium "The life of plant mitochondrial complex I" held in Munich on November 4/5, 2013. We thank Christine Schikowsky, Leibniz University Hannover/Germany, for the artwork of the article. Our research is supported by the Deutsche Forschungsgemeinschaft (grants BR1829-10/2 [HPB], BR326-11/1 [AB], FE552-9/2 [ARF], IF1655-1/1 [IF], SCHW 1719-1/1 [MS], TA624-2/2 [MT] and TA624-4/1 [MT]).

Appendix A. Supplementary data

Supplementary data to this article can be found online at http://dx.doi.org/10.1016/j.mito.2014.02.006.

References

Abu-Abied, M., Avisar, D., Belausov, E., Holdengreber, V., Kam, Z., Sadot, E., 2009. Identification of an *Arabidopsis* unknown small membrane protein targeted to mitochondria, chloroplasts, and peroxisomes. Protoplasma 236, 3–12.

Aharoni, A., Brandizzi, F., 2012. High resolution methods in plant biology. Plant J. 70, 1–4.

Ahn, B.H., Kim, H.S., Song, S., Lee, I.H., Liu, J., Vassilopoulos, A., Deng, C.X., Finkel, T., 2008. A role for the mitochondrial deacetylase Sirt3 in regulating energy homeostasis. Proc. Natl. Acad. Sci. U. S. A. 105, 14447–14452.

Allen, R.D., Schroeder, A.K., Fok, A.K., 1989. An investigation of mitochondrial inner membranes by rapid-freeze deep-etch techniques. J. Cell Biol. 108, 2233–2240.

Angerer, H., Zwicker, K., Wumaier, Z., Sokolova, L., Heide, H., Steger, M., Kaiser, S., Nübel, E., Brutschy, B., Radermacher, M., Brandt, U., Zickermann, V., 2011. A scaffold of accessory subunits links the peripheral arm and the distal proton-pumping module of mitochondrial complex I. Biochem. J. 437, 279–288.

Antonicka, H., Ogilvie, I., Taivassalo, T., Anitori, R.P., Haller, R.G., Vissing, J., Kennaway, N.G., Shoubridge, E.A., 2003. Identification and characterization of a common set of complex I assembly intermediates in mitochondria from patients with complex I deficiency. J. Biol. Chem. 278, 43081–43088.

Arabidopsis Interactome Mapping Consortium, 2011. Evidence for network evolution in an *Arabidopsis* interactome map. Science 333, 601–607.

Balmer, Y., Vensel, W.H., Tanaka, C.K., Hurkman, W.J., Gelhaye, E., Rouhier, N., Jacquot, J.P., Manieri, W., Schurmann, P., Droux, M., Buchanan, B.B., 2004. Thioredoxin links redox to the regulation of fundamental processes of plant mitochondria. Proc. Natl. Acad. Sci. U. S. A. 101, 2642–2647.

Balsa, E., Marco, R., Perales-Clemente, E., Szklarczyk, R., Calvo, E., Landazuri, M.O., Enriquez, J.A., 2012. NDUFA4 is a subunit of complex IV of the mammalian electron transport chain. Cell Metab. 16, 378–386.

Baradaran, R., Berrisford, J.M., Minhas, G.S., Sazanov, L.A., 2013. Crystal structure of the entire respiratory complex I. Nature 494, 443–448.

Binder, S., Marchfelder, A., Brennicke, A., Wissinger, B., 1992. RNA editing in intron sequences may be required for trans-splicing of nad2 transcripts in *Oenothera* mitochondria. J. Biol. Chem. 267, 7615–7623.

Bonen, L., 2008. Cis- and trans-splicing of group II introns in plant mitochondria. Mitochondrion 8, 26–34.

Börner, G.V., Mörl, M., Wissinger, B., Brennicke, A., Schmelzer, C., 1995. RNA editing of a group II intron in *Oenothera* as a prerequisite for splicing. Mol. Gen. Genet. 246, 739–744.

Brandt, U., 2006. Energy converting NADH:quinone oxidoreductase (complex I). Annu. Rev. Biochem. 75, 69–92.

Brandt, U., 2013. Inside view of a giant proton pump. Angew. Chem. Int. Ed. Engl. 52, 7358–7360.

Brangeon, J., Sabar, M., Gutierres, S., Combettes, B., Bove, J., Gendy, C., Chetrit, P., Des Francs-Small, C.C., Pla, M., Vedel, F., De Paepe, R., 2000. Defective splicing of the first nad4 intron is associated with lack of several complex I subunits in the *Nicotiana sylvestris* NMS1 nuclear mutant. Plant J. 21, 269–280.

Braun, H.P., Zabaleta, E., 2007. Carbonic anhydrase subunits of the mitochondrial NADH dehydrogenase complex (complex I) in plants. Physiol. Plant. 129, 114–122.

Brennicke, A., Zabaleta, E., Dombrowski, S., Hoffmann, M., Binder, S., 1999. Transcription signals of mitochondrial and nuclear genes for mitochondrial proteins in dicot plants. J. Hered. 90, 345–350.

Bultema, J., Braun, H.P., Boekema, E., Kouril, R., 2009. Megacomplex organization of the oxidative phosphorylation system by structural analysis of respiratory supercomplexes from potato. Biochim. Biophys. Acta 1787, 60–67.

Bykova, N.V., Egsgaard, H., Møller, I.M., 2003. Identification of 14 new phosphoproteins involved in important plant mitochondrial processes. FEBS Lett. 540, 141–146.

Cardol, P., 2011. Mitochondrial NADH:ubiquinone oxidoreductase (complex I) in eukaryotes: a highly conserved subunit composition highlighted by mining of protein databases. Biochim. Biophys. Acta 1807, 1390–1397.

Cardol, P., Vanrobaeys, F., Devreese, B., Van Beeumen, J., Matagne, R.F., Remacle, C., 2004. Higher plant-like subunit composition of mitochondrial complex I from *Chlamydomonas reinhardtii*: 31 conserved components among eukaryotes. Biochim. Biophys. Acta 1658, 212–224.

Carrie, C., Giraud, E., Duncan, O., Xu, L., Wang, Y., Huang, S., Clifton, R., Murcha, M., Filipovska, A., Rackham, O., Vrielink, A., Whelan, J., 2010. Conserved and novel functions for *Arabidopsis thaliana* MIA40 in assembly of proteins in mitochondria and peroxisomes. J. Biol. Chem. 285, 36138–36148.

Carroll, J., Fearnley, I.M., Skehel, J.M., Shannon, R.J., Hirst, J., Walker, J.E., 2006. Bovine complex I is a complex of 45 different subunits. J. Biol. Chem. 281, 32724–32727.

Cesaro, L., Salvi, M., 2010. Mitochondrial tyrosine phosphoproteome: new insights from an up-to-date analysis. Biofactors 36, 437–450.

Chapdelaine, Y., Bonen, L., 1991. The wheat mitochondrial gene for subunit I of the NADH dehydrogenase complex: a trans-splicing model for this gene-in-pieces. Cell 65, 465–472.

Choi, B., Acero, M.M., Bonen, L., 2012. Mapping of wheat mitochondrial mRNA termini and comparison with breakpoints in DNA homology among plants. Plant Mol. Biol. 80, 539–552.

Chouchani, E.T., Methner, C., Nadtochiy, S.M., Logan, A., Pell, V.R., Ding, S., James, A.M., Cochemé, H.M., Reinhold, J., Lilley, K.S., Partridge, L., Fearnley, I.M., Robinson, A.J., Hartley, R.C., Smith, R.A., Krieg, T., Brookes, P.S., Murphy, M.P., 2013. Cardioprotection by S-nitrosation of a cysteine switch on mitochondrial complex I. Nat. Med. 19, 753–759.

Cocheme, H.M., Quin, C., McQuaker, S.J., Cabreiro, F., Logan, A., Prime, T.A., Abakumova, I., Patel, J.V., Fearnley, I.M., James, A.M., Porteous, C.M., Smith, R.A., Saeed, S., Carre, J.E., Singer, M., Gems, D., Hartley, R.C., Partridge, L., Murphy, M.P., 2011. Measurement of H_2O_2 within living *Drosophila* during aging using a ratiometric mass spectrometry probe targeted to the mitochondrial matrix. Cell Metab. 13, 340–350.

Dahm, C.C., Moore, K., Murphy, M.P., 2006. Persistent S-nitrosation of complex I and other mitochondrial membrane proteins by S-nitrosothiols but not nitric oxide or peroxynitrite: implications for the interaction of nitric oxide with mitochondria. J. Biol. Chem. 281, 10056–10065.

De Longevialle, A.F., Meyer, E.H., Andres, C., Taylor, N.L., Lurin, C., Millar, A.H., Small, I.D., 2007. The pentatricopeptide repeat gene OTP43 is required for trans-splicing of the mitochondrial nad1 intron 1 in *Arabidopsis thaliana*. Plant Cell 19, 3256–3265.

De Rasmo, D., Signorile, A., Larizza, M., Pacelli, C., Cocco, T., Papa, S., 2012. Activation of the cAMP cascade in human fibroblast cultures rescues the activity of oxidatively damaged complex I. Free Radic. Biol. Med. 52, 757–764.

Dieteren, C.E., Koopman, W.J., Swarts, H.G., Peters, J.G., Maczuga, P., van Gemst, J.J., Masereeuw, R., Smeitink, J.A., Nijtmans, L.G., Willems, P.H., 2012. Subunit-specific incorporation efficiency and kinetics in mitochondrial complex I homeostasis. J. Biol. Chem. 287, 41851–41860.

Dombrowski, S., Hoffmann, M., Guha, C., Binder, S., 1999. Continuous primary sequence requirements in the 18-nucleotide promoter of dicot plant mitochondria. J. Biol. Chem. 274, 10094–10099.

Please cite this article as: Braun, H.-P., et al., The life of plant mitochondrial complex I, Mitochondrion (2014), http://dx.doi.org/10.1016/j.mito.2014.02.006

Dudkina, N.V., Eubel, H., Keegstra, W., Boekema, E.J., Braun, H.P., 2005. Structure of a mitochondrial supercomplex formed by respiratory-chain complexes I and III. Proc. Natl. Acad. Sci. U. S. A. 102, 3225–3229.

Dudkina, N.V., Kouril, R., Peters, K., Braun, H.P., Boekema, E.J., 2010. Structure and function of mitochondrial supercomplexes. Biochim. Biophys. Acta 1797, 664–670.

Dutilleul, C., Garmier, M., Noctor, G., Mathieu, C., Chetrit, P., Foyer, C.H., de Paepe, R., 2003a. Leaf mitochondria modulate whole cell redox homeostasis, set antioxidant capacity, and determine stress resistance through altered signaling and diurnal regulation. Plant Cell 15, 1212–1226.

Dutilleul, C., Driscoll, S., Cornic, G., De Paepe, R., Foyer, C.H., Noctor, G., 2003b. Functional mitochondrial complex I is required by tobacco leaves for optimal photosynthetic performance in photorespiratory conditions and during transients. Plant Physiol. 131, 264–275.

Emanuelsson, O., Nielsen, H., Brunak, S., von Heijne, G., 2000. Predicting subcellular localization of proteins based on their N-terminal amino acid sequence. J. Mol. Biol. 300, 1005–1016.

Engelsberger, W.R., Schulze, W.X., 2012. Nitrate and ammonium lead to distinct global dynamic phosphorylation patterns when resupplied to nitrogen-starved *Arabidopsis* seedlings. Plant J. 69, 978–995.

Eubel, H., Jänsch, L., Braun, H.P., 2003. New insights into the respiratory chain of plant mitochondria. Supercomplexes and a unique composition of complex II. Plant Physiol. 133, 274–286.

Eubel, H., Heinemeyer, J., Braun, H.P., 2004. Identification and characterization of respirasomes in potato mitochondria. Plant Physiol. 134, 1450–1459.

Farré, J.C., Aknin, C., Araya, A., Castandet, B., 2012. RNA editing in mitochondrial trans-introns is required for splicing. PLoS One 7, e52644.

Fey, J., Marechal-Drouard, L., 1999. Compilation and analysis of plant mitochondrial promoter sequences: an illustration of a divergent evolution between monocot and dicot mitochondria. Biochem. Biophys. Res. Commun. 256, 409–414.

Finkemeier, I., Laxa, M., Miguet, L., Howden, A.J., Sweetlove, L.J., 2011. Proteins of diverse function and subcellular location are lysine acetylated in *Arabidopsis*. Plant Physiol. 155, 1779–1790.

Fleischer, S., Brierley, G., Klouwen, H., Slautterback, D.G., 1962. The role of phospholipids in electron transfer. J. Biol. Chem. 237, 3264–3272.

Forner, J., Weber, B., Thuss, S., Wildum, S., Binder, S., 2007. Mapping of mitochondrial mRNA termini in *Arabidopsis thaliana*: t-elements contribute to 5′ and 3′ end formation. Nucleic Acids Res. 35, 3676–3692.

Fry, M., Green, D.E., 1981. Cardiolipin requirement for electron transfer in complex I and III of the mitochondrial respiratory chain. J. Biol. Chem. 246, 1874–1880.

Fukushima, T., Decker, R.V., Anderson, W.M., Spivey, H.O., 1989. Substrate channeling of NADH in mitochondrial redox processes. J. Biol. Chem. 264, 16483–16488.

Galkin, A., Moncada, S., 2007. S-nitrosation of mitochondrial complex I depends on its structural conformation. J. Biol. Chem. 282, 37448–37453.

Galkin, A., Meyer, B., Wittig, I., Karas, M., Schägger, H., Vinogradov, A., Brandt, U., 2008. Identification of the mitochondrial ND3 subunit as a structural component involved in the active/deactive enzyme transition of respiratory complex I. J. Biol. Chem. 283, 20907–20913.

Galkin, A., Abramov, A.Y., Frakich, N., Duchen, M.R., Moncada, S., 2009. Lack of oxygen deactivates mitochondrial complex I: implications for ischemic injury? J. Biol. Chem. 284, 36055–36061.

Garmier, M., Carroll, A.J., Delannoy, E., Vallet, C., Day, D.A., Small, I.D., Millar, A.H., 2008. Complex I dysfunction redirects cellular and mitochondrial metabolism in *Arabidopsis*. Plant Physiol. 148, 1324–1341.

Gawryluk, R.M., Gray, M.W., 2010. Evidence for an early evolutionary emergence of gamma-type carbonic anhydrases as components of mitochondrial respiratory complex I. BMC Evol. Biol. 10, 176.

Gebert, N., Joshi, A.S., Kutik, S., Becker, T., McKenzie, M., Guan, X.L., Mooga, V.P., Stroud, D.A., Kulkarni, G., Wenk, M.R., Rehling, P., Meisinger, C., Ryan, M.T., Wiedemann, N., Greenberg, M.L., Pfanner, N., 2009. Mitochondrial cardiolipin involved in outer-membrane protein biogenesis: implications for Barth syndrome. Curr. Biol. 19, 2133–2139.

Giegé, P., Hoffmann, M., Binder, S., Brennicke, A., 2000. RNA degradation buffers asymmetries of transcription in *Arabidopsis* mitochondria. EMBO Rep. 1, 164–170.

Giegé, P., Heazlewood, J.L., Roessner-Tunali, U., Millar, H., Fernie, A.R., Leaver, C.J., Sweetlove, L.J., 2003. Enzymes of glycolysis are functionally associated with the mitochondrion in *Arabidopsis* cells. Plant Cell 15, 2140–2151.

Giraud, E., Ng, S., Carrie, C., Duncan, O., Low, J., Lee, C.P., Van Aken, O., Millar, A.H., Murcha, M., Whelan, J., 2010. TCP transcription factors link the regulation of genes encoding mitochondrial proteins with the circadian clock in *Arabidopsis thaliana*. Plant Cell 22, 3921–3934.

Gjetting, S.K., Schulz, A., Fuglsang, A.T., 2013. Perspectives for using genetically encoded fluorescent biosensors in plants. Front. Plant Sci. 4, 234.

Graham, J.W.A., Williams, T.C.R., Morgan, M., Fernie, A.R., Ratcliffe, G., Sweetlove, L.J., 2007. Glycolytic enzymes associate dynamically with mitochondria in response to respiratory demand and support substrate channeling. Plant Cell 19, 3723–3738.

Gray, M.W., 2012. Mitochondrial evolution. Cold Spring Harb. Perspect. Biol. 4, a011403.

Grigorieff, N., 1998. Three-dimensional structure of bovine NADH:ubiquinone oxidoreductase (complex I) at 22 Å in ice. J. Mol. Biol. 277, 1033–1046.

Guénebaut, V., Vincentelli, R., Mills, D., Weiss, H., Leonard, K.R., 1997. Three-dimensional structure of NADH-dehydrogenase from *Neurospora crassa* by electron microscopy and conical tilt reconstruction. J. Mol. Biol. 265, 409–418.

Gutscher, M., Sobotta, M.C., Wabnitz, G.H., Ballikaya, S., Meyer, A.J., Samstag, Y., Dick, T.P., 2009. Proximity-based protein thiol oxidation by H_2O_2-scavenging peroxidases. J. Biol. Chem. 284, 31532–31540.

Hager, J., Pellny, T.K., Mauve, C., Lelarge-Trouverie, C., De Paepe, R., Foyer, C.H., Noctor, G., 2010. Conditional modulation of NAD levels and metabolite profiles in *Nicotiana sylvestris* by mitochondrial electron transport and carbon/nitrogen supply. Planta 231, 1145–1157.

Haili, N., Arnal, N., Quadrado, M., Amiar, S., Tcherkez, G., Dahan, J., Briozzo, P., Colas des Francs-Small, C., Vrielynck, N., Mireau, H., 2013. The pentatricopeptide repeat MTSF1 protein stabilizes the nad4 mRNA in *Arabidopsis* mitochondria. Nucleic Acids Res. 41, 6650–6663.

Håkansson, G., Allen, J.F., 1995. Histidine and tyrosine phosphorylation in pea mitochondria: evidence for protein phosphorylation in respiratory redox signaling. FEBS Lett. 372, 238–242.

Hartl, M., Finkemeier, I., 2012. Plant mitochondrial retrograde signaling: post-translational modifications enter the stage. Front. Plant Sci. 3, 253.

Hatefi, Y., Haavik, A.G., Griffiths, D.E., 1962. Studies on the electron transfer system XL: preparation and properties of mitochondrial DPNH-coenzyme Q reductase. J. Biol. Chem. 237, 1676–1680.

Hatefi, Y., 1985. The mitochondrial electron transport and oxidative phosphorylation system. Ann. Rev. Biochem. 54, 1015–1069.

Hauler, A., Jonietz, C., Stoll, B., Stoll, K., Braun, H.P., Binder, S., 2013. RNA PROCESSING FACTOR 5 is required for efficient 5′ cleavage at a processing site conserved in RNAs of three different mitochondrial genes in *Arabidopsis thaliana*. Plant J. 74, 593–604.

He, J., Duan, Y., Hua, D., Fan, G., Wang, L., Liu, Y., Chen, Z., Han, L., Qu, L.J., Gong, Z., 2012. DEXH box RNA helicase-mediated mitochondrial reactive oxygen species production in *Arabidopsis* mediates crosstalk between abscisic acid and auxin signaling. Plant Cell 24, 1815–1833.

Heazlewood, J.L., Howell, K.A., Millar, A.H., 2003. Mitochondrial complex I from *Arabidopsis* and rice: orthologs of mammalian and fungal components coupled with plant-specific subunits. Biochim. Biophys. Acta 1604, 159–169.

Heazlewood, J.L., Tonti-Filippini, J.S., Gout, A.M., Day, D.A., Whelan, J., Millar, A.H., 2004. Experimental analysis of the *Arabidopsis* mitochondrial proteome highlights signaling and regulatory components, provides assessment of targeting prediction programs, and indicates plant-specific mitochondrial proteins. Plant Cell 16, 241–256.

Heazlewood, J.L., Durek, P., Hummel, J., Selbig, J., Weckwerth, W., Walther, D., Schulze, W.X., 2008. PhosPhAt: a database of phosphorylation sites in *Arabidopsis thaliana* and a plant-specific phosphorylation site predictor. Nucleic Acids Res. 36, D1015–D1021.

Hervás, M., Bashir, Q., Leferink, N.G., Ferreira, P., Moreno-Beltrán, B., Westphal, A.H., Díaz-Moreno, I., Medina, M., de la Rosa, M.A., Ubbink, M., Navarro, J.A., van Berkel, W.J., 2013. Communication between L-galactono-1,4-lactone dehydrogenase and cytochrome c. FEBS J. 280, 1830–1840.

Hoefs, S.J., Rodenburg, R.J., Smeitink, J.A., van den Heuvel, L.P., 2012. Molecular base of biochemical complex I deficiency. Mitochondrion 12, 520–532.

Hölzle, A., Jonietz, C., Törjek, O., Altmann, T., Binder, S., Forner, J., 2011. A RESTORER OF FERTILITY-like PPR gene is required for 5′-end processing of the nad4 mRNA in mitochondria of *Arabidopsis thaliana*. Plant J. 65, 737–744.

Huang, S., Taylor, N.L., Whelan, J., Millar, A.H., 2009. Refining the definition of plant mitochondrial presequences through analysis of sorting signals, N-terminal modifications, and cleavage motifs. Plant Physiol. 150, 1272–1285.

Hurd, T.R., Requejo, R., Filipovska, A., Brown, S., Prime, T.A., Robinson, A.J., Fearnley, I.M., Murphy, M.P., 2008. Complex I within oxidatively stressed bovine heart mitochondria is glutathionylated on Cys-531 and Cys-704 of the 75-kDa subunit: potential role of CYS residues in decreasing oxidative damage. J. Biol. Chem. 283, 24801–24815.

Ito, J., Taylor, N.L., Castleden, I., Weckwerth, W., Millar, A.H., Heazlewood, J.L., 2009. A survey of the *Arabidopsis thaliana* mitochondrial phosphoproteome. Proteomics 9, 4229–4240.

Jänsch, L., Kruft, V., Schmitz, U.K., Braun, H.P., 1996. New insights into the composition, molecular mass and stoichiometry of the protein complexes of plant mitochondria. Plant J. 9, 357–368.

Johansson, F.I., Michalecka, A.M., Møller, I.M., Rasmusson, A.G., 2004. Oxidation and reduction of pyridine nucleotides in alamethicin-permeabilized plant mitochondria. Biochem. J. 380, 193–202.

Jonietz, C., Forner, J., Hölzle, A., Thuss, S., Binder, S., 2010. RNA PROCESSING FACTOR2 is required for 5′ end processing of nad9 and cox3 mRNAs in mitochondria of *Arabidopsis thaliana*. Plant Cell 22, 443–453.

Juszczuk, I.M., Flexas, J., Szal, B., Dabrowska, Z., Ribas-Carbo, M., Rychter, A.M., 2007. Effect of mitochondrial genome rearrangement on respiratory activity, photosynthesis, photorespiration and energy status of MSC16 cucumber (*Cucumis sativus*) mutant. Physiol. Plant. 131, 527–541.

Kang, P.T., Zhang, L., Chen, C.L., Chen, J., Green, K.B., Chen, Y.R., 2012. Protein thiyl radical mediates S-glutathionylation of complex I. Free Radic. Biol. Med. 53, 962–973.

Kasimova, M.R., Grigiene, J., Krab, K., Hagedorn, P.H., Flyvbjerg, H., Andersen, P.E., Møller, I.M., 2006. The free NADH concentration is kept constant in plant mitochondria under different metabolic conditions. Plant Cell 18, 688–698.

Katayama, K., Sakurai, I., Wada, H., 2004. Identification of an *Arabidopsis thaliana* gene for cardiolipin synthase located in mitochondria. FEBS Lett. 577, 193–198.

Katayama, K., Wada, H., 2012. T-DNA insertion in the CLS gene for cardiolipin synthase affects development of *Arabidopsis thaliana*. Cytologica 77, 123–129.

Keren, I., Bezawork-Geleta, A., Kolton, M., Maayan, I., Belausov, E., Levy, M., Mett, A., Gidoni, D., Shaya, F., Ostersetzer-Biran, O., 2009. AtnMat2, a nuclear-encoded maturase required for splicing of group-II introns in *Arabidopsis* mitochondria. RNA 15, 2299–2311.

Keren, I., Tal, L., des Francs-Small, C.C., Araujo, W.L., Shevtsov, S., Shaya, F., Fernie, A.R., Small, I., Ostersetzer-Biran, O., 2012. nMAT1, a nuclear-encoded maturase involved in the trans-splicing of nad1 intron 1, is essential for mitochondrial complex I assembly and function. Plant J. 71, 413–426.

Please cite this article as: Braun, H.-P., et al., The life of plant mitochondrial complex I, Mitochondrion (2014), http://dx.doi.org/10.1016/j.mito.2014.02.006

Klodmann, J., Sunderhaus, S., Nimtz, M., Jänsch, L., Braun, H.P., 2010. Internal architecture of mitochondrial complex I from *Arabidopsis thaliana*. Plant Cell 22, 797–810.

Klodmann, J., Braun, H.P., 2011. Proteomic approach to characterize mitochondrial complex I from plants. Phytochemistry 72, 1071–1080.

Klodmann, J., Rode, C., Senkler, M., Braun, H.P., 2011. The protein complex proteome of plant mitochondria. Plant Physiol. 157, 587–598.

Knoop, V., Schuster, W., Wissinger, B., Brennicke, A., 1991. Trans-splicing integrates an exon of 22 nucleotides into the nad5 mRNA in higher plant mitochondria. EMBO J. 10, 3483–3493.

Kobayashi, Y., Knoop, V., Fukuzawa, H., Brennicke, A., Ohyama, K., 1997. Interorganellar gene transfer in bryophytes: the functional nad7 gene is nuclear encoded in *Marchantia polymorpha*. Mol. Gen. Genet. 256, 589–592.

Köhler, D., Schmidt-Gattung, S., Binder, S., 2010. The DEAD-box protein PMH2 is required for efficient group II intro splicing in mitochondria of *Arabidopsis thaliana*. Plant Mol. Biol. 72, 459–467.

König, A.C., Hartl, M., Pham, P.A., Laxa, M., Boersema, P., Orwat, A., Kalitventseva, I., Plöchinger, M., Braun, H.P., Leister, D., Mann, M., Wachter, A., Fernie, A., Finkemeier, I., 2014. The *Arabidopsis* class II sirtuin is a lysine deacetylase and interacts with mitochondrial energy metabolism. Plant Physiol. (in press).

Koprivova, A., Colas des Francs-Small, C., Calder, G., Mugford, S.T., Tanz, S., Lee, B.R., Zechmann, B., Small, I., Kopriva, S., 2010. Identification of a pentatricopeptide repeat protein implicated in splicing of intron 1 of mitochondrial nad7 transcripts. J. Biol. Chem. 285, 32192–32199.

Krause, F., Reifschneider, N.H., Vocke, D., Seelert, H., Rexroth, S., Dencher, N.A., 2004. "Respirasome"-like supercomplexes in green leaf mitochondria of spinach. J. Biol. Chem. 279, 48369–48375.

Kruft, V., Eubel, H., Jänsch, L., Werhahn, W., Braun, H.P., 2001. Proteomic approach to identify novel mitochondrial proteins in *Arabidopsis*. Plant Physiol. 127, 1694–1710.

Kühn, K., Weihe, A., Börner, T., 2005. Multiple promoters are a common feature of mitochondrial genes in *Arabidopsis*. Nucleic Acids Res. 33, 337–346.

Kühn, K., Bohne, A.V., Liere, K., Weihe, A., Börner, T., 2007. *Arabidopsis* phage-type RNA polymerases: accurate *in vitro* transcription of organellar genes. Plant Cell 19, 959–971.

Kühn, K., Richter, U., Meyer, E.H., Delannoy, E., Falcon de Longevialle, A., O'Toole, N., Börner, T., Millar, A.H., Small, I.D., Whelan, J., 2009. Phage-type RNA polymerase RPOTmp performs gene-specific transcription in mitochondria of *Arabidopsis thaliana*. Plant Cell 21, 2762–2779.

Kühn, K., Carrie, C., Giraud, E., Wang, Y., Meyer, E.H., Narsai, R., des Francs-Small, C.C., Zhang, B., Murcha, M.W., Whelan, J., 2011. The RCC1 family protein RUG3 is required for splicing of nad2 and complex I biogenesis in mitochondria of *Arabidopsis thaliana*. Plant J. 67, 1067–1080.

Kwasniak, M., Pogorzelec, L., Migdal, I., Smakowska, E., Janska, H., 2012. Proteolytic system of plant mitochondria. Physiol. Plant. 145, 187–195.

Kwasniak, M., Majewski, P., Skibior, R., Adamowicz, A., Czarna, M., Sliwinska, E., Janska, H., 2013. Silencing of the nuclear *RPS10* gene encoding mitochondrial ribosomal protein alters translation in *Arabidopsis* mitochondria. Plant Cell 25, 1855–1867.

Lambert, A.J., Brand, M.D., 2004. Superoxide production by NADH:ubiquinone oxidoreductase (complex I) depends on the pH gradient across the mitochondrial inner membrane. Biochem. J. 382, 511–517.

Law, S.R., Narsai, R., Taylor, N.L., Delannoy, E., Carrie, C., Giraud, E., Millar, A.H., Small, I., Whelan, J., 2012. Nucleotide and RNA metabolism prime translational initiation in the earliest events of mitochondrial biogenesis during *Arabidopsis* germination. Plant Physiol. 158, 1610–1627.

Lazarou, M., McKenzie, M., Ohtake, A., Thorburn, D.R., Ryan, M.T., 2007. Analysis of the assembly profiles for mitochondrial- and nuclear-DNA-encoded subunits into complex I. Mol. Cell. Biol. 27, 4228–4237.

Lee, B.H., Lee, H., Xiong, L., Zhu, J.K., 2002. A mitochondrial complex I defect impairs cold-regulated nuclear gene expression. Plant Cell 14, 1235–1251.

Lee, C.P., Eubel, H., O'Toole, N., Millar, A.H., 2008. Heterogeneity of the mitochondrial proteome for photosynthetic and non-photosynthetic *Arabidopsis* metabolism. Mol. Cell. Proteomics 7, 1297–1316.

Lee, C.P., Eubel, H., O'Toole, N., Millar, A.H., 2011. Combining proteomics of root and shoot mitochondria and transcript analysis to define constitutive and variable components in plant mitochondria. Phytochemistry 72, 1092–1108.

Leon, S., Touraine, B., Ribot, C., Briat, J.F., Lobreaux, S., 2003. Iron–sulfur assembly in plant. Distinct NFU proteins in mitochondria and plastids from *Arabidopsis thaliana*. Biochem. J. 371, 823–830.

Leonard, K., Haiker, H., Weiss, H., 1987. Three-dimensional structure of NADH: ubiquinone reductase (complex I) from *Neurospora* mitochondria determined by electron microscopy of membrane crystals. J. Mol. Biol. 194, 277–286.

Li, L., Nelson, C.J., Solheim, C., Whelan, J., Millar, A.H., 2012. Determining degradation and synthesis rates of *Arabidopsis* proteins using the kinetics of progressive 15 N labeling of two-dimensional gel-separated protein spots. Mol. Cell. Proteomics 11 (M111.010025).

Li, L., Nelson, C.J., Carrie, C., Gawryluk, R.M., Solheim, C., Gray, M.W., Whelan, J., Millar, A.H., 2013. Subcomplexes of ancestral respiratory complex I subunits rapidly turn over *in vivo* as productive assembly intermediates in *Arabidopsis*. J. Biol. Chem. 288, 5707–5717.

Liere, K., Weihe, A., Börner, T., 2011. The transcription machineries of plant mitochondria and chloroplasts: composition, function, and regulation. J. Plant Physiol. 168, 1345–1360.

Liu, Y., He, J., Chen, Z., Ren, X., Hong, X., Gong, Z., 2010. ABA overly-sensitive 5 (ABO5), encoding a pentatricopeptide repeat protein required for cis-splicing of mitochondrial nad2 intron 3, is involved in the abscisic acid response in *Arabidopsis*. Plant J. 63, 749–765.

Lohrmann, J., Sweere, U., Zabaleta, E., Bäurle, I., Keitel, C., Kozma-Bognar, L., Brennicke, A., Schäfer, E., Kudla, J., Harter, K., 2001. The response regulator ARR2: a pollen-specific transcription factor involved in the expression of nuclear genes for components of mitochondrial complex I in *Arabidopsis*. Mol. Genet. Genomics 265, 2–13.

Masri, S., Patel, V.R., Eckel-Mahan, K.L., Peleg, S., Forne, I., Ladurner, A.G., Baldi, P., Imhof, A., Sassone-Corsi, P., 2013. Circadian acetylome reveals regulation of mitochondrial metabolic pathways. Proc. Natl. Acad. Sci. U. S. A. 110, 3339–3344.

Matsuo, M., Obokata, J., 2006. Remote control of photosynthetic genes by the mitochondrial respiratory chain. Plant J. 47, 873–882.

McKenzie, M., Lazarou, M., Thorburn, D.R., Ryan, M.T., 2006. Mitochondrial respiratory chain supercomplexes are destabilized in Barth syndrome patients. J. Mol. Biol. 361, 462–469.

Meyer, E.H., Heazlewood, J.L., Millar, A.H., 2007. Mitochondrial acyl carrier proteins in *Arabidopsis thaliana* are predominantly soluble matrix proteins and none can be confirmed as subunits of respiratory complex I. Plant Mol. Biol. 64, 319–327.

Meyer, E.H., Taylor, N.L., Millar, A.H., 2008. Resolving and identifying protein components of plant mitochondrial respiratory complexes using three dimensions of gel electrophoresis. J. Prot. Res. 7, 786–794.

Meyer, E.H., Tomaz, T., Carroll, A.J., Estavillo, G., Delannoy, E., Tanz, S.K., Small, I.D., Pogson, B.J., Millar, A.H., 2009. Remodeled respiration in ndufs4 with low phosphorylation efficiency suppresses *Arabidopsis* germination and growth and alters control of metabolism at night. Plant Physiol. 151, 603–619.

Meyer, E.H., Solheim, C., Tanz, S.K., Bonnard, G., Millar, A.H., 2011. Insights into the composition and assembly of the membrane arm of plant complex I through analysis of subcomplexes in *Arabidopsis* mutant lines. J. Biol. Chem. 286, 26081–26092.

Meyer, E.H., 2012. Proteomic investigations of complex I composition: how to define a subunit? Front. Plant Sci. 3, 106.

Millar, A.H., Whelan, J., Soole, K.L., Day, D.A., 2011. Organization and regulation of mitochondrial respiration in plants. Annu. Rev. Plant Biol. 62, 79–104.

Mimaki, M., Wang, X., McKenzie, M., Thorburn, D.R., Ryan, M.T., 2012. Understanding mitochondrial complex I assembly in health and disease. Biochim. Biophys. Acta 1817, 851–862.

Mitchell, P., 1961. Coupling of phosphorylation to electron and hydrogen transfer by a chemi-osmotic type of mechanism. Nature 191, 144–148.

Møller, I.M., Kristensen, B.K., 2006. Protein oxidation in plant mitochondria detected as oxidized tryptophan. Free Radic. Biol. Med. 40, 430–435.

Møller, I.M., Palmer, J.M., 1982. Direct evidence for the presence of a rotenone-resistant NADH dehydrogenase on the inner surface of the inner membrane of plant mitochondria. Physiol. Plant. 54, 267–274.

Murcha, M.W., Elhafez, D., Lister, R., Tonti-Filippini, J., Baumgartner, M., Philippar, K., Carrie, C., Mokranjac, D., Soll, J., Whelan, J., 2007. Characterization of the preprotein and amino acid transporter gene family in *Arabidopsis*. Plant Physiol. 143, 199–212.

Murphy, M.P., 2009. How mitochondria produce reactive oxygen species. Biochem. J. 417, 1–13.

Narsai, R., Howell, K.A., Millar, A.H., O'Toole, N., Small, I., Whelan, J., 2007. Genome-wide analysis of mRNA decay rates and their determinants in *Arabidopsis thaliana*. Plant Cell 19, 3418–3436.

Narsai, R., Law, S.R., Carrie, C., Xu, L., Whelan, J., 2011. In-depth temporal transcriptome profiling reveals a crucial developmental switch with roles for RNA processing and organelle metabolism that are essential for germination in *Arabidopsis*. Plant Physiol. 157, 1342–1362.

Nehls, U., Friedrich, T., Schmiede, A., Ohnishi, T., Weiss, H., 1992. Characterization of assembly intermediates of NADH:ubiquinone oxidoreductase (complex I) accumulated in *Neurospora* mitochondria by gene disruption. J. Mol. Biol. 227, 1032–1042.

Nelson, C.J., Li, L., Jacoby, R.P., Millar, A.H., 2013. Degradation rate of mitochondrial proteins in *Arabidopsis thaliana* cells. J. Proteome Res. 12, 3449–3459.

Noctor, G., Dutilleul, C., De Paepe, R., Foyer, C.H., 2004. Use of mitochondrial electron transport mutants to evaluate the effects of redox state on photosynthesis, stress tolerance and the integration of carbon/nitrogen metabolism. J. Exp. Bot. 55, 49–57.

Obata, T., Matthes, A., Koszior, S., Lehmann, M., Araújo, W.L., Bock, R., Sweetlove, L.J., Fernie, A.R., 2011. Alteration of mitochondrial protein complexes in relation to metabolic regulation under short-term oxidative stress in *Arabidopsis* seedlings. Phytochemistry 72, 1081–1091.

Ogura, M., Yamaki, J., Homma, M.K., Homma, Y., 2012. Mitochondrial c-Src regulates cell survival through phosphorylation of respiratory chain components. Biochem. J. 447, 281–289.

Okada, S., Brennicke, A., 2006. Transcript levels in plant mitochondria show a tight homeostasis during day and night. Mol. Genet. Genomics 276, 71–78.

Pagniez-Mammeri, H., Rak, M., Legrand, A., Benit, P., Rustin, P., Slama, A., 2012. Mitochondrial complex I deficiency of nuclear origin II. Non-structural genes. Mol. Genet. Metab. 105, 173–179.

Palmieri, M.C., Lindermayr, C., Bauwe, H., Steinhauser, C., Durner, J., 2010. Regulation of plant glycine decarboxylase by s-nitrosylation and glutathionylation. Plant Physiol. 152, 1514–1528.

Pellny, T.K., Van Aken, O., Dutilleul, C., Wolff, T., Groten, K., Bor, M., De Paepe, R., Reyss, A., Van Breusegem, F., Noctor, G., Foyer, C.H., 2008. Mitochondrial respiratory pathways modulate nitrate sensing and nitrogen-dependent regulation of plant architecture in *Nicotiana sylvestris*. Plant J. 54, 976–992.

Perales, M., Parisi, G., Fornasari, M.S., Colaneri, A., Villarreal, F., Gonzalez-Schain, N., Echave, J., Gomez-Casati, D., Braun, H.P., Araya, A., Zabaleta, E., 2004. Gamma carbonic anhydrase like complex interact with plant mitochondrial complex I. Plant Mol. Biol. 56, 947–957.

Perales, M., Eubel, H., Heinemeyer, J., Colaneri, A., Zabaleta, E., Braun, H.P., 2005. Disruption of a nuclear gene encoding a mitochondrial gamma carbonic anhydrase reduces

Please cite this article as: Braun, H.-P., et al., The life of plant mitochondrial complex I, Mitochondrion (2014), http://dx.doi.org/10.1016/j.mito.2014.02.006

complex I and supercomplex I + III_2 levels and alters mitochondrial physiology in *Arabidopsis*. J. Mol. Biol. 350, 263–277.
Perrin, R., Meyer, E.H., Zaepfel, M., Kim, Y.J., Mache, R., Grienenberger, J.M., Gualberto, J.M., Gagliardi, D., 2004. Two exoribonucleases act sequentially to process mature 3′-ends of atp9 mRNAs in *Arabidopsis* mitochondria. J. Biol. Chem. 279, 25440–25446.
Peters, K., Dudkina, N.V., Jänsch, L., Braun, H.P., Boekema, E.J., 2008. A structural investigation of complex I and I + III2 supercomplex from *Zea mays* at 11–13 Å resolution: assignment of the carbonic anhydrase domain and evidence for structural heterogeneity within complex I. Biochim. Biophys. Acta 1777, 84–93.
Peters, K., Niessen, M., Peterhansel, C., Spath, B., Holzle, A., Binder, S., Marchfelder, A., Braun, H.P., 2012. Complex I–complex II ratio strongly differs in various organs of *Arabidopsis thaliana*. Plant Mol. Biol. 79, 273–284.
Peters, K., Belt, K., Braun, H.P., 2013. 3D gel map of *Arabidopsis* complex I. Front. Plant Sci. 4, 153.
Pineau, B., Layoune, O., Danon, A., De Paepe, R., 2008. L-Galactono-1,4-lactone dehydrogenase is required for the accumulation of plant respiratory complex I. J. Biol. Chem. 283, 32500–32505.
Pineau, B., Bourge, M., Marion, J., Mauve, C., Gilard, F., Maneta-Peyret, L., Moreau, P., Satiat-Jeunemaître, B., Brown, S.C., De Paepe, R., Danon, A., 2013. The importance of cardiolipin synthase for mitochondrial ultrastructure, respiratory function, plant development, and stress responses in Arabidopsis. Plant Cell 25, 4195–4208.
Priault, P., Tcherkez, G., Cornic, G., De Paepe, R., Naik, R., Ghashghaie, J., Streb, P., 2006. The lack of mitochondrial complex I in a CMSII mutant of *Nicotiana sylvestris* increases photorespiration through an increased internal resistance to CO_2 diffusion. J. Exp. Bot. 57, 3195–3207.
Ramírez-Aguilar, S.J., Keuthe, M., Rocha, M., Fedyaev, V.V., Kramp, K., Gupta, K.J., Rasmusson, A.G., Schulze, W.X., van Dongen, J.T., 2011. The composition of plant mitochondrial supercomplexes changes with oxygen availability. J. Biol. Chem. 43045–43053.
Rardin, M.J., Newman, J.C., Held, J.M., Cusack, M.P., Sorensen, D.J., Li, B., Schilling, B., Mooney, S.D., Kahn, C.R., Verdin, E., Gibson, B.W., 2013. Label-free quantitative proteomics of the lysine acetylome in mitochondria identifies substrates of SIRT3 in metabolic pathways. Proc. Natl. Acad. Sci. U. S. A. 110, 6601–6606.
Rasmusson, A.G., Soole, K.L., Elthon, T.E., 2004. Alternative NAD(P)H dehydrogenases of plant mitochondria. Annu. Rev. Plant Biol. 55, 23–39.
Reiland, S., Messerli, G., Baerenfaller, K., Gerrits, B., Endler, A., Grossmann, J., Gruissem, W., Baginsky, S., 2009. Large-scale *Arabidopsis* phosphoproteome profiling reveals novel chloroplast kinase substrates and phosphorylation networks. Plant Physiol. 150, 889–903.
Reiland, S., Finazzi, G., Endler, A., Willig, A., Baerenfaller, K., Grossmann, J., Gerrits, B., Rutishauser, D., Gruissem, W., Rochaix, J.D., Baginsky, S., 2011. Comparative phosphoproteome profiling reveals a function of the STN8 kinase in fine-tuning of cyclic electron flow (CEF). Proc. Natl. Acad. Sci. U. S. A. 108, 12955–12960.
Remacle, C., Barbieri, M.R., Cardol, P., Hamel, P.P., 2008. Eukaryotic complex I: functional diversity and experimental systems to unravel the assembly process. Mol. Genet. Genomics 280, 93–110.
Rich, P., 2003. Chemiosmotic coupling: the cost of living. Nature 421, 583.
Rimmer, K.A., Foo, J.H., Ng, A., Petrie, E.J., Shilling, P.J., Perry, A.J., Mertens, H.D., Lithgow, T., Mulhern, T.D., Gooley, P.R., 2011. Recognition of mitochondrial targeting sequences by the import receptors Tom20 and Tom22. J. Mol. Biol. 405, 804–818.
Roberts, P.G., Hirst, J., 2012. The deactive form of respiratory complex I from mammalian mitochondria is a Na+/H + antiporter. J. Biol. Chem. 287, 34743–34751.
Rouhier, N., Villarejo, A., Srivastava, M., Gelhaye, E., Keech, O., Droux, M., Finkemeier, I., Samuelsson, G., Dietz, K.J., Jacquot, J.P., Wingsle, G., 2005. Identification of plant glutaredoxin targets. Antioxid. Redox Signal. 7, 919–929.
Sabar, M., De Paepe, R., de Kouchkovsky, Y., 2000. Complex I impairment, respiratory compensations, and photosynthetic decrease in nuclear and mitochondrial male sterile mutants of *Nicotiana sylvestris*. Plant Physiol. 124, 1239–1250.
Salvato, F., Havelund, J.F., Chen, M., Rao, R.S., Rogowska-Wrzesinska, A., Jensen, O.N., Gang, D.R., Thelen, J.J., Møller, I.M., 2014. The potato tuber mitochondrial proteome. Plant Physiol. 164, 637–653.
Salvi, M., Brunati, A.M., Toninello, A., 2005. Tyrosine phosphorylation in mitochondria: a new frontier in mitochondrial signaling. Free Radic. Biol. Med. 38, 1267–1277.
Sauve, A.A., 2010. Sirtuins. Biochim. Biophys. Acta 1804, 1565–1566.
Sazanov, L.A., Baradaran, R., Efremov, R.G., Berrisford, J.M., Minhas, G., 2013. A long road towards the structure of respiratory complex I, a giant molecular proton pump. Biochem. Soc. Trans. 41, 1265–1271.
Schägger, H., Pfeiffer, K., 2000. Supercomplexes in the respiratory chains of yeast and mammalian mitochondria. EMBO J. 19, 1777–1783.
Schägger, H., 2002. Respiratory supercomplexes of mitochondria and bacteria. Biochim. Biophys. Acta 10, 154–159.
Schertl, P., Sunderhaus, S., Klodmann, J., Grozeff, G.E., Bartoli, C.G., Braun, H.P., 2012. L-Galactono-1,4-lactone dehydrogenase (GLDH) forms part of three subcomplexes of mitochondrial complex I in *Arabidopsis thaliana*. J. Biol. Chem. 287, 14412–14419.
Schlame, M., Rua, D., Greenberg, M.L., 2000. The biosynthesis and functional role of cardiolipin. Prog. Lipid Res. 39, 27–288.
Schleiff, E., Becker, T., 2011. Common ground for protein translocation: access control for mitochondria and chloroplasts. Nat. Rev. Mol. Cell Biol. 12, 48–59.
Schwarzländer, M., König, A.C., Sweetlove, L.J., Finkemeier, I., 2012. The impact of impaired mitochondrial function on retrograde signalling: a meta-analysis of transcriptomic responses. J. Exp. Bot. 63, 1735–1750.
Schwarzländer, M., Finkemeier, I., 2013. Mitochondrial energy and redox signaling in plants. Antioxid. Redox Signal. 18, 2122–2144.
Senkler, M., Braun, H.P., 2012. Functional annotation of 2D protein maps: the GelMap portal. Front. Plant Sci. 3, 87.
Shikanai, T., 2007. Cyclic electron transport around photosystem I: genetic approaches. Annu. Rev. Plant Biol. 58, 199–217.
Sol, E.M., Wagner, S.A., Weinert, B.T., Kumar, A., Kim, H.S., Deng, C.X., Choudhary, C., 2012. Proteomic investigations of lysine acetylation identify diverse substrates of mitochondrial deacetylase sirt3. PLoS One 7, e50545.
Soole, K.L., Dry, I.B., James, A.T., Wiskich, J.T., 1990. The kinetics of NADH oxidation by complex I of isolated plant mitochondria. Physiol. Plant. 80, 75–82.
Steinhauser, M.L., Bailey, A.P., Senyo, S.E., Guillermier, C., Perlstein, T.S., Gould, A.P., Lee, R.T., Lechene, C.P., 2012. Multi-isotope imaging mass spectrometry quantifies stem cell division and metabolism. Nature 481, 516–519.
Stern, D.B., Bang, A.G., Thompson, W.F., 1986. The watermelon URF-1 gene: evidence for a complex structure. Curr. Genet. 10, 857–869.
Stoll, B., Stoll, K., Steinhilber, J., Jonietz, C., Binder, S., 2013. Mitochondrial transcript length polymorphisms are a widespread phenomenon in *Arabidopsis thaliana*. Plant Mol. Biol. 81, 221–233.
Sumegi, B., Srere, P.A., 1984. Complex I binds several mitochondrial NAD-coupled dehydrogenases. J. Biol. Chem. 259, 15040–15045.
Sunderhaus, S., Dudkina, N., Jänsch, L., Klodmann, J., Heinemeyer, J., Perales, M., Zabaleta, E., Boekema, E., Braun, H.P., 2006. Carbonic anhydrase subunits form a matrix-exposed domain attached to the membrane arm of mitochondrial complex I in plants. J. Biol. Chem. 281, 6482–6488.
Takenaka, M., Verbitskiy, D., van der Merwe, J.A., Zehrmann, A., Brennicke, A., 2008. The process of RNA editing in plant mitochondria. Mitochondrion 8, 35–46.
Takenaka, M., Zehrmann, A., Verbitskiy, D., Härtel, B., Brennicke, A., 2014. RNA-editing in plants and its evolution. Annu. Rev. Genet. 47, 335–352.
Tanz, S., Castleden, I., Hooper, C.M., Vacher, M., Small, I., Millar, A.H., 2013. SUBA3: a database for integrating experimentation and prediction to define the SUBcellular location of proteins in *Arabidopsis*. Nucleic Acids Res. 41, D1185–D1195.
Tian, G.W., Mohanty, A., Chary, S.N., Li, S., Paap, B., Drakakaki, G., Kopec, C.D., Li, J., Ehrhardt, D., Jackson, D., Rhee, S.Y., Raikhel, N.V., Citovsky, V., 2004. High-throughput fluorescent tagging of full-length *Arabidopsis* gene products in planta. Plant Physiol. 135, 25–38.
Ugalde, C., Vogel, R., Huijbens, R., Van Den Heuvel, B., Smeitink, J., Nijtmans, L., 2004. Human mitochondrial complex I assembles through the combination of evolutionary conserved modules: a framework to interpret complex I deficiencies. Hum. Mol. Genet. 13, 2461–2472.
Unseld, M., Marienfeld, J.R., Brandt, P., Brennicke, A., 1997. The mitochondrial genome of *Arabidopsis thaliana* contains 57 genes in 366,924 nucleotides. Nat. Genet. 15, 57–61.
Van der Laan, M., Wiedemann, N., Mick, D.U., Guiad, B., Rehling, P., Pfanner, N., 2006. A role for Tim21 in membrane-potential-dependent preprotein sorting in mitochondria. Curr. Biol. 16, 2271–2276.
Vinogradov, A.D., 1998. Catalytic properties of the mitochondrial NADH–ubiquinone oxidoreductase (complex I) and the pseudo-reversible active/inactive enzyme transition. Biochim. Biophys. Acta 1364, 169–185.
Vogel, R.O., Dieteren, C.E., van den Heuvel, L.P., Willems, P.H., Smeitink, J.A., Koopman, W.J., Nijtmans, L.G., 2007a. Identification of mitochondrial complex I assembly intermediates by tracing tagged NDUFS3 demonstrates the entry point of mitochondrial subunits. J. Biol. Chem. 282, 7582–7590.
Vogel, R.O., Smeitink, J.A., Nijtmans, L.G., 2007b. Human mitochondrial complex I assembly: a dynamic and versatile process. Biochim. Biophys. Acta 1767, 1215–1227.
Wang, Q., Fristedt, R., Yu, X., Chen, Z., Liu, H., Lee, Y., Guo, H., Merchant, S.S., Lin, C., 2012a. The γ-carbonic anhydrase subcomplex of mitochondrial complex I is essential for development and important for photomorphogenesis of *Arabidopsis*. Plant Physiol. 160, 1373–1383.
Wang, Y., Carrie, C., Giraud, E., Elhafez, D., Narsai, R., Duncan, O., Whelan, J., Murcha, M., 2012b. Dual location of the mitochondria preprotein transporters B14.7 and Tim23-2 in complex I and the TIM17:23 complex in *Arabidopsis* links mitochondrial activity and biogenesis. Plant Cell 24, 2675–2695.
Watt, I.N., Montgomery, M.G., Runswick, M.J., Leslie, A.G., Walker, J.E., 2010. Bioenergetic cost of making an adenosine triphosphate molecule in animal mitochondria. Proc. Natl. Acad. Sci. U. S. A. 107, 16823–16827.
Welchen, E., Gonzalez, D.H., 2006. Overrepresentation of elements recognized by TCP-domain transcription factors in the upstream regions of nuclear genes encoding components of the mitochondrial oxidative phosphorylation machinery. Plant Physiol. 141, 540–545.
Wissinger, B., Hiesel, R., Schuster, W., Brennicke, A., 1988. The NADH-dehydrogenase subunit 5 gene in *Oenothera* mitochondria contains two introns and is cotranscribed with the 18S–5S rRNA genes. Mol. Gen. Genet. 212, 56–65.
Wissinger, B., Schuster, W., Brennicke, A., 1991. Trans-splicing in *Oenothera* mitochondria: nad1 mRNAs are edited in exon and trans splicing group II intron sequences. Cell 65, 473–482.
Wittig, I., Carrozzo, R., Santorelli, F.M., Schägger, H., 2006. Supercomplexes and subcomplexes of mitochondrial oxidative phosphorylation. Biochim. Biophys. Acta 1757, 1066–1072.
Wu, X., Oh, M.H., Schwarz, E.M., Larue, C.T., Sivaguru, M., Imai, B.S., Yau, P.M., Ort, D.R., Huber, S.C., 2011. Lysine acetylation is a widespread protein modification for diverse proteins in *Arabidopsis*. Plant Physiol. 155, 1769–1778.
Yoshida, K., Noguchi, K., Motohashi, K., Hisabori, T., 2013. Systematic exploration of thioredoxin target proteins in plant mitochondria. Plant Cell Physiol. 54, 875–892.
Zabaleta, E., Martin, M.V., Braun, H.P., 2012. A basal carbon concentrating mechanism in plants? Plant Sci. 187, 97–104.

Please cite this article as: Braun, H.-P., et al., The life of plant mitochondrial complex I, Mitochondrion (2014), http://dx.doi.org/10.1016/j.mito.2014.02.006

Zensen, R., Husmann, H., Schneider, R., Peine, T., Weiss, H., 1992. *De novo* synthesis and desaturation of fatty acids at the mitochondrial acyl-carrier protein, a subunit of NADH:ubiquinone oxidoreductase in *Neurospora crassa*. FEBS Lett. 310, 179–181.

Zhang, X.P., Glaser, E., 2001. Interaction of plant mitochondrial and chloroplast signal peptides with the Hsp70 molecular chaperone. Trends Plant Sci. 7, 14–21.

Zhang, M., Mileykowskaya, E., Dowhan, W., 2005. Cardiolipin is essential for organization of complexes III and IV into a supercomplex in intact yeast mitochondria. J. Biol. Chem. 280, 29403–29408.

Zhang, D.S., Piazza, V., Perrin, B.J., Rzadzinska, A.K., Poczatek, J.C., Wang, M., Prosser, H.M., Ervasti, J.M., Corey, D.P., Lechene, C.P., 2012. Multi-isotope imaging mass spectrometry reveals slow protein turnover in hair-cell stereocilia. Nature 481, 520–524.

Zmudjak, M., Colas des Francs-Small, C., Keren, I., Shaya, F., Belausov, E., Small, I., Ostersetzer-Biran, O., 2013. mCSF1, a nucleus-encoded CRM protein required for the processing of many mitochondrial introns, is involved in the biogenesis of respiratory complexes I and IV in *Arabidopsis*. New Phytol. 199, 379–394.

Please cite this article as: Braun, H.-P., et al., The life of plant mitochondrial complex I, Mitochondrion (2014), http://dx.doi.org/10.1016/j.mito.2014.02.006

Publication 5

The Arabidopsis class II sirtuin is a lysine deacetylase and interacts with mitochondrial energy metabolism.

König AC*, Hartl M*, Pham PA, Laxa M, Boersema PJ, Orwat A, Kalitventseva I, Plöchinger M, Braun HP, Leister D, Mann M, Wachter A, Fernie AR, Finkemeier I.

(2014)

Plant Physiology 164(3): 1401-14.

The Arabidopsis Class II Sirtuin Is a Lysine Deacetylase and Interacts with Mitochondrial Energy Metabolism[1][C][W][OPEN]

Ann-Christine König[2,3], Markus Hartl[2,3], Phuong Anh Pham, Miriam Laxa[4], Paul J. Boersema[5], Anne Orwat, Ievgeniia Kalitventseva, Magdalena Plöchinger, Hans-Peter Braun, Dario Leister, Matthias Mann, Andreas Wachter, Alisdair R. Fernie, and Iris Finkemeier[3]*

Department I of Biology, Ludwig Maximilians University Munich, Grosshaderner Strasse 2, 82152 Martinsried, Germany (A.-C.K., M.H., M.L., A.O., I.K., M.P., D.L., I.F.); Max Planck Institute of Molecular Plant Physiology, Am Muehlenberg 1, 14476 Potsdam-Golm, Germany (P.A.P., A.R.F.); Proteomics and Signal Transduction, Max Planck Institute of Biochemistry, Am Klopferspitz 18, 82152 Martinsried, Germany (P.J.B., M.M.); Institute for Plant Genetics, Faculty of Natural Sciences, Leibniz Universität Hanover, 30419 Hanover, Germany (H.-P.B.); and Center for Plant Molecular Biology, University of Tuebingen, 72076 Tuebingen, Germany (A.W.)

The posttranslational regulation of proteins by lysine (Lys) acetylation has recently emerged to occur not only on histones, but also on organellar proteins in plants and animals. In particular, the catalytic activities of metabolic enzymes have been shown to be regulated by Lys acetylation. The Arabidopsis (*Arabidopsis thaliana*) genome encodes two predicted sirtuin-type Lys deacetylases, of which only Silent Information Regulator2 homolog (SRT2) contains a predicted presequence for mitochondrial targeting. Here, we have investigated the function of SRT2 in Arabidopsis. We demonstrate that SRT2 functions as a Lys deacetylase in vitro and in vivo. We show that SRT2 resides predominantly at the inner mitochondrial membrane and interacts with a small number of protein complexes mainly involved in energy metabolism and metabolite transport. Several of these protein complexes, such as the ATP synthase and the ATP/ADP carriers, show an increase in Lys acetylation in *srt2* loss-of-function mutants. The *srt2* plants display no growth phenotype but rather a metabolic phenotype with altered levels in sugars, amino acids, and ADP contents. Furthermore, coupling of respiration to ATP synthesis is decreased in these lines, while the ADP uptake into mitochondria is significantly increased. Our results indicate that SRT2 is important in fine-tuning mitochondrial energy metabolism.

Mitochondria are central hubs of energy metabolism in plants and animals. In addition to a fine-tuned mitochondria-to-nuclear signaling that regulates transcription of nuclear gene expression (Rhoads and Subbaiah, 2007; Schwarzländer et al., 2012), posttranslational modifications of proteins are thought to be essential for the regulation of central metabolic pathways and thus determine the plasticity of plant metabolism (Hartl and Finkemeier, 2012). In mammalian mitochondria, the regulation of metabolic functions by posttranslational Lys acetylation of proteins was recently discovered to be of great importance (Newman et al., 2012; Rardin et al., 2013). The $^{\epsilon}N$-acetylation of Lys side chains (subsequently referred to as Lys acetylation) is a reversible and highly regulated posttranslational modification of both prokaryotic and eukaryotic proteins (Sadoul et al., 2011; Xing and Poirier, 2012). Lys acetylation can have a strong impact on the biochemical function of proteins as the transfer of the acetyl group to Lys masks the positive charge, which is known to be important in many catalytic centers of enzymes, as well as for protein-protein and protein-DNA interactions. In plants, Lys acetylation was, until recently, mainly thought to occur on histone proteins as regulatory mechanism for transcription and chromatin functions (Hollender and Liu, 2008). However, several central metabolic enzymes of diverse subcellular compartments were recently discovered to be Lys acetylated in Arabidopsis (*Arabidopsis thaliana*), and in vitro deacetylation tests confirmed that Lys acetylation affects enzyme activities and protein functions (Finkemeier et al.,

[1] This work was supported by the Deutsche Forschungsgemeinschaft, Germany (Emmy Noether Programme FI–1655/1–1 and Research Unit 804 to I.F.) and the Max Planck Gesellschaft (to A.R.F., P.A.P., P.J.B., M.M.).

[2] These authors contributed equally to the article.

[3] Present address: Max Planck Institute for Plant Breeding Research, Carl von Linné Weg 10, 50829 Cologne, Germany.

[4] Present address: Leibniz University Hannover, Institute of Botany, 30419 Hannover, Germany.

[5] Present address: Eidgenössiche Technische Hochschule Zürich, Institute of Biochemistry, Schafmattstrasse 18, 8093 Zurich, Switzerland.

* Address correspondence to finkemeier@mpipz.mpg.de.

The author responsible for distribution of materials integral to the findings presented in this article in accordance with the policy described in the Instructions for Authors (www.plantphysiol.org) is: Iris Finkemeier (i.finkemeier@lmu.de).

[C] Some figures in this article are displayed in color online but in black and white in the print edition.

[W] The online version of this article contains Web-only data.

[OPEN] Articles can be viewed online without a subscription.

www.plantphysiol.org/cgi/doi/10.1104/pp.113.232496

2011; Wu et al., 2011). Although even organellar-encoded proteins, such as the β subunit of the ATP synthase and the large subunit of Rubisco, have been identified as Lys acetylated in Arabidopsis, it is as yet unclear which enzymes regulate this modification in mitochondria and chloroplasts of plants. Generally, protein acetyltransferases and deacetylases are known to catalyze the reversible modification of the $^{\varepsilon}N$-group of Lys. In addition to the classical family of histone deacetylases, a second family of protein deacetylases exists, namely the sirtuins, which are conserved across bacteria, yeast (*Saccharomyces cerevisiae*), plants, and animals (Hollender and Liu, 2008). Sirtuins catalyze an NAD^+-dependent deacetylation of acetyl-Lys in proteins and thereby produce a deacetylated Lys, as well as the metabolites nicotinamide and 2′-*O*-acetyl-ADP-ribose. Sirtuins have recently emerged as key regulators of life span, cell survival, apoptosis, and metabolism in different heterotrophic organisms (Sauve, 2010; Houtkooper et al., 2012; Sebastián et al., 2012). They are also of great interest with regard to energy metabolism, as they are NAD^+ dependent and function in a nutrient- and redox-dependent manner (Guarente, 2011). Based on phylogenetic analysis, sirtuin-type proteins can be grouped into four different classes (class I–IV), not all of which solely possess a Lys deacetylase activity. Mammalian Sirtuin5 (SIRT5) for example (class III) possesses additional Lys succinylase and demalonylase activity (Du et al., 2011). The most studied enzymes so far are mainly derived from class I (Houtkooper et al., 2012), while the function of class II-type enzymes is still somewhat obscure. To date, only the mammalian SIRT4 was characterized from this class and possessed an ADP-ribosyltransferase activity on mitochondrial Glu dehydrogenase (Haigis et al., 2006). Only very recently, additional Lys deacetylase activity was also demonstrated for SIRT4 (Laurent et al., 2013; Rauh et al., 2013). The Arabidopsis genome encodes two sirtuins from two classes, with Silent Information Regulator1 homolog (SRT1; At5g55760) from class IV and SRT2 (At5g09230) from class II (Pandey et al., 2002). Because the actual biological function of type II sirtuins in mammalian organisms is still under some debate (Newman et al., 2012), and neither sirtuin-specific activity nor function of any plant sirtuin has been demonstrated so far, it was our goal to establish the function of the predicted mitochondrial class II sirtuin SRT2 of Arabidopsis.

RESULTS

Arabidopsis *SRT2* Encodes Seven Splice Forms, of Which Two Are Degraded by Nonsense-Mediated Decay

In contrast to seven sirtuin genes in the mammalian genome, Arabidopsis possesses only two genes encoding putative sirtuin-type proteins. However, seven transcript isoforms are predicted for the Arabidopsis SRT2 gene (At5g09230.1–At5g09230.7/SRT2.1–SRT2.7, TAIR10 [The Arabidopsis Information Resource 10]), which are generated from alternative splicing (AS) of the *SRT2* precursor mRNA. Hence, we were curious to find out whether all of the annotated splice forms are expressed and whether different protein isoforms will be generated from these transcripts. We were able to detect all of the annotated as well as some additional splicing variants for *SRT2* by an analysis of high-throughput RNA sequencing data from Arabidopsis seedlings (Supplemental Fig. S1). As the protein sequences of the annotated SRT2 isoforms are very similar and mainly differ in their N- or C-terminal regions (Supplemental Fig. S1; Supplemental Table S1), we had a closer look at an AS event in intron 5 occurring in both SRT2.4 and SRT2.6 transcripts (Fig. 1A; Supplemental Fig. S2). This splice form is predicted to result in N-terminal short forms of the protein according to the Arabidopsis genome annotation (TAIR10), due to

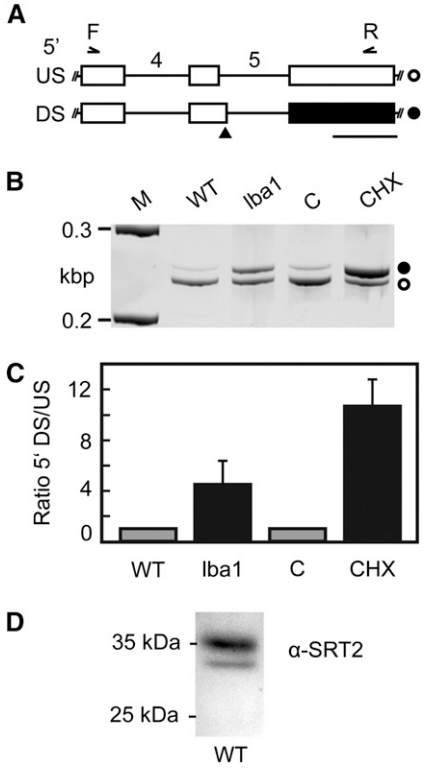

Figure 1. AS of *SRT2* precursor mRNA generates an NMD target and is regulated by polypyrimidine tract-binding protein splicing factors. A, Partial models of *SRT2* splicing variants resulting from usage of an upstream (US, top) or downstream (DS, bottom) 5′ splice site in intron 5 (introns numbered). Boxes and lines depict exons and introns, respectively. White boxes correspond to coding sequence, and black box indicates an untranslated region resulting from the introduction of a premature termination codon (black triangle) upon usage of the downstream 5′ splice site. White circle indicates SRT2 splice form 1,2,3, and 7, and black circle indicates splice form 4 and 6. Binding positions of primers used for coamplification of splicing variants in B and C are shown. Bar = length of 100 bp. B, RT-PCR analysis of AS event shown in A. For NMD impairment, *low-beta-amylase1* (*lba1*) mutant or cycloheximide (CHX) versus mock (C) treatment were analyzed. M indicates ladder with 0.2- and 0.3-kb DNA fragments. C, Quantitative analysis of splicing ratios for samples depicted in B using a bioanalyzer. Displayed are mean values (n = 3–6, ± SD). Data are normalized to the wild type (WT) or mock treatment. D, Western-blot analysis of SRT2 protein in Arabidopsis leaves.

an alternative translation start from a downstream codon. However, at the same time, the introduction of this splice site could also result in the introduction of a premature termination codon, which should result in degradation of this splicing variant by the RNA surveillance mechanism nonsense-mediated decay (NMD). To test this hypothesis, the ratio of splicing variants resulting from usage of the alternative 5′ splice sites in control and NMD-impaired samples was determined by reverse transcription (RT)-PCR (Fig. 1, B and C). Coamplification with oligonucleotides spanning the indicated region resulted in two amplification products of the expected sizes (Fig. 1B). Using the previously described missense mutant in a core NMD factor, *low-beta-amylase1* (Yoine et al., 2006), and treatment with the translation inhibitor cycloheximide, which is known to suppress NMD, a relative increase of the splicing variant derived from the downstream 5′ splice site was found, clearly supporting its NMD target identity (Fig. 1C). Hence, the open reading frame annotation in TAIR10 needs to be revised for SRT2.4 and SRT2.6. To confirm our results and to analyze the presence and localizations of the predicted protein isoforms, we performed a western-blot analysis using an SRT2-specific antibody (αSRT2) raised against the recombinant protein of the SRT2.1 splice form. The specificity of the antiserum was confirmed by the absence of the immunosignal in SRT2 knockout plants (see below; Fig. 2B). Because all predicted SRT2 proteins (TAIR10) are highly similar in the core sequence and mainly differ in their N- or C-terminal regions, all isoforms should at least theoretically be detected in the western blot in the range between 20 and 40 kD (Supplemental Fig. S1; Supplemental Table S1). However, only two protein bands were detected, with the main signal at around 36 kD (Fig. 1D). This band matches the predicted size of SRT2.1, SRT2.2, SRT2.5, and SRT2.7 with cleaved N-terminal targeting presequences (Supplemental Table S1). Hence, this mature protein isoform is referred to as SRT2A in the following. A further weaker band was detected at around 31 kD, which matches the size of the mature C-terminal short-form SRT2.3, and is subsequently referred to as SRT2B. No protein band was detected for the predicted mature protein isoforms of SRT2.4 and SRT2.6 at 25 kD, and thus the western-blot analysis confirms the absence of these protein isoforms as predicted from our NMD target analysis.

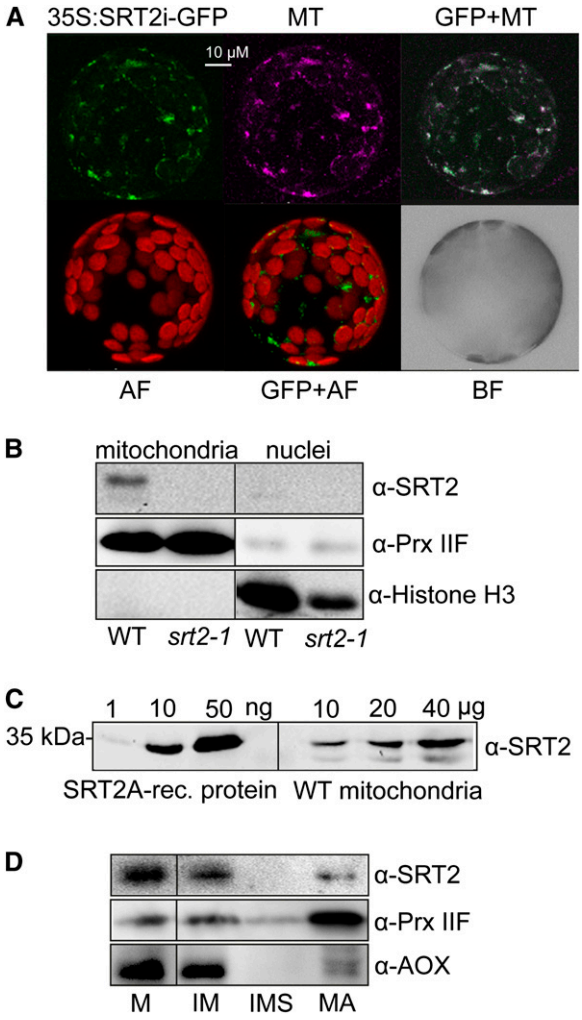

Figure 2. *SRT2*-encoded proteins localize to mitochondria in Arabidopsis. A, Arabidopsis protoplasts showing GFP localizations (green) for a full-length *SRT2* (plus introns)-GFP fusion construct (35S:SRT2i-GFP). Protoplasts were isolated from stable Arabidopsis transformants. Purple indicates the mitochondrial localization of MitoTracker (MT). GFP+MT indicates overlay image of 35S:SRT2i-GFP and MitoTracker; AF indicates autofluorescence of chloroplasts; and BF indicates bright-field image of protoplast. B, Western-blot analysis of SRT2 protein in mitochondrial and nuclear fractions. Antisera against PRX IIF was used as mitochondrial marker and histone H3 as nuclear marker, respectively. C, Western-blot analysis of SRT2 proteins in isolated mitochondria. Protein extracts of isolated mitochondria from wild-type (10, 20, and 40 μg) seedlings as well as recombinant 6× His-SRT2A protein (1, 10, and 50 ng) were analyzed by western blotting using SRT2 antiserum. D, Western-blot analysis of SRT2 protein in subfractionated Arabidopsis wild-type mitochondria. Ten micrograms of protein were loaded for each fraction. Antisera against Alternative Oxidase1 and PRX IIF were used as controls for the inner membrane and matrix proteins, respectively. M, Mitochondria; IM, inner mitochondrial membrane; IMS, intermembrane space; MA, matrix.

Arabidopsis *SRT2*-Encoded Protein Variants Are Located in Mitochondria

All annotated *SRT2* splice forms encode a predicted N-terminal presequence of different length for targeting to mitochondria (Supplemental Table S1). To determine the subcellular localization of all expressed SRT2 isoforms, the full-length genomic sequence of *SRT2* including introns and without stop codon (*SRT2i*) was cloned into the binary vector pK7WGF2 for C-terminal GFP fusion (Karimi et al., 2002). The 35S:*SRT2i*-GFP construct was stably transformed into Arabidopsis, and independent transformants were analyzed for their GFP fluorescence signal by confocal laser scanning microscopy. All transformants showed only mitochondria-localized GFP signals, which overlapped with the mitochondria- specific dye

MitoTracker Red (Invitrogen; Fig. 2A), confirming the predictions of the TargetP algorithm (Supplemental Table S1). No GFP signal was detected in the nucleus for any of the transformants (neither after transient nor stable transformation) in contrast to the report by Wang et al. (2010). We confirmed the absence of SRT2 in the nucleus and its presence in mitochondria by a western-blot analysis of enriched nuclear and mitochondrial fractions using αSRT2 and compartment specific antisera (PRX IIF for mitochondrial type II peroxiredoxin F and histone H3 for nuclei) as control, respectively (Fig. 2B). Furthermore, SRT2 was identified as fairly low-abundance protein in Arabidopsis mitochondria, with only about 0.2 ng SRT2 μg^{-1} (0.02% [w/w]) of mitochondrial protein (Fig. 2C). Further subfractionation of mitochondria into matrix, inner membrane, and intermembrane space revealed that *SRT2* is primarily localized at the inner mitochondrial membrane, while a weak signal was also detected in the matrix fraction (Fig. 2D).

Arabidopsis SRT2 Is a NAD$^+$-Dependent Lys Deacetylase

To investigate the catalytic activity of the two major SRT2 isoforms, we next overexpressed and purified both SRT2A and SRT2B proteins as N-terminally His-tagged proteins from *Escherichia coli*. A Lys-acetylated peptide of p53, which is a common substrate of different types of mammalian sirtuins, was used in a luminescence assay based on trypsin cleavage of the deacetylated peptide. Both SRT2A and SRT2B proteins were able to deacetylate the artificial p53 peptide in a concentration-dependent manner, indicating that both proteins can act as sirtuin-type deacetylases (Fig. 3A). The activity of both proteins was linear with respect to enzyme concentration in the range from 1 to 6 μg for both SRT2A and SRT2B. However, SRT2B (the C-terminally truncated form) was about 4 times less active than SRT2A (Fig. 3A). To further investigate sirtuin-specific enzyme characteristics, we tested the inhibition of both SRT2 proteins by its reaction product nicotinamide. A concentration-dependent effect of nicotinamide on SRT2 deacetylase activities was observed, which resulted in a half-maximum inhibition at about 30 mM (50% inhibition of initial activity [IC_{50}] = 29.7 mM, fitted with the solver tool of Microsoft Excel 2010) with 100 μM acetylated p53-peptide as substrate and 1 μM SRT2 enzyme (Fig. 3B). A similar nicotinamide concentration was reported for half-maximum inhibition of human poly(ADP-ribose)polymerase enzyme activity (Ungerstedt et al., 2003), while classical sirtuins usually have much higher affinities for nicotinamide as inhibitor (IC_{50} around 100 μM) under comparable reaction conditions (Schmidt et al., 2004). However, it should be noted that for competitive inhibitors, IC_{50} values are not equivalent to inhibitor constant values, and thus IC_{50} values from different enzymes are not necessarily comparable (Brandt et al., 1987).

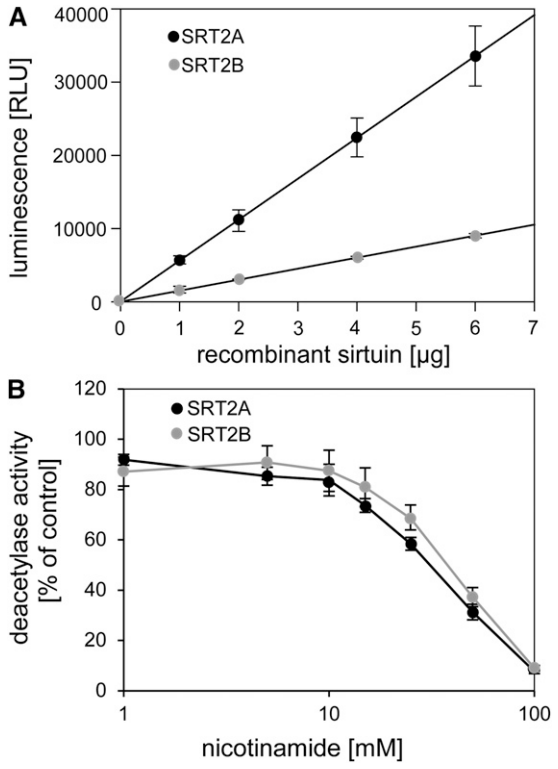

Figure 3. Arabidopsis SRT2A and SRT2B proteins possess NAD$^+$-dependent deacetylase activity. A, Linear range of SRT2A and SRT2B NAD$^+$-dependent deacetylase activities on acetylated p53 peptide using the SIRT-Glo assay (Promega). The deacetylase activities were recorded as luminescent signal from deacetylated and trypsin-digested peptides using 1 to 6 μg SRT2 recombinant proteins. B, Potency of nicotinamide concentration (1–100 mM) on SRT2A and SRT2B (1 μM each) deacetylase activities. Data are expressed as means ± SE from independent purifications of recombinant proteins ($n = 3$).

Increased Lys Acetylation of Mitochondrial Inner Membrane Complexes in *srt2-1*

To identify in vivo SRT2 protein substrates, we used the *srt2-1* knockout line (Wang et al., 2010), which is deficient in SRT2 protein (*srt2-1*; Fig. 2B), to detect changes in Lys acetylation levels of mitochondrial proteins in the mutant compared with the wild type. We also isolated a second mutant allele (*srt2-2*; Supplemental Fig. S3), which showed the same phenotype as the srt2-1 mutant, and thus *srt2-1* was used for the further experiments. Given that SRT2 is primarily located at the inner mitochondrial membrane (Fig. 2C) and changes in Lys acetylation could potentially impact protein-protein interactions and complex formation, we isolated intact protein complexes from wild-type and *srt2-1* mitochondria solubilized with digitonin and analyzed them by two-dimensional blue-native PAGE (Fig. 4). No changes in protein complex formation and composition or in protein abundances of the respiratory oxidative phosphorylation (OXPHOS) complexes were detected between the wild type and *srt2-1* (Fig. 4A). However, in the western-blot analysis using an antibody directed against acetyl-Lys, we

detected increased acetylation of the ATP synthase (complex V) subunits γ (1.9-fold ± 0.2, *n* = 6, spot 1), δ/ε (2.1-fold ± 0.6, *n* = 6, spot 2), subunit 8 (2.3-fold ± 0.7, *n* = 6, spot 3), and ATP17, which is a plant-specific subunit of the ATP synthase (10.2-fold ± 4.2, *n* = 6, spot 4) in *srt2-1* compared with the wild type (Fig. 4B; Supplemental Table S2). Furthermore, a 1.6-fold-increased Lys acetylation (1.6-fold ± 0.2, *n* = 6) of two protein complexes primarily containing the ATP/ADP carrier proteins (AAC1 to AAC3; spots 5 and 6) as well as the voltage-dependent anion channel proteins (VDAC1 to VDAC4; spots 5 and 6) were detected in the *srt2-1* mutant. However, as the VDAC proteins are localized to the outer mitochondrial membrane, it is more likely that the signal reflects the differential Lys acetylation of the AAC carrier proteins in the inner mitochondrial membrane where SRT2 is also located. To a lesser extent, the gel spot also contained two mitochondrial substrate carrier proteins of the inner mitochondrial membrane, A BOUT DE SOUFFLE (BOU; spot 6) and a di- and tricarboxylate transporter protein (spot 6; Fig. 4B; Supplemental Table S2), which possibly also partly contribute to the immune signal.

To reveal whether SRT2 is present in one of the differentially Lys-acetylated protein complexes, we detected the SRT2 protein in the two-dimensional blue-native western blot using the purified αSRT2 antibody (Fig. 4C). In agreement with the multiprotein deacetylase function of sirtuins, the SRT2 protein was not present in a specific protein complex but rather widely distributed over a whole range of protein complexes with different sizes, starting from complex I at around 1 megadalton down to smaller protein complexes of around 100 kD (Fig. 4C). As expected, the detected immune signal was absent in the *srt2-1* knockout line (Fig. 4C). Hence, the extent of Lys acetylation of the ATP synthase as well as of the protein complex containing the ATP/ADP carrier is dependent on the presence of SRT2 in plant mitochondria.

SRT2 Interacts with Several of Its Substrate Proteins

To confirm the interaction of SRT2 with the differentially Lys-acetylated protein complexes, we performed two different pull-down approaches. In the first approach,

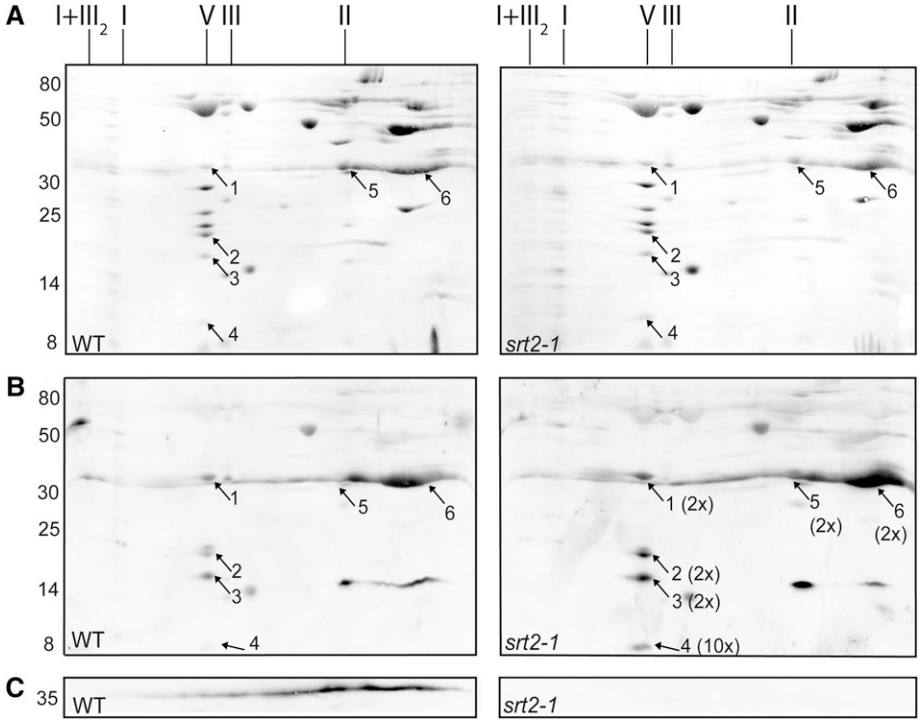

Figure 4. Differences in Lys acetylation levels in the protein complexes of wild-type (WT) and *srt2-1* mitochondria. A, PonceauS stain of wild type and *srt2-1* two-dimensional blue-native SDS-PAGE of mitochondrial protein complexes. The identity of OXPHOS complexes is indicated above the gels. The molecular mass scale (in kilodaltons) is indicated on the left. Numbers (1–6) refer to proteins identified by LC-MS/MS. ATP synthase subunit γ (1), δ/ε (2), subunit 8 (3), ATP17 (At4g30010; 4), ATP/ADP carrier proteins AAC1 to AAC3 and VDAC1 to VDAC4 (5), and ATP/ADP carrier proteins AAC1 to AAC3, VDAC1 to VDAC4, A BOUT DE SOUFFLE, and di- and tricarboxylate transporter protein (6). For a full list with protein abundances, see Supplemental Table S2. $I+III_2$, Supercomplex composed of complex I and dimeric complex III; I, complex I; V, complex V (ATP synthase); III, dimeric complex III. B, Differences in Lys acetylation levels of proteins from the wild type and *srt2-1* were detected by western-blot analysis using the anti-acetyl-Lys antibody. Numbers (1–6) refer to proteins identified by LC-MS/MS. The average fold change increase in Lys acetylation in *srt2-1* is indicated in brackets behind the numbers (*n* = 6). C, The presence and absence of SRT2 protein was detected by western-blot analysis using anti-SRT2 antiserum.

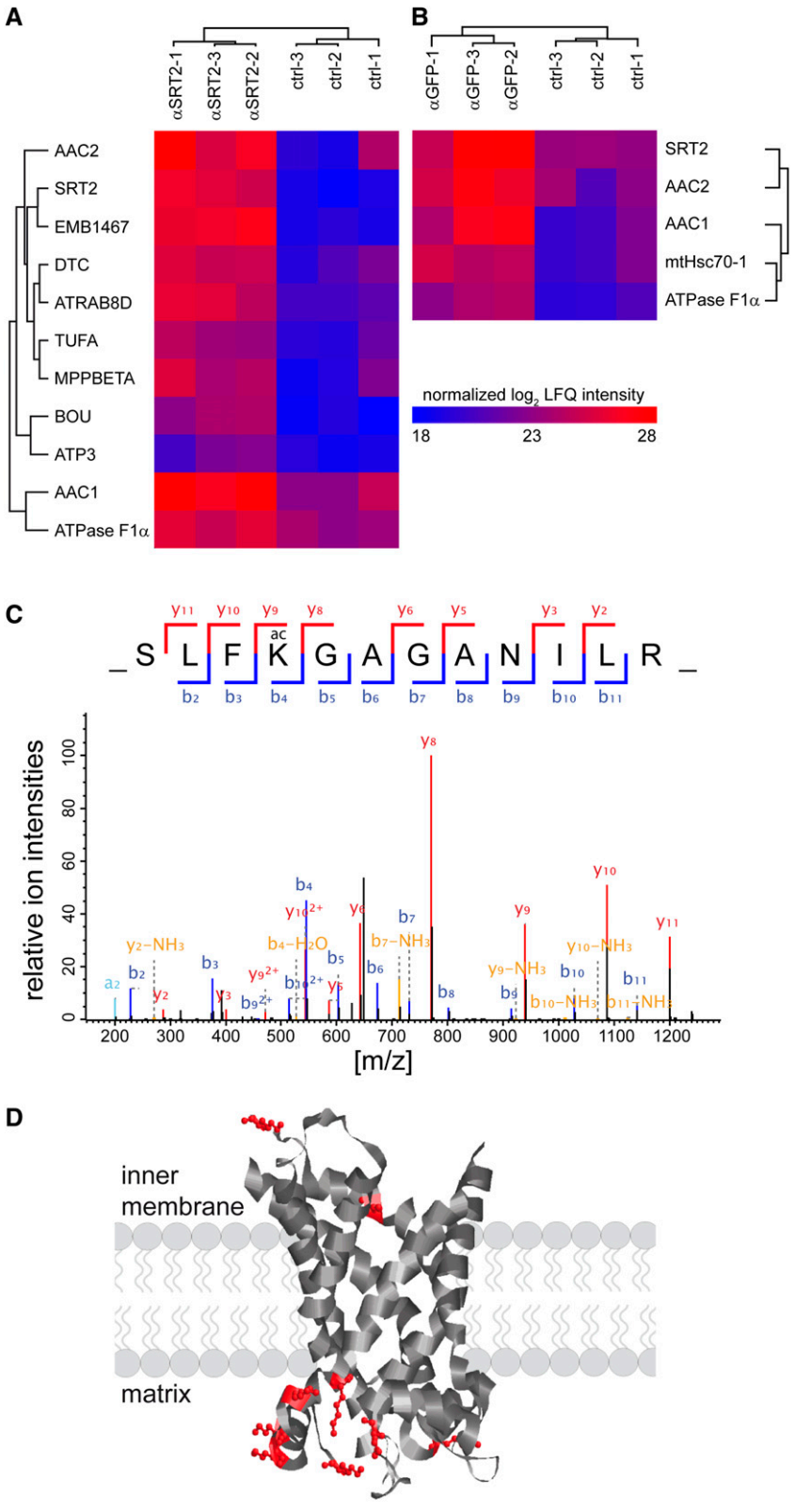

Figure 5. SRT2 interacts with several proteins of the inner mitochondrial membrane. A and B, Two-way hierarchical clustering of SRT2-interacting proteins from two different coimmunoprecipitation experiments. A, Antibody specific for Arabidopsis SRT2 (αSRT2) was incubated with mitochondrial extracts from wild-type plants ($n = 3$). B, Antibody specific for GFP (αGFP) was used on mitochondrial extracts from transgenic plants expressing a SRT2.1:GFP fusion protein (αGFP; $n = 3$). Only proteins that were significantly enriched were selected for the clustering (Student's t test with permutation-based false discovery rate < 0.05). The color code represents relative protein abundance, measured as the log-summed peptide intensities for each protein, after normalization by the label-free quantification algorithm in the MaxQuant software package. C, Tandem mass spectrometry fragmentation spectrum of the peptide containing the evolutionary conserved acetylated K345 (AAC1) site of the ATP/ADP carrier proteins. D, Scheme of the AAC1 to AAC3 protein topology in the inner mitochondrial membrane (after Klingenberg, 2008) with 11 Lys acetylation sites at the matrix- and intermembrane-exposed loops.

SRT2-interacting proteins were isolated by coimmunoprecipitation using the purified SRT2 antibody on isolated protein extracts from wild-type mitochondria (Fig. 5A). In the second approach, mitochondria from 35S:SRT2-GFP lines were isolated, and interacting proteins were copurified using GFPTrap-A beads (Chromotek; Fig. 5B). Only three different proteins were significantly enriched, alongside SRT2, in both coimmunoprecipitation approaches and identified by liquid chromatography-tandem mass spectrometry (LC-MS/MS)-based label-free quantification compared with their respective controls for background correction (Cox and Mann, 2008; Hubner et al., 2010; Fig. 5; Supplemental Table S3). Strikingly, the AAC proteins, which were significantly more Lys acetylated in *srt2-1* mitochondria (Fig. 4B), were among these proteins. Furthermore, the α subunit of the ATP synthase was more than 2-fold enriched using both approaches. Seven more proteins were identified in the αSRT2-coimmunoprecepitation analyses that were not enriched in the SRT2.1-GFP pull downs (Fig. 5; Supplemental Table S3). Among these were several additional interesting candidates, such as the 76-kD NADH dehydrogenase subunit of complex I, beta subunit of mitochondrial processing peptidase, an integral protein of complex III, which is responsible for the removal of presequences of imported precursor proteins, a GTP-binding elongation factor Tu family protein, and the member of the Ras superfamily GTPase homolog E1B, as well as three proteins, which were part of the complexes that showed increased Lys acetylation on the western blot in the *srt2-1* lines: the γsubunit of the ATP synthase, the mitochondrial carrier protein BOU, and the di- and tricarboxylate transporter (Fig. 5; Supplemental Table S3). Hence, these proteins also have to be considered as potential in vivo SRT2-interacting proteins.

To identify the actual position of the Lys acetylation sites on the SRT2-interacting proteins, we performed a further pull-down experiment using the acetyl-Lys antibody. Several of the SRT2-interacting proteins contained one or more Lys-acetylated sites (Supplemental Table S4). First and foremost, 11 Lys acetylation sites were detected on the AAC1 to AAC3 proteins (Fig. 5C; Supplemental Table S4). Nine of these sites were positioned at the loops protruding into the matrix and two into the intermembrane space. Furthermore, three Lys acetylation sites were identified on the ATP synthase complex (α and γ subunits), three sites on the di- and tricarboxylate transporter protein, and two sites on the mitochondrial heat shock protein 70-1 (Supplemental Table S4).

Mitochondrial Respiratory Control and ^{14}C-ADP Uptake Is Significantly Altered in *srt2-1* Mitochondria

Because the ATP/ADP carrier proteins (AAC1–AAC3) as well as the ATP synthase complex were identified as most robust interaction partners of SRT2 (Fig. 5) and both protein complexes also showed increased acetylation in the absence of SRT2 (Fig. 4), we tested whether the loss of SRT2 affects OXPHOS and ADP uptake of mitochondria. However, no significant changes were observed in the respiratory activities of the OXPHOS complexes I and II driven by TCA

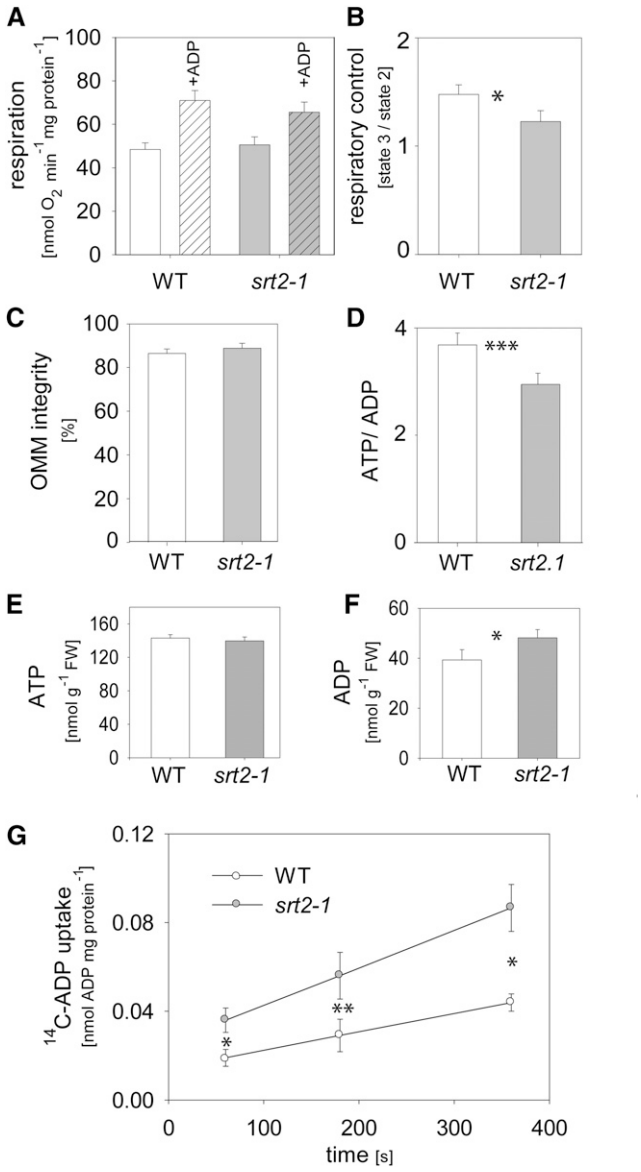

Figure 6. Loss of SRT2 affects coupling of ATP synthesis to mitochondrial respiration and ADP uptake into mitochondria. A, TCA cycle-dependent respiration (pyruvate, malate) in isolated mitochondria of wild-type (WT) and *srt2-1* seedlings. Respiratory activities were measured in state II and state III (100 μM ADP) mitochondria (n = 6, + SE). B, Respiratory control ratios calculated from respiratory activities before and after ADP addition (n = 6, ± SE). C, Integrity of the outer membrane calculated by the latency of cytochrome c oxidation before and after addition of Triton-X100 to mitochondria (n = 6, ± SE). D, ATP to ADP ratios in *srt2-1* seedlings compared with the wild type (n = 5, ± SE). E, ATP contents in *srt2-1* seedlings compared with the wild type (n = 5, ± SE). F, ADP contents in *srt2-1* seedlings compared with the wild type (n = 5, ± SE). G, Time course of ^{14}C-ADP uptake into isolated mitochondria of wild-type (white bars) and *srt2-1* seedlings (black bars; n = 5, + SE). Asterisks indicate significant difference (*$P < 0.05$, **$P < 0.01$, ***$P < 0.001$, Student's t test).

cycle-dependent malate and pyruvate oxidation (Fig. 6A). Nevertheless, the respiratory control ratio, which indicates the coupling of respiration to ATP synthesis, was significantly decreased in *srt2-1* mitochondria compared with those of the wild type (Fig. 6B). This was not due to a damage of the outer mitochondrial membrane, as the latency of cytochrome c oxidation before and after Triton-X100 addition was in both mutant and the wild type around 90% (Fig. 6C). Other explanations for a decreased coupling of respiration in the *srt2-1* mutant could be due to a decreased ATP synthase activity or an enhanced uncoupling of *srt2-1* mitochondria. When we measured the total ATP as well ADP levels in the *srt2-1* seedlings compared with the wild type, we observed a decreased ATP to ADP ratio, which was due to increased ADP but not ATP levels (Fig. 6, D–F). To test whether the mitochondrial ADP uptake rates are affected in *srt2-1*, we measured ^{14}C-ADP uptake on isolated mitochondria. Interestingly, the rate of ^{14}C-ADP uptake into *srt2-1* mitochondria was much more efficient and significantly increased compared with the wild type at each measured time point (60–360 s; Fig. 6G). In energized mitochondria, the AAC carriers usually transport matrix ATP against cytosolic ADP in a 1:1 exchange ratio, while they are unable to transport AMP (Haferkamp et al., 2002; Klingenberg, 2008). However, the AAC carrier activity is not necessarily coupled to mitochondrial ATP production, as the transport proceeds with high activity when mitochondria are completely uncoupled (Klingenberg, 2008). Hence, we conclude that SRT2 positively affects the ATP synthase activity by Lys deacetylation when NAD^+ is available as substrate, while deacetylation of the ATP/ADP carrier proteins negatively impacts their activity. In addition to increased ADP levels in *srt2-1* seedlings, also Gln and Gly levels were increased, while several metabolites of central metabolism, such as sugars (Fru, Glc, erythritol, and myoinositol), as well as some amino acids (Ser, Pro, Arg, Thr, Tyr, and Ala) and organic acids (shikimate, ascorbate, pyruvate, fumarate, and γ-aminobutyrate), were significantly decreased in abundance (Fig. 7A; Supplemental Table S5). Hence, SRT2 is most likely involved in the fine regulation of mitochondrial energy metabolism and thus indirectly also affects up- and downstream metabolic pathways in Arabidopsis (Fig. 7B).

DISCUSSION

Herein, we established that Arabidopsis SRT2 functions as mitochondrial Lys deacetylase, and we identified its first substrates and interaction partners. While mammalian mitochondria contain three different types of sirtuins (SIRT3–SIRT5) with very diverse physiological functions (Verdin et al., 2010), the Arabidopsis genome only encodes a single sirtuin gene (SRT2) for mitochondrial targeting. According to the latest Arabidopsis genome annotation (TAIR10), SRT2 potentially expresses seven protein isoforms. Here, we have demonstrated that the two nearly identical splice forms *SRT2.4* and *SRT2.6*, which are generated from an AS site in intron five, are both targets of NMD. Furthermore, we did not observe proteins corresponding to these two splicing variants in the western-blot analysis (Fig. 1) nor have we detected any of their sequence-specific peptides in the LC-MS/MS analysis (Supplemental Fig. S1).

The Native Arabidopsis SRT2 Isoforms Are 31 and 36 kD in Size and Are Localized in Mitochondria

All of the annotated SRT2 protein isoforms contain N-terminal presequences predicted for mitochondrial targeting (Supplemental Table S1). The subcellular localization analysis using a C-terminal GFP fusion to the SRT2 gene containing introns confirmed the mitochondrial localization of all expressed SRT2 isoforms (Fig. 2A). Importantly, we detected no nuclear GFP signal for SRT2, although Wang et al. (2010) exclusively observed a nuclear localization for SRT2 (Pandey et al., 2002). Furthermore, we confirmed the mitochondrial localization of the native SRT2 protein by western-blot analysis and in pull-down experiments using isolated mitochondria (Fig. 2; Supplemental Table S3). Two immune-reactive protein bands of 31 and 36 kD in size, respectively, were detected in our western-blot analysis (Figs. 1D and 2B). These two protein bands were named SRT2A and SRT2B, respectively, as they fitted to the size of the predicted processed isoforms of SRT2.1/SRT2.2/SRT2.5/SRT2.7 and SRT2.3 after removal of their presequences (Supplemental Table S1). The native SRT2 peptides identified in the LC-MS/MS analysis of the coimmunoprecipitation experiment further support this observation (Supplemental Fig. S1). Hence, we conclude that there are two mature SRT2 proteins present in plant mitochondria, which mainly differ in their C-terminal part.

The Arabidopsis Class II Sirtuin Is a Protein Deacetylase

Having confirmed that SRT2 is present in two isoforms in plant mitochondria, the question emerged what enzymatic activity these two isoforms have, because Arabidopsis sirtuins were to date merely annotated on the basis of sequence homology. Comparison of the amino acid sequence of the Arabidopsis SRT2 proteins to the mammalian sirtuins revealed that SRT2 shares the highest homology with human SIRT4 (42% amino acid sequence identity), followed by 31% identity with hSIRT3 and 25% identity with hSIRT5 (Supplemental Fig. S4). Because the true enzymatic function of the mammalian SIRT4 is still under debate (Feldman et al., 2012; Newman et al., 2012), we purified the two mature SRT2A and SRT2B proteins as N-terminally His-tagged proteins upon heterologous expression in *E. coli*. Strikingly, SRT2A and, to a slightly lesser extent, SRT2B were active as protein Lys deacetylases (Fig. 3).

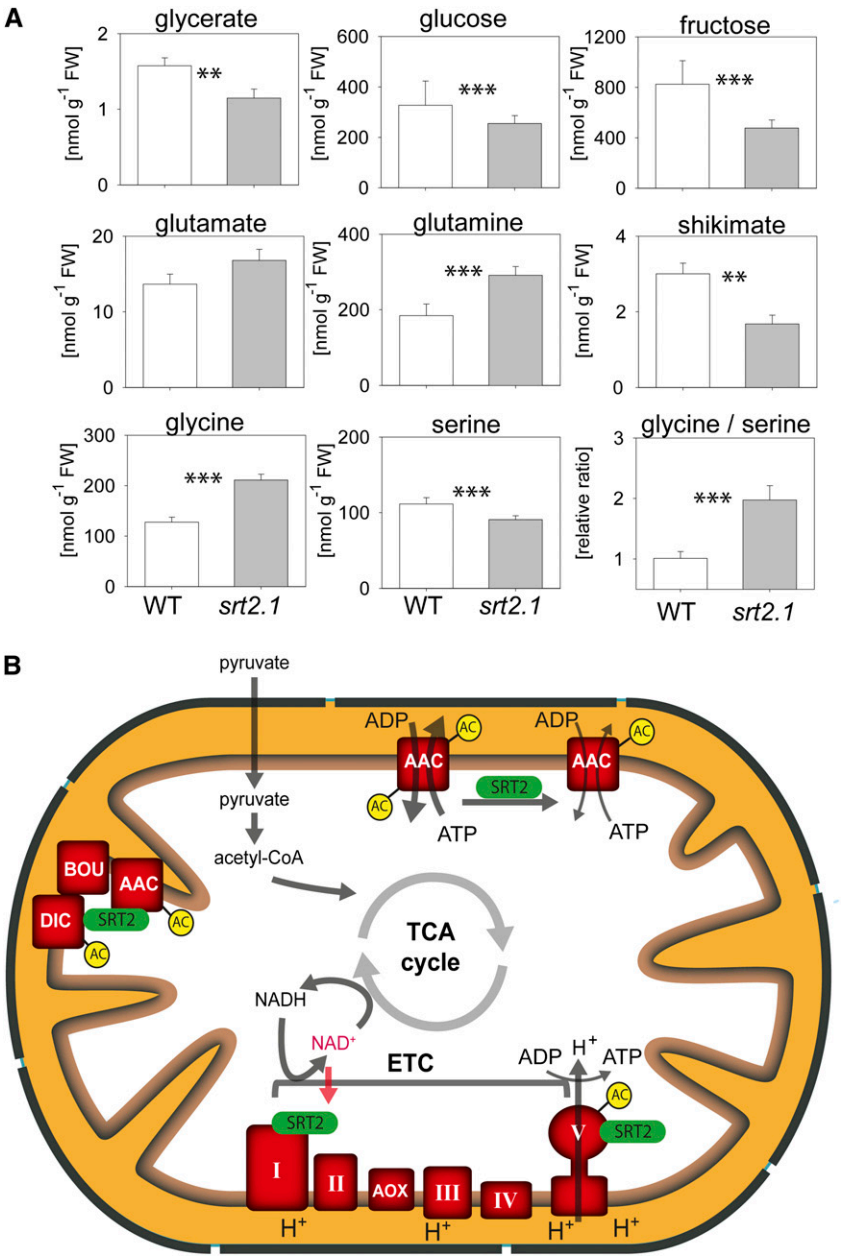

Figure 7. Metabolic phenotype of SRT2 knockout line and simplified working model for SRT2 functions in plant mitochondria. A, Metabolite contents in *srt2-1* compared with the wild type (WT; $n = 5$, ± SE). The full list of metabolites including the absolute values can be found in Supplemental Table S5. Asterisks indicate significant differences ($^*P < 0.05$, $^{**}P < 0.01$, $^{***}P < 0.001$, Student's t test). B, SRT2 is dependent on NAD^+ as substrate and interacts with the 76-kD subunit of complex I. SRT2 interacts and most likely deacetylates the ATP synthase (complex V) as well as a complex containing the AAC proteins AAC1 to AAC3, the putative di-and tricarboxylate transporter (DIC), and the metabolite transporter BOU. Lys acetylation sites of SRT2 interaction partners are indicated (AC). [See online article for color version of this figure.]

SRT2 Interacts with Proteins of the Inner Mitochondrial Membrane Involved in Energy Metabolism and Metabolite Transport

In subfractionated Arabidopsis mitochondria, most of the SRT2 immunosignal was detected to be present in the inner membrane fraction and to a lesser extent in the matrix (Fig. 2). Given that the SRT2 protein contains no membrane-spanning domain, we assume that SRT2 is associated with the inner membrane via protein-protein interactions. Several of our identified interaction partners of SRT2 are integral proteins of the inner mitochondrial membrane, such as the ATP/ADP carriers, beta subunit of mitochondrial processing peptidase, and the metabolite carrier BOU, a putative carboxylate transporter, as well as two matrix-exposed subunits of the ATP synthase (complex V) and the 76-kD matrix-exposed complex I subunit (Fig. 5). Although we did not identify a Lys acetylation site on the 76-kD subunit of the Arabidopsis complex I in *srt2-1* mitochondria (Supplemental Table S4) and complex I-dependent respiration was not affected in the mutant (Fig. 6A), it is possible that the constitutive knockout plants have been partially adapted to loss of SRT2. Binding of SRT2 to complex I is anyhow interesting, as the activity of sirtuins is generally regulated by its substrate NAD^+. Thus, SRT2 could possibly act in concert with an active complex I oxidizing NADH. The interaction of

SRT2 with complex V subunits is interesting because Arabidopsis SRT2 knockout mutant showed a decreased coupling of mitochondrial respiration to ATP synthesis, which indicates a decreased activity of complex V and which could explain the decreased in vivo Glc and Fru levels due to decreased respiratory energy conversion. Although total ATP levels were not changed, as a decrease in mitochondrial ATP production can possibly be compensated for by photosynthesis, the total ADP contents were increased, suggesting an adaptation of the cellular metabolism to the loss of SRT2. Similar observations were recently also reported for human cells deficient in SIRT4. Knockdown of SIRT4 in Human Embryonic Kidney 293 cells resulted in increased ADP/ATP ratios, while overexpression of SIRT4 showed the opposite effect (Ho et al., 2013). Furthermore, Ho et al. (2013) demonstrated that the activity of the mitochondrial ATP synthase was not affected by the loss of SIRT4 but that uncoupling of mitochondria was increased. Interestingly, uncoupling of respiration was relieved when the ATP/ADP carrier ADP/ATP Translocase2 was knocked down simultaneously with SIRT4 (Ho et al., 2013). However, Lys acetylation levels of mitochondrial proteins were not investigated in that study. It will be interesting to find out whether knockdown of the AAC carriers in the Arabidopsis *srt2-1* background would have a similar effect.

The AAC Carriers as Well as the ATP Synthase Complexes Are the Major Targets of SRT2-Dependent Deacetylation in Arabidopsis Mitochondria

Two recent studies identified the first organellar Lys-acetylated proteins in Arabidopsis (Finkemeier et al., 2011; Wu et al., 2011). Among these proteins were several plastidial proteins but only a few mitochondrial proteins, such as cytochrome c, the α subunit of the ATP synthase complex, and AAC1. Here, we detected several additional mitochondrial Lys-acetylated proteins in western-blot analysis of the two-dimensional blue-native PAGE as well as in the protein pull downs of the SRT2-interacting proteins (Fig. 7; Supplementary Table S3). The most prominent Lys-acetylated proteins we detected were several subunits of the ATP synthase complex as well as two protein complexes containing the AAC carrier proteins AAC1 to AAC3. These protein complexes were also significantly increased in Lys acetylation in *srt2-1* compared with the wild type (Fig. 4). Hence, we conclude that Arabidopsis SRT2 has very specific target proteins for deacetylation and that it does not act as universal mitochondrial protein deacetylase such as SIRT3 in mammalian mitochondria (Lombard et al., 2007; Rardin et al., 2013). Loss of mammalian SIRT3 results in the hyperacetylation of mitochondrial proteins, which is not observed upon deletion of the mouse mitochondrial SIRT4 and SIRT5 (Lombard et al., 2007). Similarly, no overall hyperacetylation of mitochondrial proteins was observed upon deletion of Arabidopsis SRT2 in our study.

The Activity of the ATP/ADP Carrier Proteins Is Dependent on SRT2

AAC carrier proteins have a central role in energy metabolism in eukaryotic cells, as they are the gateways for ATP supply to the cytosol (Haferkamp et al., 2011). Here, we identified 11 acetylation sites on the ATP/ADP carrier proteins AAC1 to AAC3 (Supplemental Table S4). Interestingly, the ADP/ATP carrier 2 was previously also identified as interacting protein of human SRT4-FLAG protein (Ahuja et al., 2007). However, Ahuja et al. (2007) did not investigate whether this interaction affected the acetylation status of ADP/ATP carrier. The AAC carrier proteins are highly conserved in sequence between species, and according to the topology model of Klingenberg (2008), most of the acetylated Lys residues can be found in the matrix-exposed loops (Fig. 5D). Only two of the identified acetylated Lys residues reside in the loops exposed to the intermembrane space. Seven of the 11 acetylated Lys residues are highly conserved between species and were also shown to be Lys acetylated in yeast, rat, mouse, and human tissue, respectively (Supplemental Fig. S5; Choudhary et al., 2009; Weinert et al., 2011; Henriksen et al., 2012; Lundby et al., 2012; Sol et al., 2012). Furthermore we detected a 1.6- to 2-fold increase in Lys acetylation of the AAC carriers in the *srt2* mutants (Fig. 4). In addition, Lys acetylation levels of three of the matrix-exposed sites were recently identified as highly increased (up to 9-fold) in SIRT3 –/– mice (Rardin et al., 2013), confirming that the AAC proteins are universal targets of sirtuins in different species. While it has reported nearly 20 years ago that fatty acids can induce an uncoupling of the ATP/ADP carriers (Brustovetsky and Klingenberg, 1994), to our knowledge, no study has yet investigated whether Lys acetylation affects the activity of these carriers. Here, we have demonstrated that an increased Lys acetylation correlated with an increased ^{14}C-ADP uptake rate in *srt2-1* mitochondria (Fig. 6G), indicating that SRT2 regulates the Lys acetylation level and activity of the carrier proteins.

In summary, we have shown that Arabidopsis SRT2 is a mitochondrial Lys deacetylase acting on specific target proteins of the inner membrane such as the ATP synthase and the ATP/ADP carriers (Fig. 7B). Although loss of SRT2 resulted neither in major structural changes of the OXPHOS complex nor in differences in the activities of the mitochondrial electron transport complexes I and II, it did cause a decreased coupling of the ATP synthase complex as well as an increase of the mitochondrial ADP uptake via the ATP/ADP carrier proteins, thereby contributing to fine-tuning of mitochondrial energy metabolism.

MATERIALS AND METHODS

Plant Material and Growth Conditions

For mitochondria isolation, Arabidopsis (*Arabidopsis thaliana*; ecotype Columbia [Col-0]) seedlings were grown in liquid culture as described in Morgan

et al. (2008). For growth on plates, Arabidopsis seeds were treated and grown the same way except that the medium was supplemented with 0.8% (w/v) phytoagar. For translation inhibition, 11-d-old seedlings were transferred to liquid one-half Murashige and Skoog medium containing 2% (w/v) Suc and 10 μg mL^{-1} cycloheximide and incubated for 4 h at room temperature (equivalent treatment for mock, but in absence of drug; Drechsel et al., 2013).

The *srt2-1* (SALK_131994.45.80) and *srt2-2* (SALK_149295.52.35) lines were obtained from the SALK collection (Ungerstedt et al., 2003). The screening for homozygous transfer DNA insertion lines was performed as described before (Finkemeier et al., 2005). Primer sequences are listed in Supplemental Table S6.

Plant Transformation

All vector constructs were verified by sequencing and transformed into *Agrobacterium tumefaciens* strain C58 followed by floral-dip transformation of Arabidopsis (Col-0) plants (Clough and Bent, 1998). Transformants were selected by germination of seeds on Murashige and Skoog-agar plates containing kanamycin (85 μM). Resistant plants were transferred to soil and propagated.

RNA Isolation and RT-PCR

Total RNA isolation and on-column DNaseI treatment was performed using the Universal RNA Purification Kit (EURx), according to the manufacturer's instructions. Avian Myeloblastosis Virus reverse transcriptase native (EURx) was used for RT with dT_{20}, followed by PCR amplification with listed oligonucleotides (Supplemental Table S6). RT-PCR products were run on 2% (w/v) agarose Tris-acetate (40 mM Tris, 20 mM acetate, 1 mM EDTA, pH 8.0) or 12% (w/v) native polyacrylamide gels (Tris-Gly native running buffer) and visualized by UV illumination upon ethidium bromide staining.

Analyses of AS Patterns

SRT2 splicing variants, derived from alternative 5′ splice site usage in intron 5, were PCR amplified from complementary DNA (primer sequences listed in Supplemental Table S6). PCR products had the expected sizes of 231 and 242 bp upon usage of the up- and downstream 5′ splice site, respectively. For PCR product quantitation, samples were analyzed with DNA 1000 chips using the Agilent 2100 Bioanalyzer according to the manufacturer's instructions. For sequence confirmation, RT-PCR products were cloned into pGEM-T vector (Promega) and sequenced (Eurofins).

GFP Construct

35S:*SIR2i*-GFP fusion construct was generated using the Gateway cloning system (Invitrogen) according to the manufacturer's protocols. Entry clones were generated with the pENTR/SD/TOPO (Invitrogen) vector. For C-terminal GFP fusion, the TAIR10 annotated genomic sequence of *SIR2.7* was amplified from Arabidopsis (Col-0) DNA using primers lacking stop codons as listed in Supplemental Table S6. LR reactions for in-frame recombination into pK7FWG2 vector (GFP fusion) were performed as described before (Karimi et al., 2002).

Protoplast Isolation and Confocal Laser Scanning Microscopy

Protoplast isolation was performed from 4-week-old Arabidopsis leaves after the tape sandwich method described by Wu et al. (2009). Staining with 200 nM MitoTracker Red (Invitrogen) was performed according to the manufacturer's protocol. Imaging was performed with a spectral TCS SP5 MP confocal laser scanning microscope (Leica Microsystems) using an argon and DPSS laser, respectively, at an excitation wavelength of 488 (eGFP) and 561 nm (MitoTracker Red). The water immersion objective lens HCX PL APO 20.0 × 0.70 IMM UV was used for imaging in multitrack mode with line switching. eGFP and MitoTracker Red fluorescence was measured at 500 to 530 nm and 620 to 660 nm, respectively.

Heterologous Expression and Purification of Recombinant SRT2 Proteins

SRT2A and SRT2B complementary DNAs were amplified by PCR excluding the coding region for the 47-amino acid signal peptide. Primer sequences are listed in Supplemental Table S6. The PCR product was cloned after restriction digestion with *Bam*HI and *Sal*I in frame into the pQE30 vector (Qiagen), which allows expression and purification of the recombinant, N-terminally 6× His-tagged protein. Expression and purification of the recombinant protein were performed in BL21* cells (Invitrogen) as described in Finkemeier et al. (2005). Vector constructs were verified by sequencing.

Sirtuin Activity Assay

The SRT2 activity assay was performed as described in the manufacturer's protocol of the SIRT-Glo assay (Promega) using 1 to 6 μg of recombinant SRT2 per reaction.

Antiserum Production

For antiserum production, a rabbit was immunized with 850 μg heterologously expressed and gel-purified SRT2A protein (Pineda). The antiserum was affinity purified against SRT2A protein after the protocol described in Tran et al. (2012).

Western-Blot Analyses

Proteins were blotted onto a nitrocellulose membrane and incubated overnight with primary antibodies as indicated in the text. Secondary anti-horseradish peroxidase antibody (ThermoFisher Scientific) was used in a 1:2,000 dilution followed by detection with SuperSignal West Dura enhanced chemiluminescent substrate (ThermoFisher Scientific).

Isolation of Organelles

Mitochondria were isolated from 10-d-old Arabidopsis seedlings grown in liquid cultures as described before (Morgan et al., 2008). The integrity of the outer membrane was determined by the latency of cytochrome c oxidation before and after addition of Triton-X100 (Sweetlove et al., 2007). Subfractionation of mitochondria was performed as described in detail in Finkemeier et al. (2005). Nuclei were isolated from 4-week-old Arabidopsis leaves as described previously (van Blokland et al., 1997).

Respiratory Measurements

Measurements of mitochondrial respiration were performed at 20°C in a Clark-type oxygen electrode (Oxygraph; Hansatech Instruments) in a basic medium (0.3 M mannitol, 5 mM KH_2PO_4, 3 mM $MgSO_4$, 10 mM KCl, 0.1% [w/v] bovine serum albumin, pH 7.5) containing 10 mM pyruvate, 10 mM malate, 100 μM thiamine pyrophosphate, and 300 μM NAD^+ as described before (Sweetlove et al., 2002). Oxygen consumption was recorded before and after addition of 1 mM ADP.

^{14}C-ADP Uptake into Isolated Mitochondria

The uptake of ^{14}C-ADP into isolated mitochondria was performed with slight modifications as described in Winkler et al. (1968) and Haferkamp et al. (2002). Mitochondrial protein (0.6 mg) was incubated for 5 min in the basic medium (0.3 M mannitol, 5 mM KH_2PO_4, 3 mM $MgSO_4$, 10 mM KCl, 0.1% [w/v] bovine serum albumin, pH 7.5) containing 5 mM Gly, 10 mM malate, and 10 mM pyruvate to energize mitochondria. ^{14}C-labeled ADP (0.1 μCi mL^{-1}) was added together with unlabeled ADP to the sample in a final concentration of 0.2 mM. Samples were taken from the reaction precisely at the indicated time and rapidly separated from media by vacuum filtration on a filter (pore size, 0.22 μm; Millipore). The mitochondria were subsequently washed twice with basic medium. Incorporated radiolabel was determined by liquid scintillation counting.

ATP and ADP Contents

ATP and ADP contents of seedlings were determined luminometrically using the KinaseGlo reagent (Promega) for detection of ATP. Extraction of metabolites was performed as described before (Finkemeier et al., 2005). ADP was converted to ATP for 1 h at 37°C by addition of 1 μg pyruvate kinase (Sigma) and 32 mM phospho*enol*pyruvate to the pH-adjusted (pH 7.5) metabolite extract.

Primary Metabolite Profiling by Gas Chromatography-Mass Spectrometry

Metabolite extraction, derivatization, and relative metabolite levels were determined using an established gas chromatography-mass spectrometry protocol as described previously (Roessner et al., 2001; Lisec et al., 2006). Metabolites were identified by comparison to database entries of authentic standards (Kopka et al., 2005; Schauer et al., 2005).

Two-Dimensional Blue-Native SDS-PAGE

Freshly isolated mitochondria (750 μg protein) were sedimented by centrifugation for 10 min at 23,700*g*. The pellet was resuspended in 75 μL of digitonin solubilization buffer. Blue-native gel electrophoresis and second gel dimension was carried out in a standard dual cooled gel electrophoresis chamber (Hoefer) with a gel dimension of 18 × 16 cm as described in Klodmann et al. (2011). Gels were either transferred to nitrocellulose membranes for western-blot analysis or stained with Coomassie colloidal blue. Protein spots were excised from gels and trypsin digested as described before (Morgan et al., 2008) and analyzed using LC-MS/MS as described below.

Protein Coimmunoprecipitation

For GFP coimmunoprecipitation, mitochondria isolated from full-length SRT2.1-GFP and SRT2.7-GFP (SRT2.7 presequence 1–67 amino acids; control) seedlings were sedimented and resuspended in immunoprecipitation buffer (50 mM Tris, pH 7.5, 150 mM NaCl, 10% [v/v] glycerol, 2 mM EDTA, 5 mM dithiothreitol, 1% [v/v] Triton-X100, 1 mM phenylmethylsulfonylfluoride, and protease inhibitor cocktail tablets [Roche]). The extract was precleared on Sepharose beads and subjected to immunoprecipitation with GFP-Trap Beads (Chromotek) overnight at 4°C. After incubation, the supernatant was discarded, and beads were washed thoroughly using IP buffer. Proteins were eluted using 0.1% (v/v) trifluoroacetic acid.

For antibody coimmunoprecipitation, affinity-purified SRT2 and citrate synthase (control) antibodies were covalently bound to protein A Sepharose (Invitrogen). Coimmunoprecipitation of SRT2 and interacting proteins was carried out as described above except that mitochondria isolated from wild-type seedlings were used. The eluted proteins were trypsin digested and analyzed by LC-MS/MS as described below.

Enrichment of Lys-Acetylated Peptides

Lys-acetylated peptides were enriched from trypsin-digested mitochondrial proteins as described before (Finkemeier et al., 2011).

Trypsin Digestion and LC-MS/MS Data Acquisition and Analysis

Proteins were denatured in 6 M urea/2 M thiourea, reduced with 1 mM dithiothreitol, and alkylated with 5 mM iodoacetamide. Proteins were digested overnight using 1 μg proteomics-grade trypsin (Roche) at 37°C. Digestion was stopped with 1% (w/v) formic acid. Peptides were desalted using Sep-Pak C18 cartridges (Waters), and peptide-containing eluates were evaporated using a speed vac. Dried peptides were redissolved in 2% (v/v) acetonitrile and 0.1% (v/v) trifluoroacetic acid before analysis. Samples were analyzed using either a Rheos Allegro UPLC (Flux Instruments) or an EASY-nLC 1000 (Thermo Fisher) coupled to an LTQ-Orbitrap XL or an Orbitrap Elite Mass Spectrometer (Thermo Fisher), respectively. Peptides were separated on 15-cm fritless, self-pulled fused silica emitters (15 cm × 0.75 μm) and packed in house with reversed-phase ReproSil-Pur C18-AQ 3-μm beads resin (Dr. Maisch GmbH). Peptides (1 μg for coimmunoprecipitations, 0.5 μg for blue-native PAGE gel spots) were loaded on the column and eluted for 120 min using a segmented linear gradient of 3% to 95% solvent B (80% [v/v] acetonitrile, 0.5% [v/v] acetic acid) at a flow rate of 250 nL min^{-1}. Survey full-scan mass spectra were acquired in the Orbitrap analyzer. The scanned mass range was 300 to 1,650 *m/z*, at a resolution of 60.000 (Orbitrap XL) or 120.000 (Elite) at 400 *m/z*, respectively, and the seven (Orbitrap XL) or 20 (Elite) most intense ions were sequentially isolated, fragmented (collision-induced dissociation at 35 eV), and measured in the linear ion trap. Peptides with a charge of +1 or with unassigned charge state were excluded from fragmentation for tandem mass spectrometry, and dynamic exclusion of maximum 500 *m/z* values prevented repeated selection of selected masses for 90 s. Ions were accumulated to a target value of 10^6 for full Fourier transform-mass spectrometry in the Orbitrap and of 10^4 for tandem mass spectrometry in the linear ion trap.

Raw data were processed using MaxQuant software (version 1.3.0.5; http://www.maxquant.org/; Cox and Mann, 2008) and searched against The Arabidopsis Information Resource protein database (build TAIR10_pep_20101214; ftp://ftp.arabidopsis.org/home/tair/Proteins/TAIR10_protein_lists/), with trypsin specificity and a maximum of two missed cleavages at a protein and peptide false discovery rate of 1%. Carbamidomethylation of Cys residues were set as fixed, and oxidation of Met, N-terminal acetylation, and Lys acetylation were set as variable modifications. Label-free quantitation of coimmunoprecipitated proteins was also performed in MaxQuant, and subsequent quantitative statistical analyses were conducted similar to the method described by Hubner et al. (2010) in Perseus (version 1.3.0.4, http://www.maxquant.org/), using the parameters specified in Supplemental Table S7.

Sequence data from this article can be found in the GenBank/EMBL data libraries under accession number SRT2 (At5g09230).

Supplemental Data

The following materials are available in the online version of this article.

Supplemental Figure S1. Amino acid sequence alignment of the seven annotated SRT2 isoforms of Arabidopsis (TAIR10).

Supplemental Figure S2. Precursor mRNA of *SRT2* is subject to alternative spicing.

Supplemental Figure S3. Characterization of SRT2 knockout lines.

Supplemental Figure S4. Amino acid sequence alignment of the different protein isoforms of Arabidopsis SRT2 with the mitochondrial human sirtuins (HsSIRT3, HsSIRT4, and HsSIRT5).

Supplemental Figure S5. Lys acetylation sites on the ADP/ATP translocator proteins AAC1 to AAC3.

Supplemental Table S1. Characteristics of putative proteins encoded by the seven *SRT2* splice forms as annotated in TAIR10.

Supplemental Table S2. Proteins identified from excised spots from two-dimensional blue-native SDS PAGE (Fig. 7) as determined by LC-MS/MS.

Supplemental Table S3. Significantly enriched proteins in label-free coimmunoprecipitation experiments.

Supplemental Table S4. Lys acetylation sites of proteins.

Supplemental Table S5. Full gas chromatography-mass spectrometry metabolite profile of shoot material from wild-type and *srt2-1* seedlings.

Supplemental Table S6. Primer list.

Supplemental Table S7. MaxQuant settings for data analysis and label-free quantification.

ACKNOWLEDGMENTS

We thank Axel Imhof (Ludwig-Maximilians-Universität Munich) for measuring time at the LTQ Orbitrap when the machine at the Ludwig-Maximilians-Universität biocenter was defective.

Received November 12, 2013; accepted January 10, 2014; published January 14, 2014.

LITERATURE CITED

Ahuja N, Schwer B, Carobbio S, Waltregny D, North BJ, Castronovo V, Maechler P, Verdin E (2007) Regulation of insulin secretion by SIRT4, a mitochondrial ADP-ribosyltransferase. J Biol Chem **282:** 33583–33592

Brandt RB, Laux JE, Yates SW (1987) Calculation of inhibitor Ki and inhibitor type from the concentration of inhibitor for 50% inhibition for Michaelis-Menten enzymes. Biochem Med Metab Biol **37:** 344–349

Brustovetsky N, Klingenberg M (1994) The reconstituted ADP/ATP carrier can mediate H+ transport by free fatty acids, which is further stimulated by mersalyl. J Biol Chem **269:** 27329–27336

Choudhary C, Kumar C, Gnad F, Nielsen ML, Rehman M, Walther TC, Olsen JV, Mann M (2009) Lysine acetylation targets protein complexes and co-regulates major cellular functions. Science **325:** 834–840

Clough SJ, Bent AF (1998) Floral dip: a simplified method for *Agrobacterium*-mediated transformation of *Arabidopsis thaliana*. Plant J **16:** 735–743

Cox J, Mann M (2008) MaxQuant enables high peptide identification rates, individualized p.p.b.-range mass accuracies and proteome-wide protein quantification. Nat Biotechnol **26:** 1367–1372

Drechsel G, Kahles A, Kesarwani AK, Stauffer E, Behr J, Drewe P, Rätsch G, Wachter A (2013) Nonsense-mediated decay of alternative precursor mRNA splicing variants is a major determinant of the *Arabidopsis* steady state transcriptome. Plant Cell **25:** 3726–3742

Du J, Zhou Y, Su X, Yu JJ, Khan S, Jiang H, Kim J, Woo J, Kim JH, Choi BH, et al (2011) Sirt5 is a NAD-dependent protein lysine demalonylase and desuccinylase. Science **334:** 806–809

Feldman JL, Dittenhafer-Reed KE, Denu JM (2012) Sirtuin catalysis and regulation. J Biol Chem **287:** 42419–42427

Finkemeier I, Goodman M, Lamkemeyer P, Kandlbinder A, Sweetlove LJ, Dietz KJ (2005) The mitochondrial type II peroxiredoxin F is essential for redox homeostasis and root growth of *Arabidopsis thaliana* under stress. J Biol Chem **280:** 12168–12180

Finkemeier I, Laxa M, Miguet L, Howden AJ, Sweetlove LJ (2011) Proteins of diverse function and subcellular location are lysine acetylated in Arabidopsis. Plant Physiol **155:** 1779–1790

Guarente L (2011) The logic linking protein acetylation and metabolism. Cell Metab **14:** 151–153

Haferkamp I, Fernie AR, Neuhaus HE (2011) Adenine nucleotide transport in plants: much more than a mitochondrial issue. Trends Plant Sci **16:** 507–515

Haferkamp I, Hackstein JHP, Voncken FGJ, Schmit G, Tjaden J (2002) Functional integration of mitochondrial and hydrogenosomal ADP/ATP carriers in the *Escherichia coli* membrane reveals different biochemical characteristics for plants, mammals and anaerobic chytrids. Eur J Biochem **269:** 3172–3181

Haigis MC, Mostoslavsky R, Haigis KM, Fahie K, Christodoulou DC, Murphy AJ, Valenzuela DM, Yancopoulos GD, Karow M, Blander G, et al (2006) SIRT4 inhibits glutamate dehydrogenase and opposes the effects of calorie restriction in pancreatic beta cells. Cell **126:** 941–954

Hartl M, Finkemeier I (2012) Plant mitochondrial retrograde signaling: post-translational modifications enter the stage. Front Plant Sci **3:** 253

Henriksen P, Wagner SA, Weinert BT, Sharma S, Bacinskaja G, Rehman M, Juffer AH, Walther TC, Lisby M, Choudhary C (2012) Proteome-wide analysis of lysine acetylation suggests its broad regulatory scope in *Saccharomyces cerevisiae*. Mol Cell Proteomics **11:** 1510–1522

Ho L, Titus AS, Banerjee KK, George S, Lin W, Deota S, Saha AK, Nakamura K, Gut P, Verdin E, et al (2013) SIRT4 regulates ATP homeostasis and mediates a retrograde signaling via AMPK. Aging **5:** 835–849

Hollender C, Liu Z (2008) Histone deacetylase genes in Arabidopsis development. J Integr Plant Biol **50:** 875–885

Houtkooper RH, Pirinen E, Auwerx J (2012) Sirtuins as regulators of metabolism and healthspan. Nat Rev Mol Cell Biol **13:** 225–238

Hubner NC, Bird AW, Cox J, Splettstoesser B, Bandilla P, Poser I, Hyman A, Mann M (2010) Quantitative proteomics combined with BAC TransgeneOmics reveals in vivo protein interactions. J Cell Biol **189:** 739–754

Karimi M, Inzé D, Depicker A (2002) GATEWAY vectors for *Agrobacterium*-mediated plant transformation. Trends Plant Sci **7:** 193–195

Klingenberg M (2008) The ADP and ATP transport in mitochondria and its carrier. Biochim Biophys Acta **1778:** 1978–2021

Klodmann J, Senkler M, Rode C, Braun HP (2011) Defining the protein complex proteome of plant mitochondria. Plant Physiol **157:** 587–598

Kopka J, Schauer N, Krueger S, Birkemeyer C, Usadel B, Bergmüller E, Dörmann P, Weckwerth W, Gibon Y, Stitt M, et al (2005) GMD@CSB.DB: the Golm Metabolome Database. Bioinformatics **21:** 1635–1638

Laurent G, German NJ, Saha AK, de Boer VC, Davies M, Koves TR, Dephoure N, Fischer F, Boanca G, Vaitheesvaran B, et al (2013) SIRT4 coordinates the balance between lipid synthesis and catabolism by repressing malonyl CoA decarboxylase. Mol Cell **50:** 686–698

Lisec J, Schauer N, Kopka J, Willmitzer L, Fernie AR (2006) Gas chromatography mass spectrometry-based metabolite profiling in plants. Nat Protoc **1:** 387–396

Lombard DB, Alt FW, Cheng HL, Bunkenborg J, Streeper RS, Mostoslavsky R, Kim J, Yancopoulos G, Valenzuela D, Murphy A, et al (2007) Mammalian Sir2 homolog SIRT3 regulates global mitochondrial lysine acetylation. Mol Cell Biol **27:** 8807–8814

Lundby A, Lage K, Weinert BT, Bekker-Jensen DB, Secher A, Skovgaard T, Kelstrup CD, Dmytriyev A, Choudhary C, Lundby C, et al (2012) Proteomic analysis of lysine acetylation sites in rat tissues reveals organ specificity and subcellular patterns. Cell Rep **2:** 419–431

Morgan MJ, Lehmann M, Schwarzländer M, Baxter CJ, Sienkiewicz-Porzucek A, Williams TC, Schauer N, Fernie AR, Fricker MD, Ratcliffe RG, et al (2008) Decrease in manganese superoxide dismutase leads to reduced root growth and affects tricarboxylic acid cycle flux and mitochondrial redox homeostasis. Plant Physiol **147:** 101–114

Newman JC, He W, Verdin E (2012) Mitochondrial protein acylation and intermediary metabolism: regulation by sirtuins and implications for metabolic disease. J Biol Chem **287:** 42436–42443

Pandey R, Müller A, Napoli CA, Selinger DA, Pikaard CS, Richards EJ, Bender J, Mount DW, Jorgensen RA (2002) Analysis of histone acetyltransferase and histone deacetylase families of *Arabidopsis thaliana* suggests functional diversification of chromatin modification among multicellular eukaryotes. Nucleic Acids Res **30:** 5036–5055

Rardin MJ, Newman JC, Held JM, Cusack MP, Sorensen DJ, Li B, Schilling B, Mooney SD, Kahn CR, Verdin E, et al (2013) Label-free quantitative proteomics of the lysine acetylome in mitochondria identifies substrates of SIRT3 in metabolic pathways. Proc Natl Acad Sci USA **110:** 6601–6606

Rauh D, Fischer F, Gertz M, Lakshminarasimhan M, Bergbrede T, Aladini F, Kambach C, Becker CF, Zerweck J, Schutkowski M, et al (2013) An acetylome peptide microarray reveals specificities and deacetylation substrates for all human sirtuin isoforms. Nat Commun **4:** 2327

Rhoads DM, Subbaiah CC (2007) Mitochondrial retrograde regulation in plants. Mitochondrion **7:** 177–194

Roessner U, Luedemann A, Brust D, Fiehn O, Linke T, Willmitzer L, Fernie A (2001) Metabolic profiling allows comprehensive phenotyping of genetically or environmentally modified plant systems. Plant Cell **13:** 11–29

Rühl C, Stauffer E, Kahles A, Wagner G, Drechsel G, Rätsch G, Wachter A (2012) Polypyrimidine tract binding protein homologs from *Arabidopsis* are key regulators of alternative splicing with implications in fundamental developmental processes. Plant Cell **24:** 4360–4375

Sadoul K, Wang J, Diagouraga B, Khochbin S (2011) The tale of protein lysine acetylation in the cytoplasm. J Biomed Biotechnol **2011:** 970382

Sauve AA (2010) Sirtuins. Biochim Biophys Acta **1804:** 1565–1566

Schauer N, Steinhauser D, Strelkov S, Schomburg D, Allison G, Moritz T, Lundgren K, Roessner-Tunali U, Forbes MG, Willmitzer L, et al (2005) GC-MS libraries for the rapid identification of metabolites in complex biological samples. FEBS Lett **579:** 1332–1337

Schmidt MT, Smith BC, Jackson MD, Denu JM (2004) Coenzyme specificity of Sir2 protein deacetylases: implications for physiological regulation. J Biol Chem **279:** 40122–40129

Schwanhäusser B, Busse D, Li N, Dittmar G, Schuchhardt J, Wolf J, Chen W, Selbach M (2011) Global quantification of mammalian gene expression control. Nature **473:** 337–342

Schwarzländer M, König AC, Sweetlove LJ, Finkemeier I (2012) The impact of impaired mitochondrial function on retrograde signalling: a meta-analysis of transcriptomic responses. J Exp Bot **63:** 1735–1750

Sebastián C, Satterstrom FK, Haigis MC, Mostoslavsky R (2012) From sirtuin biology to human diseases: an update. J Biol Chem **287:** 42444–42452

Sol EM, Wagner SA, Weinert BT, Kumar A, Kim HS, Deng CX, Choudhary C (2012) Proteomic investigations of lysine acetylation identify diverse substrates of mitochondrial deacetylase sirt3. PLoS ONE **7:** e50545

Sweetlove LJ, Heazlewood JL, Herald V, Holtzapffel R, Day DA, Leaver CJ, Millar AH (2002) The impact of oxidative stress on Arabidopsis mitochondria. Plant J **32:** 891–904

Sweetlove LJ, Taylor NL, Leaver CJ (2007) Isolation of intact, functional mitochondria from the model plant *Arabidopsis thaliana*. Methods Mol Biol **372:** 125–136

Tran HT, Nimick M, Uhrig RG, Templeton G, Morrice N, Gourlay R, DeLong A, Moorhead GB (2012) *Arabidopsis thaliana* histone deacetylase 14 (HDA14) is an α-tubulin deacetylase that associates with PP2A and enriches in the microtubule fraction with the putative histone acetyltransferase ELP3. Plant J **71:** 263–272

Ungerstedt JS, Blömback M, Söderström T (2003) Nicotinamide is a potent inhibitor of proinflammatory cytokines. Clin Exp Immunol **131:** 48–52

van Blokland R, ten Lohuis M, Meyer P (1997) Condensation of chromatin in transcriptional regions of an inactivated plant transgene: evidence for an active role of transcription in gene silencing. Mol Gen Genet **257:** 1–13

Verdin E, Hirschey MD, Finley LWS, Haigis MC (2010) Sirtuin regulation of mitochondria: energy production, apoptosis, and signaling. Trends Biochem Sci **35:** 669–675

Wang CZ, Gao F, Wu JG, Dai JL, Wei CH, Li Y (2010) Arabidopsis putative deacetylase AtSRT2 regulates basal defense by suppressing PAD4, EDS5 and SID2 expression. Plant Cell Physiol **51:** 1291–1299

Weinert BT, Wagner SA, Horn H, Henriksen P, Liu WR, Olsen JV, Jensen LJ, Choudhary C (2011) Proteome-wide mapping of the *Drosophila* acetylome demonstrates a high degree of conservation of lysine acetylation. Sci Signal **4:** ra48

Winkler HH, Bygrave FL, Lehninger AL (1968) Characterization of the atractyloside-sensitive adenine nucleotide transport system in rat liver mitochondria. J Biol Chem **243:** 20–28

Wu FH, Shen SC, Lee LY, Lee SH, Chan MT, Lin CS (2009) Tape-Arabidopsis Sandwich: a simpler Arabidopsis protoplast isolation method. Plant Methods **5:** 16

Wu X, Oh MH, Schwarz EM, Larue CT, Sivaguru M, Imai BS, Yau PM, Ort DR, Huber SC (2011) Lysine acetylation is a widespread protein modification for diverse proteins in Arabidopsis. Plant Physiol **155:** 1769–1778

Xing S, Poirier Y (2012) The protein acetylome and the regulation of metabolism. Trends Plant Sci **17:** 423–430

Yoine M, Ohto MA, Onai K, Mita S, Nakamura K (2006) The lba1 mutation of UPF1 RNA helicase involved in nonsense-mediated mRNA decay causes pleiotropic phenotypic changes and altered sugar signalling in Arabidopsis. Plant J **47:** 49–62

Publication 6

The mitochondrial lysine acetylome of Arabidopsis.

Mitochondrion.

König AC, Hartl M, Boersema PJ, Mann M, Finkemeier I.

(2014)

Mitochondrion pii: S1567-7249

Mitochondrion xxx (2014) xxx–xxx

Contents lists available at ScienceDirect

Mitochondrion

journal homepage: www.elsevier.com/locate/mito

The mitochondrial lysine acetylome of Arabidopsis

Ann-Christine König [a], Markus Hartl [a], Paul J. Boersema [b,1], Matthias Mann [b], Iris Finkemeier [a,*]

[a] Plant Proteomics, Max-Planck Institute for Plant Breeding Research, Carl-von-Linné Weg 10, 50829 Köln, Germany
[b] Proteomics and Signal Transduction, Max-Planck Institute of Biochemistry, Am Klopferspitz 18, 82152 Martinsried, Germany

ARTICLE INFO

Article history:
Received 15 December 2013
received in revised form 6 March 2014
accepted 10 March 2014
Available online xxxx

Keywords:
Lysine acetylation
Mitochondria
Acetyl-CoA
Arabidopsis
Metabolism
pH

ABSTRACT

Posttranslational modifications are essential regulators of protein functions as they can modify enzyme activities or protein–molecule interactions by changing the charge state or chemical properties of their target amino acid. The acetyl moiety of the central energy metabolite acetyl-CoA can be transferred to the ε-amino group of lysine, a process known as lysine acetylation which is implicated in the regulation of key metabolic enzymes in various organisms. Since plant mitochondria are of great importance for plant growth and development and as they house key enzymes of oxidative phosphorylation and photorespiration, it is essential to investigate the occurrence of lysine acetylation in this organelle. Here we characterised the plant mitochondrial acetylome of Arabidopsis mitochondria by LC-MS/MS analysis. In total 120 lysine-acetylated mitochondrial proteins containing 243 acetylated sites were identified. These proteins were mapped into functional categories showing that many proteins with essential functions from the tricaboxylic cycle and the respiratory chain are lysine-acetylated, as well as proteins involved in photorespiration, amino acid and protein metabolism, and redox regulation. Immuno-detection of mitochondrial proteins revealed that many lysine-acetylated proteins reside in native protein complexes. Furthermore, in vitro experiments demonstrated that lysine acetylation can occur non-enzymatically in Arabidopsis mitochondria at physiological matrix pH.

1. Introduction

Lysine acetylation is an important post-translational modification (PTM) occurring in a large number of proteins of diverse biological function and various subcellular localisations in bacteria, yeast, plant, and animal cells (Choudhary et al., 2009; Finkemeier et al., 2011; Henriksen et al., 2012; Lundby et al., 2012; Melo-Braga et al., 2012; Smith-Hammond et al., 2013; Weinert et al., 2011, 2013; Wu et al., 2011). Generally, specific protein lysine acetyltransferases (KAT) and lysine deacetylases (KDAC) catalyze the reversible modification of the N^{ε}-group of lysine. Although lysine acetylation was first discovered on histone tails (Gershey et al., 1968), which is nowadays known as an important regulator of chromatin structure and gene expression, it has recently emerged that lysine acetylation is particularly abundant in prokaryotes as well as in mitochondria of eukaryotes (Weinert et al., 2011). While in species such as *Drosophila melanogaster*, mice, rats, and humans, the mitochondrial acetylomes have already been described (Kim et al., 2006; Rardin et al., 2013; Still et al., 2013; Weinert et al., 2011), only a few mitochondrial lysine-acetylated proteins have been identified in Arabidopsis and other plants thus far (Finkemeier et al., 2011; Melo-Braga et al., 2012; Smith-Hammond et al., 2013; Wu et al., 2011). Lysine acetylation can have a strong impact on the biological function of proteins as the transfer of the acetyl group to lysine masks the positive charge, which is known to be important in many catalytic centres of enzymes, as well as for protein–protein, and protein–DNA interactions (Yang and Seto, 2008). Since lysine acetylation is dependent on the availability of acetyl-CoA, it has a huge potential to convey information on the metabolic status of mitochondria to proteins from signalling pathways (Hartl and Finkemeier, 2012; Xing and Poirier, 2012). Plant mitochondria play a central role in acetyl-CoA metabolism and they are essential integrators in metabolic signalling (Schwarzländer et al., 2012a). Furthermore, plant mitochondria have many additional functions in comparison to animal mitochondria as they house enzymes of the photorespiratory pathways in green tissues, enzymes involved in vitamin biosynthesis, as well as alternative respiratory complexes to direct the electron flow when the cell experiences stress (Sweetlove et al., 2007). This is especially important as plants are sessile organisms and often rapidly have to adapt to adverse environmental conditions (Jacoby et al., 2012). Recently, it was demonstrated that the TCA cycle often does not operate as a circle in plants but that different flux modes are possible depending on cellular demands for metabolic intermediates (Sweetlove et al., 2010). The underlining regulatory mechanisms, however, that allow the plant to flexibly redirect its metabolism are still largely unknown. Although substrate concentrations may play a pivotal role in determining enzyme activities, the potential role of PTMs in altering substrate affinities and enzyme

* Corresponding author at: Max-Planck Institute for Plant Breeding Research, Plant Proteomics, Carl-von-Linné Weg 10, 50829 Cologne, Germany. Tel.: +49 221 5062 234.
E-mail address: finkemeier@mpipz.mpg.de (I. Finkemeier).
[1] Current address: ETH Zürich, Institute of Biochemistry, Schafmattstrasse 18, 8093 Zürich, Switzerland.

http://dx.doi.org/10.1016/j.mito.2014.03.004
1567-7249/

activities is still largely unexplored in plant mitochondria (reviewed in Hartl and Finkemeier, 2012). Hence, PTMs such as lysine acetylation have the potential as powerful regulators of mitochondrial functions. In this work we present a first extensive study of the lysine acetylome of Arabidopsis mitochondria. Furthermore, we demonstrate in in vitro experiments that lysine acetylation can also occur non-enzymatically in plant mitochondria depending on the matrix pH.

2. Materials and methods

2.1. Plant growth and isolation of mitochondria

Mitochondria were isolated from 10-day-old *Arabidopsis thaliana* (Col0) total seedlings grown in liquid cultures as described in detail in Morgan et al. (2008). The integrity of the outer membrane was determined by the latency of cytochrome c oxidation before and after addition of Triton-X 100. Only mitochondria with over 90% intactness were used for further analysis.

2.2. 2D BN/SDS-PAGE

Protein (750 μg) of freshly isolated mitochondria was sedimented by centrifugation for 10 min at 23,700 ×*g*. The pellet was resuspended in 75 μl of digitonin solubilization buffer (30 mM HEPES, 150 mM potassium acetate, 10% (w/v) glycine and 5% digitonin (w/v) pH 7.4). BN-gel electrophoresis as well as second gel dimension was carried out in a standard dual cooled gel electrophoresis chamber (Hoefer) with a gel dimension of 18 × 16 cm as described in Klodmann et al. (2011). Gels were transferred to nitrocellulose membranes for Western-blot analysis and proteins stained with Ponceau S for quality control.

2.3. In vitro lysine acetylation of mitochondrial proteins

The in vitro acetylation assay was performed as described in Wagner and Payne (2013). Mitochondrial protein (30 μg) was incubated with or without 5 mM acetyl-CoA for 4 h gently mixing at room temperature (20 °C). Incubations were performed at pH 5 and pH 8 under native or denaturing conditions, respectively. For denaturing conditions proteins were heated for 10 min at 95 °C before addition of acetyl-CoA. Additionally, mitochondria were incubated with 2.5 mM potassium acetate and 0.25 mM coenzyme A (CoA) at pH 8, as described before. The samples were analyzed on a 12% (w/v) SDS-PAGE followed by immunoblotting and detection with anti-acetyl lysine antibody.

2.4. Western blot analysis of lysine-acetylated proteins

For Western blot analysis, proteins were separated by SDS-PAGE, transferred to a nitrocellulose membrane, and probed using anti-acetyl lysine antibody (ImmuneChem Pharmaceuticals). As secondary antibody either IRDye 800CW (LI-COR Bioscience) goat anti-rabbit antibody was used and detected by the Odyssey® Infrared Imaging System (LI-COR Bioscience) or anti-horseradish peroxidase antibody (ThermoFisher Scientific) was used followed by detection with SuperSignal West Dura enhanced chemiluminescent substrate (ThermoFisher Scientific).

2.5. Trypsin digestion, immuno-enrichment of lysine-acetylated peptides and LC-MS/MS data acquisition and analysis

Protein (800 μg) of mitochondrial preparations were dissolved in 4% (w/v) SDS, 0.1 M DTT, 0.1 M Tris–HCl, and pH 7.6 heated to 95 °C for 5 min and processed using the filter-assisted sample preparation protocol, as described by Wisniewski et al. (2009). Lysine-acetylated peptides were immuno-enriched from trypsin-digested mitochondrial proteins as described in detail in Finkemeier et al. (2011) with the following modification: the washing steps were increased to five, and the final two washing steps were performed with double-distilled water before elution of the peptides. After enrichment the eluted peptides were desalted using C18 Stagetips (Rappsilber et al., 2007), evaporated on a speed-vac, and redissolved in 2% (w/v) acetonitrile, 0.1% (w/v) trifluoroacetic acid before analysis. In total, we enriched lysine-acetylated peptides from three independent biological replicates, and we analyzed the samples before and after enrichment using an EASY-nLC 1000 (Thermo Fisher) coupled to an Orbitrap Elite mass spectrometer (Thermo Fisher). Peptides were separated on frit-less, self-pulled fused silica emitters (20 cm × 0.75 μm), packed in-house with reversed-phase ReproSil-Pur C18-AQ resin with 3 μm diameter (Dr. Maisch). Peptides were eluted for 120 min using a segmented linear gradient of 3% to 95% solvent B (80% acetonitrile, 0.5% acetic acid) at a flow-rate of 250 nl/min. Survey full-scan mass spectra were acquired in the Orbitrap analyzer. The scanned mass range was 300–1650 m/z, at a resolution of 120,000 at 400 m/z. The 20 most intense ions were sequentially isolated, fragmented (CID at 35 eV) and measured in the linear ion-trap. Peptides with a charge of +1 or with unassigned charge state were excluded from fragmentation for MS2, dynamic exclusion of max. 500 m/z values prevented repeated selection of selected masses for 90 s. Ions were accumulated to a target value of 10^6 for full FT-MS in the Orbitrap and of 10^4 for MS2 in the linear ion trap.

Raw data were processed using MaxQuant software (version 1.4.1.2, http://www.maxquant.org/) (Cox and Mann, 2008) and searched against *The Arabidopsis Information Resource* protein database (build TAIR10_pep_20101214, ftp://ftp.arabidopsis.org/home/tair/Proteins/TAIR10_protein_lists/) at a protein as well as peptide false discovery rate of 1%, with trypsin specificity and a maximum of two missed cleavages for total proteome measurements or of four missed cleavages for samples enriched in lysine-acetylated peptides. Carbamidomethylation of cysteine residues was set as fixed, oxidation of methionine as well as lysine acetylation were set as variable modifications. Additionally, we applied the following quality thresholds for the reliable identification of lysine-acetylated sites: MaxQuant site score >40 and localization score >0.9.

2.6. Functional classification and prediction of subcellular localization

Proteins were functionally annotated using the Mapman functional terms (Thimm et al., 2004; http://mapman.gabipd.org/, version 3.6.0RC1). Mapman annotations were loaded into the Perseus software (http://www.maxquant.org/; version 1.4.0.17) and matched based on their TAIR protein identifiers. Information on experimentally determined or computationally predicted subcellular localisation of proteins was extracted from the SUBA3 database (Tanz et al., 2013; http://suba.plantenergy.uwa.edu.au) and the consensus information was matched to the dataset using Perseus. Furthermore, we compared the recently described mitochondrial proteome of potato tuber (Salvato et al., 2014) with our dataset. Proteins which were annotated to be mitochondrially localized in either of these two references were considered very likely to be expressed in mitochondria in this study. The corresponding functional and subcellular annotations are listed in Supplemental Tables 1–3. A Fisher-exact test was computed in Perseus overall functional and localisation categories to assess if lysine-acetylated mitochondrial proteins were significantly over- or underrepresented in particular categories (at a Benjamini–Hochberg corrected false-discovery rate of 0.05%).

2.7. Generation of sequence logos using ice-logo

Sequence windows of 15 amino acids up- and downstream of the identified acetylation sites were extracted from the MaxQuant output and used to generate a sequence logo using the pLogo web application (https://plogo.uconn.edu/; version 1.2.0; O'Shea et al., 2013). pLogo applies binomial probabilities to compute the statistical significance of amino acids at the individual positions in a sequence motif. As a result it generates a sequence logo which depicts over- and underrepresented

Please cite this article as: König, A.-C., et al., The mitochondrial lysine acetylome of Arabidopsis, Mitochondrion (2014), http://dx.doi.org/10.1016/j.mito.2014.03.004

amino acids above and below the x-axis. On the y-axis the residues are scaled according to the statistical significance of the amino acid frequency in comparison to a background of sequences generated from all proteins identified. The Bonferroni-corrected significance cut-off for $p < 0.05$ is shown in the logo as a red horizontal line. The acetylated lysine site was set as a fixed position.

3. Results

3.1. Identification of Arabidopsis mitochondrial lysine-acetylated proteins

To identify lysine-acetylated mitochondrial proteins we isolated intact mitochondria from 10 day-old wildtype seedlings of three independent biological replicates. Protein extracts were digested with trypsin and enriched for lysine-acetylated proteins by immuno-purification as described in Finkemeier et al. (2011). Mitochondrial total peptide samples and the immuno-enriched fractions were then analyzed via LC-MS/MS. Before enrichment we identified a total of 901 proteins, of which 570 are predicted to be localized in the mitochondria according to the SUBA3 database (http://suba.plantenergy.uwa.edu.aul; Tanz et al., 2013) consensus information or the recently described mitochondrial proteome of potato tuber (Salvato et al., 2014) (Table 1 and Supplementary Table S1). After enriching for lysine-acetylated peptides we identified 310 proteins, of which 204 carried one or more lysine-acetylated sites (Table 1 and Supplementary Table S2). 120 of these 204 acetylated proteins are predicted to be localized in mitochondria and carry 243 acetylated sites (Supplementary Table 3).

To gain a better overview, proteins were functionally classified using MapMan ontologies (Thimm et al., 2004) and the occurrence of lysine-acetylation was tested for non-random association with all these functional terms using a Fisher-exact test (Fig. 1). Interestingly, 18% of the 120 mitochondrial lysine-acetylated proteins belong to the category of TCA cycle enzymes, which represents a significant and more than three-fold enrichment of lysine acetylated proteins in this enzyme class. Similarly, enzymes of the photorespiratory pathway (5%) and nucleotide metabolism (4%; consisting mainly of adenylate and diphosphate kinases) are significantly enriched at a similar scale. Other prominent protein classes that were lysine-acetylated included proteins of the respiratory chain (13%), of different metabolic pathways, redox regulation, or transport mechanisms but were not particularly overrepresented. However, the functional classes of protein metabolism (8%) and of proteins with unknown function (8%) appear to be underrepresented within the group of lysine-acetylated mitochondrial proteins.

Fig. 2 shows a more detailed map of proteins of the TCA cycle, respiratory chain as well as mitochondrial transporters which were identified as lysine-acetylated. The pyruvate dehydrogenase is a complex of three enzymes E1–E3, which are each encoded by several isoforms in the nuclear genome. Strikingly, seven of the eight proteins identified for the pyruvate dehydrogenase complex (PDC) were lysine-acetylated, including two proteins of the E1 pyruvate dehydrogenase/decarboxylase complex, three proteins of the E2 lipoate acetyltransferase complex, and another two of the E3 dihydrolipoate dehydrogenase complex. In every enzymatic step of the TCA cycle at least one protein appears to be lysine-acetylated. In contrast, complex I of the respiratory chain just shows one acetylated protein which is the gamma carbonic anhydrase CA2. CA2 is a matrix-exposed subunit, associated with the membrane arm of complex I and it is unique for the plant kingdom (Sunderhaus et al., 2006). For all other proteins of the respiratory chain, like complexes II and IV, cytochrome c, and the mitochondrial uncoupling protein (UCP), just one acetylated protein was discovered. Compared to the other complexes in the respiratory chain, complex V shows a rather high level of acetylated proteins with six out of 13 identified proteins. These six proteins belong to different subunits: an ATP synthase subunit g protein (ATP20-2, At4g26210), the ATP synthase d chain (ATPQ, At3g52300), an F_Ad subunit of mitochondrial ATP synthase (At2g21870), an ATP synthase β-subunit (At5g08690), an ATPase F_1 complex α-subunit protein (At2g07698), and the mitochondrially encoded protein AtMg00480, which encodes subunit 8 of the mitochondrial F_0–ATP synthase complex. Taking a closer look at the transporter families in mitochondria, we found five of 10 identified transporter proteins as lysine-acetylated, including the voltage dependent anion channels 1–3 (VDAC1–3; At3g01280), dicarboxylate/tricarboxylate carrier (At5g19760), the ATP/ADP carriers 1–3 (At3g08580, At4g28390, At5g13490), and a phosphate transporter (At5g14040) (Supplementary Tables 2, 3).

Several interesting proteins from other metabolic processes were identified, such as the serinehydroxymethyltransferase (At4g37930, At5g26780), the H- (At1g32470), P- (At4g33010; At2g26080), and T- (At1g11860) subunits of the glycine decarboxylase complex from photorespiration, and proteins from amino acid synthesis (e.g. aspartate aminotransferase 1, At2g30970; cysteine synthase, At3g61440; GABA transaminase, At3g22200) as well as degradation (e.g. DIN3, At3g06850; aldehyde dehydrogenase 12A1, At5g62530) (Supplementary Tables 2, 3).

Besides several prominent proteins in mitochondrial redox processes were identified as lysine-acetylated such as the manganese superoxide dismutase (At3g10920), the monodehydroascorbate dehydrogenase 6 (At1g63940) and the L-galactono-1,4-lactone dehydrogenase (At3g47930) involved in mitochondrial ascorbate synthesis. Prominent proteins involved in mitochondrial protein import (TOM 20-3, At3g27080; TIM9, At3g46560), processing (MPPß, At1g51980), mitochondrial protein biosynthesis (translation elongation factors, At2g45030, At4g11120), folding (e.g. HSP60, At3g2990; HSP70-1, AT4g37910) and degradation (LON1, At5g26860) were also among the identified lysine-acetylated proteins.

To identify possible specific sequence motifs surrounding acetylated lysine residues, we generated a type of sequence logo (pLogo) which computes the likelihood of amino acids being over- or underrepresented at the positions surrounding the acetylation site (Fig. 3). Glutamic acid was observed to be significantly overrepresented at position −1. Furthermore, glutamic acid, alanine and lysine appear to be enriched in several positions but did not pass the significance cut-off. Similarly, serine is underrepresented in several positions (e.g. +2, +5) but also not significantly.

3.2. Detection of lysine-acetylated proteins in native mitochondrial protein complexes

To investigate whether the identified lysine-acetylated proteins can actually be found in mitochondrial protein complexes or whether they are more likely to be excluded from these, we isolated intact protein complexes from wild-type mitochondria, solubilized the membranes with digitonin and analyzed them by two-dimensional blue-native

Table 1
Overview of identified Arabidopsis mitochondrial proteins.
Peptides from total mitochondrial extracts and from fractions immuno-enriched for lysine-acetylated peptides were analyzed with the Orbitrap Elite mass spectrometer (Supplemental Tables S1–3). K-Ac: acetylated lysine.

	Total extract	K-Ac enriched fraction[a]		
	Proteins	Proteins	K-Ac proteins	K-Ac sites
Replicate 1	770	247	166	287
Replicate 2	773	151	100	97
Replicate 3	772	218	149	216
Total	858 (901)[c]	310	204	348
Mitochondrial[b]	564 (570)[c]	207	120	243

[a] Selection criteria for identifications: peptide and protein FDR < 1%, K-Ac site score > 40, K-Ac site localization probability > 0.9; contaminant non-plant proteins were removed.
[b] Mitochondrial localization was inferred from the consensus annotation of the SUBA3 database and from a comparison to the mitochondrial proteome of potato tuber (Salvato et al., 2014).
[c] Numbers in parentheses represent the combined numbers of identified proteins from total extract proteins and K-Ac enriched fractions.

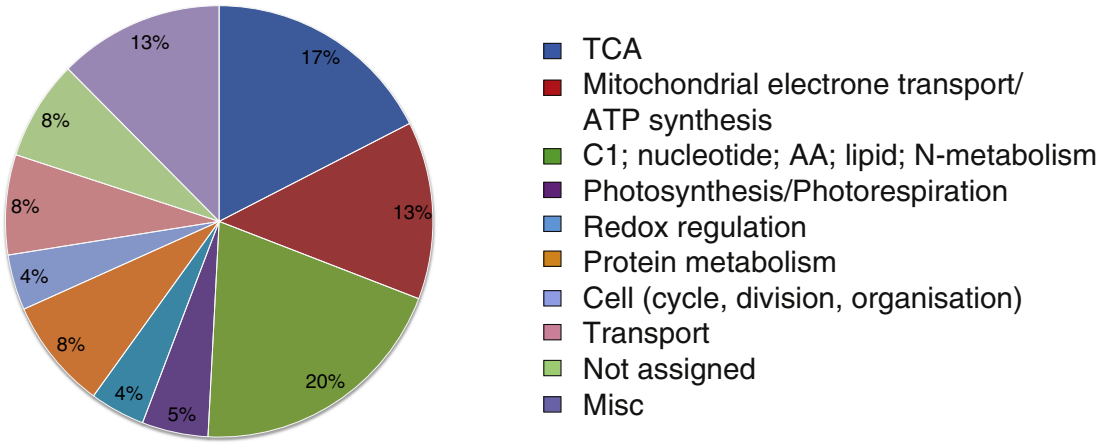

Mapman bin	No. of observed proteins in bin	Identified K-ac proteins in bin	enrichment factor	p-value	Benj. Hoch. FDR
Photosynthesis (PS)	9	7	3.69	0.000366	0.003781
PS.photorespiration	8	6	3.56	0.001403	0.043955
TCA / org. transformation.TCA	26	18	3.29	6.81E-08	6.41E-06
TCA / org transformation	31	21	3.22	8.31E-09	2.57E-07
nucleotide metabolism	9	6	3.17	0.003355	0.025999
protein	101	12	0.56	0.004107	0.025465
not assigned	154	12	0.37	2.98E-07	4.62E-06
not assigned.unknown	91	7	0.37	0.00015	0.007045

Fig. 1. Functional categories of lysine-acetylated mitochondrial proteins from *Arabidopsis thaliana*. Hundred-twenty mitochondria-localized lysine-acetylated proteins were identified by LC-MS/MS analysis and functionally classified using MapMan ontologies (see Supplementary Table 1). A Fisher exact test was performed to identify over- and underrepresented functional categories among the 120 lysine-acetylated proteins compared to the total number of 570 identified mitochondrial proteins. The enrichment factor indicates significantly under- and overrepresented categories, respectively. p-Values were adjusted using the Benjamini–Hochberg correction for false-discovery rate (FDR) determination. AA, amino acid; C1, one carbon metabolism; K-Ac, acetylated lysine; TCA, tricarboxylic acid.

PAGE (BN-PAGE) followed by Western blot analysis using the anti-acetyllysine antibody (Fig. 4A, B). The Ponceau S stain of the Western blot shows all major proteins of the respiratory complexes (Fig. 4A). Complex I only appears in the supercomplex together with complex III which indicates that the isolated mitochondria were highly intact. Comparing the Ponceau S stain (Fig. 4A) with the detected lysine-acetylated proteins (Fig. 4B) it becomes clear that lysine-acetylated proteins can be detected within the protein complexes and that not all but only specific proteins are lysine-acetylated. For the identification of proteins we used the GelMap software package (http://www.gelmap.de; Klodmann et al., 2011) which can be used to annotate and evaluate two-dimensional blue native gels. Supercomplex I + III (1.5 MDa in the first dimension) shows more acetylated proteins than we could identify in our LC-MS/MS approach of immuno-precipitated proteins (Table 1). It is conceivable that not all lysine-acetylated sites can be detected by LC-MS/MS analysis, as the length or the physico-chemical properties of tryptic peptides might not be suitable for unambiguous detection via mass spectrometry. Within the supercomplex I + III a lysine-acetylated protein matching the CA2 subunit of complex I was detected at around 30 kDa, which we also identified by LC-MS/MS (Supplementary Tables 2, 3). Other lysine-acetylated proteins were detected at around 50 kDa which include the MPPα as well as MPPβ subunit of complex III. The most intense signals for lysine-acetylated proteins were detected in complex V which is in accordance with the LC-MS/MS data. This includes the ATPase F_1 complex α- and β-subunit subunit at around 50–60 kDa. According to GelMap, these two proteins appear to be present in a number of spots at around 50–60 kDa which could explain the unresolved signals in this area. Between 25 kDa and 30 kDa the F_Ad subunit of mitochondrial ATP synthase and around 15 kDa subunit 8 of the mitochondrial F_0–ATP synthase complex were detected. The γ- as well as the δ-subunits of complex V were not identified by LC-MS/MS but were still found to be lysine-acetylated in the Western blot. The voltage dependent anion channel proteins (VDAC1–3) can be detected in a complex of around 110 kDa in the first dimension while the single proteins run at around 30 kDa in the second dimension. These spots were also detected to be lysine-acetylated in the LC-MS/MS analysis, as well as the ADP/ATP-carrier proteins 1–3 (AAC1–3) which co-migrate in the same complex (Supplementary Table 3). Proteins from the TCA cycle and likewise the PDC are not clearly detectable on the BN-PAGE.

3.3. pH-dependent in vitro acetylation of mitochondrial proteins

Wagner and Payne (2013) recently demonstrated that protein lysine acetylation in mammalian mitochondria can occur non-enzymatically. To investigate whether non-enzymatic lysine acetylation can also occur in plant mitochondria, we incubated membrane-ruptured mitochondria (frozen in −80 °C) with 5 mM acetyl-CoA in different buffers. Mitochondria were treated with non-denaturing buffer at pH 5 to mimic apoplastic environment and at pH 8, the pH of the mitochondrial

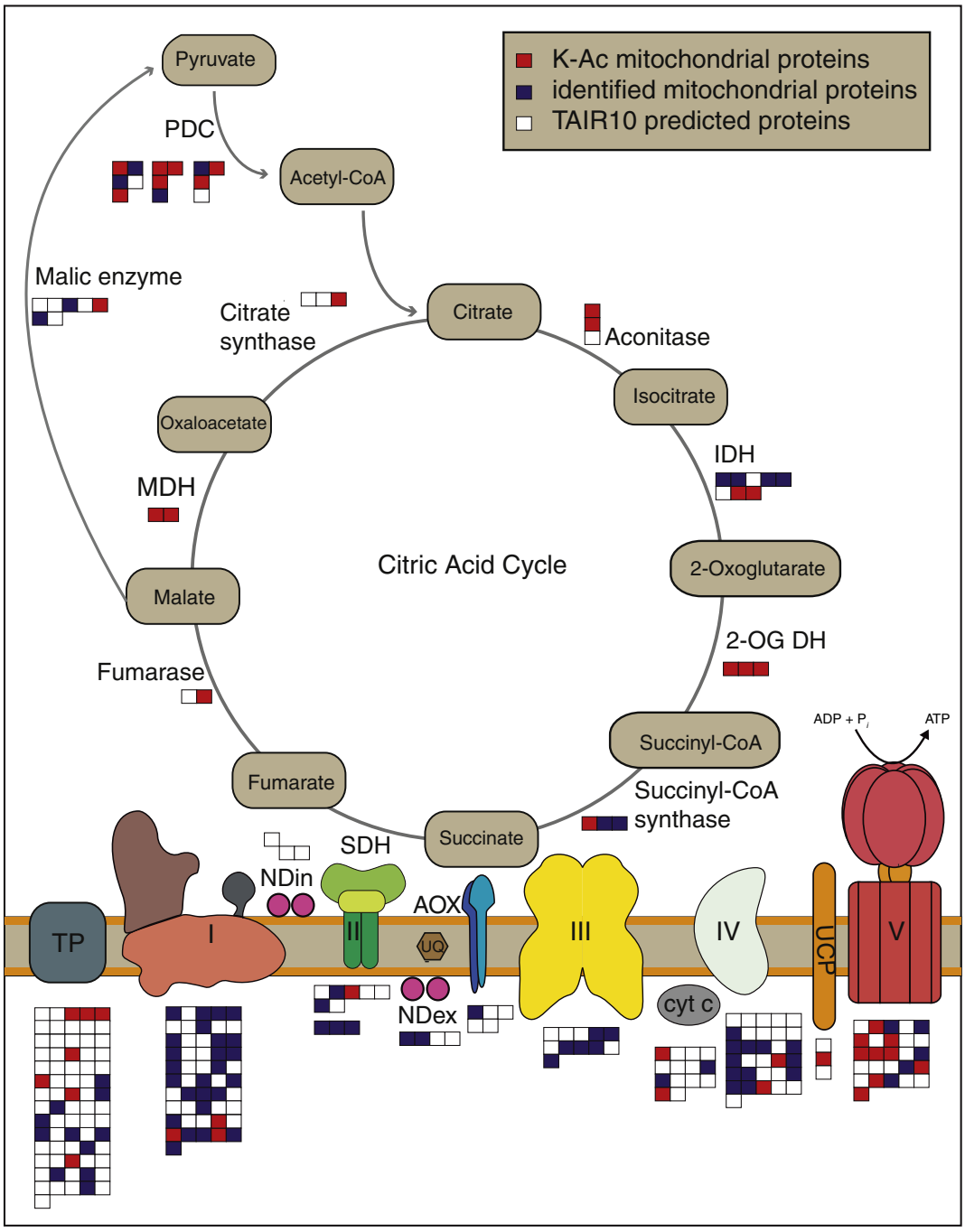

Fig. 2. Overview of identified Arabidopsis lysine-acetylated proteins from mitochondrial energy metabolism. Protein functional categories were annotated using MapMan (Thimm et al., 2004). Boxes in blue indicate identified non-acetylated proteins before enrichment, red boxes show identified lysine-acetylated proteins and white boxes indicate TAIR10 proteins not identified in the LC-MS/MS analyses. AOX, alternative oxidase; TCA, tricarboxylic acid; TP, transporter; I, complex I; II, complex II; III, complex III; IV, complex IV. (For interpretation of the references to color in this figure legend, the reader is referred to the web version of this article.).

matrix. Additionally, mitochondria were analyzed under denaturing condition achieved by heat inactivation. Mitochondria which were not treated with acetyl-CoA and just NAD^+ in the buffer show already a basic acetylation level, as demonstrated by our results from LC-MS/MS and BN-PAGE (see also Supplementary Fig.S1). After treatment with acetyl-CoA the acetylation level of proteins increased significantly in the samples at pH 8, especially in the denatured sample due to unfolding of proteins followed by exposure of internal lysine residues to the medium. This leads us to the conclusion that lysine acetylation can occur independent of lysine acetyltransferases at a slightly basic pH in mitochondria, as it also occurred in samples inactivated by heat. Mitochondria treated with acetyl-CoA under acidic buffer conditions at pH 5 do not show increased lysine acetylation, even after heat inactivation. To reveal if acetate can cause the same effect mitochondria were treated with 2.5 mM potassium acetate, but no changes in acetylation levels were detected.

4. Discussion

4.1. The function of lysine acetylation in plant mitochondria

A first step to gain insights on the function of lysine acetylation in plant mitochondria is to identify the acetylated target proteins. In this work we present a first extensive overview of the mitochondrial

Fig. 3. Sequence logo of the lysine-acetylated amino acid motif. The sequence plot was generated with the pLogo-tool (http://plogo.uconn.edu; O'Shea et al., 2013) using the sequences bordering the 233 identified lysine-acetylated sites (11 sequences were omitted because they did not cover the full length) and comparing them to 21,469 sequences generated from the sequences of all proteins identified. The pLogo depicts under- and over-represented amino acids which are scaled to their $\log_{10}$-odds of the binomial probability — as a direct measure of a residue's likelihood of being statistically significantly over- or underrepresented. The horizontal red line indicates the threshold of the Bonferroni corrected p-value of $p < 0.05$. (For interpretation of the references to color in this figure legend, the reader is referred to the web version of this article.).

lysine acetylome of Arabidopsis. In comparison to our previous work (Finkemeier et al., 2011) we achieved an improved enrichment of lysine-acetylated mitochondrial proteins, mainly by increasing the washing steps before elution of the immunoenriched acetylated peptides and by using the high resolution Orbitrap Elite (Thermo Fisher) mass spectrometer for analysis. Here we achieved an enrichment of about 60% lysine-acetylated proteins identified in the elutions after immunoenrichment (Table 1). We identified 120 mitochondrial proteins that were lysine-acetylated and which contained a total number of 243 lysine-acetylated sites (Table 1). These proteins were from various functional categories (Fig. 1, Supplementary Table 1). Salvato et al. (2014) recently published a comprehensive list of the mitochondrial potato tuber proteome. Without enrichment they identified 30 lysine-acetylated proteins, of which several proteins are also included in our study such as the NAD-dependent isocitrate dehydrogenase, however the identified lysine-acetylated sites are not identical with ours. Most of the lysine-acetylated peptides identified by Salvato et al. (2014) are acetylated at the C-terminus, which we regard as false-positives and which are excluded from the analysis, see Choudhary et al. (2009) for discussion. Similar to bacteria and animals, all of the Arabidopsis TCA cycle enzymes were identified to be lysine-acetylated in our study (Wang et al., 2010; Zhao et al., 2010). For bacteria and human liver cells it was demonstrated that lysine acetylation is dependent on the nutrient status of the cells and that the acetylation status of the metabolic enzymes regulates the activity of glycolysis as well of the TCA cycle (Wang et al., 2010; Zhao et al., 2010). Whether a similar regulation mechanism exists for Arabidopsis will be interesting to find out in future studies. Recently, we demonstrated that the activity of the Arabidopsis citrate synthase enzyme CS4 is activated by reduction of disulphide bridges via thioredoxin (Schmidtmann et al., 2014). Here we identified an acetylated lysine in close proximity (+7 AA) to Cys365 which regulates the redox sensitivity of the enzyme. Citrate is a major determinant of cytosolic acetyl-CoA levels through the action of ATP-dependent citrate-lyase (ACL) (Fatland et al., 2002, 2005). ACL is reported as mainly cytosolic enzyme, however we identified a lysine acetylation site on an ACL isoform (At2g20420) that is predicted to be targeted to mitochondria and which was also found in several other mitochondrial proteomic studies of Arabidopsis (e.g. Kruft et al., 2001) according to SUBA3 database (Tanz et al., 2013). Additionally, we identified a lysine-acetylated dicarboxylate/tricarboxylate carrier (At5g19760) that transports citrate (Picault et al., 2002). Therefore it will be interesting to find out whether mitochondrial lysine acetylation indirectly regulates the pools of cytosolic acetyl-CoA levels by altering mitochondrial citrate levels. Besides enzymes of the TCA cycle, a remarkable amount of lysine acetylation sites were discovered on the PDC complex in our study. This result is of great interest as the PDC converts pyruvate to acetyl-CoA which is the substrate for lysine acetylation. It is conceivable that product inhibition of plant mitochondrial PDC activity by acetyl-CoA (Tovar-Mendez et al., 2003) is additionally mediated by lysine acetylation. It should be noted that the bacterial acetyl-CoA synthetase, which presents an alternative source of acetyl-CoA, is also regulated by lysine acetylation (Starai et al., 2002). For many years it is known that phosphorylation of the E1 subunit of the PDC regulates the activity of the enzyme (Miernyk and Randall, 1987; Tovar-Mendez et al., 2003). In future studies, it will be interesting to find out whether these two modifications interplay in the regulation of the PDC activity.

Compared to the PDC and TCA cycle we identified far fewer lysine acetylation sites on proteins of the respiratory chain. For complex I we only identified the CA2 subunit, which is involved in complex I assembly (reviewed in: Braun et al., 2014), as lysine-acetylated by LC-MS/MS. Knockout plants of CA2 show a 80% reduction in complex I and no supercomplex (I + III) formation (Perales et al., 2005). Recently it was reported that the loss of complex I in mice leads to a general increase in mitochondrial protein acetylation (Karamanlidis et al., 2013). It remains an open question whether the same effect occurs in plants and if lysine acetylation of CA2 could function in controlling the amount of complex I. Strikingly complex V, the ATP synthase complex, showed the highest number of acetylated proteins in the respiratory chain. The acetylated complex V subunits can also be found in the holocomplex as shown in the BN-PAGE analysis (Fig. 4). Complex V of other species (such as yeast, Drosophila, mice, rats) was also identified as highly lysine-acetylated (Henriksen et al., 2012; Lundby et al., 2012; Rardin et al., 2013; Weinert et al., 2011). Although complex V contains many lysine acetylation sites, which are also conserved between species, nearly nothing is known about their impact on ATP synthase function thus far. Indeed many of the enzymes involved in respiration have previously been identified to carry multiple PTMs, such as phosphorylation, oxidation, glutathionylation, and nitrosylation (reviewed in: Millar et al., 2005; Schwarzländer and Finkemeier, 2013). In future experiments it will be interesting to find out whether the different PTMs have distinct or overlapping functions in regulation of enzyme activities or protein–protein interactions.

Please cite this article as: König, A.-C., et al., The mitochondrial lysine acetylome of Arabidopsis, Mitochondrion (2014), http://dx.doi.org/10.1016/j.mito.2014.03.004

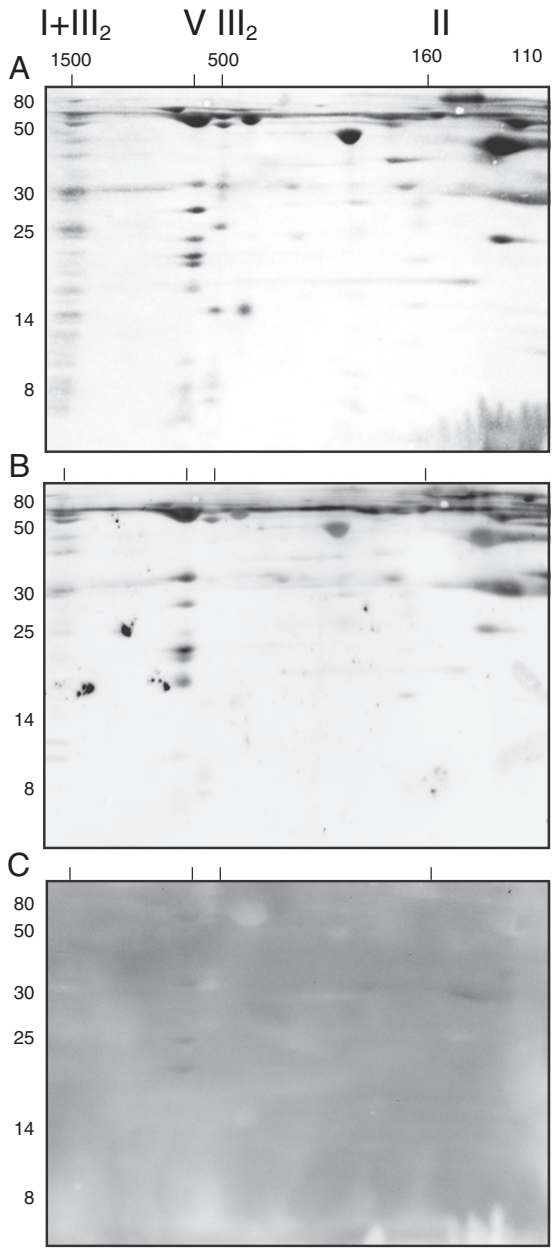

Fig. 4. Detection of lysine acetylation in the protein complexes of Arabidopsis mitochondria analyzed by 2D BN/SDS-PAGE and Western blot. (A) Ponceau S stain of 2D BN/SDS-PAGE of mitochondrial protein complexes. The identity of OXPHOS complexes is indicated above the gels. I + III2, supercomplex composed of complex I and dimeric complex III; I, complex I; V, complex V (ATP synthase); III, dimeric complex III. The molecular mass scale (in kDa) is indicated on the left. (B) Lysine-acetylated proteins from Arabidopsis mitochondria detected by Western blot analysis using the anti-acetyllysine antibody. (C) Competition assay with 3 mg of acetylated bovine serum albumin and anti-acetyllysine antibody prior detection by Western blot analysis.

4.2. Regulation of lysine acetylation in mitochondria

The acetylation of proteins is usually catalyzed by lysine acetyltransferases (KAT) in the nucleus and cytosol of cells and it is still debated whether mitochondrial KATs do exist. In a recent study, GCN5L1 [GCN5 (general control of amino acid synthesis 5)-like 1] was discovered to be additionally localized within human mitochondria and it was reported that it promotes acetylation of electron transport chain (ETC) subunits thereby altering mitochondrial oxygen consumption (Scott et al., 2012). Until now, GCN5L1 is the only KAT reported to reside inside mitochondria. One reasonable explanation for the failure to identify mitochondrial KATs is that lysine acetylation could also occur non-enzymatically in mitochondria. Because of the unique physiological conditions concerning the slightly alkaline pH and elevated acetyl-CoA levels in mitochondria compared to the cytosol, the chemical non-enzymatic acetylation is favoured within the mitochondrial matrix (Wagner and Payne, 2013). We performed a similar assay as described in Wagner and Payne (2013) with isolated mitochondria of Arabidopsis and could confirm their results. By addition of externally supplied acetyl-CoA at pH 8 we observed an increase in mitochondrial protein acetylation. Heat inactivation of the mitochondrial protein extracts before addition of acetyl-CoA confirmed the theory of non-enzymatic acetylation (Fig. 5). Non-enzymatic acetylation does not exclude the action of KATs. Rather a combined operation of spontaneous lysine acetylation and enzyme-catalyzed acetylation can be expected. Deacetylases have been identified in a variety of organisms with the most prominent belonging to the sirtuin (SIRT) family of NAD-dependent deacetylases (Blander and Guarente, 2004). Sirtuins are generally efficient in removing lysine acetylation sites from proteins and are known to be involved in life span extension, cell survival, apoptosis, as well as metabolism in different heterotrophic organisms (Houtkooper et al., 2012; Newman et al., 2012; Sauve, 2010; Sebastian et al., 2012). While mammalian mitochondria contain three types of sirtuins (Newman et al., 2012), Arabidopsis only possesses two different sirtuin-type proteins of which one is residing in mitochondria (König et al., 2014). We recently demonstrated that the Arabidopsis sirtuin 2 has only very specific targets, and that it regulates the lysine acetylation status of the AAC carrier proteins as well of several subunits of the ATP synthase (König et al.,

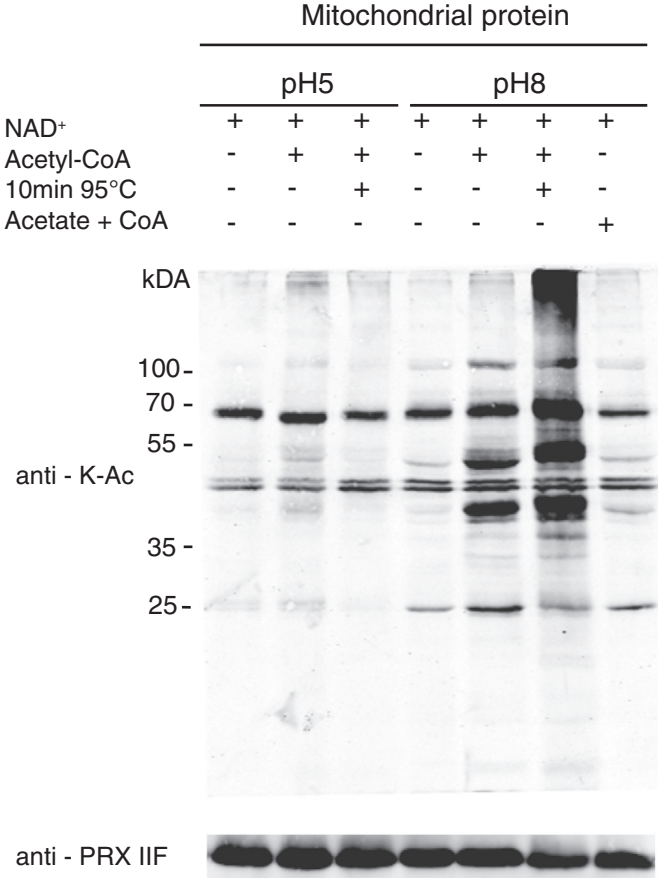

Fig. 5. pH-dependent non-enzymatic lysine acetylation of isolated mitochondrial proteins. Mitochondrial protein extract was treated with 5 mM acetyl-CoA for 4 h at pH 5 and pH 8 under native and denatured conditions, respectively. Potassium acetate and coenzyme A (CoA) were used alternatively. Acetylated proteins were detected using the anti-acetyllysine antibody. Detection of the mitochondrial peroxiredoxin II F (PRX IIF) protein using anti-PRX IIF antiserum (Finkemeier et al. (2005)) indicates equal loading of proteins.

2014). Furthermore, it was recently reported that repression of mitochondrial Sirt3 expression in mammalian cells results in increased acetylation of the OSCP subunit of the ATP synthase complex which leads to decreased intracellular ATP levels (Wu et al., 2013). Interestingly, the OSCP subunit was one of the ATP synthase subunits not identified as lysine-acetylated in our study. Thus, acetylation of OSCP might be controlled by a yet unknown mitochondrial deacetylase in Arabidopsis.

5. Conclusion

Here we have demonstrated that lysine acetylation is an abundant protein modification occurring on mitochondrial proteins of 10-day-old Arabidopsis plants. Many proteins involved in metabolism were identified among the 120 lysine-acetylated mitochondrial proteins. As shown in in vitro analyses, lysine acetylation potentially occurs non-enzymatically in plant mitochondria, especially at an elevated pH. Many interesting research question emanate from our findings which will be crucial to be answered in future work: (i) Do the recently described mitochondrial pH flashes (Schwarzländer et al., 2012b) also affect the acetylation status of mitochondrial proteins, and does this have a functional relevance?; (ii) What proportion of the metabolic enzymes are actually lysine-acetylated and does lysine acetylation have a regulatory role in plant mitochondrial metabolism?; (iii) Do specific plant mitochondrial lysine acetyltransferases exist?; (iv) Is acetyl-CoA involved in metabolic signalling in plant mitochondria and does it convey its information via lysine acetylation? To answer these questions will be critical for our understanding of the regulatory mechanisms of mitochondrial energy metabolism in plants and it might shed new light on mechanisms that allow plants to redirect their metabolism under adverse environmental conditions.

Acknowledgement

We thank Anne Orwat (LMU Munich) for the technical assistance. This work was supported by the Deutsche Forschungsgemeinschaft, Germany (Emmy Noether Programme FI-1655/1-1) and the Max Planck Gesellschaft.

Appendix A. Supplementary data

Supplementary data to this article can be found online at http://dx.doi.org/10.1016/j.mito.2014.03.004.

References

Blander, G., Guarente, L., 2004. The Sir2 family of protein deacetylases. Annu. Rev. Biochem. 73, 417–435.

Braun, H.P., Binder, S., Brennicke, A., Eubel, H., Fernie, A.R., Finkemeier, I., Klodmann, J., König, A.C., Kühn, K., Meyer, E., Obata, T., Schwarzländer, M., Takenaka, M., Zehrmann, A., 2014. The life of plant mitochondrial complex I. Mitochondrion. http://dx.doi.org/10.1016/j.mito.2014.02.006 [Epub ahead of print] (pii: S1567-7249(14)00020-8).

Choudhary, C., Kumar, C., Gnad, F., Nielsen, M.L., Rehman, M., Walther, T.C., Olsen, J.V., Mann, M., 2009. Lysine acetylation targets protein complexes and co-regulates major cellular functions. Science 325, 834–840.

Cox, J., Mann, M., 2008. MaxQuant enables high peptide identification rates, individualized p.p.b.-range mass accuracies and proteome-wide protein quantification. Nat. Biotechnol. 26, 1367–1372.

Fatland, B.L., Ke, J.S., Anderson, M.D., Mentzen, W.I., Cui, L.W., Allred, C.C., Johnston, J.L., Nikolau, B.J., Wurtele, E.S., 2002. Molecular characterization of a heteromeric ATP-citrate lyase that generates cytosolic acetyl-coenzyme A in Arabidopsis. Plant Physiol. 130, 740–756.

Fatland, B.L., Nikolau, B.J., Wurtele, E.S., 2005. Reverse genetic characterization of cytosolic acetyl-CoA generation by ATP-citrate lyase in Arabidopsis. Plant Cell 17, 182–203.

Finkemeier, I., Goodman, M., Lamkemeyer, P., Kandlbinder, A., Sweetlove, L.J., Dietz, K.J., 2005. The mitochondrial type II peroxiredoxin F is essential for redox homeostasis and root growth of Arabidopsis thaliana under stress. J Biol Chem. 280, 12168–12180.

Finkemeier, I., Laxa, M., Miguet, L., Howden, A.J., Sweetlove, L.J., 2011. Proteins of diverse function and subcellular location are lysine acetylated in Arabidopsis. Plant Physiol. 155, 1779–1790.

Gershey, E.L., Vidali, G., Allfrey, V.G., 1968. Chemical studies of histone acetylation. The occurrence of epsilon-N-acetyllysine in the f2a1 histone. J. Biol. Chem. 243, 5018–5022.

Hartl, M., Finkemeier, I., 2012. Plant mitochondrial retrograde signaling: post-translational modifications enter the stage. Front. Plant Sci. 3, 253.

Henriksen, P., Wagner, S.A., Weinert, B.T., Sharma, S., Bacinskaja, G., Rehman, M., Juffer, A. H., Walther, T.C., Lisby, M., Choudhary, C., 2012. Proteome-wide analysis of lysine acetylation suggests its broad regulatory scope in Saccharomyces cerevisiae. Mol. Cell. Proteomics 11, 1510–1522.

Houtkooper, R.H., Pirinen, E., Auwerx, J., 2012. Sirtuins as regulators of metabolism and healthspan. Nat. Rev. Mol. Cell Biol. 13, 225–238.

Jacoby, R.P., Li, L., Huang, S., Pong Lee, C., Millar, A.H., Taylor, N.L., 2012. Mitochondrial composition, function and stress response in plants. J. Integr. Plant Biol. 54, 887–906.

Karamanlidis, G., Lee, C.F., Garcia-Menendez, L., Kolwicz Jr., S.C., Suthammarak, W., Gong, G., Sedensky, M.M., Morgan, P.G., Wang, W., Tian, R., 2013. Mitochondrial complex I deficiency increases protein acetylation and accelerates heart failure. Cell Metab. 18, 239–250.

Kim, S.C., Sprung, R., Chen, Y., Xu, Y., Ball, H., Pei, J., Cheng, T., Kho, Y., Xiao, H., Xiao, L., Grishin, N.V., White, M., Yang, X.J., Zhao, Y., 2006. Substrate and functional diversity of lysine acetylation revealed by a proteomics survey. Mol. Cell 23, 607–618.

Klodmann, J., Senkler, M., Rode, C., Braun, H.P., 2011. Defining the protein complex proteome of plant mitochondria. Plant Physiol. 157, 587–598.

König, A.C., Hartl, M., Pham, P.A., Laxa, M., Boersema, P., Orwat, A., Kalitventseva, I., Plochinger, M., Braun, H.P., Leister, D., Mann, M., Wachter, A., Fernie, A., Finkemeier, I., 2014. The Arabidopsis class II sirtuin is a lysine deacetylase and interacts with mitochondrial energy metabolism. Plant Physiol. 164, 1401–1414.

Kruft, V., Eubel, H., Jänsch, L., Werhahn, W., Braun, H.P., 2001. Proteomic approach to identify novel mitochondrial proteins in Arabidopsis. Plant Physiol. 127, 1694–1710.

Lundby, A., Lage, K., Weinert, B.T., Bekker-Jensen, D.B., Secher, A., Skovgaard, T., Kelstrup, C.D., Dmytriyev, A., Choudhary, C., Lundby, C., Olsen, J.V., 2012. Proteomic analysis of lysine acetylation sites in rat tissues reveals organ specificity and subcellular patterns. Cell Rep. 2, 419–431.

Melo-Braga, M.N., Verano-Braga, T., Leon, I.R., Antonacci, D., Nogueira, F.C., Thelen, J.J., Larsen, M.R., Palmisano, G., 2012. Modulation of protein phosphorylation, N-glycosylation and Lys-acetylation in grape (*Vitis vinifera*) mesocarp and exocarp owing to *Lobesia botrana* infection. Mol. Cell. Proteomics 11, 945–956.

Miernyk, J.A., Randall, D.D., 1987. Some kinetic and regulatory properties of the pea mitochondrial pyruvate dehydrogenase complex. Plant Physiol. 83, 306–310.

Millar, A.H., Heazlewood, J.L., Kristensen, B.K., Braun, H.P., Møller, I.M., 2005. The plant mitochondrial proteome. Trends Plant Sci. 10, 36–43.

Morgan, M.J., Lehmann, M., Schwarzländer, M., Baxter, C.J., Sienkiewicz-Porzucek, A., Williams, T.C., Schauer, N., Fernie, A.R., Fricker, M.D., Ratcliffe, R.G., Sweetlove, L.J., Finkemeier, I., 2008. Decrease in manganese superoxide dismutase leads to reduced root growth and affects tricarboxylic acid cycle flux and mitochondrial redox homeostasis. Plant Physiol. 147, 101–114.

Newman, J.C., He, W., Verdin, E., 2012. Mitochondrial protein acylation and intermediary metabolism: regulation by sirtuins and implications for metabolic disease. J. Biol. Chem. 287, 42436–42443.

O'Shea, J.P., Chou, M.F., Quader, S.A., Ryan, J.K., Church, G.M., Schwartz, D., 2013. pLogo: a probabilistic approach to visualizing sequence motifs. Nat. Methods 10, 1211–1212.

Perales, M., Eubel, H., Heinemeyer, J., Colaneri, A., Zabaleta, E., Braun, H.P., 2005. Disruption of a nuclear gene encoding a mitochondrial gamma carbonic anhydrase reduces complex I and supercomplex I + III2 levels and alters mitochondrial physiology in Arabidopsis. J. Mol. Biol. 350, 263–277.

Picault, N., Palmieri, L., Pisano, I., Hodges, M., Palmieri, F., 2002. Identification of a novel transporter for dicarboxylates and tricarboxylates in plant mitochondria. Bacterial expression, reconstitution, functional characterization, and tissue distribution. J. Biol. Chem. 277, 24204–24211.

Rappsilber, J., Mann, M., Ishihama, Y., 2007. Protocol for micro-purification, enrichment, pre-fractionation and storage of peptides for proteomics using StageTips. Nat. Protoc. 2, 1896–1906.

Rardin, M.J., Newman, J.C., Held, J.M., Cusack, M.P., Sorensen, D.J., Li, B., Schilling, B., Mooney, S.D., Kahn, C.R., Verdin, E., Gibson, B.W., 2013. Label-free quantitative proteomics of the lysine acetylome in mitochondria identifies substrates of SIRT3 in metabolic pathways. Proc. Natl. Acad. Sci. U. S. A. 110, 6601–6606.

Salvato, F., Havelund, J.F., Chen, M., Rao, R.S., Rogowska-Wrzesinska, A., Jensen, O.N., Gang, D.R., Thelen, J.J., Møller, I.M., 2014. The potato tuber mitochondrial proteome. Plant Physiol. 164, 637–653.

Sauve, A.A., 2010. Sirtuins. Biochim. Biophys. Acta 1804, 1565–1566.

Schmidtmann, E., Konig, A.C., Orwat, A., Leister, D., Hartl, M., Finkemeier, I., 2014. Redox regulation of Arabidopsis mitochondrial citrate synthase. Mol. Plant 7, 156–169.

Schwarzländer, M., König, A.C., Sweetlove, L.J., Finkemeier, I., 2012a. The impact of impaired mitochondrial function on retrograde signalling: a meta-analysis of transcriptomic responses. J. Exp. Bot. 63, 1735–1750.

Schwarzländer, M., Murphy, M.P., Duchen, M.R., Logan, D.C., Fricker, M.D., Halestrap, A.P., Muller, F.L., Rizzuto, R., Dick, T.P., Meyer, A.J., Sweetlove, L.J., 2012b. Mitochondrial 'flashes': a radical concept repHined. Trends Cell Biol. 22, 503–508.

Schwarzländer, M., Finkemeier, I., 2013. Mitochondrial energy and redox signaling in plants. Antioxid. Redox Signal. 18, 2122–2144.

Scott, I., Webster, B.R., Li, J.H., Sack, M.N., 2012. Identification of a molecular component of the mitochondrial acetyltransferase programme: a novel role for GCN5L1. Biochem. J. 443, 655–661.

Sebastian, C., Satterstrom, F.K., Haigis, M.C., Mostoslavsky, R., 2012. From sirtuin biology to human diseases: an update. J. Biol. Chem. 287, 42444–42452.

Smith-Hammond, C.L., Swatek, K.N., Johnston, M.L., Thelen, J.J., Miernyk, J.A., 2013. Initial description of the developing soybean seed protein Lys-N-acetylome. J. Proteome 96C, 56–66.

Starai, V.J., Celic, I., Cole, R.N., Boeke, J.D., Escalante-Semerena, J.C., 2002. Sir2-dependent activation of acetyl-CoA synthetase by deacetylation of active lysine. Science 298, 2390–2392.

Still, A.J., Floyd, B.J., Hebert, A.S., Bingman, C.A., Carson, J.J., Gunderson, D.R., Dolan, B.K., Grimsrud, P.A., Dittenhafer-Reed, K.E., Stapleton, D.S., Keller, M.P., Westphall, M.S., Denu, J.M., Attie, A.D., Coon, J.J., Pagliarini, D.J., 2013. Quantification of mitochondrial acetylation dynamics highlights prominent sites of metabolic regulation. J. Biol. Chem. 288, 26209–26219.

Sunderhaus, S., Dudkina, N.V., Jansch, L., Klodmann, J., Heinemeyer, J., Perales, M., Zabaleta, E., Boekema, E.J., Braun, H.P., 2006. Carbonic anhydrase subunits form a matrix-exposed domain attached to the membrane arm of mitochondrial complex I in plants. J. Biol. Chem. 281, 6482–6488.

Sweetlove, L.J., Fait, A., Nunes-Nesi, A., Williams, T., Fernie, A.R., 2007. The mitochondrion: an integration point of cellular metabolism and signalling. Crit. Rev. Plant Sci. 26 (1).

Sweetlove, L.J., Beard, K.F., Nunes-Nesi, A., Fernie, A.R., Ratcliffe, R.G., 2010. Not just a circle: flux modes in the plant TCA cycle. Trends Plant Sci. 15, 462–470.

Tanz, S.K., Castleden, I., Hooper, C.M., Vacher, M., Small, I., Millar, A.H., 2013. SUBA3: a database for integrating experimentation and prediction to define the SUBcellular location of proteins in Arabidopsis. Nucleic Acids Res. 41, D1185–D1191.

Thimm, O., Blasing, O., Gibon, Y., Nagel, A., Meyer, S., Kruger, P., Selbig, J., Muller, L.A., Rhee, S. Y., Stitt, M., 2004. MAPMAN: a user-driven tool to display genomics data sets onto diagrams of metabolic pathways and other biological processes. Plant J. 37, 914–939.

Tovar-Mendez, A., Miernyk, J.A., Randall, D.D., 2003. Regulation of pyruvate dehydrogenase complex activity in plant cells. Eur. J. Biochem./FEBS 270, 1043–1049.

Wagner, G.R., Payne, R.M., 2013. Widespread and enzyme-independent N-epsilon-acetylation and N epsilon-succinylation of proteins in the chemical conditions of the mitochondrial matrix. J. Biol. Chem. 288, 29036–29045.

Wang, Q., Zhang, Y., Yang, C., Xiong, H., Lin, Y., Yao, J., Li, H., Xie, L., Zhao, W., Yao, Y., Ning, Z.B., Zeng, R., Xiong, Y., Guan, K.L., Zhao, S., Zhao, G.P., 2010. Acetylation of metabolic enzymes coordinates carbon source utilization and metabolic flux. Science 327, 1004–1007.

Weinert, B.T., Iesmantavicius, V., Wagner, S.A., Scholz, C., Gummesson, B., Beli, P., Nystrom, T., Choudhary, C., 2013. Acetyl-phosphate is a critical determinant of lysine acetylation in *E. coli*. Mol. Cell 51, 265–272.

Weinert, B.T., Wagner, S.A., Horn, H., Henriksen, P., Liu, W.R., Olsen, J.V., Jensen, L.J., Choudhary, C., 2011. Proteome-wide mapping of the Drosophila acetylome demonstrates a high degree of conservation of lysine acetylation. Sci. Signal. 4, ra48.

Wisniewski, J.R., Zougman, A., Mann, M., 2009. Combination of FASP and StageTip-based fractionation allows in-depth analysis of the hippocampal membrane proteome. J. Proteome Res. 8, 5674–5678.

Wu, X., Oh, M.H., Schwarz, E.M., Larue, C.T., Sivaguru, M., Imai, B.S., Yau, P.M., Ort, D.R., Huber, S.C., 2011. Lysine acetylation is a widespread protein modification for diverse proteins in Arabidopsis. Plant Physiol. 155, 1769–1778.

Wu, Y.T., Lee, H.C., Liao, C.C., Wei, Y.H., 2013. Regulation of mitochondrial F(o)F(1)ATPase activity by Sirt3-catalyzed deacetylation and its deficiency in human cells harboring 4977 bp deletion of mitochondrial DNA. Biochim. Biophys. Acta 1832, 216–227.

Xing, S., Poirier, Y., 2012. The protein acetylome and the regulation of metabolism. Trends Plant Sci. 17, 423–430.

Yang, X.J., Seto, E., 2008. Lysine acetylation: codified crosstalk with other posttranslational modifications. Mol. Cell 31, 449–461.

Zhao, S., Xu, W., Jiang, W., Yu, W., Lin, Y., Zhang, T., Yao, J., Zhou, L., Zeng, Y., Li, H., Li, Y., Shi, J., An, W., Hancock, S.M., He, F., Qin, L., Chin, J., Yang, P., Chen, X., Lei, Q., Xiong, Y., Guan, K.L., 2010. Regulation of cellular metabolism by protein lysine acetylation. Science 327, 1000–1004.

Please cite this article as: König, A.-C., et al., The mitochondrial lysine acetylome of Arabidopsis, Mitochondrion (2014), http://dx.doi.org/10.1016/j.mito.2014.03.004

Publication 7

Identification of lysine-acetylated mitochondrial proteins and their acetylation sites.

Hartl M *, **König AC***, Finkemeier I.

(2014)

Submitted to Springer, Plant Mitochondria: Methods and Protocols

Chapter 9

Identification of lysine-acetylated mitochondrial proteins and their acetylation sites

Markus Hartl*, Ann-Christine König*, Iris Finkemeier

*these authors contributed equally to this work.

To whom correspondence should be addressed:
Dr. Iris Finkemeier
Plant Proteomics
Max-Planck Institute for Plant Breeding Research
Carl-von-Linné Weg 10
50829 Köln, Germany

Tel.: +49 (221) 5062 - 234
Fax: +49 (221) 5062 - 207
Email: finkemeier@mpipz.mpg.de

Summary

The $^{\varepsilon}$N-acetylation of lysine (K) side chains is a highly conserved post-translational modification of both prokaryotic and eukaryotic proteins. Lysine acetylation not only occurs on histones in the nucleus but also on many mitochondrial proteins in plants and animals. As the transfer of the acetyl group to lysine eliminates its positive charge, lysine acetylation can affect the biological function of proteins. This chapter describes two methods for the identification of lysine-acetylated proteins in plant mitochondria using an anti-acetyl lysine antibody. We describe the Western blot analysis of a two-dimensional blue native polyacrylamide gel electrophoresis with an anti-acetyl lysine antibody as well as the immuno-enrichment of lysine-acetylated peptides followed by liquid chromatography tandem mass spectrometry (LC-MS/MS) data acquisition and analysis.

Key words: lysine acetylation, mitochondria, Arabidopsis, protein complexes, BN-PAGE

1. Introduction

Plant mitochondria function in the fundamental energy metabolism and have additional unique properties when compared to their mammalian relatives. Besides oxidative phosphorylation which produces energy in form of ATP, plant mitochondria also host enzymes for photorespiration as well as alternative electron complexes to limit oxidative stress in the cell. These metabolic pathways have to be tightly regulated and adjusted to the always changing environmental conditions plants are experiencing. Posttranslational modifications (PTMs) have the capability to regulate central metabolic pathways as well as to maintain the flexibility of the organellar metabolism [5]. One recently emerging PTM in prokaryotes and eukaryotes with predicted key regulatory function in metabolic pathways is the lysine acetylation of proteins [2, 3, 16, 18, 21]. Lysine acetylation was first investigated on histones where it affects chromatin structure and gene expression [8], but lately it was also identified to occur on non-histone proteins. However, lysine acetylation depends on the availability of acetyl-coA, a central metabolite of several metabolic pathways, which indicates that information on the metabolic state of the cell could directly be sensed and transduced via lysine acetylation [10, 21]. Also in plants there is mounting evidence that lysine acetylation affects protein functions as well as enzyme activities [7, 14, 20]. Especially plant mitochondrial proteins show a high abundance of lysine-acetylated proteins [22] but due to the overall low abundance of mitochondria in the cell it is challenging to detect lysine-acetylated mitochondrial proteins in whole cell extracts. Here, we present two methods to

detect and analyze mitochondrial lysine-acetylated proteins with the help of an anti-acetyllysine antibody: (1) The detection of lysine-acetylated proteins in native mitochondrial protein complexes, (2) the identification of lysine-acetylated peptides and sites via immuno-enrichment of lysine-acetylated peptides followed by LC-MS/MS data acquisition and analysis.

The two-dimensional blue-native PAGE (BN-PAGE) is a relevant method to determine protein complex compositions of supercomplexes and it is especially useful for membrane bound complexes lacking an internal charge [11]. To explore the extent of lysine acetylation in plant mitochondria, intact protein complexes from mitochondria are isolated and solubilization of membranes occurs with digitonin. Separation of protein complexes is carried out by BN-PAGE as explained in Klodmann et al., 2011 [13] and followed by Western blot analysis using the anti-acetyllysine antibody as well as Ponceau S stain after immunotransfer for quality control. The Ponceau S stain visualizes all the abundant mitochondrial proteins (Fig.1).

The BN-PAGE approach yields valuable information on the lysine acetylation state of proteins and protein complexes. However, it falls short of identifying the actual acetylation sites of particular proteins of interest, which is most relevant for understanding the functional or structural implications of a particular modification. Generating site-specific antibodies is costly, time consuming, and technically not always feasible. Thus the identification of lysine acetylation sites using liquid chromatography tandem mass spectrometry (LC-MS/MS) became a valuable alternative. The identification of lysine-acetylated protein peptides by LC-MS/MS is based on the detection of a 42.01 Da increase in peptide mass using high-resolution accurate mass LC-MS/MS [1, 6, 12]. In principle this technique allows the identification and to some extent also quantification of peptides at a proteome-wide scale. However, LC-MS/MS also has technical limitations, which mainly depend on the properties of a protein and the peptides generated from it. Thus it is possible that certain lysine acetylation sites escape detection, for example due to inadequate peptide length or unfavorable physicochemical properties which prevent it from reaching the detector of the MS. Despite these limitations LC-MS/MS is currently the most powerful technique available to identify and quantify lysine-acetylated peptides.

Here we provide a procedure for sample preparation and enrichment for lysine-acetylated peptides from plant mitochondria (Fig.2), which we previously applied successfully to identify 243 acetylated lysine sites on 120 mitochondrial proteins from *Arabidopsis thaliana* [22]. We deliberately chose not to include a detailed protocol for LC-MS/MS, as this would

require referring to a particular instrumental setup which would be of limited use to a wider community. However, as very similar results can be obtained with a range of LC-MS/MS setups from different vendors, we will provide basic measurement parameters which should enable users to develop a suitable protocol for the instruments at hand. For the same reason, we also do not include procedures for data analysis because these are in many cases platform-dependent.

Our sample preparation procedure for the identification of lysine-acetylated peptides comprises two major steps:

1. Extensive solubilization and digestion of proteins. These are absolute prerequisites for deep proteome coverage. Given that many membrane proteins are essential for mitochondrial function and metabolism, their solubilization should be facilitated by the method applied. In this protocol we use a filter assisted sample preparation (FASP), which was originally described by Wisniewksi et al. [19], and which we slightly adapted for our purpose. It has the advantage of solubilizing proteins very well and of removing compounds interfering with LC-MS/MS, without the need of precipitating the protein. Nevertheless, other approaches might be similarly successful.

2. Enrichment of lysine-acetylated peptides. This step is absolutely necessary because the abundance of acetylated peptides can be rather low and thus their detection would be hampered by the bulk of non-acetylated peptides. So far the only method available for enrichment of lysine-acetylated peptides uses an anti-acetyl-lysine antibody [2, 9, 15] and the protocol presented here largely follows this method.

We highly recommend desalting samples after the enrichment. We prefer using custom-made C18 StageTips, as described in detail by Rappsilber et al. [17], but other approaches are possible. As each mass spectrometry laboratory usually has its own preferred standard procedure for sample clean-up, we do not provide a protocol for this step.

Figure 1: Detection of lysine acetylation in mitochondrial protein complexes of Arabidopsis analyzed by 2D BN/SDS-PAGE and Western blot.

(A) PonceauS stain of 2D BN/SDS-PAGE of mitochondrial protein complexes. The identity of OXPHOS complexes is indicated above the gels. I+III_2, supercomplex composed of complex I and dimeric complex III; I, complex I; V, complex V (ATP synthase); III_2, dimeric complex III. The molecular mass scale (in kDa) is indicated on the left.

(B) Lysine-acetylated proteins from Arabidopsis mitochondria detected by Western blot analysis using the anti-acetyllysine antibody.

Figure 2: Workflow for the identification of lysine-acetylated peptides using LC-MS/MS.

After cell lysis, proteins are digested enzymatically and lysine-acetylated peptides are enriched using an anti-acetyl lysine antibody. Enriched peptides are separated and measured using nano-LC-MS/MS, raw data are computationally processed to identify the peptides and acetylated lysines.

2. Materials

2.1. Materials for BN-PAGE and anti-acetyllysine immunoblotting

2.1.1. First dimension BN-PAGE

For the first dimension of the BN-PAGE see Chapter 8 (Materials: 2.1. Components for Casting and Running a BN-Gel).

2.1.2. Materials for sample preparation

For material for sample preparation see Chapter 8 (Materials: 2.3. Components for Sample Preparation).

2.1.3. Components for preparing the gel strip for second dimension

Denaturing solution 1% (w/v) sodium dodecyl sulfate (SDS), 1% (v/v) ß-mercaptoethanol

2.1.4. Second dimension (Tricine-SDS-PAGE) components

1. Tricine gel buffer: 3 M Tris-HCl pH 8.45, 0.3% (w/v) SDS
2. Acrylamide 40%: Rotiphorese® Gel 40 (37.5:1) (Carl ROTH)
3. Anode buffer: 0.2 M Tris-HCl pH 8.9
4. Cathode buffer : 0.1 M Tris-HCl, 0.1 M Tricine, 0.1% (w/v) SDS, pH 8.25
5. Overlay-solution: 1 M Tris-HCl pH 8.45. 0.1% (w/v) SDS
6. 87% (v/v) and 100% (v/v) glycerol
7. Gel buffer BN (6X): 1.5 M amino caproic acid, 150 mM BisTris, pH 7 (store at 4°C)
8. SDS solution: 10% (w/v) SDS
9. N,N,N',N'-tetramethylethylenediamine (TEMED)
10. Ammonium persulfate (APS): 10% (w/v) solution in water

11. 70% (v/v) ethanol
12. Hoefer SE600 Standard Dual Cooled Vertical Unit

2.1.5. Western blot components

1. Nitrocellulose membrane (GE Healthcare Life Science Whatman™)
2. Grade 3MM Chr Cellulose Chromatography Papers (GE Healthcare Life Science Whatman™)
3. Western blot transfer buffer: 0.048 M Tris-HCl, pH 8.3, 0.039 M glycine, 20% (v/v) methanol
4. Trisbuffered saline (TBS): 0.05 M Tris-HCl pH 7.5, 0.15 M NaCl
5. TBS containing 0.05% (v/v) Tween-20 (TBST).
6. Blocking solution: 2% (w/v) gelatin from cold water fish skin (SIGMA) in TBS
7. Plastic container
8. Bag sealer (Severin, Folio FS 3602)
9. Plastic bags (Sekuroka®-disposal bags, ROTH)
10. Ponceau S staining solution: 0.1% (w/v) PonceauS in 5% (v/v) acidic acid
11. Orbital Shaker (ELMI Large Sky Line Digital DOS-10L / 20L)
12. Scissor
13. Anti-acetyllysine antibody (ImmuneChem Pharmaceuticals)
14. Anti-horseradish peroxidase antibody (ThermoFisher Scientific)
15. SuperSignal West Dura enhanced chemiluminescent substrate (Thermo Fisher Scientific)
16. Fastblot Semi-Dry Electrophoretic Transfer Apparatus B44 (Biometra)
17. Fusion Imaging System (PEQLAB)

2.2. Materials for digestion of mitochondrial proteins and immuno-enrichment of lysine-acetylated peptides

2.2.1. Filter-assisted sample preparation (FASP)

1. SDS-lysis buffer: 4% (w/v) SDS, 0.1 M dithiothreitol (DTT) in 100 mM Tris-HCl pH 7.6
2. Urea buffer: 8 M urea in 0.1 M Tris-HCl pH 8.5. Prepare 25 ml per sample (see **Note 1**).
3. IAA solution: 0.05 M iodoacetamide in urea buffer. Prepare 1 ml per sample (see **Note 1**).
4. Proteomics-grade trypsin (for example Trypsin Gold, Promega)
5. ABC buffer: 0.05M NH_4HCO_3 in water. Prepare 20 ml per sample
6. Buffer A: 0.05% (v/v) formic acid in ultrapure water
7. Buffer B: 80% (v/v) acetonitrile (HPLC-grade), 0.05% (v/v) formic acid in ultrapure water

8. Methanol
9. 10% trifluoroacetic acid (TFA) in ultrapure water
10. 660 nm protein assay with compatibility reagent (Pierce - Thermo Scientific)
11. Centrifugal filter device (CFD): Amicon Ultra-4 30k MWCO (Millipore) or similar
12. Bench-top centrifuge for microfuge tubes
13. Bench-top centrifuge, accommodating 15 ml conical-bottomed tubes, ideally in a swinging-bucket rotor at a speed of 4000 x g
14. Heat block
15. Microvolume UV-VIS photometer (for example NanoDrop 2000, Thermo Scientific)
16. Vacuum-concentrator (for example Concentrator 5301, Eppendorf)
17. Sep-Pak C18 1 cc cartridge, 100 mg sorbent per cartridge, 55-105 µm particle size (Waters)

2.2.2. Immuno-enrichment of lysine-acetylated peptides

1. 20% (v/v) acetonitrile (MS grade) in ultrapure water
2. Tris-buffered saline buffer (TBS): 50 mM Tris-HCl, 150 mM NaCl, pH 7.6, stored at 4°C
3. 1.5 ml Protein LoBind tubes (Eppendorf), and 1.5 ml microcentrifuge tubes
4. Ultrapure water
5. Acetyllysine antibody, immobilized to beaded agarose (Immunechem, ICP0388)
6. GELoader® tips (Eppendorf) or similar gel-loading pipette tips
7. Rolling wheel at 4°C
8. Ice for cooling samples
9. Universal pH indicator paper, pH 1-11
10. Ultrasonic bath

3. Methods

3.1. BN-PAGE and anti-acetyllysine immunoblotting

3.1.1. First dimension BN-PAGE

For preparation of the first dimension see Chapter 8 (Methods: 3.1 Preparation of a BN Gel).

3.1.2 Sample preparation for first dimension

For BN sample preparation see Chapter 8 (Methods: 3.2 Sample Preparation for BN Gel and CN Gel)

3.1.3. Transfer of gel strip of first dimension onto second dimension

1. Cut out lane of interest from first dimension with a razor blade.
2. Incubate in denaturing solution for 30 min shaking (100 rpm) at room temperature (20°C - 25°C).
3. Wash gel strip in distilled water 2x to avoid ß- mercaptoethanol contamination.

3.1.4 Second dimension (Tricine-SDS-PAGE)

Second dimension is carried out in a Hoefer SE600 Standard Dual Cooled Vertical Unit chamber or a comparable gel electrophoresis system. All procedures are performed at room temperature.

1. Wash glass plates of running chamber 3x with 70% (v/v) ethanol and then 3x with distilled water.
2. Place strip of first dimension at the upper part of one glass plate where usually the comb is situated.
3. Place second glass plate exactly on top of the first plate using 0.7 mm spacers and assemble plates (see **Note 2**).
4. For the 16.5% *Tricine-SDS-PAGE* prepare resolving gel as well as spacer gel in parallel (Table 1). Shortly before pouring the gel add APS and TEMED.
5. For pouring the second dimension, first add resolving gel then the spacer gel solution into the assembled glass plates and overlay it with overlay solution (see **Note 3**).
6. The sample gel (Table 2) is prepared after polymerization of resolving and spacer gel. Shortly before pouring the gel add APS and TEMED.
7. Remove overlay solution; add sample gel until the upper edge of the gel strip and let the sample gel polymerize before transferring the glass plates into the running chamber (see **Note 4**).
8. Add the anode buffer and the cathode buffer to the lower and upper chamber of the gel unit.
9. Run the second dimension for 13h with 30 mA max. and 500 V per 1 mm spacer width.

3.1.5. Western blot

For Western blotting, the Fastblot Semi-Dry Electrophoretic Transfer Apparatus B44 (Biometra) has been used. All procedures were carried out at room temperature. For detection of the chemiluminescent substrate the Fusion Imaging System from PEQLAB was used.

1. Cut 8 pieces of cellulose chromatography paper in the size of the gel of the second dimension as well as one piece of nitrocellulose membrane.
2. Soak 4 pieces of cellulose chromatography paper in Western blot transfer buffer and then transfer them onto the Fastblot.
3. Shortly incubate the nitrocellulose membrane in Western blot transfer buffer and place it on top of the cellulose chromatography papers.
4. Remove the gel from the second dimension carefully from the glass plates and discard the sample gel. Shortly incubate the gel in Western blot transfer buffer and place it on top of the nitrocellulose membrane.
5. Add another 4 layers of cellulose chromatography papers soaked in Western blot transfer buffer on top of the gel (see **Note 5**).
6. Assemble the blotting system. Transfer of proteins onto the nitrocellulose membrane is carried out at 320 mA for 90 min (see **Note 6).**
7. After transfer disassemble the blotting system and remove the nitrocellulose membrane carefully.
8. To assess the success of the transfer the nitrocellulose membrane is placed in a plastic container and incubated in Ponceau S staining solution for 1 min. The membrane should be completely covered with staining solution (see **Note 7**)**.**
9. For de-staining, wash nitrocellulose membrane 3x for 5min with TBS, slightly shaking.
10. Add blocking solution until the nitrocellulose membrane is completely covered and incubate for 60 min, slightly shaking.
11. After blocking wash the nitrocellulose membrane 3x for 10 min with TBST, slightly shaking.
12. Seal the nitrocellulose membrane in a plastic bag with one side left open (see **Note 8**)**.**
13. Dilute anti-acetyllysine antibody 1:2000 in 12 ml TBST and pour the solution into the open side of the plastic bag containing the nitrocellulose membrane. Seal the open side of the plastic sheets and incubate 16 h shaking at 150 rpm.
14. Remove nitrocellulose membrane from the plastic sheets and wash as in **step 11**.
15. Dilute the anti-horseradish peroxidase antibody 1:1000 in 12 ml TBST and proceed as in **step 12 and 13** but incubate just for 1h.
16. Repeat **step 14**.
17. For visualization of lysine-acetylated proteins, SuperSignal West Dura enhanced chemiluminescent substrate is used and for detection a chemiluminescence imager (see **Note 9**).

3.2. Identification of lysine-acetylated peptides

3.2.1 Protein digestion using FASP

All steps are carried out at room temperature unless indicated else. Placing SDS or urea containing buffers on ice or at 4 °C can lead to precipitation.

1. Purified mitochondria (see Chapter 2) (corresponding to at least 0.5 to 1 mg mitochondrial protein) are pelleted at 15000 x g for 10 min at 4°C in a microcentrifuge tube (see **Note 10**). For better coverage, we recommend processing at least three independent biological replicates. Pellets can be snap-frozen in liquid nitrogen and stored at -80°C until further processing.
2. Resuspend the pellet in 400 µl SDS lysis buffer, vortex until the pellet is resuspended and place for 5 min in a heat block at 95°C, vortexing two times for 20 seconds in between.
3. Sonicate sample in an ultrasonic bath for 1 min.
4. Centrifuge for 20 min in a benchtop centrifuge at top speed (15000 to 21000 x g) and room temperature.
5. Transfer the supernatant to a new tube without disturbing any sedimented material.
6. Repeat steps 4 and 5 once.
7. Determine the amount of protein using the 660 nm protein assay with compatibility reagent according to the manufacturer's instructions.
8. Add 2 ml urea buffer to the CFD and centrifuge for 5 min to condition the membrane. Stop the centrifuge after approximately one minute and check the buffer retention. In rare cases unusually fast flow-through occurs, which indicates a leak in the membrane. Such damaged units cannot be used and must be replaced.
9. Dilute the sample with urea buffer to a total volume of 4 ml and transfer to the CFD (see **Note 11**) – final SDS concentration must not exceed 0.5%.
10. Centrifuge at 4000 x g for 15 min (or until at least ten-fold concentration).
11. Discard flow-through, add another 4 mL urea buffer and repeat centrifugation.
12. Discard flow-through, add 1 ml IAA solution, mix gently for 1 min with a pipette without touching the membrane and incubate for 30 min at room temperature in darkness.
13. Centrifuge the CFD at 4000 x g for 10 min, discard flow-through.
14. Add 4 ml of urea buffer to the CFD and centrifuge at 4000 x g for 15 min or until at least ten-fold concentration. Discard the flow-through and repeat this step twice.
15. Add 4 ml ABC buffer to the CFD and centrifuge at 4000 x g for 15 min or until at least ten-fold concentration. Discard the flow-through and repeat this step twice.

16. Transfer the CFD to new 15 ml collection tubes.

17. Add 1 ml ABC buffer containing trypsin at an enzyme to protein ratio of 1:100 (e.g. 10 µg trypsin for 1 mg protein) and gently mix with a pipette (do not touch the membrane while pipetting), (see **Note 12**).

18. Tighten the lid of the tube well and incubate the CFD at 37°C overnight.

19. Centrifuge the CFD at 4000 x g for 10 min. The eluate now contains the peptides.

20. Add 1 ml ABC buffer to the CFD (rinsing the filters when adding the buffer) and repeat the centrifugation.

21. Repeat step 20.

22. Assess the peptide yield on a microvolume UV-VIS photometer at 280 nm, assuming an absorption of 1 for a peptide concentration of 1 mg ml^{-1}. Typical yields are approximately 50 to 60% of the starting amount.

23. Acidify the eluate to a final concentration of 1% TFA.

24. Condition a C18 SepPak cartridge by flushing it with 3 ml methanol, 3 ml buffer B, and then 3 ml buffer A.

25. Slowly load peptide sample on the cartridge.

26. Wash with 3x 1 ml of buffer A

27. Elute two times with 0.6 ml buffer B into a 1.5 ml Protein LoBind tube.

28. Evaporate the sample to complete dryness on a vacuum concentrator, if necessary overnight. After drying, peptides can be stored for short term at -20°C or for long term at -80°C.

3.2.2. Enrichment of lysine-acetylated peptides

Sample preparation can be carried out at room temperature to facilitate dissolution of peptides. All steps involving the anti-acetyl lysine antibody should be carried out on ice or at 4°C.

1. Re-dissolve dried peptides in 50 µL 20% acetonitrile, vortex vigorously and let rest for 10 min. Then add 450 µl TBS and vortex (see **Note 13**).

2. Check the pH of the solution by pipetting 1 µl of sample on pH indicator paper (see **Note 14**).

3. Assess the peptide yield on a microvolume UV-VIS photometer at 280 nm, assuming an absorption of 1 for a peptide concentration of 1 mg ml^{-1}.

4. Take an aliquot of 10 µg and store it for measuring the background proteome (see **Note 15**)

5. Transfer 50 µL antibody bead slurry to a 1.5 ml Protein LoBind tube with a cut 200 µl pipette tip (see **Note 16**).
6. Wash beads 3 x 5 min with 1 ml TBS on a rolling wheel. Centrifuge at 1000 x g in between washes and carefully remove the supernatant (see **Note 16**).
7. Add the re-dissolved peptides to the beads and incubate overnight at 4°C on a rolling wheel.
8. Wash beads 4 x 5 min with 1 ml TBS on a rolling wheel at 4°C.
9. Wash beads 2 x shortly with ultrapure water to reduce the salt concentration, centrifuging in between at 1000 x g for 1 min.
10. Elute 3 x 5 min with 50 µl 0.1% TFA, mixing the beads gently with the pipet and letting them rest for the remaining time period. Centrifuge in between at 2000 x g and try to recover as much liquid as possible without transferring beads using gel-loading tips.
11. Assess the peptide concentration of the combined eluates on a microvolume UV-VIS photometer at 280 nm as in step 3. Usually the concentration is very low (only a few µg yield in total). Higher concentrations might indicate massive background contamination.
12. Clean-up combined eluates on StageTips and run the samples on an LC-MS/MS system.

3.2.3 Guidelines for measuring the samples on LC-MS/MS

In general every high-resolution accurate mass nano-UHPLC-MS/MS setup used for shotgun proteomics can be used for measuring these samples. Typically we run them on self-pulled capillary columns with 75 µm diameter, packed with 20 to 50 cm C18 reversed-phase material (for example: 1.9 µm ReproSil-Pur C18-AQ, Dr. Maisch GmbH). The column is kept at 50°C in a column oven throughout the run. We inject max. 1 to 2 µg peptides and separate them at a flow rate of 250 nl min^{-1} with a 90 min linear gradient from 2% to 30% buffer B in buffer A (buffer A: 0.1% (v/v) formic acid; buffer B: 80% (v/v) acetonitrile 0.1% (v/v) formic acid), followed by a 5 min linear gradient to 60% buffer B, and then a 5 min linear gradient to 95% buffer B. If sample complexity is high the gradient time should be prolonged accordingly (for example to a total of 4 h runtime) or fractionation should be considered. We typically detect the peptides on a Q-Exactive MS (Thermo Scientific) in positive mode with a scanned mass range of 300-1650 m/z, at a resolution of 70,000 and an AGC target value of 3e6. The ten most intense ions are selected for MS2 at a resolution of 35,000 with an isolation window of 1.6 m/z and an AGC target of 1e6. Peptides with a charge of +1 or with unassigned charge state are excluded from fragmentation for MS2, dynamic exclusion prevents repeated selection of selected masses for 20 s. We process raw data using MaxQuant software

(http://www.maxquant.org/) [4] and search against The Arabidopsis Information Resource protein database (http://www.arabidopsis.org), with trypsin specificity and a maximum of four missed cleavages at a protein and peptide false discovery rate of 1%. Carbamidomethylation of cysteine residues were set as fixed, oxidation of methionine, N-terminal acetylation and lysine acetylation as variable modifications.

4. Notes

1. Urea and IAA solutions must be freshly prepared. Prepare the urea buffer early in advance. It needs time to dissolve but should not be heated above room temperature to prevent formation of isocyanate and carbamylation of proteins. The IAA solution should be stored in the dark until use.
2. Place the edges of the plates exactly on top of each other before touching the gel strip. Do not adjust the second glass plate when it already touches the gel strip because this could damage it.
3. For pouring the *Tricine-SDS-PAGE,* start with the resolving gel, trying not to touch the gel strip with the solution. Directly after pouring, take the assembled glass plates with the resolving gel parallel to the surface and slowly add the spacer gel. Add half of the spacer gel solution on the left side and the other half on the right side of the gel strip. The spacer gel should not touch the gel strip in order to have space for the sample gel. Add overlay solution on top of the spacer gel in the same way like the spacer gel was added. Slowly put the gel back in a vertical position and let the gel polymerize for 1h.
4. Pour the sample gel from one side into the glass plates avoiding air bubbles in between sample gel and gel strip. This is achieved by holding the glass plates tilted while pouring.
5. Try to avoid air bubbles between the different layers of paper.
6. The current to be applied depends on the gel size. For the Fastblot Semi-Dry Electrophoretic Transfer Apparatus B44 (Biometra) 2 mA cm^{-2} are recommended.
7. We recommend documenting the result of the Ponceau S stain with a scanner or a camera. The membrane should be washed with distilled water until proteins become clearly visible.
8. Cut a plastic bag with a scissor into two separate sheets. Place the nitrocellulose membrane carefully on one sheet of and put the second sheet on top of the nitrocellulose membrane. Seal three sides of the plastic sheets close to the borders of the nitrocellulose membrane with one side remaining open.
9. The SuperSignal West Dura enhanced chemiluminescent substrate contains two components (Luminol/Enhancer Solution and Stable Peroxide Buffer) which have to be mixed

together in a volume proportion of 1:1. The mixture is then added immediately on top of the membrane making sure that it is covered completely.

10. The amount of mitochondrial protein will mainly be dictated by the quality and number of isolations. We consider 0.5 mg total protein as the absolute minimum. Ideally, 0.8 mg or more should be used to obtain a high number of identified acetylation sites. In general the number of identified sites correlates with the amount of peptides used in the enrichment step [15].

11. We recommend using 4 ml centrifugation devices (for example Amicon Ultra-4, Millipore) for digesting samples in the range of 0.3 to 3 mg total protein. For larger amounts the protocol can also be scaled up to devices such as Amicon Ultra-15 (Millipore).

12. To reach more complete digestion, it is possible to additionally digest the sample with LysC. For example LysC is added at an enzyme to protein ratio of 1:100 and the sample is incubated for 2 h at room temperature, before adding trypsin and incubating overnight as specified.

13. If the peptides do not dissolve well, the sample can also be placed in an ultrasonic bath for 5 min. Higher amounts of 20% acetonitrile can also help to redissolve the pellet, however bear in mind that the antibody tolerates only low amounts of acetonitrile.

14. Formic acid remaining after desalting and evaporation on the vacuum concentrator can lower the pH substantially. After adding the TBS buffer check whether the pH is in the desired range and, if necessary, correct by adding small amounts of 1 M Tris-HCl pH 7.6.

15. We recommend desalting this aliquot directly on C18 StageTips [17] and keeping the sample until measurement at -20°C.

16. 50 µl slurry corresponds to 100 µg antibody. A ratio of 100 µg antibody per 1 mg of peptides, results in a reasonable compromise between the number of sites identified and the costs for the antibody. The antibody is quite sensitive to temperature changes and cannot be re-used in our experience.

17. Take care not to lose beads while washing. Gel-loading tips are useful for taking off the remaining buffer close to the beads.

References

1. Borchers C, Parker CE, Deterding LJ et al. (1999) Preliminary comparison of precursor scans and liquid chromatography-tandem mass spectrometry on a hybrid quadrupole time-of-flight mass spectrometer. Journal of chromatography. A 854:119-130
2. Choudhary C, Kumar C, Gnad F et al. (2009) Lysine acetylation targets protein complexes and co-regulates major cellular functions. Science 325:834-840
3. Close P, Creppe C, Gillard M et al. (2010) The emerging role of lysine acetylation of non-nuclear proteins. Cellular and molecular life sciences : CMLS 67:1255-1264
4. Cox J, Mann M (2008) MaxQuant enables high peptide identification rates, individualized p.p.b.-range mass accuracies and proteome-wide protein quantification. Nature biotechnology 26:1367-1372
5. Deribe YL, Pawson T, Dikic I (2010) Post-translational modifications in signal integration. Nature structural & molecular biology 17:666-672
6. Dormeyer W, Ott M, Schnolzer M (2005) Probing lysine acetylation in proteins: strategies, limitations, and pitfalls of in vitro acetyltransferase assays. Molecular & cellular proteomics : MCP 4:1226-1239
7. Finkemeier I, Laxa M, Miguet L et al. (2011) Proteins of diverse function and subcellular location are lysine acetylated in Arabidopsis. Plant physiology 155:1779-1790
8. Gershey EL, Vidali G, Allfrey VG (1968) Chemical studies of histone acetylation. The occurrence of epsilon-N-acetyllysine in the f2a1 histone. The Journal of biological chemistry 243:5018-5022
9. Guan KL, Yu W, Lin Y et al. (2010) Generation of acetyllysine antibodies and affinity enrichment of acetylated peptides. Nature protocols 5:1583-1595
10. Hartl M, Finkemeier I (2012) Plant mitochondrial retrograde signaling: post-translational modifications enter the stage. Frontiers in plant science 3:253
11. Heinemeyer J, Lewejohann D, Braun HP (2007) Blue-native gel electrophoresis for the characterization of protein complexes in plants. Methods in molecular biology 355:343-352
12. Kim JY, Kim KW, Kwon HJ et al. (2002) Probing lysine acetylation with a modification-specific marker ion using high-performance liquid chromatography/electrospray-mass spectrometry with collision-induced dissociation. Analytical chemistry 74:5443-5449
13. Klodmann J, Senkler M, Rode C et al. (2011) Defining the protein complex proteome of plant mitochondria. Plant physiology 157:587-598
14. Koenig AC, Hartl M, Pham PA et al. (2014) The Arabidopsis class II sirtuin is a lysine deacetylase and interacts with mitochondrial energy metabolism. Plant Physiol
15. Mertins P, Qiao JW, Patel J et al. (2013) Integrated proteomic analysis of post-translational modifications by serial enrichment. Nature methods 10:634-637
16. Norvell A, Mcmahon SB (2010) Rise of the Rival. Science 327:964-965
17. Rappsilber J, Mann M, Ishihama Y (2007) Protocol for micro-purification, enrichment, pre-fractionation and storage of peptides for proteomics using StageTips. Nature protocols 2:1896-1906
18. Weinert BT, Wagner SA, Horn H et al. (2011) Proteome-wide mapping of the Drosophila acetylome demonstrates a high degree of conservation of lysine acetylation. Science signaling 4:ra48
19. Wisniewski JR, Zougman A, Nagaraj N et al. (2009) Universal sample preparation method for proteome analysis. Nature methods 6:359-362
20. Wu X, Oh MH, Schwarz EM et al. (2011) Lysine acetylation is a widespread protein modification for diverse proteins in Arabidopsis. Plant Physiol 155:1769-1778
21. Xing S, Poirier Y (2012) The protein acetylome and the regulation of metabolism. Trends in plant science 17:423-430
22. König AC, Hartl M, Boersema P et al. (2014) The mitochondrial lysine acetylome of Arabidopsis. Mitochondrion, in press

Table1: Preparation of resolving gel and spacer gel for second dimension. Amount of solutions is calculated for two 16.5% Tricine SDS PAGEs.

	Resolving Gel (30 ml)	Spacer Gel (10 ml)
Acrylamide 40% (w/v)	12.4 ml	2.5 ml
Tricine gel buffer	10 ml	3.4 ml
Glycerol 87% (v/v)	4 ml	-
Distilled water	3.6 ml	4.1 ml
APS 10% (w/v)	100 µl	34 µl
TEMED	10 µl	3.4 µl

Table2: Preparation of sample gel for second dimension. Amount of solutions is calculated for two sample gels.

	Sample Gel (10 ml)
Acrylamide 40% (w/v)	2.5 ml
Gel buffer BN (6X)	3.4 ml
Glycerol 100% (v/v)	1 ml
SDS 10% (w/v)	100 µl
Distilled water	2.9 ml
APS 10% (w/v)	83 µl
TEMED	8.3 µl

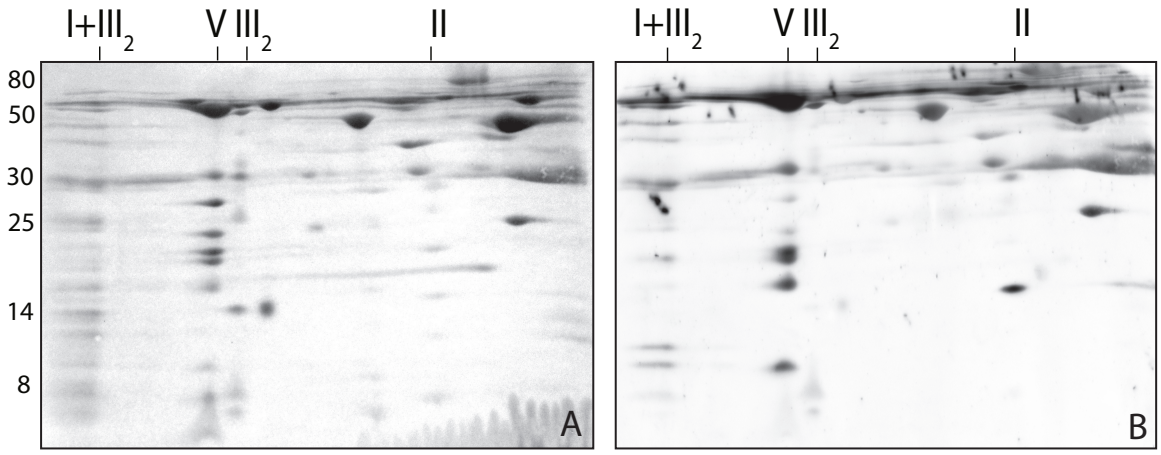

Figure 1: Detection of lysine acetylation in mitochondrial protein complexes of Arabidopsis analyzed by 2D BN/SDS-PAGE and Western blot.

(A) PonceauS stain of 2D BN/SDS-PAGE of mitochondrial protein complexes. The identity of OXPHOS complexes is indicated above the gels. $I+III_2$, supercomplex composed of complex I and dimeric complex III; I, complex I; V, complex V (ATP synthase); III_2, dimeric complex III. The molecular mass scale (in kDa) is indicated on the left.

(B) Lysine-acetylated proteins from Arabidopsis mitochondria detected by Western blot analysis using the anti-acetyllysine antibody.

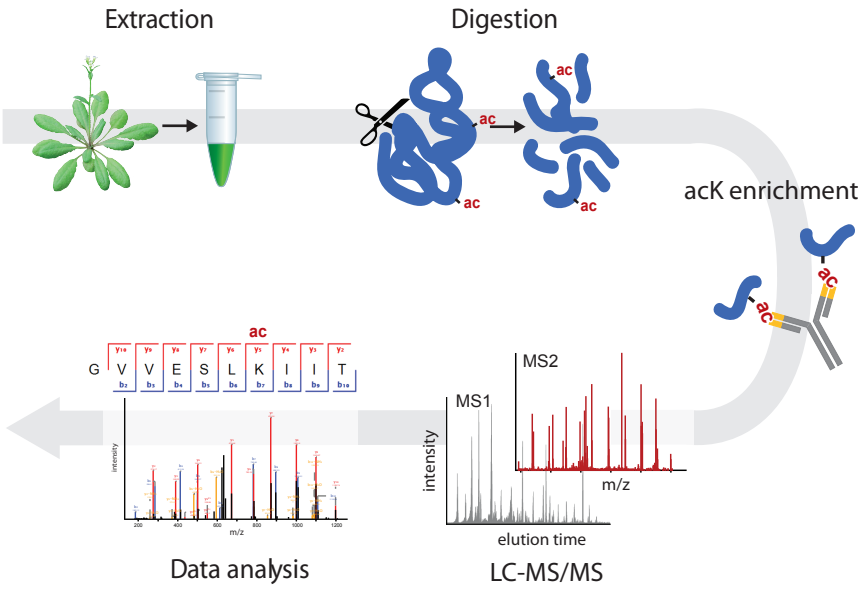

Figure 2: Workflow for the identification of lysine-acetylated peptides using LC-MS/MS.

After cell lysis, proteins are digested enzymatically and lysine-acetylated peptides are enriched using an anti-acetyl lysine antibody. Enriched peptides are separated and measured using nano-LC-MS/MS, raw data are computationally processed to identify the peptides and acetylated lysines.